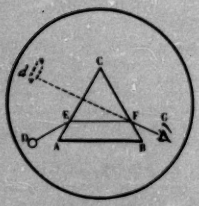

optics and spectroscopy

volume viii
number 1
january 1960

OPTICAL SOCIETY OF AMERICA

RUSSIAN EDITORIAL STAFF

Editor: S. E. FRISH

Assistant Editor: P. P. FEOFILOV
Corresponding Secretary: L. S. SAZONOV

Associate Editors:

M. M. GUREVICH M. A. EL'IASHEVICH A. A. LEBEDEV V. P. LINNIK
S. L. MANDEL'SHTAM I. V. OBREIMOV V. K. PROKOF'EV
N. N. SOBOLEV A. N. TERENIN A. I. TUDOROVSKII

Translated on the Initiative of
THE OPTICAL SOCIETY OF AMERICA, INC.
With a Grant-in-Aid from
THE NATIONAL SCIENCE FOUNDATION

TRANSLATION EDITORIAL STAFF

Scientific Editors

FRED W. BEHNKE, *Perkin-Elmer Corp.*

CYRUS FELDMAN, *Oak Ridge National Laboratory*

GEORGE HERRMAN, *Columbia University*

Administrative Editor: PATRICIA R. WAKELING, *OSA*

Published monthly by the Optical Society of America, Inc. Executive office: 1155 Sixteenth Street, N.W., Washington, D.C. Subscriptions for one year to members of the Society: Associates $13.00; Regular members and Fellows $17.00. Subscriptions for non-members of the Society: One year U. S. and Possessions, $25.00; Foreign $28.00. Back numbers: $3.00 per copy. Subscriptions, changes of address and undeliverable copies should be referred to the Executive offices in Washington, D.C. The office of publication is 2500 South State Street, Ann Arbor, Michigan. Second class postage paid at Ann Arbor, Michigan.

Printed in the U.S.A. by Edwards Brothers, Inc., Ann Arbor, Michigan.

AN INVESTIGATION OF THE INTENSITY RATIO OF THE POLARIZED COMPONENTS IN THE RADIATION OF THE "LUMINOUS" ELECTRON

F. A. Korolev and O. F. Kulikov

Received 25 April 1959

The ratio of the intensities of the polarized components of the electromagnetic radiation emitted by electrons accelerated in a synchrotron has been measured photographically in the visible region of the spectrum (6000-4000 A) for different maximum energies of the accelerated electrons (150, 200, and 250 Mev). Satisfactory agreement was found between the experimental and theoretical results calculated for the total radiation of electrons which are continuously accelerated to the maximum energy.

The electromagnetic radiation of electrons originating in modern cyclical accelerators is created by the acceleration of the particles, and plays an extremely important role in this process. Besides the expenditure of the accelerated particle's energy in the radiation, which can be rather large (in the case of the betatron, it constitutes the limit to the maximum energy of the accelerated electrons), this radiation can excite the particles to oscillation (increasing their energy, in the case of the synchrotron) and to the separation of the majority of them from the acceleration process long before they achieve the maximum energy. Hence, the investigation of this radiation and its properties is very important for the current theory of accelerators. Furthermore, the character of the radiation allows one to judge the behavior of the particles in the acceleration process, and a knowledge of its properties is also necessary from this point of view. Finally, experimental investigation of this radiation allows one to test the theory of the ultrarelativistic motion of the electron in a magnetic field.

The theory of the radiation in question, which was first predicted by the Soviet physicists Ivanenko and Pomeranchuk in 1944,[1] describes a number of its properties. We should stop and consider the main points, even if briefly, since they characterize important special features of this radiation. From the classical theory of the "luminous" electron, as developed in references 2-6, it follows that the spectrum of this radiation consists of a series of closely-spaced discrete lines, the frequencies of which ω_n are multiples of the basic frequency of revolution of the electrons ω in the orbit of the accelerator, i.e., $\omega_n = n\omega$, where n is the harmonic number, and $\omega = c/R$ (R is the radius of the electron orbit and c is its velocity). The quantity of energy which is radiated by the electron in unit time is proportional to the fourth power of the electron's energy; the frequency of the radiation peak is proportional to the third power of the energy. For high energies (beginning at 30-50 Mev) this frequency approaches the visible region of the spectrum, and the radiation can be observed directly by eye (hence the phenomenon is called the "luminous" electron effect). Furthermore, all of the radiation is concentrated essentially within a solid angle of the order of $\Delta\phi \cong mc^2/E$ (m is the mass of the electron, c is the speed of light, E is the energy of the electron), with its vertex at the position of the electron, and its axis directed along the instantaneous velocity of the electron. The radiation is polarized, i.e., there exist two directions of oscillation for the electric vector—parallel to the magnetic field, but perpendicular to the velocity (π-component) and perpendicular to both the magnetic field and the velocity (σ-component). Each of these components of polarization possesses a characteristic angular distribution of intensity. The total intensity of radiation is different in the two polarized components (the σ-component is more intense) and their intensity ratio changes as a function of the wavelength and energy of the electrons. The ratio of the total spectral intensities I_σ/I_π is equal to seven (see, for example, reference 16). These are the chief properties of the radiation.

Experimentally, the radiation was first indirectly observed by Blewett in 1946,[7] and thereafter directly by Suits[8] and by Haber.[9] The Pollock group noticed the first indications of the polarization of the radiation—they observed the σ-component which is the stronger of the two. In our work[11] we discovered the second polarized component of the radiation and studied in detail the angular distribution of intensity in both components. The first attempts to measure the intensity ratio of the polarized components for mono-energetic electrons were also undertaken at that time.[12]

In the present work, the intensity ratio of the polarized components of "luminous" electron radiation was measured as a function of the wavelength for different energies of particle acceleration. First of all, a calculation was made of the intensity ratio of the components for radiation summed over the entire time of electron acceleration, from the moment of injection to the attainment of a given maximum energy. Using expressions (36) and (37) from the paper of Sokolov and Ternov,[13] and assuming that the energy of the accelerated particles increases according to a sinusoidal law, we obtained formulas suitable for calculating the average power of the linearly polarized radiation of one electron over the entire spectrum.[14] The calculation carried out according to these formulas allowed the direct comparison of theory with experiment, and made it possible to do without any special contrivance for isolating mono-energetic radiation of the electrons, which substantially enhanced the optical speed of the apparatus and somewhat reduced the experimental errors. The work was carried out on the electron synchrotron of the Physical Institute of the Academy of Sciences of the USSR, with a maximum electron energy of 280 Mev.[15]

The radiation of the accelerated electrons was observed through a tube in the porcelain sector of the synchrotron chamber. The axis of the tube was directed tangentially to the equilibrium orbit of the electrons. The tube terminated in a transparent window for observing the radiation. The window was provided with a guard to protect it from the rapid contamination by diffusion pump oil, which would darken under the action of the short wavelength part of the electron radiation, and thus absorb part of the radiant energy.

The optical arrangement consisted of an ISP-22 quartz spectrograph with an auxiliary polarizing Wollas-

ton prism installed between the collimator and the dispersing prism of the spectrograph, plus a condensing system. The arrangement is shown schematically in Fig. 1.

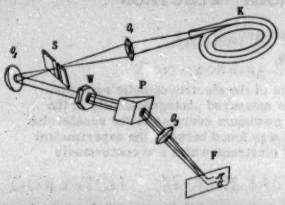

Fig. 1. Optical diagram of the apparatus. K, cynchrotron chamber; O_1, condensing system; S, spectrograph slit; O_2, collimating mirror of the spectrograph; W, Wollaston Prism; P, Cornu dispersing prism; O_3, objective of spectrograph; F, photographic plate.

Because of the presence in the system of a Wollaston prism, it was possible to photograph both polarized components simultaneously on one photographic plate. The condensing system projected all the radiation from a small section of the orbit onto the spectrograph slit; the image was 1-2 mm high. The condenser consisted of two fused quartz lenses which permitted the collection along the vertical of the entire cone of electron radiation. The width of the spectrograph slit was 0.015 mm. The spectrograph was situated in the same room as the synchrotron, so that the separation between the tube in the acceleration chamber and the spectrograph slit was about 2.5 meters. The alignment of the spectrograph with the source of radiation was conducted visually. With the aid of two mirrors and an OT-1 telescope, the image of the section of the orbit projected by the condensing system onto the spectrograph slit could be observed with the aid of two mirrors and an optical tube OT-1, from another location, safely shielded from γ-radiation.

As already noted above, the spectrum was recorded photographically. Besides the emission spectra of the polarized components of "luminous" electrons, two iron spectra were photographed along the edges of the plate for wavelength calibration, along with the spectrum of an incandescent lamp taken through a 9-step attenuator, for the conversion of optical density values into radiation intensities.

The typical appearance of a spectrogram is shown in Fig. 2. The spatial separation of the polarized components was incomplete for large images, and the polarized components in the spectrum of the incandescent lamp are therefore partially superimposed. As can be seen from the spectrogram presented, the radiation of "luminous" electrons has the form of a continuous spectrum, because with the given dispersion it is impossible to resolve the individual lines (harmonics of the basic frequency). The sharp variation in the intensity of the π- and σ-components with wavelength is due to the spectral sensitivity of the photographic plates used. The same effect is noted for the incandescent lamp. The spectra of the radiation broaden on the plate as the wavelength decreases because of defocusing, due to the fact that the condensing system consists of quartz lenses which are not corrected for chromatic aberration. The intensity dip in the middle of the π-component spectrum is explained by the specific angular distribution of intensity

Fig. 2. Spectrograms of "luminous" electron radiation. 1—iron spectra; 2—incandescent lamp spectra, taken through a step-filter with exposures of 15 and 1.5 min; 3—spectra of the π- and σ-components (electron energy 250 Mev, exposure 15 sec); 4—the same, with 18 sec exposure. Lines of the iron spectrum, with their wavelengths: 0.3—5927 A; 0.1—5005 A; 0—5005 A; 5—4528 A.

along the vertical, which is characteristic of this component (see reference 11). This distribution is observed for the given condensing system in the focal plane, which is very close to the image plane because of the long distance from the radiation source to the spectrograph. On defocusing the image, we still observe this distribution on the plate. It does not disappear with decreasing wavelength because of the strong increase in the linear dispersion of the spectrograph in this region of the spectrum (4000-2000 A).

The photographs obtained were processed by the method of photographic photometry with the aid of an MF-4 microphotometer. The step-filters were first calibrated for definite wavelengths by the use of fairly narrow band-pass interference filters (half-width of order 50 A). Emulsion calibration curves were constructed for selected wavelengths for each plate from the photometric data obtained with the step-filter. Thereafter, the distribution of density across the spectrum of the polarized components was estimated for these same wavelengths. With the aid of the characteristic curves, the density values for the polarized components were converted to intensities. A typical example of such an intensity distribution curve is shown in Fig. 3. To decrease the errors in the photometry, the green background surface of the condensing slit of the microphotometer was silvered,

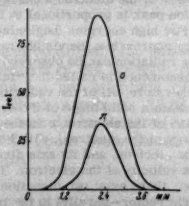

Fig. 3. Intensity distribution curves for the π- and σ-components of polarization of "luminous" electrons. λ6000 A; electron energy—250 Mev; exposure—17 sec.

and all measurements (calibration of the attenuator steps as well as measurement of the spectrograms) were performed with the same dimensions for the condensing and measuring slits of the microphotometer. The areas under the intensity curves were then measured with a planimeter for the π- and σ-components and the ratio I_σ/I_π determined. Using the data of the photometer measurements of the step-filter, the correction coefficient to the ratio I_σ/I_π for each of the wavelengths was found separately. The correction was required because the intensity ratio of the polarized beams obtained from the natural light source (incandescent lamp) by means of a Wollaston prism varied with wavelength in the present arrangement.

The ratio of the intensities of the components of polarization of the "luminous" electron were studied for three values of the maximum energy of accelerated electrons—150, 200, and 250 Mev. The results of the experiment are presented in Figs. 4 and 5. Although the experimental error is fairly large (about 16%) there is an obvious difference in the intensity ratios of the polarized components for different maximum acceleration energies of the electrons, and a general tendency towards an increase in the ratio with decreasing wavelength of radiation. The results obtained, as can be seen from the graphs, are found to be in satisfactory agreement with theory.[13, 14]

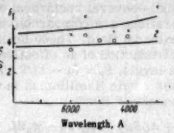

Fig. 4

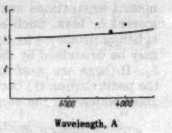

Fig. 5

Fig. 4. Comparison of experimental (points) and theoretical (lines) values of the ratio I_σ/I_π for electrons of different energies. Curve 1—150 Mev; curve 2—250 Mev.

Fig. 5. Comparison of the experimental (points) and theoretical (lines) values of the ratio I_σ/I_π for electrons accelerated to an energy of 200 Mev.

The comparatively large experimental error is a result of the following: In the construction of the characteristic curves of photographic plates, the greatest inaccuracy is encountered in the regions of under- and overexposure. In photographing spectra of "luminous" electrons, it is impossible to obtain photographs in which the entire density distribution curve for both polarized components lies within the linear portion of the calibration curve, owing to the fact that parts of these curves are in the region of underexposure. For the less intense π-component, a large part of the contour is in the underexposed region, since in photographing we usually tried to get the maximum densities for both components to fall on the linear portion of the calibration curve. This was the basic source of error. Furthermore, in operating the spectrograph near the synchrotron, it turned out that the prisms and optics of the spectrograph blackened noticeable under the influence of the synchrotron radiation. This was an additional source of error, although it was taken into account to some degree by the above mentioned correction factor applied to the ratio I_σ/I_π. Besides this, the diffusion pump oil which covered the optical window of the synchrotron, blackening under the action of the synchrotron radiation, turned out to have a depolarizing effect (although to a lesser degree) on the "luminous" electron radiation. However, it was impossible to correct for this factor because the clouding over of the window continuously increased during the operation of the synchrotron. In view of these errors, the agreement of experiment with theory should be considered satisfactory.

The authors express their sincere thanks to M. S. Rabinovich and A. Ya. Belyak for every kind of assistance in carrying out the experiment.

REFERENCES

1. D. D. Ivanenko and I. Ya. Pomeranchuk. Doklady Akad. Nauk SSSR **44**, 343 (1944).
2. D. D. Ivanenko and A. A. Sokolov. Doklady Akad. Nauk SSSR **59**, 1551 (1948).
3. D. D. Ivanenko and A. A. Sokolov. Vestnik Moscok. Gosudarst. Univ. No. 11, 95 (1948).
4. I. Schwinger. Phys. Rev. **75**, 1912 (1949).
5. D. D. Ivanenko and A. A. Sokolov. "Klassicheskaya teoriya polya." (Classical Field Theory), Moscow, 1951.
6. L. A. Artsimovich and I. Ya. Pomeranchuk. Zhur. Eksptl. i Teoret. Fiz. **16**, 379 (1946).
7. I. Blewett. Phys. Rev. **69**, 87 (1946).
8. Sci. News Letter **51**, 339 (1947).
9. H. Haber. Electronics **20**, 136 (1947).
10. F. R. Elder, A. M. Gurewitsch, R. V. Lengmuir, and H. C. Pollock. Phys. Rev. **71**, 829 (1947).
11. F. A. Korolev, V. S. Markov, E. M. Akimov, and O. F. Kulikov. Doklady Akad. Nauk SSSR **110**, 542 (1956).
12. F. A. Korolev, E. M. Akimov, V. S. Markov, and O. F. Kulikov. Trudy X Vsesoyuz. Soveshchaniya Spektr., **2**, L'vov, 1958. (Proceedings of the Tenth All-Union Conference on Spectroscopy).
13. A. A. Sokolov and I. M. Ternov. Zhur. Eksptl. i Teoret. Fiz. **31**, 473 (1956).
14. O. F. Kulikov. Izvest. Vysshikh Ucheb. Zavedenii **3**, 95 (1959).
15. A. Ya. Belyak, V. I. Veksler, V. N. Kanunnikov, P. A. Cherenkov, and B. N. Yablokov. "Uskoriteli elementarnykh chastits." (Elementary Particle Accelerators), Moscow, 1957.
16. A. A. Sokolov. "Vvedenie v kvantovuiu elektrodinamiku." (Introduction to Quantum Electrodynamics), Moscow, 1958.

GROUND STATES OF BOUND PARAMAGNETIC RARE EARTH IONS IN AN EXTERNAL MAGNETIC FIELD

N. V. Afanas'eva

Received 3 February 1959

The case of a crystalline field of tetragonal symmetry is examined. Matrix elements of the crystalline potential are calculated, taking account of the interaction of levels in the presence of an external magnetic field, and the coefficients of the spin Hamiltonian are determined for all the rare earth ions. It is determined which energy levels are capable of paramagnetic resonance absorbtion.

INTRODUCTION

In studying the magnetic properties of rare earth ions in crystals, one considers first of all the interaction of these ions with the crystal lattice. For the trivalent rare earth ions, which have well-shielded f shells, the interaction of the ion with the crystalline lattice is comparatively weak, leading to splitting of the energy levels which is small by comparison with the multiplet splitting. Calculations show that the splitting of the levels for a given value of the quantum number J under the influence of a crystal field amounts to roughly 100 cm^{-1}.[1]

However, the strength of this interaction is different for different ions: the interaction is weaker the higher the multiplicity of the electronic state of the ion, and decreases with increasing atomic number by virtue of the increase in effective nuclear charge.

When an ion having total angular momentum $\mathbf{J} = \mathbf{L} + \mathbf{S}$ is put into an external magnetic field H, the vector J precesses about the field direction at a definite rate. Level E_J, with a certain value of J, splits into 2J + 1 equally spaced components. These levels, which correspond to different orientations of J, have additional energies $E_M = Mg\beta H$, where M is the magnetic quantum number, β is the Bohr magneton, and g is a numerical factor of the order of unity. (g = 1 when there is only orbital angular momentum and g = 2 for pure spin angular momentum.)

Transitions may occur between the levels thus obtained, subject to the selection rule $\Delta M = \pm 1$ and $h\nu = g\beta H$.[2] The quantum number M completely characterizes the sublevels in a magnetic field. In the strongest magnetic fields obtainable externally, βH amounts to perhaps 5 cm^{-1}, which is very small by comparison with the multiplet splittings in rare earth atoms. However, in the fields existing in crystalline lattices states of different M are mixed, and it becomes necessary to consider the influence of the field on the magnetic properties of the ions.

Comparing theory with experimental results obtained in paramagnetic resonance experiments, it is possible to give a satisfactory qualitative and quantitative description of the interaction of paramagnetic ions of the rare earths with the ions, atoms, and molecules surrounding them in the crystalline lattice, and to find out which levels are capable of leading to paramagnetic resonance absorption.

CALCULATION: METHODS AND RESULTS

For bound rare-earth ions, we will choose the perturbation operator for the ground states (taking account of the action of external magnetic fields) in the form

$$\hat{H} = \beta g \mathbf{J}\mathbf{H} + pN\mathbf{J}\mathbf{H} + Q\frac{1}{2}(J_x J_z + J_z J_x)IJ_z - \gamma\beta_N \mathbf{H}\mathbf{I}, \qquad (1)$$

where g is the Landé factor for the free ion, N is a numerical factor, β and β_N are the Bohr and nuclear magnetons, and γ is the gyromagnetic ratio of the nucleus.

$$P = \frac{2\gamma^2\beta^2_N}{r^3},$$

where I is the nuclear spin, Q is a constant describing the nuclear quadrupole moment, and H is the magnitude of the external magnetic field.

We will select a group of low-lying levels whose mutual separations are small—several reciprocal centimeters or less. Such separations are comparable to the splitting produced by the external field. These levels may be described by the introduction of an effective spin S_Γ. If there are n of these levels, $S_\Gamma = (n - 1)/2$. Thus the perturbation (1) becomes a spin Hamiltonian in variables which are the components of S_Γ.

$$\hat{H} = D_{ij}S_iS_j + \beta g_{ij}H_iS_j + A_{ij}S_iI_j + Q_{ij}I_iI_j - \gamma\beta_N \mathbf{H}\mathbf{I}, \qquad (2)$$

where D is the fine structure constant and A is the hfs constant.

We will examine the ground states of the ions with the goal of finding the quantum number J in a tetragonal field with predominantly cubic components. The potential in the tetragonal system takes the form

$$V = B_{20}\sum_k (3z_k^2 - r_k^2) + B_{40}\sum_k (35z_k^4 - 30r_k^2z_k^2 + 3r_k^4) + 2B_{44}\sum_k (x_k^4 - 6x_k^2y_k^2 + y_k^4) \qquad (3)$$

$$+ B_{60}\sum_k (231r_k^6 - 315r_k^4z_k^2 + 105r_k^2z_k^4 - 5z_k^6) + \ldots,$$

where B_{20}, B_{40}, ... are parameters of the crystal lattice, x_k, y_k and z_k are the coordinates of the k'th electron, and r_k is its distance from the nucleus of the ion. To find the matrix elements of the potential we will use the "equivalent operator" method.[1]

In the presence of an external magnetic field it is important to consider matrix elements corresponding to states with quantum numbers J and J + 1; that is, we must consider the interaction of these states. This necessity springs from the fact that the separations of the low-lying levels of europium and samarium, for example, are comparable to the energy of thermal motion.

In second-order perturbation theory we find matrix elements for the potential of a crystalline field between levels of different J.

$$\left\langle J+1,\ J_z \middle| \sum_k 3z_k^2 - r_k^2 \middle| J,\ J_z \right\rangle = F^2\alpha_1 J_z\sqrt{(J+1)^2 - J_z^2},$$

$$\left\langle J+1,\ J_z \middle| \sum_k 35z_k^4 - 30r_k^2z_k^2 + 3r_k^4 \middle| J,\ J_z \right\rangle =$$

$$= F^4\beta_1 J_z\left[7\left(J_z^2 - 3/^2 - 6J + 2\right)\sqrt{(J+1)^2 - J_z^2}\right.$$

etc. There are well-defined relations between the coefficients α_l, β_l, ... and the coefficients α, β, ... of the equivalent operators, which we used previously.[1] It should be pointed out that these results are correct for both normal and inverted terms.

For ions with fewer than 7 electrons, J refers to the ground state and is equal to L − S, whereas when there are more than 7 electrons the ground state goes with J + 1, which is equal to L + S.

In solving the problem we shall use the eigenfunctions we found by perturbation theory (Table 1) as a basis for describing the total angular momentum.

Table 1

Ion	Term and ground state	Wave function
Ce^{+++}	$^2F_{5/2}$, doublet	$\psi_{\pm a} = \sqrt{\frac{1}{6}}\psi_{\pm 3/2} - \sqrt{\frac{5}{6}}\psi_{\mp 5/2}$
Yb^{+++}	$^2F_{7/2}$, doublet	$\psi_{\pm a} = \sqrt{\frac{3}{4}}\psi_{\pm 7/2} - \sqrt{\frac{1}{4}}\psi_{\mp 5/2}$
Pr^{+++}	$^3H_4$, singlet	$\sqrt{\frac{5}{24}}\psi_4 + \sqrt{\frac{7}{12}}\psi_0 + \sqrt{\frac{5}{24}}\psi_{-4}$
Tm^{+++}	$^3H_6$, singlet	$\sqrt{\frac{7}{16}}\psi_6 + \sqrt{\frac{1}{8}}\psi_0 + \sqrt{\frac{7}{16}}\psi_{-6}$
Nd^{+++}	$^4J_{9/2}$, doublet	$\sqrt{\frac{9}{24}}\psi_{\pm 9/2} + \sqrt{\frac{7}{12}}\psi_{\pm 1/2} + \sqrt{\frac{1}{24}}\psi_{\mp 7/2}$
Er^{+++}	$^4J_{15/2}$, quadruplet	$N\left(\psi_{\pm 15/2} - \frac{a_1 - E_1}{a}\psi_{\pm 11/2} + \frac{a_1 - E_2 - a^2}{a}\psi_{\mp 7/2} + \frac{a^2 d - (a - E_3)}{a\,(a_1 - E_3)}\psi_{\mp 11/2}\right)$ $N\left(\psi_{\pm 13/2} - \frac{a_2 - E_2}{b}\psi_{\pm 9/2} + \frac{(a_2 - E_2)(a_2 - E_3 - b^2)}{bf}\right.$ $\left. \times\psi_{\mp 5/2} - \frac{[(a_2 - E_2)(a_2 - E_3) - b^2]\,e}{a_2 - E_3\,bf}\psi_{\mp 11/2}\right)$
Pm^{+++}	$^5I_4$, triplet	$\frac{1}{\sqrt{2}}(\psi_2 - \psi_{-2})$; $\sqrt{\frac{7}{8}}\psi_{\pm 3} - \sqrt{\frac{1}{8}}\psi_{\mp 1}$ $N\left(\psi_0 - \frac{a_1 - E_1}{a}\psi_1 + \frac{2e\,(a_1 - E_1)}{a\,(a_2 - E_1)}\psi_0 - \frac{a_1 - E_1}{a}\psi_{-1} + \psi_0\right)$ $N\left(\psi_{\pm 2} - \frac{a_2 - E_1}{b}\psi_{\pm 3} + \frac{(a_2 - E_1)(a_2 - E_2) - b^2}{bf}\psi_{\mp 1} - \frac{d\,[(a_2 - E_1)(a_2 - E_2) - b^2]}{bf\,(a_2 - E_1)}\psi_{\mp 3}\right)$
Sm^{+++}	$^6H_{5/2}$, doublet	$\sqrt{\frac{1}{6}}\psi_{\pm 5/2} - \sqrt{\frac{5}{6}}\psi_{\mp 3/2}$
Dy^{+++}	$^6H_{15/2}$, doublet	$N\left[\psi_{\pm 15/2} - \frac{a_1 - E_1}{a}\psi_{\pm 11/2} + \frac{(a_1 - E_1) - a^2}{a}\psi_{\mp 7/2} + \frac{a^2 d - (a_1 - E_1)}{a\,(a_1 - E_1)}\psi_{\mp 11/2}\right]$
Tb^{+++}	$^7F_6$, singlet	$\sqrt{\frac{7}{16}}\psi_6 + \sqrt{\frac{1}{8}}\psi_0 - \sqrt{\frac{7}{16}}\psi_{-6}$

Table 1 shows how states with different magnetic quantum numbers M are mixed by the crystal field of the symmetry chosen. N is a normalizing factor, so chosen that the squared coefficients of the component functions add to unity.; α_1 are the diagonal matrix elements of the potential, and a, b, c, etc., are the off-diagonal elements. E_1 are the energy levels.

As has been shown previously,[4] holmium and promethium ions have triplet ground states in a cubic field. For them the perturbation (1) may be written by means of the spin Hamiltonian (2) with an effective spin of 1 and tetragonal symmetry:

$$\hat{H} = DS_z^2 + \beta g_i S_i H_i + A_i S_i I_i - \gamma_i \beta_n H_i I_i + Q_i I_i^2 ,$$

where i = x, y, z; the expression is summed over identical indices.

$$g_x = g_y = g_\perp,\ g_z = g_\parallel,\ A_x = A_y = B,\ A_z = A,\ A \neq B,\ g_\parallel \neq g_\perp .$$

For γ_i the difference is unimportant and can be ignored. The fine structure coefficient D is determined from the splitting of this triplet into a singlet and a doublet in a tetragonal field. For praseodymium, terbium, and thulium the ground states are singlets; they are not split in the magnetic field, and therefore we shall examine higher levels which are triplets. (See reference 1) These are capable of giving paramagnetic resonance absorption. The wave functions belonging to these levels are given in Table 2.

Calculations show that in a purely cubic field, the symmetry of the spin Hamiltonian is cubic; that is, D = 0, $g_\parallel = g_\perp$, A = B.

The presence of a moderate tetragonal component of the crystal field in this case gives a significant splitting of the neighboring triply degenerate level into a singlet and a doublet. Hence only weak magnetic transitions can be observed between the components of the doublet. Such transitions are forbidden by the selection rules.

The ions of cerium, neodymium, samarium, dysprosium, and ytterbium have doubly degenerate ground states in the limit, as tetragonal symmetry goes over to cubic. These are ions with half-integral J. Their perturbation may be described by a spin Hamiltonian with effective spin $\frac{1}{2}$, with tetragonal symmetry and D = 0.

In the limit, as tetragonal symmetry goes over to cubic, $g_\parallel = g_\perp$ and A = B. For the erbium ion, which has a quadruplet ground state in a cubic field, it is reasonable to propose a large tetragonal crystal field component and consider that the splitting which it produces is significantly larger than that produced by the external magnetic field. The quadruplet is split into two doublets, and if there is a significant separation between them, no paramagnetic resonance occurs, corresponding to transitions between members of different doublets. Each doublet is to be considered separately.

It should be pointed out that calculations for the erbium ion give a significant anisotropy of g_i and A_{ii}, but the g_i are related to one another in the same way as the hyperfine splitting constants.

The results of the calculations agree rather well for erbium with the conclusions of Judd and Wong on the rare earth double nitrates (C_{3v} symmetry). They assume that the symmetry of $Er_2Mg_3(NO_3)_{12} \cdot 24H_2O$ is nearly icosahedral.

It should be mentioned that no paramagnetic resonance was found in $Ho_2Mg_3(NO_3)_{12} \cdot 24H_2O$ at 4.2°K and a frequency of 9.23 kMc up to 14,000 gauss field strength.

Paramagnetic resonance studies in the frequency range from 0.32 to 1.18 cm^{-1} and at temperatures from 13 to 20°K have been carried out up to 13,000 gauss on the ethylsulfates of the rare earths with an even number of 4f electrons (Pr^{+3}, Pm^{+3}, Tb^{+3}, Ho^{+3}, Tu^{+3}). Considering the non-Kramers degeneracy under suitable crystal field symmetry, remarkable agreement is obtained with theoretical calculations, inasmuch as with Pm^{+3} and Tm^{+3} resonance was not observed. These experimental data support the correctness of our results for the praseodymium, terbium, and thulium ions in the presence of a small tetragonal contribution to the cubic crystal field.

The general results of these calculations agree fairly well with existing experimental data.[7-10] Table 3 gives the g-values obtained for the limit of a cubic field. For the Gd^{+++} ion ($^8S_{7/2}$) the ground state can be described with a spin Hamiltonian in which the only variables are the components of the total ionic spin. The limiting case of transition to a cubic field is in good agreement with experimental findings.[9, 11]

In conclusion, I consider it my pleasant duty to thank M. V. Vol'kenshtein for his counsel on questions touched upon in this work.

Table 2

Ion	Wave function
Tb^{+++}	$\sqrt{\frac{1}{2}}(\psi_3-\psi_{-3})$
	$\sqrt{\frac{11}{32}}\psi_{\pm2}-\sqrt{\frac{3}{16}}\psi_{\pm1}+$
	$+\sqrt{\frac{15}{32}}\psi_{\pm3}$
Pr^{+++}	$\sqrt{\frac{1}{2}}(\psi_3-\psi_{-3})$
	$\sqrt{\frac{3}{8}}\psi_{\pm3}-\sqrt{\frac{1}{8}}\psi_{\pm1}$
Tm^{+++}	$\sqrt{\frac{1}{2}}(\psi_1-\psi_{-1})$
	$\sqrt{\frac{11}{32}}\psi_{\pm2}-\sqrt{\frac{3}{16}}\psi_{\pm1}+$
	$+\sqrt{\frac{15}{32}}\psi_{\pm3}$

Table 3

Ion	$g_\parallel = g_\perp$
Ce^{+++}	0.855
Yb^{+++}	1.144
Pr^{+++}	0.799
Tm^{+++}	1.165
Nd^{+++}	0.739
Pm^{+++}	0.599
Ho^{+++}	1.253
Sm^{+++}	0.287
Dy^{+++}	1.334
Tb^{+++}	1.501
Gd^{+++}	1.994
Er^{+++}	$g_\parallel = 1.199$, $g_\perp = 2.743$
	$g_\parallel = 1.182$, $g_\perp = 3.113$

REFERENCES

1. N. V. Afanas'eva. Opt. i Spektr. **5**, 629 (1958).
2. B. Bleaney and K. Stevens. Rep. Progr. Phys. **16**, 108 (1953).
3. G. Harrison and F. Bitter. Phys. Rev. **57**, 15 (1940).
4. N. V. Afanas'eva. Opt. i Spektr. **5**, 110 (1958).
5. B. R. Judd and E. Wong. J. Chem. Phys. **28**, 1097 (1958).
6. I. M. Baker and B. Bleaney. Proc. Roy. Soc. **A245**, 156 (1958).
7. B. Bleaney, H. Scovil, and R. S. Trenam. Proc. Roy. Soc. **223**, 15 (1954).
8. B. R. Judd. Proc. Roy. Soc. **A232**, 458 (1955).
9. Ch. Ryter. Helv. Phys. Acta **30**, 353 (1957).
10. R. Lacroix and Ch. Ryter. Arch. Sci. **9**, 96 (1956).
11. R. Lacroix and Ch. Ryter. Compt. rend. **24**, 2812 (1956).

SPECTROSCOPIC DETERMINATION OF THE NUCLEAR MOMENTS OF THE ODD ISOTOPES OF GADOLINIUM

N. I. Kaliteevskii, M. P. Chaika, I. Kh. Pacheva, and E. E. Fradkin

Received 19 June 1959

The hfs splitting of the 5015 A, 5103 A, and 5251 A lines of Gd^{157} and Gd^{155} were obtained by the photoelectric method. The ratios $Q_{155}/Q_{157} = 0.8$ and $\mu_{155}/\mu_{157} = 0.79$ were determined. The deformation parameters and gyromagnetic ratios g_k and g_R were calculated for both isotopes.

In the last few years a considerable number of studies have been published concerning the hyperfine structure of spectral lines of gadolinium. Speck[1] and Kopfermann et al.[2] investigated in detail the isotopic shift in the spectrum of gadolinium. Separated isotopes were used in these studies and a significant violation of equidistance was observed in the case of the lighter isotopes, which show a considerably different degree of nuclear deformation than the lighter ones. It was shown that

$$\frac{\Delta\nu(152-154)}{\Delta\nu(158-160)} \simeq 3$$

Therefore, substantial corrections were applied to data obtained in earlier investigations[3,4] of natural mixtures of gadolinium isotopes, in which Gd^{152} and Gd^{154} are present in low concentrations.

A number of investigations have been dedicated to the determination of the nuclear moments of Gd^{155} and Gd^{157}. Murakava,[5] studying the hfs of some lines of a gadolinium sample of natural isotopic composition, arrived at the conclusion that $I \geq 5/2$ for both odd isotopes. Speck,[1] using separated isotopes of gadolinium, determined that the best analysis of composite curves can be made by assuming that $I = 3/2$. From this spin value for Gd^{155} and Gd^{157} he determined the magnetic and quadrupole moments of odd isotopes of gadolinium. This study used the photographic method of registering hfs. Because of the use of this method and of the low abundance of the isotopes of interest, some uncertainty arose in the processing of the experimental data. The data of this study will be discussed in detail along with the discussion of the results of our investigation.

The most reliable values of the spin ($I = 3/2$) and magnetic moments of the nuclei of Gd^{155} and Gd^{157} were obtained by Low[6] and also by Prokhorov and Manenkov,[8] who studied the spectrum of the gadolinium ion, using paramagnetic resonance. The absolute values of the magnetic moments and their ratio $\mu_{155}/\mu_{157} = 0.75$, as derived in these independent investigations, were in good agreement.

We undertook a photoelectric investigation of the hfs of spectra of separated isotopes of Gd in order to determine the quadrupole moments of Gd^{155} and Gd^{157}, and also to confirm the spin values of these nuclei by optical methods. The earlier values of quadrupole moments could have been distorted by systematic and accidental experimental errors.

I. DESCRIPTION OF THE EXPERIMENT

The hyperfine structure of the atomic lines of gadolinium, 5015.04 A ($z'^9G_3 - a'^7F_3^o$), 5103.45 ($z'^9G_4 - a'^7F_4^o$), and 5251.18 ($z'^9G_3 - a'^7F_3^o$) was investigated. A photoelectric spectrometer with a Fabry-Perot interferometer was used. This instrument has been described in detail in references 7 and 8. Since these lines are in the green region of the spectrum, the FEU-17 photomultiplier having the best available signal/noise ratio for small photo currents was selected. In order to decrease the fluctuation of the photo current the recording was made with the aid of an amplifier having a large time constant, $\tau = RC = 25$ sec.

The spectrum of gadolinium was produced by a hollow cathode tube. About 2 mg of Gd_2O_3 were mixed with

an equal volume of graphite powder and placed in the hollow cathode. Spectroscopically pure argon was used as the carrier gas. After a short breaking-in period, the tube gave a stable emission of gadolinium lines for many hours. When the brightness of the lamp decreased, a new portion of gadolinium oxide mixed with graphite powder was introduced.

Since the hfs. components of gadolinium lines are very close, the resolving power of the spectrograph is very important in determining the position of the components. At the present time, there is no accepted criterion for the resolution of photoelectric recordings, but the conditions set by different authors are very close to each other. For an evaluation of the actual resolving power, we accepted two lines as resolved if the dip between them was significantly above the noise leve.[9] The actual resolving power at the exit of the spectrometer is determined by the instrumental width of the line, the real width of the line, and the fluctuation of the recordings.

The instrumental width of the line is defined by the Airy function (for a given coefficient of reflection of the mirrors), by the defects of the surface of the mirrors, and by the transmission function of the exit diaphragm. We used Fabry etalons 30 and 40 mm thick. The free spectral ranges were 166 and 125×10^{-3} cm^{-1} respectively.* The coefficient of reflectivity of the dielectric mirrors of our etalon was around 92%. The surfaces of the etalon had a deviation from the parallelism of the order of several hundredths of a band. In order to decrease the broadening caused by surface defects, the interferometer was diaphramed down to a diameter of 3 cm. Under these conditions, the resolving power of the interferometer was ≈1,000,000. The spectral width of the exit diaphragm was 7 mK and contributed only a small amount of broadening.

*In later discussion we will use the notation 1×10^{-3} cm^{-1} = 1 mK (milliKayser), which is widely used in the foreign literature.

Doppler broadening was the main factor in determining the width of a component at the exit of the spectrometer. To decrease the broadening, the cathode of the discharge tube was cooled by liquid air and the discharge current was lowered to 30 ma. The inside diameter of the cathode was 8 mm and its length ~30 mm. The current density was therefore around 4 ma/cm², if we assume that it was constant over the entire inside surface of the cathode. Under these conditions, the width of the line (after taking account of instrumental width) corresponded to a gas temperature of about 250°K. Figure 1 shows line width at the exit slit of the spectrometer as a function of discharge tube current. The noncoincidence of the curves for different isotopes of Gd can apparently be explained by the fact that one of the isotopes was excited in a pure aluminum tube and the other in a duralumin tube. These materials have different thermal conductivities; therefore, the temperatures of the gases inside the tubes are not equal.

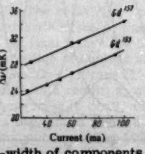

Fig. 1. Line-width of components as a function of discharge current.

The real resolving power at the exit slit of the spectrometer can be expressed as the smallest distance between distinctly resolved components. Components separated by ~25 mK were distinctly resolved. The resolving power of the equipment was therefore,

$$R = \frac{\nu}{\delta\nu} > \frac{20.000}{25 \cdot 10^{-3}} = 0.8 \cdot 10^{6}.$$

II. PROCESSING OF THE EXPERIMENTAL DATA

The isotopic compositions of the samples of gadolinium used in this investigation are given in the Table 1.

Table 1. Isotopic Composition (in %)

No.	Sample	152	154	155	156	157	158	160
1	Gd^{155}	< 0.1	0.5	97.3	1.7	0.5	< 0.1	< 0.1
2	Gd^{157}	—	—	0.6	1.7	91.4	5.2	1.1
3	$Gd_{nat.}$	0.2	2.86	15.61	20.59	16.42	23.45	20.87

The table shows that the samples were highly enriched in one isotope. In spite of this, the presence of other isotopes had to be taken into account in determining the distances between the hyperfine structure components of the isotope under investigation. The hfs components of gadolinium lines are located very close to each other. In order to resolve them, the light source had to be operated under special conditions which minimized the line-width. Despite this, it was impossible to resolve all the components. The distance between the last weak components of the line Gd[155] 5103 is ~13mK. In order to separate these lines even with an interferometer of infinite resolving power, the temperature of the source would have to be below 160°K.

A study of all the recordings of the structure of gadolinium lines shows that these curves can be analyzed only by assuming that four components of Gd^{157} and Gd^{155} are present. This leads to the spin-value I = 3/2 for both odd isotopes. To determine the location of the indicated components accurately, it was necessary to take account of all superposed components of other isotopes, even when they were very weak. The intensity of the superposed components could be easily determined from the known isotopic composition of a sample. In order to determine their location, the following two methods, based on the isotopic shift of the line under investigation, were used.

1. Several orders of interference of one isotope were recorded. This discharge tube was then replaced by another containing natural gadolinium. Several orders of interference of the same line of natural gadolinium were recorded on the same chart paper, without interrupting the scanning (see Fig. 2). Thus, the positions of the components of Gd^{156}, Gd^{158}, and Gd^{160} with respect to the structure of Gd^{157} or Gd^{155} were found by direct extrapolation.

2. After recording several orders of interference of the sample under investigation, the jaws of the slit were moved so that a neighboring line of argon passed through the exit slit of the monochromator, and several orders of the argon line were recorded. The same procedure was adopted for the recordings of natural gadolinium. The argon line was simultaneously recorded on the chart paper along with each of the two line structure tracings, thus making it possible to measure the relative positions of the components of different isotopes.

The analysis of the line structure into its components was performed as follows: The tracing was corrected for the change in intensity, and the mean curve for several

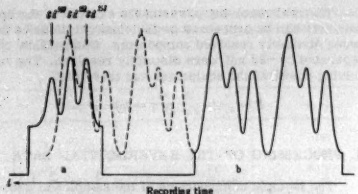

Fig. 2. Relative positions of the hfs components of Gd^{157} and of even isotopes of the line 5015 A. The solid lines are photoelectric recordings of the spectrum of Gd of natural isotopic composition (a) and of Gd^{157} (b); dashed curve is a transposed (from b) recording of Gd^{157}.

orders of interference was found. The relative intensities of the components were calculated assuming the spin of nucleus to be $^3/_2$. Then the most intense component was constructed with its maximum little below the corresponding point on the tracing. At first, the contributions of other components were only roughly estimated. All of the remaining components had the same form as the first one. The distances between them were chosen such that the composite curve (taking account of the components of other isotopes) would best coincide with the tracings. Examples of such analyses for the lines 5015 and 5103 A are given in Fig. 3.

III. CALCULATION OF NUCLEAR CONSTANTS FROM THE EXPERIMENTAL DATA

The spectral lines of gadolinium investigated originate from transitions between the terms $a''F_J$ and $z''G_J$ (see Fig. 4). Each term is split into four hyperfine sublevels ($I = ^9/_2$). In this experiment, only the most intense diagonal transitions were observed, the consequently the method of processing was designed especially for this case. We measured the intervals between the hfs components of the line under investigation, which depend on the hfs splitting of the upper and the lower terms. The distance between two hfs components can be described by the following expression:

$$\sigma(i-e)=\frac{1}{2}A(C_i-C_e)-\frac{1}{2}A'(C'_i-C'_e)$$
$$+B[C_i(C_i+1)-C_e(C_e+1)]$$
$$-B'[C'_i(C'_i+1)-C'_e(C'_e+1)],$$

where C_i is a combination of quantum numbers

$$C_i=F_i(F_i+1)-J(J+1)-I(I+1),$$

A and B are the interval factors for the lower term (unprimed), and A′ and B′ for the upper term (primed). For the line 5103 ($z''G_8 - a''F_7$) we thus obtained

$$\sigma(1-2)=\left\{\frac{17}{2}A(a^7F_7)+442B(a^7F_7)\right\}$$
$$-\left\{\frac{19}{2}A(z^9G_8)+570B(z^9G_8)\right\}, \quad (1)$$

The values of $\sigma(1-3)$ and $\sigma(1-4)$ were obtained similarly.

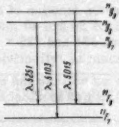

Fig. 4. Transition diagram for the gadolinium lines investigated.

In making further calculations to obtain the magnetic (μ) and quadrupole (Q) moments of Gd^{157} and Gd^{155}, we started out with the following assumptions:

1. It was assumed that the levels $a''G_J$ and $z''G_J$ were formed by LS coupling. The validity of this supposition and the errors in the determination of μ and Q connected with departure from LS coupling will be discussed later in detail.

2. The interval factors A for terms $a''F_J$ and $z''G_J$ are expressed by the one-electron hfs constants of valence electrons a_s, a_p, and a_d. The contribution of the constant a_d for lines 5015 and 5103 is small. Therefore, at the available accuracy of measurement, the separation can be calculated using only a_s and a_p.

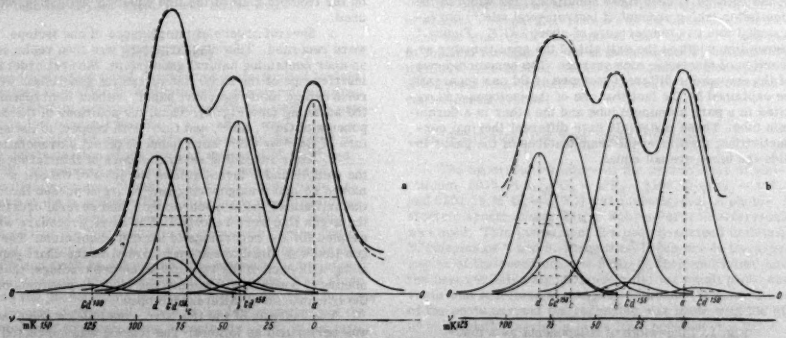

Fig. 3. Analysis of the structure of Gd^{157} lines 5015 A (a) and 5103 A (b) into components. The upper solid line is an average of the recordings. The dashed curve is the sum of the components obtained from the analysis.

Table 2. Values of σ(mK), Q,* and Linear Combinations of a_s, a_d, and a_p

	λ 5015 A						λ 5103 A						λ 5251 A
	Gd^{157}				Mean values		Gd^{155}		Mean values	Gd^{157}	Gd^{155}	Mean values	Gd^{157}
σ(1–2)	−44.8	−47.4	−47.0	−44.7	−45.0	—	−35.9	−36.0	—	−38.6	−30.8	−29.9	—	−36.1
σ(1–3)	−74.2	−77.5	−77.6	−73.7	−74.3	—	−59.2	−59.3	—	−64.8	−51.5	−50.2	—	−65.5
σ(1–4)	−87.5	−92.0	−94.5	−89.8	−91.2	—	−72.3	−72.3	—	−81.7	−64.4	−62.6	—	−88.0
$a_s - 1.70a_p + 0.07a_d$	−56.5	−59.2	−60.5	−57.6	−58.3	−58.4	−46.3	−46.3	−46.3	—	—	—	—	—
$a_d - 2.06a_p + 0.30a_s$	—	—	—	—	—	—	—	—	—	−55.5	−43.0	−42.7	−43.3	—
$a_p - 1.94a_p + 0.61a_d$	—	—	—	—	—	—	—	—	—	—	—	—	—	−55.7
$Q \cdot 10^{24}$ cm² { a	1.6	1.7	1.6	1.5	1.4	1.6	1.2	1.2	1.2	1.5	1.3	1.2	1.2	1.5
b	2.1	2.3	2.1	1.9	1.9	2.1	1.8	1.8	1.8	2.0	1.8	1.8	1.8	2.3

*For Gd 5251, only one measurement was available. The nuclear constants were calculated by averaging the data lines 5015 and 5103.

3. The quadrupole moment is calculated from the interval factor B by the well-known formula

$$B = -\frac{3}{8}\left(\frac{a}{2\pi}\right)\frac{Q}{IJ(2I-1)(2J-1)}\left\langle\frac{3\cos^2\theta - 1}{r^3}\right\rangle_{JJ}.$$

Then, from three equations of type (1), the values of linear combination of a_s and a_p, and also the value of Q can be calculated for each line investigated. The magnitude of the quadrupole moment depends essentially on the value of $(\overline{1/r^3})$. At the same time, a_s and a_p, and also their linear combinations which are used for the calculation of magnetic moments of isotopes, depend very little on $(\overline{1/r^3})$. Table 2 presents the experimental values of σ which were obtained by analyzing the hfs curves for lines 5015, 5103, and 5251; the linear combinations of a_s and a_p, and the values of Q calculated for two values of $(\overline{1/r^3})$. In the row denoted by $Q \times 10^{24}$ cm² the upper line corresponds to the values of the quadrupole moment taken from reference 1, and the lower line was obtained by the evaluation of $(\overline{1/r^3})$, which will be discussed later. Each column in the Table 2 corresponds to a separate experiment. The mean values are derived from several orders of interference.

The ratio of magnetic and quadrupole moments, which depends very little on $(\overline{1/r^3})$, can be determined from the data in Table 2. From the mean values of the measurements for lines λ5015 and 5103, the following was obtained:

$$\frac{Q_{155}}{Q_{157}} = 0.8 \pm 0.1, \quad \frac{\mu_{155}}{\mu_{157}} = 0.79 \pm 0.02.$$

It appeared that the quadrupole moment, Q_{157}, is greater than Q_{155}. A similar situation exists for the magnetic moments of these nuclei.

The absolute values of the magnetic moments of odd gadolinium isotopes can be derived from hfs constants by using the Fermi-Segrè-Goudsmit formula:

$$a_s = \frac{8}{3}\frac{R\pi^2 Z Z_a^2 \cdot F_s(Js)}{1836 n_a^3}\frac{dn_a}{dn}(1-\delta)(1-\varepsilon)\frac{\mu_I}{I}.$$

Brix[11] evaluated the expression

$$\frac{Z_a^2}{n_a^3}\cdot\frac{dn_a}{dn},$$

finding it to be 0.319. The relativistic correction $F_s(\frac{1}{2}, 64)$ according to Kopfermann's[12] tables, was 1.595. The corrections applied to the final figure for the volume of the nucleus for the distribution of nuclear charges $(1-\delta)$[13] and nuclear magnetism $(1-\varepsilon)$[14] are (1 − 0.053) and (1 − 0.16) respectively. As a result, a_s was found to be $a_s = 0.266\,(\mu_I/I)$, where a_s is in cm⁻¹, and μ is in nuclear magnetos (μ_I). From the data in Table 2, we obtained a_s = −70 mK with an error not exceeding 10%.

From this, the following values are obtained

$$\mu(Gd^{157}) = -0.40 \pm 0.04\ \mu_I$$

$$\mu(Gd^{155}) = -0.32 \pm 0.04\ \mu_I$$

These data agree satisfactorily with the values obtained by the method of paramagnetic resonance[3,4] and the data in reference 1.

In order to calculate the absolute magnitude of the quadrupole moments, the errors introduced by the evaluation of $(\overline{1/r^3})$ need to be investigated in detail. For the terms $a''F_s$ and $a''F_7$, it is necessary to determine the mean value of $(1/r^3)$, in the state defined by the 5d valence electrons. For the terms $z''F_s$ and $z''G_s$, it is necessary to evaluate $(\overline{1/r^3})_{5d}$ and $(\overline{1/r^3})_{6p}$, which are determined by one-electron fine structure constants ζ_{nl}:

$$\left(\frac{\overline{r_0}}{r_{nl}}\right)^3 = \frac{\zeta_{nl}}{Ra^2 Z_l H_r(lz_l)},$$

where a_0 is the Bohr radius and Z_l is the effective charge of the nucleus. The values $\zeta_{5d} = 864$ cm⁻¹ and $\zeta_{6p} = 1240$ cm⁻¹ are taken from Speck[2] and are based on Murakava's work.[3] Then, using the values $Z_l = Z - 4$ (for 6p electrons) and $Z_l = Z - 11$ (for 5d electrons), $H_r(1.58) = 1.10871$ and $H_r(2.53) = 1.0202$,[12] we obtained:

$$\left(\frac{\overline{a_0}}{r}\right)^3_{5d} = 2.8 \text{ and } \left(\frac{\overline{a_0}}{r}\right)^3_{6p} = 3.3.$$

In reference 3, however, no explanation is given for the selection of the values of ζ_{5d} and ζ_{6p}. From Russel's[15] data which contained a full description of the gadolinium spectrum, the values $\zeta_{5d} = 630 \pm 30$ cm⁻¹ and $\zeta_{6p} = 900$ cm⁻¹ were calculated from the fine structure of the terms $4f^7 5d^2 6s(^{11}F_J)$ and $4f^7 5d^2(a^{10}F)6p(z^{11}G_J)$. The values for the effective charge of the nucleus $Z_l = Z - 18.6$ for p electrons, as estimated by Barnes and Smith,[16] and $Z_l = Z - 18.6$ for d electrons, as taken from reference 17, appeared to be more accurate. These gave the values

$$\left(\frac{a_0}{r}\right)^3_{5d} = 2.3 \text{ and } \left(\frac{a_0}{r}\right)^3_{6p} = 2.4.$$

The error of this expression for 5d electrons does not exceed 10%; the LS coupling for the F terms appears to be very satisfactory. The error of the expression for 6p electrons may reach 80%, which leads to an error of the same order in the absolute values of the quadrupole moments.

Using Speck's evaluation of $(\overline{a_0/r})^3$ for our experimental data (see Table 2, row a), we obtained the values

$$Q_{157} = 1.6 \cdot 10^{-24} \text{ cm}^2 \text{ and } Q_{155} = 1.2 \cdot 10^{-24} \text{ cm}^2.$$

From our evaluation of $(\overline{a_0/r})^3$ and Z_l, the following values were obtained:

$$Q_{157} = 2 \cdot 10^{-24} \text{ cm}^2, \quad Q_{155} = 1.6 \cdot 10^{-24} \text{ cm}^2.$$

Because of the uncertainty in the determination of the error for the values of the quadrupole moment, it is difficult to say which approach is better. Regardless of the error of calculation, we found $Q_{157} > Q_{155}$. In reference 1, the opposite relationship was found between the quadrupole moments of odd gadolinium isotopes.

EVALUATION OF RESULTS

It is interesting to compare our results with the data derived from Coulomb excitation of the nuclei of gadolium as given in references 18 and 19. Internal quadrupole moments $Q_0(Gd^{157}) = 8 \times 10^{-24}$ cm² and $Q_0(Gd^{155}) = 7.6 \times 10^{-24}$ cm² are given in reference 18. In later work,[19] only the value $Q_0(Gd^{157}) = 11.5 \times 10^{-24}$ cm² was determined. We obtained $Q_0(Gd^{157}) = 10 \times 10^{-24}$ cm² and $Q_0(Gd^{155}) = 8 \times 10^{-24}$ cm² using our data and the formula

$$Q = Q_0 \frac{I(2I-1)}{(I+1)(2I+3)}$$

Consequently, the results obtained by two independent methods agree only in order of magnitude.

The deformation parameter, δ, of the nuclei investigated can be determined from our data by the formula,[21]

$$Q_0 = \frac{4}{5} ZR^2 \left(1 + \frac{2}{3}\delta\right),$$

where $R = 1.2 \times 10^{-13} A^{1/3}$. We obtained $\delta_{157} \sim 0.37$, $\delta_{155} = 0.31$, and $\delta_{155}/\delta_{157} = 0.8$. The last ratio is obtained directly from the ratio Q_{155}/Q_{157} of the quadrupole moments. This value was accurate, because it depends only slightly on the possible errors in the determination of the electron wave functions. This result is in full agreement with the data on the change of the deformation of nuclei of rare-earth elements as derived from the properties of even isotopes.[20]

The gyromagnetic ratios of internal and collective motion g_k and g_R can be calculated from the experimental values of the deformation parameters and the above-mentioned magnetic moments μ_{155} and μ_{157}. It is known that

$$\mu = \frac{I}{I+1}(Ig_k + g_R),$$

where μ, g_k, and g_R are expressed in nuclear magnetons. The value of g_k was calculated by the scheme of Nilsson. The coefficients of the components of the wave function of an odd nucleide were extrapolated from Nilsson's table[21] for the ground state of gadolinium ($N = 5$, $I = 3/2$, $h_{9/2}$) in the region of great deformations ($0.31 < \delta < 0.41$). We obtained

$$\frac{g_{R155}}{g_{R157}} = 0.9 \pm 0.1.$$

using $\delta_{155}/\delta_{157} = 0.8$. From these values, the following useful relation can be derived

$$\left(\frac{g_R}{g_k}\right)_{157} = 1.1\left(\frac{g_R}{g_k}\right)_{155} + 0.2.$$

The calculation of the values g_k, according to this scheme, is connected with the absolute values of the deformation parameters δ_{155} and δ_{157}, and is adversely affected by any error in the determination of Q_0. Assuming $Q_{0157} = 10 \times 10^{-24}$ cm², we obtained $g_{k157} = -0.9$ and $g_{k155} = -0.8$. Using these values for g_k, and $\mu_{157} = -0.40$ and $\mu_{155} = -0.32$, we obtained $g_{R155} = g_{R157} = 0.7$ which differs markedly from the theoretical approximate value, $g_R \simeq Z/A = 0.4$.

Our values of g_k and g_R are in good agreement with the data of de Boer et al.[19] for Gd^{157} ($g_k = -0.86$ and $g_R = 0.65$), but they disagree with earlier measurements by Bjerregard and Meyer-Berkhout[18] ($g_k = -0.60$ and $g_R = 0.28$). Their experimentally determined ratio Gd_{155}/Gd_{157} is in good agreement with our value.

The authors are grateful to V. S. Zolotarev for furnishing the separated isotopes of gadolinium, and to L. K. Peker for valuable advice in the evaluation of the results.

REFERENCES

1. D. R. Speck. Phys. Rev. **101**, 1725 (1956).
2. H. Kopfermann, L. Krüger, and A. Steudel. Ann. Physik **20**, 258 (1957).
3. K. Murakawa. Phys. Rev. **96**, 1543 (1954).
4. S. Suwa. Phys. Rev. **86**, 247 (1952); J. Phys. Soc. Japan **8**, 377 (1953).
5. W. Low. Phys. Rev. **103**, 1309 (1956).
6. A. A. Manenkov and A. M. Prokhorov. Zhur. Eksptl. i Teoret. Fiz. **33**, 1116 (1957).
7. N. I. Kaliteevskii, G. M. Malyshev, and M. P. Chaika. Opt. i Spektr. **6**, 820 (1959).
8. N. I. Kaliteevskii and M. P. Chaika. Vestnik Leningrad. Gosudarst. Univ. No 16, 51 (1959).
9. G. M. Malyshev, M. P. Chaika, E. E. Fradkin, and V. B. Skidan. Opt. i Spektr. **7**, 780 (1959).
10. M. P. Chaika and E. E. Fradkin. Opt. i Spektr. **7**, 820 (1959).
11. P. Brix. Z. Physik **132**, 579 (1952).
12. H. Kopfermann. "Kernmomente," pp. 431-435. Frankf. a. Main, 1956.
13. M. G. Grawford and A. L. Schawlow. Phys. Rev. **76**, 1316 (1949).
14. A. Bohr and V. F. Weisskopf. Phys. Rev. **77**, 94 (1950).
15. H. Russel. J. Opt. Soc. Am. **40**, 550 (1950).
16. R. G. Barnes and W. V. Smith. Phys. Rev. **93**, 95 (1954).
17. K. Murakawa. Phys. Rev. **98**, 1285 (1955).
18. J. H. Bjerregard and U. Meyer-Berkhout. Z. Naturforsch. **11a**, 273 (1956).
19. J. de Boer, M. Martin, and P. Marmier. Helv. Phys. Acta **31**, 578 (1958).
20. K. Alder, A. Bohr, T. Huus, B. Mottelson, and A. Winter. Revs. Modern Phys. **28**, 432 (1956). (See "Deformatsiya Atomnykh Yader," p. 1. Moscow, 1958.)
21. S. G. Nilsson. Kgl. Danske Videnskab. Selskab., Mat.-Fys. Medd. **29**, 1 (1955). (See "Deformatsiya Atomnykh Yader," p. 232. Moscow, 1958.)

ENHANCEMENT OF SENSITIVITY IN THE SPECTRAL ISOTOPE ANALYSIS OF LEAD

M. S. Kashtan, E. V. Sobotovich, and T. N. Khlopina

Received 9 June 1959

A method of introducing an analyzed sample into a hollow cathode discharge tube was carried out, which permits the improvement of a number of important characteristics of the spectral isotope analysis method.

The purpose of the present work was the study of the possibility of determining isotope composition of very small quantities of lead using a spectrometer, made according to the type of arrangement NIFI LGU.[1,2]

It was of considerable interest to attain, without essential change in the scheme of the instrument, an increase of sensitivity and an enhancement of the accuracy of analysis.

The arrangement employed for the experiments was the substitution of the single-prism monochromator NIFI by a spectrograph ISP-51, as proposed by Zaidel and Zhiglinskii, which increased illumination 7 to 8 times. A change in the design of the housing of the photomultiplier made by us and the use of a Fabry-Perot etalon of greater transparency* increased the illumination of the arrangement 6 to 7 times. This permitted the elimination of cooling of the photomultiplier by liquid air.

*We consider it our pleasant duty to express gratitude to F. A. Korolev for submitting high quality multiple-layer dielectric mirrors.

When using a hollow cathode discharge tube the method of introducing the sample to be examined appears to be critical. This determines, to a great degree, such important characteristics of the method as: (1) the sample size of analyzed element that is necessary for the analysis to be performed, (2) the stability of luminescence of the analytical line, and (3) the magnitude of continuous background, dependent on molecular and continuous spectra emitted in the hollow cathode discharge tube.

A hollow cathode discharge tube cooled by liquid air was used in the experiments. The design of the discharge tube was similar to that described in the work of Kaliteevskii and Chaika.[3] For a quick replacement of analyzed samples the hollow cathode tube was prepared as a small detachable metallic pot.[3] A number of constructional modifications of the hollow cathode that were made by us insured its more penetrating cooling, the dependability of electrical connections in conditions of cooling the cathode with liquid air, and also permitted the enhancement of the stability of discharge. Spectroscopically pure argon was used as a filling gas.

A number of researchers[4,5] consider that the most efficient method of introducing the sample to be examined into the hollow cathode tube appears to be its uniform spreading on the walls of the cathode pot. Yet when small quantities of the sample are used this leads to an undesirably high consumption of the analyzed element. Therefore, for the most effective utilization of a sample when changing to the analysis of very small quantities of lead it is necessary to determine from which part of the surface of the hollow cathode tube the entry of atoms of the sample into discharge is most probable. This problem has not yet been elucidated.

In the design of the cooled hollow cathode tube employed by us, the entry of atoms of sample into discharge occurs as a result of cathode sputtering. Special investigations were carried out in order to determine that part of the bottom of the pot from which the atoms of the analyzed material enter the discharge.

1. The bottom of the pot of the hollow cathode tube was covered with a flat metallic target on which a thin layer of lead amounting to 0.2 and 0.3 mg was evenly spread. The surface of the target was examined when the intensity of the analytical line was falling to zero during the time the discharge tube was in operation. It appeared that only its clearly limited central part, which constituted approximately $\frac{1}{8}$ to $\frac{1}{4}$ of the whole target area, was free from lead.

2. The target of metallic lead was placed on the bottom of the pot of an easily sputtered metal in discharge such as copper. After half an hour to an hour of burning in the discharge tube at a discharge current of 50 to 60 ma, on the target surface a densely deposited layer of copper in the form of a ring around the central part was observed, on which were marked only hardly noticeable traces of copper.

The investigations made disclosed that the atoms of the analyzed sample enter into discharge principally from that part of the hollow cathode pot (later called the working surface), above which is concentrated the brightest axial part of the negative glow. In addition to this, that part of the bottom over which the Crooke's dark space is located is most densely covered with the sputtered material of the pot.

For spectral isotope analysis of lead salts such as PbI_2, $PbCl_2$, PbO[1,6] are generally used. When these salts were used we had to work at a discharge current of the order of 50 ma. Although this was accompanied by a number of undesired phenomena, the reduction of the magnitude of the discharge current was limited by the decrease in the intensity of the analytical line Pb I 4057.8A.

When using currents of the 50 ma order a decrease of intensity and instability of illumination of the line Pb I 4057.8A were observed, which apparently resulted from the fact that the products of cathode sputtering of the pot material and the products of chemical reactions in the discharge cover the surface of the analyzed sample, by which the subsequent entry of atoms of lead into the zone of glow is hampered. Moreover, at the discharge current of the order of 50 ma and more, the continuous background, obtained on graphical records, many times exceeds the magnitude of instrument background. This is explained by the presence in a given spectral region of molecular and continuous spectra of the discharge tube and by superimposition of the fringe of the nearby argon line, the intensity of which at the current of 50 ma exceeds the intensity of the lead analytical line.

The experiments performed showed that the substitution of salts by metallic lead permits the reduction of the discharge current from 50 ma to 5-6 ma. At the same time the previous intensity of the analytical line is secured (in both cases the intensity of the line Pb I 4057.8A is such that, due to the effect of self-absorption it can

still be practically disregarded). At such a reduction in the magnitude of the discharge current, the ratio of the intensity of the background to the intensity of the analytical line decreases, the stability of its illumination increases, and also the broadening of lines dependent on the Doppler effect diminishes, which brings about the possibility of enhancing the contrast of the arrangement. Besides this, with the decreased discharge current its stabilization is facilitated and the consumption of liquid air for cooling the hollow cathode tube is reduced. The time of burning of the discharge tube that is required for performing the analysis is reduced to 10 to 15 min when salts are substituted by metallic lead which enhances the effectiveness of the utilization of the sample.

It follows from what was stated above that for the analysis of very small quantities of lead the most expedient method appears to be the application of the analyzed sample as a metalic lead on the working surface of the hollow cathode tube. In our case the working surface of a diameter of about 3 mm was located in the center of the detachable target, completely covering the bottom of the pot.

We rejected the method of electrolytic deposition of metallic lead because when very small quantities of lead of the order of some tens of micrograms or less are used, one has to deal with electrolytes of very small concentration from which lead practically does not deposit on the cathode.[7]

We worked out the means of depositing very small quantities of lead on the metallic targets by the pyrochemical method. This method permits the depositing of any desired small quantities of lead as metal on the working surface of the hollow cathode.

The principle of the method is as follows. The solution of lead nitrate is evaporated in a tiny boat of tantalum or stainless steel (9) which is then put into a quartz tube (1) of the diameter of 10 to 12 mm (Fig. 1). Nearer one of the ends of the tube there is a quartz diaphragm (2) with an aperture of the diameter equal to the diameter of the working surface of the hollow cathode tube. A flat target (3) of 7.5 mm diameter is placed in a special fixture (4) of the cooler (5) and put together with it into the quartz tube almost reaching the brace of the diaphragm (2). At one end the tube is hermetically sealed with a mushroomlike device (6) mounted on the body of the cooler—and at the other end—with a quartz ground joint (7). The tube is inserted in a specially made tubular furnace (8) of an inside diameter of 12 to 14 mm, an outside diameter of 40 to 45 mm, a length of 80 to 90 mm, power 250 to 300 watts. Next, electrolytic hydrogen is passed through the tube. In 3 to 4 min after switching on

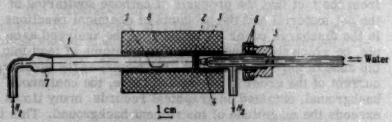

Fig. 1. Apparatus for the deposition of very small quantities of metallic lead on the working surface of the hollow cathode tube.

the furnace the temperature in the tube rises to 850-900°C. At this temperature the lead is sublimed and then is condensed on the cool central part of the target. The time of evolution is 10 to 12 min. Ninety percent completeness of the evolution is attained, which was ascertained with the aid of a radioactive indicator.*

*For the verification 10^{-13} to 10^{-12} gm of Pb^{212} (ThB) was used, which was put into the tiny tantalum boat as lead nitrate.

A photograph of a section of the automatic recorder band E PP – 09 is shown in Fig. 2. For 50 μgm of metallic lead at the current of 5 ma graphical records were obtained of hyperfine structure of the line Pb I 4057.8A drawn by the Fabry-Perot etalon of 15 mm thickness.

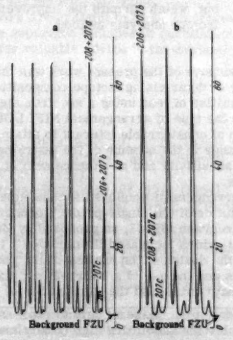

Fig. 2. Graphical records of hyperfine structure of line Pb I 4057.8A obtained with a sample of 0.05 mg. Intensities of components STS of Pb^{207} isotope are related as 207a : 207b : 207c = 9 : 1 : 5.

Graphical record (a) refers to the case of ordinary lead and (b) to a radiogenic one. The background on the graphical records amounted respectively to 0.7% and 0.6% of the total intensity of all components. This corresponds to the contrast of the arrangement, which is equal to the theoretically calculated value of contrast of the Fabry-Perot interferometer employed; that is, the background on the graphical record appears to be purely the apparatus background. From the graphical record a high stability of illumination of the analytical line is also seen. Repeatability of the ratio of the intensities of individual components to the total intensity of corresponding interference order is characterized by the mean values shown in the table and the magnitude of mean quadrature errors of ratios, determined after 5 successive measurements for samples of various isotope composition. It follows from the data given that the repeatability amounts to ±0.3-0.5% for isotopes with a relative content above 20%.

Sample	$\frac{I\ (206+207a)}{\sum I_i}$	$\frac{I\ (206+207b)}{\sum I_i}$	$\frac{I\ (207c)}{\sum I_i}$	$\frac{I\ (204)}{\sum I_i}$
1	0.6275 ± 0.0011	0.2669 ± 0.0007	0.0900 ± 0.0004	0.0256 ± 0.0004
11	0.6194 ± 0.0025	0.2777 ± 0.0018	0.0829 ± 0.0005	0.0200 ± 0.0005
719	0.2682 ± 0.0031	0.6532 ± 0.0021	0.0553 ± 0.0024	0.0193 ± 0.0011
142	0.1647 ± 0.0017	0.7814 ± 0.0017	0.0539 ± 0.0033	—
653	0.1216 ± 0.0013	0.8322 ± 0.0008	0.0462 ± 0.0008	—

Apparently, spectral isotope analysis and the study of hyperfine structure of lines for very small quantities of a number of other elements, e.g., Sn, Cd, Bi, Ag, Tl, Zn will also prove more effective when employing the method of introducing very small quantities of metal in

the hollow cathode, proposed in the present work.

Thus the work performed leads to the following results:

1. The quantity of lead sufficient for analysis was reduced to 0.05 to 0.10 mg. Further reduction in the sample size without decreasing the accuracy of analysis is limited only by parameters of spectral arrangement.

2. The stability of luminescence of lead in the hollow cathode was enhanced, which increased the repeatability of the results of analysis; e.g., for isotopes of a relative content of about 20% and more, the repeatability amounted to 0.3-0.5% instead of 2-3% as was the case in the work with the salts.

3. The magnitude of continuous background was brought up to the magnitude of the apparatus background of the Fabry-Perot etalon. This speaks favorably for the accuracies of analysis and extremely simplified method of interpreting the graphical records.

REFERENCES

1. A. G. Zhiglinskii. Opt. i Spektr. 3, 9 (1957).
2. A. N. Zajdel, A. G. Zhiglinski, and J. Cajko. Czech. J. Phys. 8, 530, 665 (1958).
3. N. I. Kaliteevskii and M. P. Chaika. Opt. i Spektr. 1, 606 (1956).
4. H. Kopfermann. Z. Physik 75, 363 (1932).
5. S. Tolanskii. "Spektroskopiya vysokoi razreshaiushchei sily." (High Resolution Spectroscopy) IL, Moscow, 1955.
6. I. K. Brody, F. S. Tomkins, and M. Fred. Spectrochim. Acta 8, 329 (1957).
7. V. I. Lainer and N. T. Kudryavtsev. "Osnovy galvanostegii t.1." (Principles of Electrodeposition) vol. 1, Metallurgizdat, 1953.

ELECTRONIC ABSORPTION SPECTRA OF SOME INDAN HOMOLOGS

M. M. Kusakov, E. A. Prokof'eva, and M. V. Shishkina

Received 15 July 1959

In this work the ultraviolet spectra of some indan derivatives are presented and a discussion of them is developed.

Hydrocarbons of the indan series are one of the least studied types of aromatic hydrocarbons. Referenced 1-7 are devoted to the synthesis of these compounds, and only one work[1] contains data on the ultraviolet and infrared absorption spectra of some methyl- and dimethylindans. Together with these, a series of investigations is known in which the presence of indan and its homologs in petroleum fractions,[8-10] in the transformation products of hydrocarbons,[11] and also in the products of coal processing is indicated.

In connection with the necessity of obtaining a more complete characterization of these compounds, E. S. Pokrovskaya et al. effectuated the synthesis of hydrocarbons of the indan series with one, two, and three substituents of various structures[12-15] and carried out a comprehensive study of their properties, including spectral properties.

The present communication is devoted to consideration of the electronic absorption spectra of fifteen indan derivatives, measured on a "Uvispek" spectrophotometer. The measurements were carried out at 10A intervals over the range 2200-2850 A (at 5A intervals in regions where the absorption changed abruptly) at room temperature in isooctane solutions.

The following hydrocarbons were characterized by means of their absorption spectra over the range just stated: indan, ten monosubstituted indans, three disubstituted indans, and two trisubstituted indans.

The results of the measurements are presented in the form of graphs of the dependence of log $\varepsilon(\lambda)$ (ε is the molar extinction coefficient) on the wavelength expressed in A.

Measurements were made, on the average, two or three times for all the compounds, which, on account of their ease of oxidation, were studied immediately after synthesis and purification or else after storage sealed in a nitrogen atmosphere. The accuracy of the determination of the absorption intensity ε amounted to 1-2%. The wavelengths were determined with an accuracy of 5A. The boiling point of each of the hydrocarbons synthesized had a range of 0.5-1.5°C.

For comparison, the spectrum of indan, with the structural formula

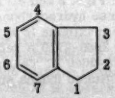

was measured; it coincided sufficiently well with the spectra known from the literature.[1, 16] The ultraviolet spectra of all the indan derivatives presented in this work have not been previously described.

The absorption spectra of indan and of isopropyl-, isobutyl-, and hexylindan containing the substituent groups in the five-membered ring are represented in Fig. 1 and Table 1. The conditions of synthesis of these hydrocarbons and their fundamental physicochemical characteristics are presented in references 12-14. The absorption spectra of the three homologs listed are very close to each other and analogous to the spectrum of indan, which might have been expected, inasmuch as the substituent group in the molecules of these hydrocarbons is located in the five-membered ring, which itself does not absorb in this region of the spectrum.

Because of the fact that the electronic absorption spectra of aromatic compounds are practically independ-

Table 1. Position of the Maxima and Minima (in A) in the Absorption Spectra of Indan and its Monosubstitution Products (Substituent in the Naphthenic Ring)

Indan	2735 (3.17)	2700 (2.78)	2670 (3.08)	2630 (2.90)	2600 (2.97)
Isopropylindan	2737 (3.26)	2710 (2.87)	2670 (3.22)	2628 (3.06)	2600 (3.09)
Sec-butylindan	2738 (3.22)	2712 (2.82)	2672 (3.18)	2628 (3.00)	2607 (3.04)
(2-Hexyl)indan	2733 (3.14)	2705 (2.77)	2665 (3.10)	2625 (2.92)	2602 (2.94)
1-Methylindan	2735 (3.18)	2712 (2.85)	2664 (3.08)	2630 (2.85)	2600 (2.90)

Note. In Tables 1–4, the values of log ε are given in parentheses.

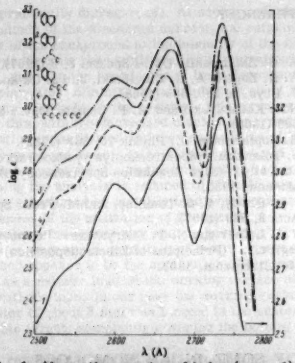

Fig. 1. Absorption spectra of indan (curve 1); 1-isopropylindan (curve 2); 1-secondary-butylindan (curve 3); 1-(2-hexyl)indan (curve 4).

ent of the structure of a saturated substituent, it proved possible to compare these spectra with the known spectrum of 1-methylindan[1] and to establish that the substituent in the molecules of the three indans studied is located in position 1 (see Table 1).

As is known from the conditions of synthesis, the seven remaining monosubstituted indans contain the substituent groups in the benzene ring.

The absorption spectra of the monosubstituted indans are presented in Figs. 2 and 3. The intensity distribution in the band of these hydrocarbons is one and the same: the most intense maximum is at 2765-2775 A, a double maximum in the 2680-2710 A region, and a secondary maximum at 2620-2640 A. Thus the absorption bands of all the monosubstituted indans studied, though having one

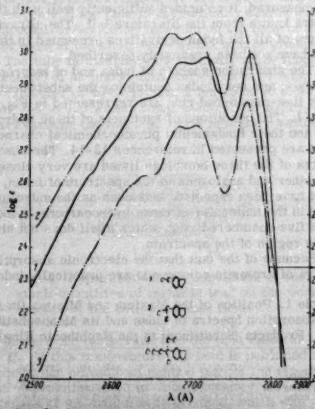

Fig. 2. Absorption spectra of 5-ethylindan (curve 1); 5-isopropylindan (curve 2); 5-(2-ethylhexyl)indan (curve 3).

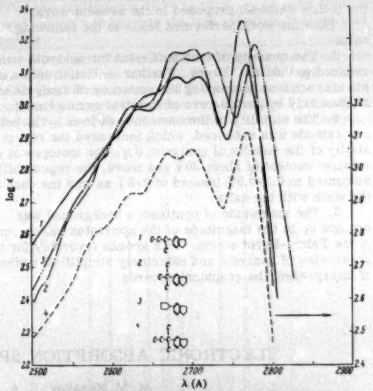

Fig. 3. Absorption spectra of 5-isobutylindan (curve 1); 5-tertiarybutylindan (curve 2); 5-cyclopentylindan (curve 3); 5-isoamylindan (curve 4).

and the same contour, are somewhat shifted with respect to one another. As can be seen from Fig. 2 and Table 2, the absorption spectrum of ethylindan occupies the longest-wavelength position relative to the spectra of isopropyl- and 2-ethylhexylindan, which have a higher degree of branching in the substituent. An analogous regularity is observed in the spectra of the isomeric butylbenzenes[17] and for a whole series of spectra of aklylbenzenes.[18-20] The greatest shift of the absorption band relative to the absorption band of benzene is possessed by those alkylbenzenes in which a CH_3 or CH_2 group, which has the most mobile electrons which can resonate with the benzene ring or migrate into it, directly adjoins the ring. The smallest shift of the absorption band is observed for the aklylbenzenes in which the substituent is attached to the benzene ring through a quaternary carbon atom. Attempts at finding a theoretical basis for this regularity in the absorption spectra of alkylbenzenes are contained in references 21-24.

From a comparison of the spectra of isobutyl- and tertiary-butylindan (Fig. 3, curves 1, 2), it can be seen that the absorption band of tertiary-butylindan is shifted toward the short wavelength side by 5A relative to the band of isobutylindan, and by 15A relative to the spectrum of ethylindan (see also Table 2), which, as already noted above, corresponds completely with the observations in the spectra of isomeric alkylbenzenes.

Table 2. Position of the Maxima and Minima (in A) in the Absorption Spectra of Monosubstitution Products of Indan (Substituent in the Aromatic Ring)

5-Methylindan[1]	2787 (3.27)	2763 (2.89)	2727 (3.20)	2705 (3.12)	2686 (3.13)	2658 (2.84)
Ethylindan	2780 (3.00)	2755 (2.78)	2722 (3.00)	2705 (2.97)	2690 (2.97)	2645 (2.86)
Isopropylindan	2768 (3.10)	2742 (2.87)	2713 (3.06)	2692 (3.04)	2681 (3.06)	2640 (2.94)
Isobutylindan	2770 (3.13)	2745 (2.89)	2712 (3.09)	2695 (3.07)	2683 (3.08)	2645 (2.96)
Tert-butylindan	2765 (3.26)	2740 (2.93)	2706 (3.17)	2680 (3.15)	2690 (3.18)	2630 (3.00)
Isoamylindan	2770 (3.11)	2740 (2.88)	2705 (3.06)	2687 (3.03)	2670 (3.05)	2640 (2.92)
Cyclopentylindan	2780 (3.07)	2734 (2.96)	2725 (3.18)	2705 (3.13)	2695 (3.14)	2645 (3.03)
(2-Ethylhexyl)indan	2770 (3.24)	2745 (2.97)	2710 (3.18)	2695 (3.16)	2690 (3.17)	2640 (3.02)
4-Methylindan[1]	2734 (2.73)	2723 (2.47)	2676 (2.67)		2643 (2.72)	2640 (2.64)

The absorption band of cyclopentylindan (Fig. 3, curve 3) has a marked shift toward the longer wavelength

side relative to the other two bands, which is caused by the naphthenic character of the substituent. Analogous displacements have previously been observed in the spectra of cyclopentylbenzenes[20, 25, 26] and have been interpreted in reference 27. The intensity distribution in the absorption band of cyclopentylindan is analogous to the intensity distribution in the band of the other alkylindans. This generality of the contour of the absorption bands of monosubstituted indans and their localization on the wavelength scale, allowing for the insignificant shifts caused by the varying structure of the side chains, permit us to assume that all seven monosubstituted indan derivatives have similar structures. Comparison of their spectra with the known spectra of the methylindans which have the methyl groups in the benzene ring (see Table 2) leads to the conclusion that the substituent groups in the seven indans listed occupy position 5 (the β-position).

The absorption spectra of diethyl-, diisopropyl-, and diisobutylindan are presented in Fig. 4. The intensity and position of the absorption maxima in the spectra of these hydrocarbons are very close to each other, which indicates the adherence of the structure of the three disubstituted indans to a single type. The small shift of the absorption band of diethylindan toward longer wavelengths (Table 3) is caused, just as in the case of the monosubstituted indans, by the linear structure of the ethyl chains in the substituents. The unavailability of spectra of the corresponding dimethylindans does not permit us to establish the position of the substituent groups in this case. From steric considerations, it is most likely that this substitution corresponds to the 5,7 or 4,6 positions (which are one and the same) in the indan molecule. However, it may also be that the substituents are placed next to each other, in the 5,6 positions. The benzene nucleus of the indan molecule would thereby become quasi-symmetrically tetrasubstituted, and in the spectrum of such a molecule the characteristics of the spectrum of 1,2,4,5-tetramethylbenzene (durene) might possibly be repeated. In the present case, the spectra of all three dialkylindans correspond to the absorption maxima of durene with respect to both relative intensities and position of the maxima (Table 3).

It should be noted that, aside from the general region of absorption, there is no other similarity in the spectra of indan and ortho-xylene. The five-membered ring attached to the benzene ring in the indan molecule radically changes the character of the electronic absorption spectrum, increasing the absorption intensity several-

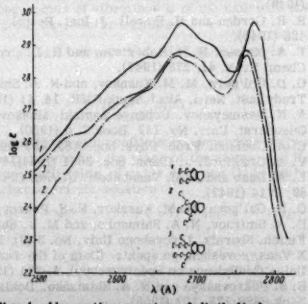

Fig. 4. Absorption spectra of diethylindan (curve 1); diisopropylindan (curve 2); diisobutylindan (curve 3).

Table 3. Position of the Maxima and Minima (in A) in the Absorption Spectra of Disubstitution Products of Indan (Substituents in the Aromatic Ring)

Durene*	2775 (2.83)	2750 (2.73)	2720 (2.78)	2680 (2.81)	—
Diethylindan	2775 (2.98)	2750 (2.82)	2715 (2.92)	2685 (2.97)	2645 (2.86)
Diisopropylindan	2768 (2.88)	2736 (2.75)	2700 (2.84)	2677 (2.87)	2642 (2.76)
Diisobutylindan	2767 (2.88)	2740 (2.78)	2705 (2.86)	2682 (2.88)	—

*The spectrum of durene was measured on the "Uvispek" spectrophotometer under the same conditions.

fold and intensifying the vibrational structure. There is a hypothesis that a condensed naphthenic ring in aromatic molecules makes the molecule more planar and rigid,[28] which is also the cause of the intensification of the vibrational structure of the electronic spectrum.

It is possible that the introduction of a few sufficiently heavy substituent groups in the benzene nucleus of indan leads to some deformation of the molecule, and that the character of the vibrations of di- and trisubstituted indans (substitution in the benzene ring!) becomes close to the character of the vibrations of the corresponding tetra- and pentasubstituted benzenes. It is curious that the measured spectra of triisopropyl- and tricyclohexylindan in which all three substituents have been introduced into the benzene ring have a still greater resemblance to the pentasubstituted benzenes with respect to the position of the absorption maxima, the intensity distribution within the absorption band, and the absolute magnitude of the absorption (Fig. 5, Table 4). The question may arise as to

Table 4. Position of the Maxima and Minima (in A) in the Absorption Spectra of Trisubstitution Products of Indan

Triisopropylindan	2700 (2.72)	2742 (2.85)	2786 (2.88)
Tricyclohexylindan	2700 (2.71)	2742 (2.84)	2785 (2.87)
Pentamethylbenzene[25]	2700 (2.56)	2753 (2.49)	2792 (2.47)

why, in the spectra of the trisubstituted indans, there is not observed a long wavelength shift of the absorption band of tricyclohexylindan relative to the band of triisopropylindan (Table 4), such as is observed for the spectra of cyclopentylindan and isopropylindan (Fig. 3). The relative position of the absorption bands of the cyclopentyl and the cyclohexyl derivatives of indan on the one hand and of the alkyl derivatives of indan on the other correspond completely to the shifts of the absorption bands in the corresponding benzene derivatives, as has been shown in references 20, 25, and 26, and an explanation of this phenomenon from the point of view of molecular orbital theory is given in reference 27. Thus the electronic ab-

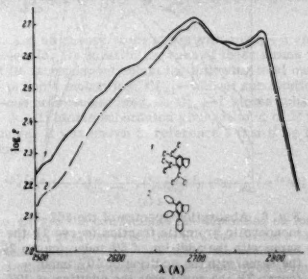

Fig. 5. Absorption spectra of triisopropylindan (curve 1); tricyclobexylindan (curve 2).

sorption spectra of the 15 indan derivatives possess the same fundamental regularities as do the spectra of the analogous benzene derivatives.

The position and contour of the absorption band of the indan hydrocarbons is fundamentally determined by the number and position of the substituent groups in the molecule, in connection with which it appears possible to determine the structure of indan hydrocarbons by means of comparison with the electronic absorption spectra of simpler homologs of indan, for example, the methylindans.

In the spectra of the indan hydrocarbons studied, with one, two, and three substituents in the benzene nucleus, shifts within the limits of 5-15 A are observed, depending on the structure of the substituent groups. However, the intensity distribution in the absorption band remains one the same for hydrocarbons which have different characters and different degrees of branching in the side chain.

The electronic absorption spectra of the indans and their pecularities noted in this work permit us to re-identify the individual synthetic indan hydrocarbons, to determine the number and position of the sutstituent groups, and in certain cases to indicate the character of the substituent as well.

In connection with the fact that the wavelengths of the absorption maxima in the spectra of indan hydrocarbons for the most part coincide with the wavelengths of the maxima of the alkylbenzenes, while the absorption intensity of the indans is only 2 to 3 times as great as the absorption intensity of the benzenes, the presence of indan hydrocarbons in monocyclic aromatic petroleum fractions is rather difficult to determine on the basis of ultraviolet absorption spectra.

The intensity maximum in the absorption spectra of the benzene fractions of ligroins, kerosenes, and oils from the most varied petroleums is at 2650-2680 A.[29-31] The intensity maximum in the spectra of the indan hydrocarbons known from reference 1 and studied in the present work is at 2730-2770 A. Therefore, with the presence of indan hydrocarbons in monocyclic aromatic petroleum fractions, one would expect a general increase in the intensity and a displacement of the peak of the absorption band into the 2730-2770 A region in the ultraviolet absorption spectra of the fractions.

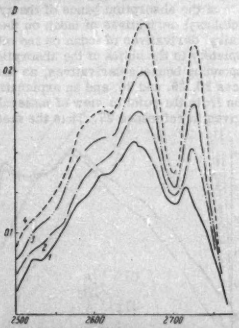

Fig. 6. Absorption spectra of the 169-174° monocyclic aromatic fraction (curve 1); the same with the addition of 5% indan (curve 2); the same with the addition of 10% indan (curve 3); the same with the addition of 20% indan (curve 4).

By means of comparison of synthetic mixtures of a kerosene-benzene fraction with indan, we succeeded in finding a redistribution of intensity in the absorption band only when the indan content amounted to 20% of the quantity of aromatic hydrocarbons in the fraction (Fig. 6).

REFERENCES

1. J. Entel, C. H. Rouf, and H. C. Howard. Anal. Chem. **25**, 1303 (1953).
2. B. B. Elsner and K. J. Parker. J. Chem. Soc. 592 (1957).
3. H. El. Hass, A. Deluzarche, and A. Maillard. Compt. rend. **245**, 540 (1957).
4. A. Maillard, A. Deluzarche, and H. El. Hass. Compt. rend. **245**, 185 (1957).
5. W. M. Kutz, J. E. Nikels, and B. B. Corson. J. Am. Chem. Soc. **70**, 4026 (1948).
6. M. S. Carpenter and W. M. Easter. J. Org. Chem. **19**, 96 (1954).
7. P. Cagniant, A. Deluzarche, and G. Chatelus. Compt. rend. **224**, 1064 (1947).
8. A. F. Plate. Sbornik. "Sostav i svoistva neftei i benzino-kerosinovykh fraktsii." (Collection: Composition and Properties of Petroleums and Benzene-Kerosene Fractions), p. 217, Moscow, 1957.
9. A. V. Topchiev, I. A. Musaev, A. N. Kislinskii, and G. D. Gal'pern. Sbornik "Sostav i Svoistva neftei i benzino-kerosinovykh fraktsii." (Collection: Composition and Properties of Petroleums and Benzene-Kerosene Fractions), p. 252, Moscow, 1957.
10. R. B. Williams, S. H. Hastings, and J. A. Anderson. Anal. Chem. **24**, 1911 (1952).
11. V. T. Aleksanyan, Kh. E. Sterin, and S. A. Ukholin. Izvest. Akad. Nauk SSSR, Ser. Fiz. **23**, 1177 (1959).
12. A. V. Topchiev, E. S. Pokrovskaya, and T. G. Stepantseva. Doklady Akad. Nauk SSSR **119**, 1164 (1958).
13. E. S. Pokrovskaya. Trudy Inst. Nefti, Akad. Nauk SSSR (in press).
14. A. V. Topchiev, N. E. Tsytovich, and E. S. Pokrovskaya. Doklady Akad. Nauk SSSR **128**, 558 (1959).
15. E. S. Pokrovskaya and T. G. Stepantseva. Doklady Akad. Nauk SSSR **55**, 841 (1947).
16. R. A. Friedel and M. Orchin. "Ultraviolet Spectra of Aromatic Compounds." New York, 1951.
17. R. Stair. J. Research Natl. Bur. Standards **42**, 587 (1949).
18. R. R. Gordon and H. Powell. J. Inst. Petrol. **31**, 428 (1945).
19. F. A. Matsen, N. N. Robertson, and R. L. Chuoke. Chem. Revs. **41**, 273 (1947).
20. G. D. Gal'pern, M. M. Kusakov, and N. A. Shimanko. Trudy Inst. Nefti, Akad. Nauk SSSR, **14**, 11 (1959).
21. A. N. Nesmeyanov. Uchenye Zapiski, Moskov. Gosudarst. Univ. No. 132, Book 7, 5 (1950).
22. C. A. Coulson. Proc. Phys. Soc. **A65**, 933 (1952).
23. V. A. Crawford. J. Chem. Soc. 2061 (1953).
24. L. A. Daub and J. M. Vandenbelt. J. Am. Chem. Soc. **69**, 2714 (1947).
25. G. D. Gal'pern, M. M. Kusakov, E. S. Pokrovskaya, B. A. Smirnov, N. A. Shimanko, and M. V. Shishkina. Fizich. Sbornik, L'vovskogo Univ. No. 3 (8); Mater. X Vses. soveshch. po spektr. (Data of the Tenth All-Union Conference on Spectroscopy), **1**, 334 (1957).
26. E. S. Pokrovskaya and N. A. Shimanko. Doklady Akad. Nauk SSSR **123**, 109 (1958).
27. W. W. Robertson, J. F. Musik, and F. A. Matsen. J. Am. Chem. Soc. **72**, 3260 (1950).

28. E. Merkel and Ch. Wiegand. Naturwissenshaften **34**, 122 (1947).
29. N. G. Adams and D. M. Richardson. Anal. Chem. **23**, 129 (1951).
30. A. V. Topchiev, L. M. Rozenberg, M. M. Kusakov, and M. V. Shishkina. Izvest. Akad. Nauk, Ordel. Khim. Nauk 1109 (1956).
31. M. M. Kusakov, S. S. Nifontova, E. S. Pokrovskaya, B. A. Smirnov, N. A. Shimanko, and M. V. Shishkina. Fizich. Sbornik, L'vovskogo Univ. No. 3 (8); Mater. X Vses. soveshch. po spektr. (Data of the Tenth All-Union Conference on Spectroscopy), 1, 321 (1957).
32. H. Conrad-Billroth. Z. physik. Chem. **B29**, 170 (1935).

RELATION BETWEEN VIBRATION FREQUENCIES OF ISOTOPIC MOLECULES (THE SUMS RULES AND THE RULES FOR THE PRODUCT SUMS OF THE FREQUENCY SQUARE POWERS)

L. M. Sverdlov

Received 8 May 1959

In the author's previous works, the rules for the sums of the products of the vibrations frequencies of isotopic molecules have been derived. In the present work, the rules have been expanded for the cases of powers of frequencies in the system of isotopic molecules

1. Some years ago, we obtained the whole complex of relations connecting the vibration frequencies of the isotopic molecules.[1-4] In particular the rules were established for the sums of the products[2] of the squares of the frequencies λ_i—

$$\sum_{i \neq j} \lambda_i \lambda_j,$$

taking the product of two, and

$$\sum_{i \neq j \neq k} \lambda_i \lambda_j \lambda_k$$

taking the product of three, etc.*

*The work of reference 2 was published in 1952. After six years, the article by Bigeleisen[5] appeared, which gives a result for the relation of the squares of frequencies, taking the product of two, $\Sigma \lambda_i \lambda_j$, i.e., a particular case of the sum rules of the products. Besides that, a similar case for $\Sigma \lambda_i^2$ was developed in this article.

It is shown in the present work that similar relations are also correct for the λ_i powers of the system of isotopic molecules.

2. Let us consider an N-atomic molecule $a_1, a_2, \ldots a_n$, which has $n = 3N - 6$ degrees of freedom. The characteristic frequencies of vibrations ω of the molecule are obtained from the secular equation

$$|D_{ij} - \delta_{ij}\lambda| = 0 \quad (i, j = 1, 2, \ldots, n; \ \lambda = \omega^2), \tag{1}$$

where

$$D_{ij} = \sum_{t=1}^{n} A_{it} K_{tj};$$

A_{it} are the kinematic coefficients, depending on geometrical parameters and the mass of the atoms, and K_{ij} are the force coefficients. Secular equation (1) is equivalent to the characteristic equation

$$\lambda^n - s_1\lambda^{n-1} + s_2\lambda^{n-2} - \ldots + (-1)^{n-1}s_{n-1}\lambda + (-1)^n s_n = 0, \tag{2}$$

where

$$s_1 = \sum_{i=1}^{n} \lambda_i, \quad s_2 = \sum_{i \neq j=1}^{n} \lambda_i \lambda_j, \ \ldots, \ s_n = \prod_{i=1}^{n} \lambda_i. \tag{3}$$

On the other hand, taking into consideration that s_k is a sum of all principal minors of the determinant of the matrix $\| D_{ij} \|$ of order k we have

$$s_1 = \sum_{\alpha=1}^{N} d_{\alpha}\varepsilon_{\alpha}, \quad s_2 = \sum_{\alpha,\beta=1}^{N} d_{\alpha\beta}\varepsilon_{\alpha}\varepsilon_{\beta}, \ \ldots, \ s_k = \sum_{\alpha,\beta,\ldots,\varkappa}^{N} d_{\alpha\beta\ldots\varkappa}\varepsilon_{\alpha}\varepsilon_{\beta}\ldots\varepsilon_{\varkappa}. \tag{4}$$

Here the d's are the coefficients depending upon the geometrical parameters and force coefficients and are invariant under isotope replacement; $\varepsilon_{\alpha} = m/m_{\alpha}$, where m is a standard mass, and m_{α} is a mass of the atom a_{α}.

If we raise the matrix $\| D_{ij} \|$ to the power of the order p, then as is known from the theory of matrices,[6] the characteristic elements of the matrix $\| D_{ij}^p \|$ are equal to the characteristic elements of matrix $\| D_{ij} \|$ of degree p, that is, $\lambda_1^p, \lambda_2^p, \ldots \lambda_n^p$. Consequently, the following characteristic equation will correspond to the matrix $\| D_{ij}^p \|$

$$\lambda^n - \sigma_{1,p}\lambda^{n-1} + \sigma_{2,p}\lambda^{n-2} - \ldots + (-1)^{n-1}\sigma_{n-1,p}\lambda + (-1)^n\sigma_{n,p} = 0, \tag{5}$$

where

$$\sigma_{1,p} = \sum_{i=1}^{n} \lambda_i^p, \quad \sigma_{2,p} = \sum_{i \neq j=1}^{n} \lambda_i^p \lambda_j^p, \ \ldots, \ \sigma_{n,p} = \prod_{i=1}^{n} \lambda_i^p. \tag{6}$$

Considering that D_{ij} is a linear function of ε_{α}, it follows that D_{ij}^p represents the homogeneous equation of degree p of ε_{α}. Consequently, $\sigma_{k,p}$ represents some homogeneous polynomical of degree kp of ε_{α}.

$$\sigma_{1,p} = \sum_{\alpha,\ldots,\varkappa}^{N} b_{\alpha\beta\ldots\varkappa}\varepsilon_{\alpha}\varepsilon_{\beta}\ldots\varepsilon_{\varkappa}, \quad \sigma_{2,p} = \sum_{\alpha\beta,\ldots,\varkappa\rho}^{N} b_{\alpha\beta\ldots\varkappa\rho}\varepsilon_{\alpha}\varepsilon_{\beta}\ldots\varepsilon_{\varkappa}\varepsilon_{\rho}, \ \ldots. \tag{7}$$

3. Let us choose some group with any $k + 1$ atoms in the molecule. By substituting each of these atoms with one of its isotopes, we obtain the following total number of the isotopic molecules: C_{k+1}^0—without substitution, C_{k+1}^1—one atom substituted, ... C_{k+1}^i—i atoms substituted, C_{k+1}^{k+1}—$(k + 1)$ atoms substituted giving a total of 2^{k+1} molecules. It was shown in reference 3 that if we have a function

$$\Phi_k^i(a_{\alpha}a_{\beta}\ldots a_{\varkappa}) = \sum_j C_j [f_{j1}(m_1) f_{j2}(m_2)\ldots f_{jk}(m_k)]$$

(where C_j are the coefficients not depending on mass; $f_{jr}(m_{\alpha})$ is an arbitrary function of mass of the 1 atom; the index k indicates the number of the products; the index i indicates the number of the substituted atoms, and in the brackets are shown the substituted atoms) then the function satisfies the following identity:

$$\sum_{i=0}^{k+1}(-1)^i C^i_{k+1}\Phi^i_k(a_\alpha a_\beta \dots a_i)=0, \quad (k=1, 2, \dots, N-1). \tag{8}$$

Here C^1_{k+1} indicates the number of different functions Φ^1_k which correspond to the i-substituted molecules. Let us examine the various cases.

A. Sum Rules for the Powers of the Squares of the Frequencies. Put $\Phi^1_k(a_\alpha a_\beta \dots a_1)=\sigma_{1p}(a_\alpha a_\beta \dots a_1)$. Applying (8) we obtain

$$\sum_{i=0}^{p+1}(-1)^i C^i_{p+1}\sigma^i_{1p}(a_\alpha a_\beta \dots a_i)=0, \quad (p=1, 2, \dots, N-1), \tag{9}$$

where

$$c_{11}=\sum_{j=1}^{n}\lambda_j, \quad c_{12}=\sum_{j=1}^{n}\lambda_j^2, \quad c_{13}=\sum_{j=1}^{n}\lambda_j^3, \quad \dots, \quad c_{1,\,s-1}=\sum_{j=1}^{n}\lambda_j^{s-1}.$$

B. Rules for the Sum of the Products for the Powers of the Squares of the Frequencies. $\Phi^1_k(a_\alpha a_\beta \dots a_1)=\sigma^l_{1p}(a_\alpha a_\beta \dots a_1)$ ($l=2, 3, 4 \dots$). Substituting in (8) we have

$$\sum_{i=0}^{lp+1}(-1)^i C^i_{lp+1}\sigma^l_{1p}(a_\alpha a_\beta \dots a_i)=0, \quad (lp=2, 3, \dots, N-1), \tag{10}$$

where

$$c_{21}=\sum_{j\neq k}^{n}\lambda_j\lambda_k; \quad c_{22}=\sum_{j\neq k}^{n}\lambda_j^2\lambda_k^2; \quad c_{23}=\sum_{j\neq k}^{n}\lambda_j^3\lambda_k^3, \dots$$

$$c_{31}=\sum_{j\neq k\neq l}^{n}\lambda_j\lambda_k\lambda_l; \quad c_{32}=\sum_{j\neq k\neq l}^{n}\lambda_j^2\lambda_k^2\lambda_l^2, \dots \text{and so forth.}$$

C. Raising s_1 (Eq. 4) to the pth power, we obtain the homogeneous polynomical of degree lp of ε_α. Introduce the definitions

$$\Delta_{1p}=s_1^p=\left(\sum_{i=1}^{n}\lambda_i\right)^p;$$

$$\Delta_{2p}=s_2^p=\left(\sum_{i\neq j}^{n}\lambda_i\lambda_j\right)^p, \quad \dots, \quad \Delta_{lp}=s_l^p=\left(\sum\lambda_i\lambda_j\dots\lambda_l\right)^p. \tag{11}$$

Putting $\Phi^1_k(a_\alpha a_\beta \dots a_1)=\Delta^1_{1p}(a_\alpha a_\beta \dots a_1)$ and applying (8), we have

$$\sum_{i=0}^{p+1}(-1)^i C^i_{p+1}\Delta^i_{1p}(a_\alpha a_\beta \dots a_i)=0, \quad (p=1, 2, \dots, N-1). \tag{12}$$

where

$$\Delta_{11}=\sum_{i=1}^{n}\lambda_i; \quad \Delta_{12}=\left(\sum_{i=1}^{n}\lambda_i\right)^2; \quad \Delta_{13}=\left(\sum_{i=1}^{n}\lambda_i\right)^3, \text{ and so forth.}$$

Let us call (12) the sum rule for the powers of the sum of the squares of the frequencies

$$\sum_{i=0}^{lp+1}(-1)^i C^i_{lp+1}\Delta^i_{1p}(a_\alpha a_\beta \dots a_i)=0, \quad (lp=2, 3, \dots, N-1), \tag{13}$$

where

$$\Delta_{21}=\sum_{i\neq j}^{n}\lambda_i\lambda_j; \quad \Delta_{22}=\left(\sum_{i\neq j}^{n}\lambda_i\lambda_j\right)^2; \quad \Delta_{23}=\left(\sum_{i\neq j}^{n}\lambda_i\lambda_j\right)^3;$$

$$\Delta_{31}=\sum^{n}\lambda_i\lambda_j\lambda_k; \quad \Delta_{32}=\left(\sum\lambda_i\lambda_j\lambda_k\right)^2, \dots$$

Let us call (13) the sum rule for the powers of the sum of the products of the squares of the frequencies.

D. Sum Rules for the Mixed Products of the Squares of the Frequencies. Considering (4) and (7) we have that the products $(s_k s_l)$, $(\sigma_{kp}\sigma_{1r})$, and $(s_k\sigma_{1r})$ represent the homogeneous polynomicals, which correspond to degree k + l, (kp + lp), and (k + lp) of ε_α. Applying (8) the following three relations are obtained:

$$\sum_{i=0}^{k+l+1}(-1)^i C^i_{k+l+1}\left(s^i_k s^i_l\right)(a_\alpha a_\beta \dots a_i)=0,$$

$$(k+l=3, 4, \dots, N-1). \tag{14}$$

$$\sum_{i=0}^{p(k+l)+1}(-1)^i C^i_{p(k+l)+1}\left(\sigma^i_{1p}\sigma^i_{lp}\right)(a_\alpha a_\beta \dots a_i)=0,$$

$$[p(k+l)=3, 4, \dots, N-1)]. \tag{15}$$

$$\sum_{i=0}^{k+lp+1}(-1)^i C^i_{k+lp+1}\left(s^i_k\sigma^i_{lp}\right)(a_\alpha a_\beta \dots a_i)=0,$$

$$(k+lp=3, 4, \dots, N-1). \tag{16}$$

Some of the derived relations are linearly dependent, due to the formula which connects the coefficients s_k and σ_{1k} of the characteristic equations (2) and (5) (see reference 6, p. 77)

$$s_n=-\frac{1}{k}\left[s_{n-1}c_{11}+s_{n-2}c_{12}+\dots+(-1)^{k-1}s_{n,\,n-1}+(-1)^k c_{1k}\right] \quad (k=1, 2, \dots, n). \tag{17}$$

4. The rules (9), (10), (12)-(16) are satisfied for the frequencies of the harmonic vibrations and are a good approximation for the observed values of the frequencies. For the case when the system of isotopic molecules has the same symmetry, the indicated rules are satisfied by the vibrations of each type of symmetry. But if the isotopic molecules have a different symmetry, then the examined relations are satisfied only for those types whose symmetry is preserved. Otherwise, it is necessary to use the general relations (9), (10), (12)-(16).

The relations obtained could be utilized to test the correctness of the frequencies interpretations of the system of isotopic molecules and to determine the unknown frequencies. For example, applying the sum rules, the sum rules of the products, and the products rules, it is possible to calculate eighteen frequencies of nonplanar vibrations of the six deuteroethylenes and three frequencies of ethylene.

5. To illustrate this, apply some of the obtained relations to deuterobenzene

$$\sum\lambda_i^2(C_6H_6)+[3\sum\lambda_i^2(o\text{-}C_6H_4D_2)+2\sum\lambda_i^2(m\text{-}C_6H_4D_2)+\sum\lambda_i^2(p\text{-}C_6H_4D_2)]+\sum\lambda_i^2(o\text{-}C_6H_3D_4)=4\sum\lambda_i^2(C_6H_5D)+[2\sum\lambda_i^2(1,2,3\text{-}C_6H_3D_3)+2\sum\lambda_i^2(1,2,4\text{-}C_6H_3D_3)]. \tag{18a}$$

$$\sum\lambda_i^2(C_6H_6)+[2\sum\lambda_i^2(o\text{-}C_6H_4D_2)+3\sum\lambda_i^2(m\text{-}C_6H_4D_2)+\sum\lambda_i^2(p\text{-}C_6H_4D_2)]+\sum\lambda_i^2(m\text{-}C_6H_2D_4)=4\sum\lambda_i^2(C_6H_5D)+[\sum\lambda_i^2(1,2,3\text{-}C_6H_3D_3)+2\sum\lambda_i^2(1,2,4\text{-}C_6H_3D_3)+\sum\lambda_i^2(1,3,5\text{-}C_6H_3D_3)]. \tag{18b}$$

$$\sum\lambda_i^2(C_6H_6)+[2\sum\lambda_i^2(o\text{-}C_6H_4D_2)+2\sum\lambda_i^2(m\text{-}C_6H_4D_2)+2\sum\lambda_i^2(p\text{-}C_6H_4D_2)]+\sum\lambda_i^2(p\text{-}C_6H_2D_4)=4\sum\lambda_i^2(C_6H_5D)+4\sum\lambda_i^2(1,2,4\text{-}C_6H_3D_3). \tag{18c}$$

Three more relations are obtained by replacing H with D and D with H

$$\sum\lambda_i^4(C_6H_6)+[4\sum\lambda_i^4(o\text{-}C_6H_4D_2)+4\sum\lambda_i^4(m\text{-}C_6H_4D_2)+2\sum\lambda_i^4(p\text{-}C_6H_4D_2)]+[2\sum\lambda_i^4(o\text{-}C_6H_3D_3)+2\sum\lambda_i^4(m\text{-}C_6H_3D_3)+\sum\lambda_i^4(p\text{-}C_6H_3D_3)]=5\sum\lambda_i^4(C_6H_5D)+[3\sum\lambda_i^4(1,2,3\text{-}C_6H_3D_3)+6\sum\lambda_i^4(1,2,4\text{-}C_6H_3D_3)+\sum\lambda_i^4(1,3,5\text{-}C_6H_3D_3)]+\sum\lambda_i^4(C_6HD_5). \quad (19)$$

Analogous relations are obtained by replacing H with D and D with H

$$\sum\lambda_i^5(C_6H_6)+[6\sum\lambda_i^5(o\text{-}C_6H_4D_2)+6\sum\lambda_i^5(m\text{-}C_6H_4D_2)+3\sum\lambda_i^5(p\text{-}C_6H_4D_2)]+[6\sum\lambda_i^5(o\text{-}C_6H_3D_4)+6\sum\lambda_i^5(m\text{-}C_6H_3D_4)+3\sum\lambda_i^5(p\text{-}C_6H_3D_4)]+\sum\lambda_i^5(C_6D_6)=6\sum\lambda_i^5(C_6H_5D)+[6\sum\lambda_i^5(1,2,3\text{-}C_6H_3D_3)+12\sum\lambda_i^5(1,2,4\text{-}C_6H_3D_3)+2\sum\lambda_i^5(1,3,5\text{-}C_6H_3D_3)]+6\sum\lambda_i^5(C_6HD_5). \quad (20)$$

Let us also demonstrate one numerical example by applying (9) and (12) to the frequencies of the nonplanar vibration of deuteroethylene, which are indicated in reference 2.

$$\frac{1}{4}\left[\sum\lambda_i^3(C_2H_4)+\sum\lambda_i^3(C_2D_4)\right]+\frac{1}{2}\left[\sum\lambda_i^3(t\text{-}C_2H_2D_2)+\sum\lambda_i^3(c\text{-}C_2H_2D_2)+\sum\lambda_i^3(a\text{-}C_2H_2D_2)\right]=\sum\lambda_i^3(C_2H_3D)+\sum\lambda_i^3(C_2HD_3).$$

Here the left-hand side is equal to 2.929927 and the right-hand side to 2.930817; the difference is 0.00089

$$\frac{1}{4}\left[\left(\sum\lambda_i\right)^3(C_2H_4)+\left(\sum\lambda_i\right)^3(C_2D_4)\right]+\frac{1}{2}\left[\left(\sum\lambda_i\right)^3(t\text{-}C_2H_2D_2)+\left(\sum\lambda_i\right)^3(c\text{-}C_2H_2D_2)+\left(\sum\lambda_i\right)^3(a\text{-}C_2H_2D_2)\right]=\left(\sum\lambda_i\right)^3(C_2H_3D)+\left(\sum\lambda_i\right)^3(C_2HD_3).$$

The left-hand side is equal to 23,853577, and the right-hand side to 23,907672; the difference is 0.054095.

REFERENCES

1. L. M. Sverdlov. Doklady Akad. Nauk SSSR **78**, 1115 (1951).
2. L. M. Sverdlov. Doklady Akad. Nauk SSSR **86**, 513 (1952).
3. L. M. Sverdlov. Doklady Akad. Nauk SSSR **88**, 249 (1953).
4. L. M. Sverdlov. Doklady Akad. Nauk SSSR **94**, 451 (1954).
5. J. Bigeleisen. J. Chem. Phys. **28**, 694 (1958).
6. F. R. Gantmakher. "Teoriya Matrits." (The Theory of Matrices), GITTL, Moscow, 1953.

FREQUENCIES OF THE FUNDAMENTAL VIBRATIONS OF THE SO_3 MOLECULE

G. A. Khachkuruzov

Received 18 June 1959

Of the proposed frequency assignments for the fundamental vibrations of the SO_3 molecule, the most satisfactory was given by Gerding and Lecomte. The defect in this assignment consists of the fact that, in it, the frequencies of three fundamental vibrations (ν_1, ν_2, ν_3) correspond to the free molecule in the gas, while the frequency of the fourth fundamental vibration ν_4 corresponds to the nonfree SO_3 molecule in the liquid. Use of the results of experimental investigations into the equilibrium of the decomposition reaction of SO_3 into SO_2 and O_2 has permitted the establishment of the value ν_4 = 440 cm^{-1} for the free sulfur trioxide molecule.

Present-day knowledge of the vibrational frequencies of the SO_3 molecule is based only on the results obtained by Gerding, Nijveld, and Muller[1] in a study of the Raman spectra of liquid and gaseous sulfur trioxide, and on the results obtained by Gerding and Lecomte[2] in a study of the infrared spectrum of gaseous sulfur trioxide.

According to the latter, the frequencies of the fundamental vibrations of the SO_3 molecule are

$$\nu_1 = 1069\ см^{-1};\ \nu_2 = 652\ см^{-1};\ \nu_3 = 1333\ см^{-1};\ \nu_4 = 532\ см^{-1}. \quad (1)$$

Here ν_1 is the frequency of the planar symmetric vibration, ν_2 is the frequency of the nonplanar vibration, and ν_3 and ν_4 are the frequencies of the doubly degenerate planar vibrations (antisymmetric stretching and deformational). In the Raman spectrum, the vibrations with the frequencies ν_1, ν_2, and ν_4 are active, and in the infrared spectrum the vibrations with the frequencies ν_2, ν_3, and ν_4 are active.

In the Raman spectrum of sulfur trioxide vapor,[1] there was found only one SO_2 line at 1069 cm^{-1}, the identification of which with the frequency ν_1 follows from polarization measurements.[3,4] The detailed analysis of the Raman spectra of liquid sulfur trioxide carried out by Gerding, Nijveld, and Muller[1] permitted the conclusion that, of the large number of observed lines, only three lines: at 1068, 532, and 1389 cm^{-1} could be ascribed to the monomeric SO_3 molecule. The results of measurements of the degree of depolarization of the lines at 532 and 1389 cm^{-1} [3,4] led these authors to the conclusion that they are due to the fundamental vibrations of the molecule with frequencies ν_2 and ν_4.

In the infrared spectrum of gaseous SO_3 (see reference 2), there were observed two bands of moderate intensity at 652 and 1123 cm^{-1} and a very intense band at 1333 cm^{-1}. Gerding and Lecomte identified the band centers at 652 and 1333 cm^{-1} with the frequencies ν_2 and ν_3, while the diffuse band at 1123 cm^{-1} was ascribed to an admixture of SO_3 in the sulfur trioxide sample investigated.

Thus, in the assignment presented in reference 2 for the fundamental vibration frequencies of the SO_3 molecule (1), the values of the frequencies ν_1, ν_2, and ν_3 may be considered as sufficiently accurately established. For the frequency of the deformational vibration ν_4, Gerding

and Lecomte took the value 532 cm^{-1}, determined in reference 1 on the basis of the Raman spectra of liquid sulfur trioxide and its mixtures with sulfur dioxide. However, in the vibrational spectra of gaseous sulfur trioxide[1,2] this frequency was not observed.

It should be noted that in liquid sulfur trioxide the intermolecular interactions are very strong, in consequence of which the formation of polymeric molecules S_2O_6, etc., is observed. The very significant forces of intermolecular interaction in liquid sulfur trioxide manifest themselves in a difference between the fundamental vibration frequencies of the monomeric SO_3 molecules in liquid sulfur trioxide and those of the free SO_3 molecules in the gas. As an example, we may point out the significant difference between the ν_3 frequency of the monomeric SO_3 molecule in the liquid (1389 cm^{-1})[1] and the free SO_3 molecule in the gas (1333 cm^{-1}).[2] Therefore, the fact that the line at 532 cm^{-1} which is observed in the Raman spectrum of sulfur trioxide may be ascribed to the monomeric molecule SO_3 and may be interpreted as the ν_4 frequency of this molecule, does not by any means indicate that this frequency will have the same value for the free SO_3 molecule as well.

The unsatisfactory nature of the frequency assignment of the SO_3 molecule proposed by Gerding and Lecomte was discovered some time ago in attempts to use these frequencies for evaluation of the thermodynamic functions of gaseous sulfur trioxide and for subsequent determination of the heat of the reaction

$$SO_3\,(gas) = SO_2\,(gas) + \frac{1}{2}\,O_2\,(gas) \qquad (2)$$

on the basis of the experimental values of the equilibrium constant. The thermodynamic functions of gaseous sulfur trioxide evaluated on the basis of frequencies (1), in conjunction with the thermodynamic functions of SO_2 and O_2 and the experimental values for the equilibrium constant of reaction (2), led to values for the heat of reaction (2) at 0°K which varied systematically, depending on the temperature at which the equilibrium constant was determined. In consequence of this, the assignment of the SO_3 frequencies proposed by Gerding and Lecomte was reconsidered by Stephenson (see references 5 and 6).

Stephenson proposed to identify the line at 532 cm^{-1}, observed by Gerding, Nijveld, and Muller in the Raman spectrum of liquid sulfur trioxide, with the frequency ν_2, and to interpret the band at 1123 cm^{-1}, observed by Gerding and Lecomte in the infrared spectrum of the gas, as the overtone $2\nu_4$. Thus Stephenson took ν_4 equal to 560 cm^{-1}. The assignment of the frequencies ν_1 and ν_3 was not subject to doubt. Thus, according to Stephenson, the fundamental vibration frequencies of SO_3 have the following values:

$$\nu_1 = 1069\ cm^{-1};\ \nu_2 = 532\ cm^{-1};\ \nu_3 = 1333\ cm^{-1};\ \nu_4 = 560\ cm^{-1}. \qquad (3)$$

However, the determination of the thermodynamic functions of gaseous sulfur trioxide in a satisfactory way with the help of frequencies (3) was also unsuccessful. Evaluated in the harmonic-oscillator, rigid-rotator approximation, these functions also led to a temperature "drift" of the value of ΔH_0° for reaction (2), using the experimental values of the equilibrium constant. Stockmayer, Kavanagh, and Mickley[6] erroneously ascribed this drift to the circumstance that, in evaluating the thermodynamic functions of SO_3 according to frequencies (3), the anharmonicity of the vibrations of the SO_3 molecule was not taken into consideration. However, for the temperature interval 700-1200°K, in which the experimental values for the equilibrium constant of reaction (2) were determined, the contribution of the anharmonicity of the vibrations of the SO_3 molecule in the evaluation of the thermodynamic functions cannot be substantial, as the example of such molecules as SO_2 and CO_2 testifies. In order to determine the thermodynamic functions of SO_3 on the basis of frequencies (3), the authors[6] were compelled, with the help of very arbitrary assumptions, to take anomalously high values for two anharmonicity constants.

One should also note the unsatisfactory nature, from the point of view of available spectral data, of the frequency assignment for SO_3 proposed by Stephenson. The frequencies ν_3 and ν_4, determined by Stephenson as 532 and 560 cm^{-1} respectively, as was shown above, must be active in the infrared spectrum, while Gerding and Lecomte[3] observed no absorption of any sort in the region from 500 to 650 cm^{-1}. Furthermore, in the frequency assignment for SO_3 proposed by Stephenson, the intense band in the infrared spectrum at 652 cm^{-1} was ignored, though there is no doubt of its belonging to the SO_3 molecule, while the weak band at 1123 cm^{-1} was taken into the calculation, though its belonging to the SO_3 molecule was not shown.

As has already been pointed out, the probable cause of the lack of correspondence between the calculated values for the thermodynamic functions of gaseous sulfur trioxide based on frequencies (1) and the experimental values for the equilibrium constant of reaction (2) is the circumstance that a value corresponding to the vibration of the nonfree SO_3 molecules in the liquid, but not corresponding to the vibration of the free SO_3 molecules in the gas, was taken for the frequency ν_4. In view of this, we decided to make use of the available data from the study of the equilibrium of reaction (2) as well as the data[7] on the structure of the SO_3 molecule, together with the values (1) for the frequencies ν_1, ν_2, and ν_3, for an approximate determination of the frequency ν_4.

The experimental determination of the values of the equilibrium constant of reaction (2) has been carried out by many investigators in connection with the fact that this reaction is the basis of the industrial processes for the manufacture of sulfuric acid. The methodological merits and defects of previous investigations of the equilibrium of reaction (2) have been considered by Kapustinskii and Shamovskii.[8] The most reliable measurements, as far as method is concerned, were carried out by Bodenstein and Pohl,[9] Taylor and Lehner,[10] and Kapustinskii and Shamovskii.[9,11]

The heat of the reaction

$$SO_3\,(l) = SO_2\,(g) + \frac{1}{2}\,O_2\,(g)$$

was determined by Roth, Grau, and Meichsner[12] at 293.15°K on the basis of the results of a series of calorimetric measurements ($\Delta H_{293.15}$ = 33.66 ± 0.06 kcal/mol). From measurements of the vapor pressure of sulfur trioxide[13,14] it follows that the heat of vaporization of sulfur trioxide equals 10.22 ± 0.10 kcal/mol. Therefore the heat of reaction (2) at 293.15°K equals

$$\Delta H^\circ_{293.15} = +23.44 \pm 0.16\ \text{kcal/mol}. \qquad (4)$$

The connection between the equilibrium constant of reaction (2) and the heat of this reaction at 293.15°K may be defined by the following equation:

$$R \ln K_p = \Delta\Phi_T^{(293)} - \frac{\Delta H^\circ_{293.15}}{T}, \qquad (5)$$

where

$$\Phi_T^{(293)} = -\frac{\Phi^\circ_T - H^\circ_{293.15}}{T} = \Phi^*_T - \frac{H^\circ_{293.15} - H^\circ_0}{T}. \qquad (6)$$

In expression (6), Φ°_T denotes the isobaric thermo-

dynamic potential and Φ_T^* the reduced isobaric thermodynamic potential

$$\left(\Phi_T^* = -\frac{\Phi_T^0 - H_0^0}{T}\right),$$

which is directly related to the statistical sum over the states of the molecule ($\Phi_T^* = R \ln Q_T$).

In accordance with Eq. (5), the change in the thermodynamic function $\Phi_T^{(293)}$ may be evaluated by the formula

$$\Delta\Phi_T^{(293)} = R \ln K_p + \frac{\Delta H_{293.15}^0}{T}. \qquad (7)$$

On the other hand, by definition

$$\Delta\Phi_T^{(293)} = \Phi_T^{(293)}(SO_3) + \frac{1}{2}\Phi_T^{(293)}(O_2) - \Phi_T^{(293)}(SO_3). \qquad (8)$$

where, in accordance with (6), the values $\Phi_T^{(293)}(SO_3)$, $\Phi_T^{(293)}(O_2)$, and $\Phi_T^{(293)}(SO_3)$ may be evaluated by the formulas of statistical thermodynamics on the basis of the molecular constants of SO_2, O_2, and SO_3.

The details of the calculation of $\Delta\Phi_T^{(293)}$ of reaction (2) by formulas (7) and (8) are presented in reference 15. The results of these calculations are presented in the figure, on which are entered the experimental values of $\Delta\Phi_T^{(293)}$, calculated by formula (7) on the basis of the experimental values of the equilibrium constant of reaction (2) obtained in references 8-10, 16, and of the values (4) for the heat of the reaction at 293.15°K. Beside this, the calculated values of $\Delta\Phi_T^{(293)}$, evaluated according to formula (8), are entered on the figure (curves I-V). The calculated values for the functions of SO_2 and O_2, based on the known values for the molecular constants of these compounds, and the calculated values of $\Phi_T^{(293)}(SO_3)$ were used for this. The latter were evaluated, on the basis of the known values for the geometric parameters of the SO_3 molecule,[7] in five variants corresponding to the following assumptions about the values of the fundamental vibration frequencies: I—the values (1) proposed by Gerding and Lecomte;[2] II—the values (3) proposed by Stephenson;[3] III—ν_1, ν_2, ν_3 the same as in (1), ν_4 = 460 cm^{-1}; IV—the same, but ν_4 = 440 cm^{-1}; V—the same, but ν_4 = 420 cm^{-1}.

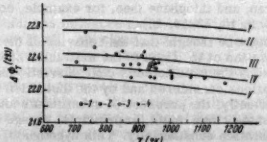

Values of $\Delta\Phi_T^{(293)}$ (in cal/mole-deg) for the reaction $SO_3 = SO_2 + \frac{1}{2}O_2$. Experimental values: 1—Knietsch;[16] 2—Bodenstein and Pohl;[9] 3—Taylor and Lehner;[10] 4—Kapustinskii and Shamovskii.[6,11] Curves I-V—calculated values.

From the figure it can be seen that each variant of the calculated values of $\Delta\Phi_T^{(293)}$ lies on a smooth curve which is almost a straight line. The bulk of the experimental points are concentrated between lines III and V, near line IV. The points corresponding to the measurements of Bodenstein and Pohl,[9] which, as shown in reference 8, are the most exact, lie particularly close to line IV. The points based on the data of Knietsch[16] are the most scattered, in accordance with their significantly lesser accuracy.

The arrangement of the experimental and calculated values for the quantity $\Delta\Phi_T^{(293)}$ on the figure shows that the sets of fundamental frequencies of SO_3 proposed by Gerding and Lecomte[2] (line I) and by Stephenson[3] (line II) are erroneous. The results of the calculation of the quantity $\Delta\Phi_T^{(293)}$ according to variant IV, to which the following set of fundamental frequencies of SO_3 corresponds:

$$\nu_1 = 1069\ cm^{-1};\ \nu_2 = 652\ cm^{-1};$$

$$\nu_3 = 1333\ cm^{-1};\ \nu_4 = 440\ cm^{-1}. \qquad (9)$$

agree best with the results of the experimental measurement of the equilibrium constant of reaction (2).

The error in the frequency ν_4 determined in this way is estimated as $\pm 30 cm^{-1}$.

It appears desirable to investigate the infrared spectrum of gaseous sulfur trioxide over a considerably broader region than that described in reference 2. It would be particularly interesting to investigate the long wavelength region of the infrared spectrum of SO_3, in order to verify the accuracy of the value of the frequency ν_4 found in the present work.

REFERENCES

1. H. Gerding, W. J. Nijveld, and G. J. Muller. Z. physik. Chem. 35B, 193 (1937).
2. H. Gerding and J. Lecomte. Physica 6, 737 (1939).
3. S. Bhagavantam. Indian J. Phys. 5, 63 (1930).
4. S. Venkateswaran. Phil. Mag. 15, 263 (1933).
5. D. M. Yost and H. Russell. "Systematic Inorganic Chemistry of the 5th and 6th Group Nonmetallic Elements." Prentice-Hall, New York, 1944.
6. W. H. Stockmayer, G. M. Kavanagh, and H. S. Mickley. J. Chem. Phys. 12, 408 (1944).
7. K. J. Palmer. J. Am. Chem. Soc. 60, 2360 (1938).
8. A. F. Kapustinskii and L. M. Shamovskii. Trudy Vses. n.-issl. inst. mineral'nogo syr'ya (Transactions of the All-Union Scientific Research Institute of Mineral Resources), No. 109, p. 55, ONTI, Moscow, Leningrad, 1936.
9. M. Bodenstein and W. Pohl. Z. Elektrochem. 11, 373 (1905).
10. G. B. Taylor and S. Lehner. Z. physik. Chem., Bodenstein-Festband, 30 (1931).
11. A. F. Kapustinskii and L. M. Shamovskii. Acta Physicochim. URSS 4, 791 (1936).
12. W. A. Roth, R. Grau, and A. Meichsner. Z. anorg. Chem. 193, 161 (1930).
13. A. Smith and P. Schoenmaker. J. Chem. Soc. 125, 2554 (1924); 1108 (1926).
14. R. Grau and W. A. Roth. Z. anorg. Chem. 188, 186 (1930).
15. G. A. Khachkuruzov. Sbornik tr. GIPKh po fiz. Khim. no. 45 (in press).
16. R. Knietsch. Ber. V Kongr. angew. Chem. 1, 613 (1903).

ON POLARIZATION RELATIONSHIPS IN RAMAN SPECTRA OF MOLECULES WITH A HIGH DEGREE OF CONJUGATION

Ya. S. Bobovich and M. Ya. Tsenter

Received 4 June 1959

The influence of conjugation on the polarization state of the Raman lines of 26 aromatic compounds has been studied. It has been established that the degree of depolarization of all lines for the majority of the substances studied tends toward the value 0.5.

The hypothesis is expressed that the observed effect is associated with the presence, in molecules with a high degree of conjugation, of a particular direction of the maximum polarizability α, and consequently of the derivative $\partial\alpha/\partial q$ also.

The polarization state of Raman lines, as is well known, is closely connected with the vibration type and with the symmetry of the resting and of the vibrating molecule. The quantities which characterize the polarization state of the lines—the degrees of depolarization ρ—are subject to a number of exact and approximate rules, which make it possible to decide, for each given molecule, about the shape of the ellipsoid of the derivative of the polarizability with respect to the normal coordinate, $\partial\alpha/\partial q$, and consequently also about the symmetry of the corresponding vibration.[1] Thus, for example, it turns out that upper limit values of ρ (near 0.86) are characteristic of antisymmetric vibrations, while low values, on the other hand, are characteristic of totally symmetric vibrations. In the particular case of highly symmetrical molecules (with tetrahedral symmetry or higher), the degree of depolarization ρ of the totally symmetric vibrations becomes zero. For diatomic molecules, and also for the characteristic vibrations of isolated bonds, the limiting possible value of ρ equals 0.5. This corresponds to a completely anisotropic $\partial\alpha/\partial q$ ellipsoid, elongated in the direction of the bond.

The available experimental material gives good confirmation of the polarization rules. Beside this, facts are described in the literature which testify to the substantial influence of conjugation on the polarization relationships in spectra. Studying series of para-, ortho-, and meta-derivatives of nitrobenzene, Bobovich and Vol'kenshtein[2] showed that in the first and second cases, as the electropositivity of the substituent increases, the degree of depolarization ρ of the totally symmetric stretching vibration of the nitro group increases, tending toward the limiting value 0.5.* With the limiting value of this quantity there was associated a completely anisotropic $\partial\alpha/\partial q$ ellipsoid of the nitro group, oriented along its symmetry axis. In the meta derivatives, on the contrary, the degree of depolarization of the same line was independent of the nature of the substituent and equal to 0.22. Shorygin[3] obtained analogous results for some aromatic nitro compounds. Sushchinskii and Tiulin,[4] and also Yakovleva[5], established an increase of the degree of depolarization, in comparison with an isolated bond in a simpler case—for the vibration of conjugated multiple carbon-carbon bonds. Later, a similar phenomenon was observed for a large number of new compounds in the work of Bobovich and Perekalin.[6] The behavior of the antisymmetric vibration of the benzene ring proved extremely interesting. According to the data of Yakovleva,[5] Shorygin,[7] and Bobovich and Perekalin,[8] the line of this vibration becomes partially polarized as the conjugation increases. The impression is given that the form of this vibration changes, depending on the conjugation.

*Here and hereafter we consider that a high degree of conjugation is determined not only by the number of conjugated bonds, but also by the presence in the molecule, in the para or ortho positions, of groups which are opposite with respect to their electron-donor and -acceptor properties.

We set ourselves the task of systematically investigating the question of the influence of conjugation on the polarization state of Raman lines, on the basis of various vibrations of the widest possible range of materials. All measurements were carried out by the photoelectric method. Information on the experimental setup is contained in references 6, 8, and 9. In place of the model described in reference 9, we used a domestic variant of this apparatus (DFS-12). In all cases the samples were excited by the blue mercury line (4358 A).

The data obtained by us on the degree of depolarization of the lines are collected in Table 1. From the table it can be seen that the degree of depolarization of all lines for the majority of the substances studied tends to one and the same critical value, namely, 0.5. This phenomenon has a universal character, appearing equally well in the characteristic vibrations of isolated bonds (NO, C=C, C≡C, C≡N), in the totally symmetric and antisymmetric vibrations of the NO_2 group, and in the complex vibrations of various rings: benzene, naphthalene, furan, and thiophene (see, for example, compounds 1, 2, 4–7, 9, 10, 12–14, 16).

It might be thought that the behavior of the degree of depolarization of the lines in the molecules studied by us is caused by the insufficiently characteristic nature of the vibrations considered and by the distortion of their form. Actually, the presence of substituents and side chains on the rings might, in principle, change the form of the vibration substantially. This hypothesis, however, appears doubtful if we compare with one another the data for m-dinitrobenzene, toluene, and the xylenes (21–25), and most of the other compounds of Table 1 which contain benzene rings. It turns out that there are cases where the substituents do not influence the form of the vibrations at all. Judging from literature sources, such cases are widespread.[10]

An increase in conjugation is usually accompanied by a shift of the long wavelength absorption band of the molecules into the visible region. Most of the substances contained in Table 1, therefore, have a more or less intense color. This means that the Raman spectra of these substances are being excited under conditions close to optical resonance. Thus, for example, the maximum of the absorption band of nitrosodimethylaniline (1) lies at 4000 A and that of the furyl nitro derivative (2) at 3780 A, while the exciting line has a wavelength of 4358 A; i.e., in essence, it falls within the absorption band. How res-

Table 1. Degree of Depolarization ρ in Raman Spectra of Some Aromatic Compounds

No.	Compound	Solvent, concentration in moles/liter	Vibrational frequency (in cm^{-1}) and degree of depolarization
1		CCl_4, $5.5 \cdot 10^{-4}$	1420 (NO, 0.46)
2	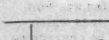	CCl_4, $1 \cdot 10^{-2}$	1140 (0.44), 1335 (NO_2, symm., 0.46), 1465 (0.45), 1620 (C=C, 0.48)
		Acetone, $5 \cdot 10^{-4}$	1335 (NO_2, symm., 0.46), 1620 (C=C, 0.50)
3	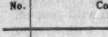	CCl_4, $6.3 \cdot 10^{-2}$	1335 (NO_2, symm., 0.41), 1620 (C=C, 0.34)
4*		CCl_4, $2 \cdot 10^{-2}$	1180 (0.46), 1280 (0.48), 1325 (NO_2, symm., 0.47), 1500 (NO_2, ant., 0.40)
		Acetone, $4 \cdot 10^{-2}$	1180 (0.39), 1280 (0.32), 1325 (NO_2, symm., 0.49), 1500 (NO_2, ant., 0.45), 1600 (benz. r, ant., 0.45), 1625 (C=C, 0.42)
5*	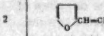	CCl_4 + acetone, $1.8 \cdot 10^{-2}$	1180 (0.36), 1260 (0.35), 1335 (NO_2, symm., 0.42), 1610 (benz. r, ant., 0.48), 1625 (C=C, 0.44)
		Acetone, $6.2 \cdot 10^{-2}$	1610 (NO_2, ant., 0.55)
6†		Acetone, $2.4 \cdot 10^{-2}$	1325 (NO_2, symm., 0.43), 1610 (benz. r, ant., 0.49), 1660 (C=C, 0.43)
7		CCl_4 + acetone, $3.6 \cdot 10^{-2}$	1255 (0.47), 1335 (NO_2, symm., 0.39), 1590 (benz. r, ant., 0.45), 1630 (C=C, 0.44)
		Acetone, $6 \cdot 10^{-2}$	1510 (NO_2, ant., 0.58)
8	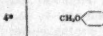	CCl_4, $6.3 \cdot 10^{-2}$	1110 (0.37), 1185 (0.32), 1210 (0.32), 1260 (0.33), 1300 (0.34), 1350 (NO_2, symm., 0.43), 1590 (benz. r, ant., 0.49), 1640 (C=C, 0.46)
		Acetone, $1 \cdot 10^{-1}$	1110 (0.31), 1350 (NO_2, symm. 0.44), 1590 (benz. r., ant., 0.55)
9		CCl_4 + acetone, $2 \cdot 10^{-2}$	1325 (NO_2, symm., 0.50), 1510 (NO_2, ant., 0.43), 1590 (benz. r, ant., 0.61)
		Acetone,	1325 (NO_2, symm., 0.43)
10	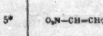	CCl_4 + acetone, 10^{-2}	1335 (NO_2, symm., 0.50)
11†	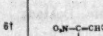	Acetone, $1 \cdot 10^{-1}$	1340 (NO_2, symm., 0.42), 1500 (NO_2, ant., 0.50), 1600 (benz. r, ant., 0.50)
12	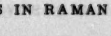	H_2O, $6 \cdot 10^{-2}$	1150 (0.49), 1190 (0.57), 1280 (0.54), 1350 (NO_2, symm., 0.50), 1500 (benz. r, ant., 0.80), 1625 (C=C, 0.58)
13	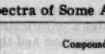	CCl_4, $1.8 \cdot 10^{-2}$	1335 (NO_2, symm., 0.33), 1570 (naph. r., ant., 0.56)
14	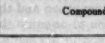	Acetone, $1 \cdot 10^{-1}$	1345 (NO_2, symm., 0.40), 1580 (benz. r., ant., 0.51), 1610 (C=C, 0.42), 2230 (C≡N, 0.48)
15	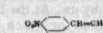	Acetone, satd.	1335 (NO_2, symm. 0.35), 1590 (benz. r., ant., 0.60)
16	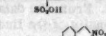	CCl_4 + acetone, $2 \cdot 10^{-2}$	990 (0.40), 1055 (0.47), 1210 (0.55), 1280 (0.39), 1370 (0.47), 1420 (0.48), 1585 (0.46)
17†	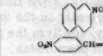	Acetone, 1.6	1610 (benz. r., ant., 0.55), 1640 (C=C, 0.28)
18	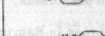	Dichloroethane, $7 \cdot 10^{-1}$	1000 (benz. r., symm., 0.28), 1190 (0.44), 1590 (benz. r., ant., 0.59), 1620 (C=C, 0.49)
19	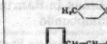	Acetone	1010 (benz. r., symm., 0.27), 1145 (0.45), 1590 (benz. r., ant., 0.61), 2220 (C≡C, 0.49)
20†	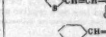	Acetone, $5 \cdot 10^{-1}$	1345 (NO_2, symm., 0.28), 1510 (NO_2, ant., 0.72), 1600 (benz. r., ant., 0.55)
21	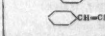	Acetone,	1340 (NO_2, symm., 0.28), 1530 (NO_2, ant., 0.97), 1600 (benz. r., ant., 1.0)
22	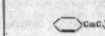	Pure	1010 (benz. r., symm., 0.03), 1040 (benz. r., symm., 0.02), 1590 (benz. r., ant., 0.88)
23		Pure	215 (0.86), 270 (0.92), 530 (0.30), 730 (0.07), 1000 (benz. r., symm., 0.04), 1250 (0.10), 1370 (0.48), 1500 (benz. r., ant., 0.93)
24	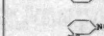	Pure	1590 (benz. r., ant., 0.88)
25		Pure	1590 (benz. r., ant., 0.93)
26		Acetone, satd.	1380 (naph. r., symm., 0.31), 1575 (naph. r., ant., 0.86)

Abbreviations: symm. – totally symmetric vibration; ant – antisymmetric vibration; benz. r. – benzene ring; naph. r. – naphthalene ring.

*In comparison with reference 6, the data given are more precise.
†Data copied from reference 6.

onance conditions influence the polarization state of Raman lines is still not clear. However, it is not possible to exclude, a priori, the possibility of such an influence, and consequently also of a connection between it and the observed phenomena.

If this should be so, then evidently, in colorless substances which do not absorb in the region of the exciting line, polarization effects would always be absent. This is contradicted, however, by the data on the spectra of styrene (17), stilbene (18), and tolan (19), which are characterized by the fairly distinct tendency of the quantity ρ toward the value 0.5. Thus the phenomenon of optical resonance must also be rejected as a possible cause of the observed regularity.*

*We do not exclude the possibility of relatively weak effects associated with the proximity of an absorption band.

The thought presents itself that the peculiar behavior of the degree of depolarization of Raman lines in the cases studied is controlled by the specific structure of the molecules. This consists in the fact that, in highly conjugated molecules, there is always a direction along which, chiefly on account of the delocalized π-electrons, the polarizability α takes on a maximum value. Thus, for example, for molecules with a long chain of conjugated bonds, with unsaturated rings, and with electropositive and electronegative groups in the para position, the symmetry axis passing through all the listed structural elements of the molecule will be in this particular direction. It is entirely natural and probable that the change in the polarizability α in the process of vibration of the nuclei will also be at a maximum in the same direction. Then to any vibration, practically independently of its form, there must always correspond a sufficiently elongated $\partial\alpha/\partial q$ ellipsoid, where q is the normal coordinate of the vibration. In this case, as was noted above, according to theoretical concepts, the degree of depolarization of the line must be very close to 0.5.

The results of polarization measurements in the spectrum of one of the representatives of the meta-derivatives—dinitrobenzene (21)—may serve as a serious argument in favor of the point of view expressed above. As is well known, a meta position of groups prevents conjugation. Correspondingly, polarization anomalies are not observed in the compound studied. In particular, the line of the antisymmetric vibration of the benzene ring proves to be depolarized, in contradistinction, for example, to nitrobenzene (20), where it is noticeably polarized. Analogous results are also obtained for the spectra of naphthalene, toluene, and the xylenes, where the influence of conjugation is relatively small and there is no clearly defined direction in the molecules.

It is interesting to compare the degree of depolarization of the lines with their intensity. It is known that the

intensity of the lines increases with an increase in conjugation. Consequently, there must exist a parallelism between the tendency of the lines to strengthen and the tendency of the degree of depolarization to assume the value 0.5. In Table 2, such a comparison is presented for part of the molecules investigated by us. At the beginning of the table are placed compounds for which the ρ values are particularly close to 0.5. From the data presented, it can be seen that the intensity of the lines also decreases approximately monotonically in the same direction. These results, consequently, confirm the proposed interpretation of the polarization phenomena.

Table 2. Intensity Coefficients of Lines in Raman Spectra of Some Aromatic Compounds

No.	Compound	Vibration frequency (in cm^{-1}) and line on a relative scale
1*	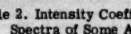	1335 (255), 1620 (95)
2	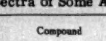	1330 (75), 1510 (5.8), 1600 (3)
3*	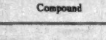	1325 (40), 1500 (3.7), 1600 (19), 1625 (10)
4	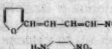	1420 (30), 1585 (54)
5*	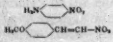	1335 (3.4), 1510 (0.45), 1590 (4.1), 1630 (4.8)
6	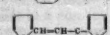	1345 (4.0), 1590—1610 (3.6)
7	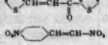	1340 (6.5), 1590 (4.0), 1635 (2.5)
8		1010 (0.9), 1145 (2.2), 1590 (2.8), 2220 (4.8)
9	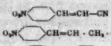	1335 (2.0), 1570 (0.7)
10	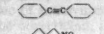	1380 (0.44), 1575 (0.08)
11*	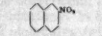	1340 (0.4), 1530 (0.13), 1600 (0.14)
12		1590 (0.02)

*Data copied from reference 6.

Thus, in the spectra of highly conjugated systems, the degree of depolarization of all Raman lines which are due to stretching vibrations ceases to be characteristic. Instead of symmetry of the vibration with respect to the equilibrium configuration, symmetry with respect to the particular direction of maximum polarizability α takes on the decisive role. The appearance of a change in the form of the vibration is created. The degrees of depolarization of lines in the spectra of such systems can no longer be used for identification of the form of the vibration, nor consequently for molecular structural analysis.

REFERENCES

1. M. V. Vol'kenshtein, M. A. El'yashevich, and B. I. Stepanov. "Kolebaniya molekul." (Molecular Vibrations), 2, GTTI, Moscow-Leningrad, 1949; M. V. Vol'kenshtein. Zhur. Eksptl. i Teoret. Fiz. 18, 138 (1948).
2. Ya. S. Bobovich and M. V. Vol'kenshtein. Doklady Akad. Nauk SSSR, 71, 1045 (1950).
3. P. P. Shorygin. Dokt. diss., Fiziko-khimich. Inst. im. Karpova (Doctoral dissertation, Karpov physicochem. Institute), Moscow, 1949.
4. M. M. Sushchinskii and V. I. Tiulin. Doklady Akad. Nauk SSSR 45, 505 (1954).
5. T. V. Yakovleva. Kand. diss., Inst. vysokomolekulyarnykh soedinenii (Dissertation, Institute of High-Molecular Compounds) Akademii Nauk SSSR, 1953.
6. Ya. S. Bobovich and V. V. Perekalin. Doklady Akad. Nauk SSSR 121, 1028 (1958); Zhur. Fiz. Khim. (in press).
7. P. P. Shorygin. Doklady Akad. Nauk SSSR 78, 469 (1951).
8. Ya. S. Bobovich and V. M. Pivovarov. Zhur. Eksptl. i Teoret. Fiz. 29, 696 (1955).
9. B. A. Koselev. Opt. i Spektr. 1, 597 (1956).
10. K. Kohlrausch. "Spektry kombinatsionnogo rasseyaniya." (Raman Spectra), pp. 329-330, Moscow, 1952.

STUDY OF THE INTERACTION BETWEEN PYRIDINE AND WATER BY INFRARED ABSORPTION SPECTRA

A. N. Sidorov

Received 23 May 1959

The infrared spectra of solutions of water in pyridine and in a pyridine-carbon tetrachloride mixture have been studied. It is concluded that two types of water-pyridine aggregates exist in these solutions. The first type is a molecule of water bonded through its H atoms to two molecules of pyridine; the second is a molecule of water bonded to a molecule of pyridine by only one H atom. It is supposed that in the second case the water molecule has an enhanced reactivity. The absorption bands of pyridine molecules which are associated with water are for the most part displaced toward the high-frequency side, which is apparently connected with a displacement of the electron cloud of the pyridine molecule toward the side of the attached water molecule. The spectral changes in pyridine on interaction with water are similar to its changes on adsorption on porous glass, where the pyridine molecule is attached to the surface hydroxyl group with its protonized hydrogen atom. A new interpretation of the spectrum of liquid water in the region of the stretching vibrations of its molecules is proposed.

Organic bases, particularly pyridine, have the property of activating water molecules absorbed on methylated porous glass, thereby promoting the replacement of surface methoxyl groups by hydroxyl.[1] Like the adsorbed water molecules, the surface hydroxyl groups of porous glass are also activated in the presence of pyridine, as is manifested by an increase in the rate of photoreduction of dyes adsorbed on porous glass.[2] In this connection, we have undertaken a study of some details of the interaction of pyridine and water as shown by infrared absorption spectra.

The spectral measurements in this work were carried out on a double-beam Carl Zeiss, Jena, UR-10 infrared spectrophotometer with NaCl and LiF prisms.

Let us consider first the question of the interpretation of the spectrum of liquid water in the region of the stretching vibrations of its molecules.

ON THE INTERPRETATION OF THE SPECTRUM OF LIQUID WATER

Despite the fact that the infrared spectrum of liquid water has been repeatedly studied in the course of the last decades, there is, up to now, no detailed interpretation of this spectrum, and it attracts the attention of investigators as much as ever. In particular, the region of the stretching vibrations of the H_2O, D_2O, and HDO molecules has been studied in the recent works of Bulanin.[3] It was found that the HDO absorption bands located at 3420 and 2510 cm^{-1} have no structure, while the H_2O and D_2O bands have two components each: 3425 and 3290 cm^{-1}, and 2550 and 2435 cm^{-1}, respectively. In view of this, the inference was drawn that the structure of the H_2O and D_2O bands is explained not by different types of aggregates of water molecules but by the activity of both the antisymmetric ν_3 (high-frequency component) and symmetric ν_1 (low-frequency component) molecular vibrations in the infrared absorption spectrum of liquid water. The absence of structure in the HDO absorption band serves, in our opinion, as conclusive confirmation of this inference. However, the question of the assignment of the components of the H_2O and D_2O absorption bands to definite vibrational types requires a more detailed discussion.

In the D_2O absorption band, aside from the components at 2550 and 2435 cm^{-1}, Bulanin found a third intense component with an absorption maximum at 2510 cm^{-1}, which was ascribed by him to absorption by an admixture of HDO. However, close inspection of the contour of the H_2O absorption band shows that, aside from the components at 3425 and 3290 cm^{-1}, there is a third component of this band also, at approximately 3480 cm^{-1}. This component was distinctly observed by Errera and coworkers,[4] who succeeded in recording the H_2O absorption band with a maximum optical density not greater than the 0.5. When working at higher optical densities (about 2.0 in Bulanin's work), the 3480 cm^{-1} component apparently does not appear sufficiently distinctly, in consequence of overlapping by the broad adjacent component. In Fig. 1 is presented the Raman spectrum of liquid water.* Three components are clearly seen in this spectrum: at 3250, 3430, and around 3480 cm^{-1}. Obviously, the D_2O absorption band must also consist of three components. We may then believe that the maximum at 2510 cm^{-1} observed by Bulanin in the D_2O spectrum corresponds not to an admixture of HDO but to the D_2O vibrations proper, although superposition of the HDO band may contribute in some degree to the intensity of this maximum.

*The Raman spectrum of water was measured on a DFS-12 spectrometer with the kind assistance of Ya. S. Bobovich and T. P. Tulub.

Fig. 1. Raman spectrum of liquid water.

According to the data of Hornig and collaborators,[5] the absorption band of ice also consists of three components. By analogy with the interpretation given by these authors for the absorption band of ice, we may propose the following interpretation for the absorption band of water in the region of the stretching vibrations of its molecules (see Table 1).

Table 1. Position and Interpretation of the Absorption Bands of Liquid Water Corresponding to its Stretching and Deformational Vibrations

Position of the bands (frequencies in cm^{-1})			Interpretation of the bands
H_2O	D_2O	HDO *	
3480 ± 20	2580 ± 20	2510 ± 5	ν_1
3425 ± 10	2510 ± 10	3420 ± 10	ν_3
3290 ± 20	2435 ± 20	2930 ± 10	$2\nu_2$
1645 ± 5	1215 ± 5	1460 ± 5	ν_2

*The absorption bands of HDO were measured: ν_1 for the mixture H_2O:D_2O (4:1); ν_3 for the mixture H_2O:D_2O (1:4); $2\nu_2$ for the mixture H_2O:D_2O (1:2). As in Bulanin's work, no structure was found for the HDO absorption band.

To the interpretation presented in Table 1 a few notes should be added. First of all, the absorption band of the first overtone of the HDO deformational vibration at 2930 cm^{-1} is a weak band. The absorption coefficient of the corresponding H_2O and D_2O bands (3290 and 2435 cm^{-1}) is much greater. Such an increase in intensity for the $2\nu_2$ bands of the H_2O and D_2O molecules may be caused by strong Fermi resonance between the vibrations ν_1 and $2\nu_2$. In the case of the HDO molecule, the corresponding frequencies are located far apart and there is no Fermi resonance. Greinacher, Lüttke, and Mecke,[6] and also Saumagne and Josien,[7] studied the changes in the ν_1 and ν_3 frequencies of H_2O molecules in various organic solvents. It was found that, as the donor-acceptor interaction between the H_2O molecules and the solvent molecules grows stronger, the ν_3 frequency falls off faster than ν_1. Thus, the difference $\nu_3 - \nu_1$ amounts to 104 cm^{-1} for water vapor, 91 cm^{-1} for a solution of water in CCl_4, 84 cm^{-1} in nitromethane, and 64 cm^{-1} in dioxane.[8] Considering the interpretation given in Table 1 for the spectrum of liquid water, it may be presumed that, as the intermolecular interaction increases, the difference $\nu_3 - \nu_1$ continues to change in the same direction, becoming negative for liquid water, ice, and a solution in pyridine (see below). For liquid water this difference will amount to minus 55 cm^{-1}, and for ice[5] to minus 110 cm^{-1}.

INTERACTION OF PYRIDINE AND WATER

1. The spectra of solutions of H_2O in pyridine have been repeatedly investigated.[4, 6, 7] In these spectra a broad absorption band of associated water has been found, but no structure within this band. Saumagne and Josien[7] found in the spectrum of a solution of water in a pyridine-carbon tetrachloride mixture, aside from the broad absorption band at 3400 cm^{-1}, a narrow intense band at 3678 cm^{-1}. They assumed that in this case each water molecule is attached to a pyridine molecule by only one hydrogen atom, according to the scheme

$$H\diagup O{-}H \cdots NC_5H_5. \qquad (I)$$

On interaction of water with pyridine according to such a scheme, a disturbance of the interaction between the vibrations ν_1 and ν_3 of the water molecule will take place,

and, to a first approximation, the stretching vibrations of the water molecule will break up into two isolated vibrations: a vibration of the unassociated OH group with the frequency ν_{free} = 3678 cm^{-1}, and a vibration of the associated OH group with the frequency $\nu_{ass.}$ = 3400 cm^{-1}.[7]

In Fig. 2 are presented the absorption spectra obtained by us for solutions of H_2O and D_2O in a pyridine-carbon tetrachloride mixture and in pure pyridine. In the spectrum of the solution of H_2O in the pyridine + CCl_4 mixture, there are observed three bands with maxima at 3685, 3390, and 3205 cm^{-1} (in reference 7, spectral measurements around 3200 cm^{-1} were not carried out).

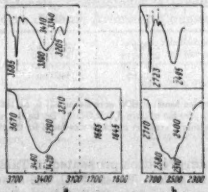

Fig. 2. Absorption spectra of solutions of water. a—H_2O; b—D_2O; below—in pyridine, 1 mole/liter, thickness 0.07 mm, pyridine in the reference beam; above—in a mixture of pyridine + CCl_4 (1:50 by volume), the concentration of water in the mixture corresponding to a ratio of 1 molecule of H_2O to 60 molecules of pyridine, thickness 10 mm pyridine + CCl_4 mixture in the reference beam; crosses indicate the bands of a solution of water in CCl_4.

The band with an absorption maximum at 3390 cm^{-1} in turn consists of three components, which makes it similar to the corresponding band of liquid water. Hence one may draw the conclusion that this band cannot belong to an isolated vibration of the associated OH group, as was assumed in reference 7, since if it did it would not show structure. A triple band with a maximum at 3390 cm^{-1} can belong only to water molecules with undisturbed symmetry. Such molecules may consist of water molecules bonded simultaneously by two hydrogen atoms according to the scheme

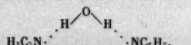

(II)

However, it appears that aggregates bonded to two molecules of pyridine are bulky and may easily decompose, as a result of collisions, with the separation of one pyridine molecule. Consequently, we have a definite dynamic equilibrium between the amounts of aggregates of water molecules with one pyridine molecule (type I) and aggregates with two pyridine molecules (type II). The absorption bands with frequencies 3685 cm^{-1} and 3205 cm^{-1} in the spectrum of a solution of water in a pyridine + CCl_4 mixture correspond, apparently, to the vibrations of the free and associated hydroxyl groups in aggregates of type I (ν_{free} and $\nu_{ass.}$).

In the spectrum of a solution of D_2O in a pyridine + CCl_4 mixture, we found bands at 2495 and 2723 cm^{-1} (Fig. 2). The first of these bands corresponds to D_2O molecules associated according to type II, the second to the ν_{free} frequency for aggregates of type I. We did not succeed in finding the $\nu_{ass.}$ band for these aggregates, in view of the absorption of CO_2 and CCl_4 in this region. One's attention is attracted by the absence of structure in the absorption band of D_2O molecules bonded to two pyridine molecules in carbon tetrachloride. This may be explained by superposition of the absorption bands corresponding to the frequencies ν_1, ν_3, and $2\nu_2$, as a result of their proximity. Such an explanation is justified if we take into account the fact that the frequency ν_3, and consequently $2\nu_2$ also, of the water molecules is raised on interaction with pyridine in comparison with the corresponding frequency of liquid water,[8] while the frequency ν_1 falls off (compare the data in Table 1 and in Fig. 2).

The interaction of water with solvent molecules in pyridine at a concentration of the order of 1 mole/liter, which has in general the same character as when a mixture of pyridine + water is dissolved in carbon tetrachloride, is complicated by the interaction of water molecules with one another. The latter manifests itself, first, in the presence of two absorption bands corresponding to the frequency ν_2 in the spectra of solutions of water in pyridine: 1645 and 1665 cm^{-1} (Fig. 2). The first of these bands coincides in position with the corresponding band of liquid water. The interaction of water molecules with one another in pyridine solution manifests itself, secondly, by the fact that in the spectrum of a solution of D_2O in pyridine, in contradistinction to a solution of D_2O in a pyridine + CCl_4 mixture, all three frequencies (ν_1, ν_3, and $2\nu_2$) may be observed. Reduction of the concentration of water in the pyridine leads to a relative reduction in the intensity of the 1645 cm^{-1} band and to a reduction in the width of the triple absorption band (ν_1, ν_3, and $2\nu_2$). Thus, if for liquid H_2O the width of the triple band equals 360 cm^{-1}, for 1- and 0.2-molar solutions in pyridine it equals 320 and 290 cm^{-1} respectively. This gives evidence of a reduction in the interaction of water molecules with one another along with the reduction of their concentration in the pyridine. For a solution of H_2O in a pyridine + CCl_4 mixture (Fig. 2), the width of the triple band amounts to 175 cm^{-1} in all. In this case, the interaction of water molecules with one another is apparently negligibly small, in consequence of their low concentration in the mixture.

In the spectrum of a 1-molar solution of H_2O in pyridine, aside from the ν_1, ν_3, and $2\nu_2$ absorption bands, there are also observed a relatively weak narrow band at 3670 cm^{-1} (the corresponding band for D_2O is located at 2710 cm^{-1})* and a small bump on the slope of the triple band around 3210 cm^{-1} (Fig. 2). Apparently, in a solution of water in pure pyridine as well as in its solution in a pyridine + CCl_4 mixture, there exists a certain relatively small quantity of water molecules bonded to pyridine by only one hydrogen atom, according to type I. The band at 3670 cm^{-1} corresponds to the ν_{free} frequency of these molecules, the band at 3210 cm^{-1} to the $\nu_{ass.}$ frequency. The main bulk of the water molecules in pyridine solution are associated with two pyridine molecules according to type II. Apparently, there also exist aggregates of water molecules with one another, as evidenced by the presence of the ν_2 band, which is like the corresponding band of liquid water, and by the change in width of the triple band with a change in the concentration of water in the pyridine.

The ν_{free} absorption band around 3670 cm^{-1} is observed both in dilute (~0.2%) and in concentrated solutions of H_2O in pyridine, such as 10, 20, and even 50% (by volume) solutions. In 10% solution, this band is suffi-

*The absorption band around 3670 cm^{-1} is present in the spectra presented in Errera's article[4] for solutions of H_2O and HDO in pyridine, although this band is not mentioned in the text of the article.

ciently well resolved, but at higher concentrations it appears as a shoulder on the slope of the triple absorption band of the H_2O stretching vibrations. One may suppose that when there is a considerable excess of water in mixtures with pyridine, there exist only aggregates of type I, aside from aggregates of water molecules with one another. The absorption band around 3670 cm^{-1} must be absent in this case, since the vibration ν_{free} is perturbed by adjacent water molecules. For the same reason, the vibration $\nu_{ass.}$ must also change.

Inasmuch as the absorption spectrum of water molecules bonded to pyridine by two H atoms simultaneously, according to scheme II, differs only slightly from the spectrum of liquid water, it may be supposed that the activity of such water molecules in the replacement reaction of surface methoxyl groups of porous glass by hydroxyl groups[1] is not great, as is also true for molecules of liquid water. Those water molecules which are bonded to pyridine by only one H atom, according to scheme I, in consequence of which the symmetry of these molecules is destroyed, are apparently active in this reaction. The position of the $\nu_{ass.}$ absorption band in such molecules (about 3210 cm^{-1}) bears witness to the highly protonic character of the hydrogen atom in a water molecule when it is bonded to the nitrogen atom of a pyridine molecule.

2. The influence of water on the vibrations of pyridine molecules was investigated in detail by Chiorboli[2] by means of the Raman spectrum of mixtures of pyridine with water. He showed that the displacements of the absorption bands of pyridine on interaction with water, phenol, and acetic acid were alike in sign and differed only in magnitude, increasing with an increase in the acidic properties of the addend. This confirms the acid-base character of the interaction of water molecules with pyridine, whether it takes place according to scheme I or to scheme I.

In Fig. 3 is presented the infrared absorption spectrum obtained by us for a mixture of pyridine + D_2O, of composition 1:1 by volume, and for comparison the spectrum of a solution of pyridine in CCl_4. The frequencies of the absorption bands of pyridine and their displacements on interaction with D_2O are given in Table 2. The displacements of the pyridine bands for a composition of 3 parts H_2O + 1 part pyridine (by volume) coincide with those given in the table.

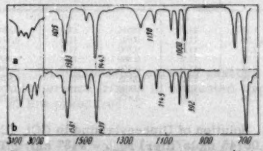

Fig. 3. a—mixture of pyridine + D_2O (1:1 by volume), liquid D_2O in the reference beam; b—pyridine in CCl_4 (3% by volume), thickness 0.27 mm., CCl_4 in the reference beam.

Almost all the absorption bands of pyridine shift toward the high-frequency side on interaction with water. It is characteristic here that the greatest relative shifts are observed for those pyridine bands (for example, the bands at 991 and 1581 cm^{-1}) corresponding to molecular vibrations which are symmetric with respect to the axis which passes through the nitrogen atom and the center of the pyridine molecule (we have made use of the interpretation of the pyridine frequencies presented in Chiorboli's work[2]). Apparently this is caused by the fixed orientation of the pyridine molecules relative to an attached water molecule. The increase in the vibrational frequencies of the pyridine molecule is then associated with the displacement of the electron cloud of its conjugated system of bonds toward the side of the addend molecule.

Table 2. Position of the Absorption bands of Pyridine under Various Conditions (the Displacements $\Delta\nu$ are Evaluated with Respect to Liquid Pyridine; in cm^{-1})

Liquid pyridine	Pyridine in CCl_4*	Pyridine + D_2O†	
ν	ν	ν	$\Delta\nu$
705.2	702.6	707.0	+ 1.8
748.5	—	752.9	+ 4.4
991.1	991.7	1000	+ 9
1030	1030	1034	+ 4
1068	1068	1068	0
1147	1145	1150	+ 3
1217	1217	1217	0
1438	1439	1443	+ 5
1483	1482	1487	+ 4
1581	1581	1593	+12
1598	1598	1615	+17
3001	3002	3014	+13
3026	3028	3042	+16
3054	3058	3061	+ 7
3079	3079	3087	+ 8

*3% by volume, thickness 0.275 mm; carbon tetrachloride in the reference beam.

†Mixture 1:1 by volume; D_2O in the reference beam.

3. The absorption spectrum of pyridine absorbed on deuterated porous glass has previously been obtained by Nikitin. Here there were observed changes in the frequencies of the stretching vibrations of the CH bonds of pyridine, produced by the interaction of its molecules with the surface OD groups.[3] Comparison of these changes with the changes produced by the interaction of pyridine with D_2O (Fig. 3, Table 2) shows that in general they are alike (the changes in frequency and in intensity of corresponding absorption bands are alike in sign in the two cases and differ only in absolute magnitude). This similarity serves to confirm the assumption that the pyridine molecule interacts with only one of the two hydrogen atoms of the water molecule.

Using Nikitin's procedure, we succeeded in observing, in the spectrum of a sample of deuterated porous glass of 0.1 mm thickness, absorption bands at 1596 and 1620 cm^{-1} when pyridine was adsorbed, corresponding to the 1581 and 1598 cm^{-1} bands of liquid pyridine. Thus these bands also are displaced, on adsorption, to the same side as on interaction of pyridine with water. The magnitude of the shift of the pyridine absorption bands characterizes the acidity of those molecular groupings to which the pyridine molecule is attached.

The absorption band of the surface OD groups perturbed by interaction with pyridine is located at 2260 cm^{-1}; i.e., displaced by 500 cm^{-1} relative to the band of free OD groups. The band at 2260 cm^{-1}, as might have been expected, has no structure.

The author expresses his deep gratitude to academician A. N. Terenin for his advice and constant help in the work.

REFERENCES

1. A. N. Sidorov. Zhur. Fiz. Khim 30, 995 (1956); A. N. Terenin and A. N. Sidorov. Optiko-mekhanicheskaya promyshlennost' (The optico-mechanical industry), No. 1, 1 (1959).

2. A. V. Karyakin. Zhur. Fiz. Khim 30, 986 (1956).
3. M. O. Bulanin. Opt. i Spektr. 2, 557 (1957).
4. J. Errera, R. Gaspart, and H. Sack. J. Chem. Phys. 8, 63 (1940).
5. D. F. Hornig, H. F. White, and F. P. Reding. Spectrochim. Acta 12, 338 (1958).
6. E. Greinacher, W. Lüttke, and R. Mecke. Z. Elektrochem. 59, 23 (1955).
7. P. Saumagne and M. L. Josien. Bull. Soc. chim. France, No. 6, 813 (1958).
8. P. Chiorboli. Annali Chim. 47, 443 (1957).
9. V. A. Nikitin. Opt. i Spektr. 1, 593 (1956).

Ed. Note: In the Errata given in the April Russian issue, it is pointed out that Fig. 1 (page 25) and Fig. 2 (page 26) are not clear. The curves which represent absorption spectra in these figures were damaged during the preparation of the plates, the result being that the absorption bands at 3480 cm^{-1} (Fig. 1) and at 3460 cm^{-1} (Fig. 2) are indistinct.

DETERMINATION OF THE ABSOLUTE VALUE OF PARAMETERS CHARACTERIZING INTENSITY IN THE INFRARED ABSORPTION SPECTRUM IN THE CASES OF THE ABSENCE OF TIME DISTORTIONS II.

V. M. Chulanovsky, I. V. Peisakhson, and D. N. Shchepkin

Received 1 June 1959

Experimental comparison is derived from three methods developed by the authors for the determination of spectral parameters in four different absorption bands. It is shown that all methods give practically the same significances of optical density in the maximum.

In our first article[1] three methods were proposed for the determination of true spectral parameters in the absence of time distortions. The fundamental purpose of the experimental part of the given work was in the comparison of these methods and in the explanation of the feasibility of their use in practicable spectral apparatus.

The work was carried out with the aid of a Perkin-Elmer monochromator (prism of LiF) in combination with an FEOU-18 amplifier and an EPP-09 self-recorder. Before the start of the measurements, the balance of the instrument was examined, and the entrance and exit slits were measured and brought up to the same width. The measurements were carried out for points as described in detail in reference 1.

Four bands with a different half width, belonging to four different substances and possessing a slightly different contour shape, were investigated (see Tables 1-4).

The meaning of the symbols used in the tables: S—the geometrical slit width; $\Delta\nu_0$—the normal spectral slit width, $\Delta\nu_e$—the effective spectral slit width; b—the observed half-width of the band (its width at $K = \frac{1}{2} K_m$); b_0—the true half-width, calculated at a given slit width on the assumption of the dispersion shape of the contour (formula 22);* K_m—the optical density, observed in the absorption maximum; k_m—the true optical density, calculated at a given slit width on the presumption of the dispersion shape of the contour (formula 21); k_m^*—the true optical density calculated for three points (formula 25).

*Here and further on, the numbering of formulas is according to part I.[1]

The relative error of the calculation of k_m and b_0, determined for the scattering of points, amounts to 0.4-0.7%. The maximum deviation of separate measurements from the average significants does not exceed 1% to slit widths up to 0.4 of the half-width of the band.

Figure 1 permits the estimation of the degree of certainty of the determination of K_m for different significants of $\Delta\nu_e$.

In the combined Table 5, besides the average significants b_0, k_m, k_m^*, obtained from Tables 1-4, the significants $b_{0\,ext.}$ and $k_{m\,ext.}$, extrapolated to $\Delta\nu_e = 0$ with respect to formulas (15) and (16) are brought in.

The observed significants K_m and b_0^2 are represented in Fig. 2. The significants $k_{m\,ext.}$ and $b_{0\,ext.}^2$ are designated on the ordinate axis. As evident from the figure, by extrapolating k and b into the region $\Delta\nu_e < 0.4b$,

Table 1. Chloroform. $\nu_{C-H} = 3020\ cm^{-1}$, Thickness of the Layer is 26μ, $\Delta\nu_0 = 1.25\ cm^{-1}$

S (μ)	$\Delta\nu_e$ (cm^{-1})	b (cm^{-1})	K_m	b_0 (cm^{-1})	k_m	k_m^*
30	2.02	15.8	0.851	15.4	0.881	0.884
50	2.92	16.1	0.828	15.6	0.846	0.850
70	3.70	16.4	0.819	15.7	0.847	0.848
80	4.42	16.6	0.814	15.8	0.853	0.856
90	4.94	17.0	0.805	15.7	0.850	0.846
100	5.46	17.5	0.791	15.9	0.843	0.835

Table 2. Methyl Ethyl Ketone. $\nu_{C=O} = 3417\ cm^{-1}$ (1st Overtone), Thickness of the Layer is 96μ, $\Delta\nu_0 = 1.6\ cm^{-1}$

S (μ)	$\Delta\nu_e$ (cm^{-1})	b (cm^{-1})	K_m	b_0 (cm^{-1})	k_m	k_m^*
40	3.28	33.2	0.985	33.0	0.993	0.993
70	5.54	33.8	0.956	33.1	0.974	0.986
80	6.26	33.8	0.956	32.8	0.978	0.975
90	6.95	34.4	0.955	33.2	0.983	0.975
100	7.70	34.8	0.963	33.3	0.995	1.015
120	9.22	35.1	0.938	33.0	0.984	1.000

Table 3. Hexyne. $\nu_{C\equiv C} = 2120\ cm^{-1}$, Thickness of the Layer is 34μ, $\Delta\nu_0 = 0.6\ cm^{-1}$

S (μ)	$\Delta\nu_e$ (cm^{-1})	b (cm^{-1})	K_m	b_0 (cm^{-1})	k_m	k_m^*
70	1.45	11.7	0.844	11.5	0.881	0.884
90	1.76	11.8	0.862	11.6	0.871	0.874
120	2.49	11.8	0.860	11.3	0.881	0.886
150	2.84	11.9	0.860	11.2	0.888	0.892
170	3.21	12.0	0.850	11.3	0.884	0.884
200	3.78	12.2	0.835	11.2	0.876	0.884
220	4.13	12.3	0.828	11.2	0.874	0.884
270	5.00	12.6	0.815	11.1	0.873	0.870

Table 4. Solution of Diphenylamine in CCl_4 (Concentration—0.00745 mole/liter) $\nu_{N-H} = 3437\ cm^{-1}$, Thickness of the Layer is 2 cm, $\Delta\nu_0 = 1.60\ cm^{-1}$

S (μ)	$\Delta\nu_e$ (cm^{-1})	b (cm^{-1})	K_m	b_0 (cm^{-1})	k_m	k_m^*
60	4.8	26.0	1.815	25.1	1.84	1.83
80	6.25	26.4	1.780	25.4	1.84	1.83
110	8.3	27.0	1.745	25.2	1.85	1.84

Table 5

Substance	$b_{0\,ext}$	b_0	$K_{m\,ext}$	k_m	k_m^*
Chloroform	15.4	15.6	0.848	0.850	0.850
Methyl ethyl ketone	32.9	33.1	0.982	0.980	0.990
Diphenylamine in CCl_4	25.2	25.2	1.846	1.845	1.835
Hexyne	11.6	11.3	0.878	0.878	0.883

where it must be linear, a rather large number of independent measurements can be used for this in order that the extrapolation might be made accurately.

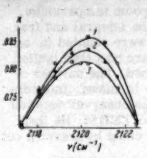

Fig. 1

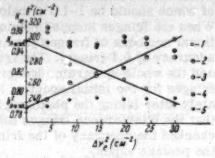

Fig. 2

Fig. 1. Recording of absorption curve K of hexynene in the neighborhood of the maximum at different significants of $\Delta\nu_e$ (b_0 = 11.5 cm^{-1}). The significants $\Delta\nu_e$ (cm^{-1}): curve 1—2.5; curve 2—3.75; curve 3—5.

Fig. 2. Linear extrapolation of significants k_m and b^2 to zero significant $\Delta\nu_e^2$ for the CH band of chloroform (3020 cm^{-1}). 1—observed significant k_m; 2—observed significant b_0^2; 3—significant k_m^*, corrected for three points (formula 25) at $\Delta\nu_e$, indicated on the abscissa axis; 4—the same by correction with respect to formula (21); 5—the same for b_0 with respect to formula (22).

Good coincidence of significants k_m^*, determined for three points near the maximum, with significants obtained by two other methods, offers particular interest. As was indicated in reference 1, the practical significance of this method is determined by the feasibility of using it not only for isolated bands. The data in Table 5 are obtained for points far from the maximum of the band at the value h, approximately equal to 0.1b (at some point of the curve's asymmetry ±h lies at a different height).

In the case of isolated peaks for which it is impossible to determine the half-width of the band, the invariableness of the quantity k_m^*, calculated at some diminishing significants of h, is the test of the admissibility of the selection of the value h.

However, as our calculation showed, for symmetrical bands with a dispersion distribution of intensity, the demand on the quantity h is not great.

If we designate the ratio h:b/2 by α, the ratio $\Delta\nu_e$:b/2 by β, and the ratio of the permitted value of deviation Δk_m from the true significant k_m by $\Delta k_m/k_m$, then it is not difficult to show that

$$\alpha^2 = \frac{6+\beta^2}{\beta^2\frac{k_m}{\Delta k_m}-6-\beta^2}.$$

Thus, for the permitted error of the determination of k_m to 1% and the equality of the effective slit width to half of the half-width of the band, the quantity h can amount to about 25% for b/2. Examination of this assertion on an experimental curve with different significants of h and $\Delta\nu_e$ for hexyne confirmed its density, although this curve differs perceptibly from the dispersion curve. On looking for the cause of this condition, very favorable for practical work, it was found that a small correction had to be applied to K_m, amounting to less than 7-8% at $\Delta\nu_e < 0.4b$.

The value $b_{0\ ext.}$ for a solution of diphenylamine in CCl_4 (Table 5) at a concentration of 0.00745 mole/liter compared with the value obtained by Russel and Thompson[2] at those same conditions. Using formula (7a) for $\Delta\nu_e$ at β = 0.85, they obtained the value 24.5 cm^{-1} for b_0. By the examination of their data with respect to formula (7) and by the use of linear extrapolation (15) the value $b_{0\ ext.}$ = 25.1 is obtained, which is practically no different from ours—25.2 cm^{-1}.

REFERENCES

1. V. M. Chulanovsky, I. V. Peisakhson, and D. N. Shchepkin. Opt. i Spektr. 7, 763 (1959).
2. R. A. Russel and H. W. Thompson. Spectrochim. Acta 9, 133 (1957).

THE DISPERSION CURVE OF GASEOUS N-PENTANE

E. F. Yamshchikov

Received 20 June 1959

The dispersion curve of gaseous n-pentane is given. A simple method of counting the interference fringes is suggested, applicable to measurement of the dispersion curves of gases at low pressures.

INTRODUCTION

In reference 1 the oscillator strengths were calculated for gases (methane, ethane, propane) using Friberg's data[2] and for liquids (hexane, pentane, octane) using the authors' data. A straight line relationship between the oscillator strength and the number of carbon atoms per molecule was obtained for gases. For the liquids hexane, pentane, and octane the oscillator strengths did not lie on the straight line on which the oscillator strengths of methane, ethane, and propane lie. The purpose of the present work is to measure the dispersion curve of gaseous n-pentane and to calculate the oscillator strength f.

THE APPARATUS

A Jamin interferometer was used for the experiment. The interferometer plates, 20 mm thick, were made of fused quartz. A tube of length 17.26 cm closed by plane parallel fused quartz windows was placed in each side of the interferometer. One tube was pumped out to a pressure not above 0.1 mm Hg, the other was filled with the vapor of the substance under study. Thin gaskets of polythene or kapron (a type of nylon) were very successful for sealing the tubes (see Fig. 1). The apparatus shown in Fig. 1 was placed in a drying oven and heated to 110-120°C for 15 min, after which the screws were tightened. The vacuum was checked with an electric discharge; the

character of the discharge did not change for several months.

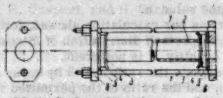

Fig. 1. Method of sealing the interferometer tube. 1, Assembly rods; 2, interferometer tube; 3, polythene gasket; 4, plane-parallel quartz windows; 5, cardboard washers; 6, brass assembly plates.

The n-pentane was obtained from Academician B. A. Kazanskii's laboratory. The following method was used to fill the tube (Fig. 2). A glass T-connector 2 led from the tube with the plane-parallel windows. One end of the T was joined to a vertical tube 3 which was filled with pentane, the other end led to the pump. The vertical tube 3 was filled with pentane, after which its upper end was sealed off. The pentane was frozen with liquid nitrogen and the system was evacuated completely (which was verified by the movement of the interferometer fringes). Then tap 4 was closed, the pentane was warmed, and the interference fringes moved. The freezing of the pentane was repeated until the zero fringe of the interferometer no longer changed its position after freezing. At the same time the laboratory temperature was measured. The pentane vapor density was calculated from the ideal gas equations and from the saturated vapor pressure corresponding to the temperature of branch 3. An arc between iron electrodes was used as a light source. The light from a super-high pressure krypton lamp passed between the electrodes (see Fig. 3). In this way the iron line spectrum was superimposed on the continuous krypton lamp spectrum. This made it easier to follow the movement of the interference fringes.

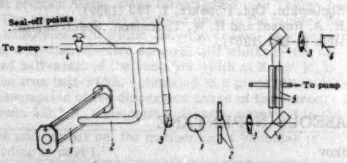

Fig. 2 Fig. 3

Fig. 2. Method of filling the system with pentane. 1, Interferometer tube; 2, glass T-connector; 3, vertical tube with liquid pentane; 4, vacuum tap.

Fig. 3. Diagram of the apparatus. 1, Super-high pressure krypton lamp; 2, iron arc electrodes; 3, condenser lenses; 4, interferometer plates; 5, interferometer tubes; 6, spectrograph slit.

COUNTING THE FRINGES

The observer fixed his attention on one line in a krypton lamp spectrum, of known wavelength (we used Kr 5570.29 A). The pentane vapor was frozen out with liquid nitrogen. A reference cross-hair was placed at the spectrograph slit a little distance from the center of the zero fringe. The pentane vapor pressure was raised by slowly lowering the level of the liquid nitrogen, and the fringes began to move. The observer counted the number of fringes crossing the reference cross-hair. When the liquid nitrogen had been removed from the pentane, the branch tube was immersed in a bath, for instance, a Dewar flask filled with water the temperature of which should be 1-1.5°C below room temperature. When the fringes stopped moving the integral and fractional numbers of fringes passing were counted (to an accuracy of 0.1 fringe). The iron arc was then ignited and the whole spectrum photographed. The number of fringes for the initial spectral line is known. Immediately after taking the photograph the observer verified that the interference fringes had not shifted. He then checked the accuracy of the fringe count by freezing out the pentane vapor.

There are well known difficulties involved in counting the fringes in this way. First, it takes about half an hour to count the fringes. Secondly, after counting the fringes about 20 min is required to set up the fringes for the photograph. The observer's eye will get very tired after this time which may lead to errors in counting the fringes. Thirdly, the observer must be very experienced in this type of measurement. We therefore tried to reduce these difficulties and used the following method of counting the interference fringes.

As is well known $(\mu - 1)d = n\lambda$, and so the refractive index of a gas, generally speaking, can be expressed through the number of interference fringes passing. Since the refractive index of gases at low pressures is proportional to the density, at constant temperature T the refractive index varies linearly with the pressure. If we plot this relationship graphically for different wavelengths using coordinates n and P (the gas pressure) we get a family of straight lines passing through the origin. Figure 4 shows two straight lines of this family for wavelengths λ_1 and $\lambda_2 (\lambda_1 > \lambda_2)$. Then the desired number of fringes n_1 and n_2 for pressures P_1 and P_2 can be determined if we have merely measured $n_2 - n_1$. In fact, from similar triangles LCD and MOC we can calculate, using simple geometry, that

$$\left.\begin{aligned} n_1 &= \frac{\Delta_1}{\Delta_2 - \Delta_1}\,\delta n \\ n_2 &= \frac{\Delta_2}{\Delta_2 - \Delta_1}\,\delta n \end{aligned}\right\} \tag{1}$$

$$\frac{n_2}{n_1} = \frac{\Delta_2}{\Delta_1}, \tag{2}$$

where $\delta n = n_2 - n_1$, is determined experimentally, and $\Delta_2 = n_2' - n_2$ and $\Delta_1 = n_1' - n_1$, are calculated from a reduction of the spectrograms taken at pressures P_2 and P_1 respectively. Further, the refractive index of gases under standard conditions (P = 760 mm Hg and T = 0°C) is given by:

$$(\mu_0 - 1) = (\mu - 1)\frac{760\,(1 + \alpha T)}{P} \tag{3}$$

and

$$n_0 = nK, \tag{4}$$

where n_0 is the number of fringes for standard conditions and n is the number of fringes at pressure P and temperature T, while

$$K = \frac{760\,(1 + \alpha T)}{P}$$

where

$$\alpha = \frac{1}{273}.$$

If we now plot n on the y-axis and 1/K on the x-axis, we obtain straight lines (Fig. 5) similar to those shown in

Fig. 4, and all the preceding considerations are also valid here.

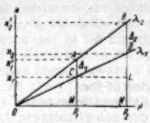

Fig. 4

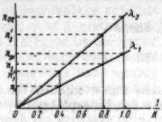

Fig. 5

Fig. 4. The refractive index of a gas plotted against pressure for constant temperature; the refractive index is expressed as the number of fringes n for two wavelengths λ_1 and λ_2.
Fig. 5. The refractive index of a gas plotted against pressure and temperature; the refractive index is expressed as the number of fringes n for two wavelengths λ_1 and λ_2.

Therefore, if we measure only the difference $n_2 - n_1$ of the fringer between pressures P_1 and P_2 and temperatures T_1 and T_2 we can determine n_1 and n_2 from Eq. (1); it is sufficient to calculate n_1 and n_2 to the nearest fringe, since fractions can be obtained from the spectrogram (see Fig. 6).

Equation (2) checks the accuracy of the values of n_1 and n_2 obtained. Knowing n_1 and n_2 we can obtain the desired value n_0 from Eq. (4) or graphicaliy (Fig. 5).

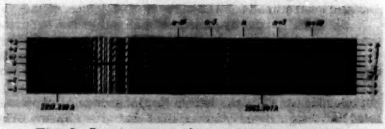

Fig. 6. Spectrogram of n-pentane vapor in the ultraviolet. P = 453.40 mm Hg; room temperature = 23.3°C.

This method of counting fringes enables us to reduce by 3 to 4 times the number of fringes counted, and also gives a check on the accuracy of the count, making it unnecessary to count the fringes in the reverse direction.

CHECK ON THE APPARATUS

Before being used for measurements with n-pentane, the apparatus was calibrated. For this purpose we used it to measure the dispersion curve of dry air. Our results agreed well with those of Meggers and Peters in the wavelength range 5000 to 2500 A.[3]

THE MEASUREMENTS

Using the method we have described, we measured the dispersion curve of n-pentane vapor. The temperature of the liquid pentane was raised from the temperature of liquid nitrogen to +0.12°C; as a check the fringes were counted as this was done; then the spectrum was photographed at this temperature; the liquid pentane was warmed to +21.74°C, the fringes being counted again, and a second photograph of the spectrum was taken.

$d = 172.6$ mm, $\lambda_1 = 5570.29$ A (Kr), $\lambda_2 = 2562.54$ A (Fe)

Temperature (°C)									
Liquid pentane	Room	P (mm Hg, corr.)	$(1+\alpha t)$	K	$n(\lambda_1)$	k	$n'(\lambda_2)$	$n_0(\lambda_1)$	$(n_0-1)\cdot 10^6$
0.12	23.5	184.33	1.0861	4.4780	123.4	176.7	300.1	552.6	1783
21.74	23.3	453.40	1.0853	1.8119	303.8	434.5	738.1	550.1	1778

The Table gives the data of these measurements. n_1 and n_2 were calculated from these data and Eq. (1) and values of 123.0 and 303.4, respectively, were obtained. We see that this calculation verifies the fringe count to an accuracy of one fringe. Since the measurements of the refractive index were made to an accuracy of 5×10^{-6}, its absolute value at 0°C and 760 mm Hg was rounded off to 1.001780 at $\lambda = 5570.29$ A. The dispersion curve for n-pentane vapor was calculated for wavelengths between 5800 and 2330 A.

RESULTS

The dispersion curve of n-pentane vapor was measured by the method described above. The curve was then interpolated by Sellmeier's formula (for 760 mm Hg pressure and 0°C temperature):

$$\mu^2 = A + \frac{B}{\nu_0^2 - \nu^2}, \qquad (5)$$

where $A = 1.0007532$, $\nu_0^2 = 93.1340 \times 10^8$, and $B = 25.2124 \times 10^8$. Figure 7 gives the curve of the discrepancies calculated by the least squares method.

The oscillator strength $f = 9.74$ was calculated from the coefficient B. Figure 8 gives the relation between the oscillator strength and the number of carbon atoms in the molecule of some saturated hydrocarbons.

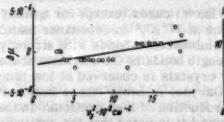

Fig. 7

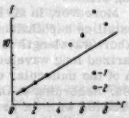

Fig. 8

Fig. 7. Curve of the discrepancies $\Delta\mu$ from the dispersion formula (5) for n-pentane vapor. The circles indicate the values of the difference $\mu_{calc.} - \mu_{meas.}$. $\Delta\mu = -1.8165 \times 10^{-6} + 0.1671 \times 10^{-34}\nu^2$.
Fig. 8. Relation between the oscillator strength f and the number of carbon atoms C in the molecule of saturated hydrocarbons. (1) Data from reference 1; (2) our data.

Finally, I acknowledge with deep gratitude I. V. Obreimov's help and constant interest in the work.

REFERENCES

1. I. V. Obreimov and T. N. Shkurina. Izvest. Akad. Nauk SSSR, Ord. Khimich. No. 5, 889 (1955).
2. Sten Friberg. "Messungen der Refraction und Dispersion in Gasförmigen Kohlenwasserstoffen," Lund, 1933.
3. W. F. Meggers and C. G. Peters. Bull. Bur. Standards 14, 697 (1918).

ON THE INTRINSIC LUMINESCENCE OF CRYSTALLINE NAPHTHALENE

M. T. Shpak and E. F. Sheka

Received 8 June 1959

The luminescence spectrum of crystalline naphthalene was studied in the region of the intrinsic absorption. It was shown that this luminescence can be explained by transitions from exciton bands of the crystal.

The analysis of the experimental data on luminescence spectra of molecular crystals carried out in the survey by Broude, Prikhot'ko, and Rashba[1] shows that of all the cases of luminescence examined, none can be interpreted as exciton luminescence, i.e., due to transitions from exciton levels to levels of the ground state of the crystal. Actually, the luminescence is associated with radiation due to impurities or structural defects which are always present in real crystals. It has recently been shown, for instance, that phenanthrene always contains traces of anthracene,[2] diphenyl acetylene and dibenzyl contain stilbene,[3] naphthalene contains β-methylnaphthalene and β-naphthol,[4] and that light absorbed by these crystals is re-emitted from the lowest excited levels of these impurities. Furthermore, it is sufficient that the crystals contain only ~0.01% or 0.001% by weight of impurities (such concentrations of impurities are practically impossible to detect by chemical methods of analysis) for practically all the fluorescence at low temperatures to take place from levels of the impurity molecules. On the other hand, it was recently shown that the luminescence of crystalline anthracene at 20.4°K may be associated with the presence of defects in the crystals being studied.[5]

Moreover, in all known cases (except for a study of crystalline naphthalene at 77°K),[6] no resonance matching of short wavelength luminescence bands with strongly polarized long wavelength bands of the intrinsic absorption of the molecular crystals is observed at low temperatures. According to Davydov's theory[7] these latter are associated with the production of free excitons. In the survey mentioned above,[1] it is noted that the exciton nature of luminescence has been proven conclusively only in the case of 1,1'-diethylpseudoisocyanine chloride and several closely related polymers.[8] In the case of molecular crystals, the role of excitons at low temperatures is primarily to transfer the excitation energy from the primary lattice to impurity centers at which the fluorescence takes place.

The fact that strongly polarized short wavelength bands were observed during an investigation of crystalline naphthalene at T = 77°K, and that these bands matched in resonance with the corresponding bands in the absorption spectrum,[6] and the publication of new data on the origin of long wavelength electronic transitions in the absorption spectrum of crystalline naphthalene[4] indicated the need for an investigation of the nature of the luminescence of crystalline naphthalene.

EXPERIMENT

The details of the experimental method have been described previously.[3] The investigations were carried out over a wide range of temperatures (20.4, 77, 200-210, 293, and 330-340°K). In the latter case a quartz cell with a single crystal of naphthalene was installed in a massive copper oven. Medium quartz spectrographs were used for obtaining the spectra (ISP-22 and Hilger E2, slit widths 0.02-0.05 mm). A krypton lamp (type GSVD-120) served as a light source for obtaining the absorption spectra; luminescence was excited by light from a SVDSh-1000 mercury lamp. The required regions of the spectrum were isolated with the aid of a double quartz monochromator. Since there are a number of bands[9] in the luminescence spectrum of crystalline naphthalene in the region of intrinsic absorption, which have been associated by several investigators with selective reflection of the exciting light,[10] we performed our excitations by using the 2530-2400 A region of the mercury lamp's emission spectrum. This region is remote from the origin of the naphthalene luminescence spectrum. A Glan-Thompson prism mounted in front of the spectrograph slit served as an analyzer.

Large single crystals of naphthalene (d ~ 0.5-7 mm) and crystals grown from melts in quartz cells (d ~ 1-300 μ) were used for the study.

Chemically pure naphthalene was subjected to further purification by zone melting. In reference 4 it was shown that by using this method of purifying naphthalene one can obtain preparations in which the impurity content (in particular β-methylnaphthalene, whose presence has been held responsible for the known luminescence of naphthalene[9]) was significantly lower than that given by any other purification methods known to us. In our work, in order to improve the purification we varied the length of the melted zone during the purification process (from 3 to 1.2 cm). This was accomplished by auxiliary cooling of the ampoule. In addition to this the rate of travel of the zone and the ratio of the over-all length of the ampoule to the length of the zone were varied. The number of sweeps was increased to 45. The ampoule containing the naphthalene was filled with nitrogen. This made it possible to obtain purer preparations than those which were used in the work of reference 4. The purity of the preparations was checked qualitatively by means of the absorption spectrum. The 31,060 cm^{-1} band, associated with the presence of the impurity β-methylnaphthalene[4] in the naphthalene was not observed in the absorption spectrum of the 7 mm single crystal of naphthalene at 20.4°K. Quantitative data on the impurity content of the naphthalene could not be obtained.

RESULTS AND DISCUSSION

The luminescence spectrum of crystalline naphthalene at 20.4°K is well known.[9, 10] It begins with a band at 31,060 cm^{-1} that is matched in resonance with a similar band in the absorption spectrum. It was shown in reference 4 that this band is associated with the β-methylnaphthalene impurity in the naphthalene.

In this paper we will not dwell on the changes in the impurity luminescence of naphthalene and their dependence

on β-methylnaphthalene concentration (a separate paper will be devoted to this problem), but we will consider the luminescence spectrum located on the short wavelength side of the 31,060 cm^{-1} band. Figure 1 shows the origins of the luminescence spectra of naphthalene crystals at 20.4°K, in which the concentration of β-methylnaphthalene is decreased in the direction indicated by the arrow. The figure shows that in the spectra of very pure naphthalene samples there appears a luminescence band weakly polarized along the a-direction with a frequency of 31,480 ± 3 cm^{-1} (henceforth we will refer to this as the A-band), which practically coincides with the strongly polarized A_1-band (ν = 31,476 cm^{-1}) in the absorption spectrum of crystalline naphthalene.[11] The intensity of this increases as one considers samples of higher purity. On the long wavelength side of this band there were weak satellite bands 54 and 120 cm^{-1} away from the main band.

In references 9 and 10 a band with a frequency of 31,463 cm^{-1} was observed in the luminescence spectrum of crystalline naphthalene at 20.4°K. This band, which we did not observe, is apparently also associated with selective reflection of poorly filtered exciting light in the region of absorption of the A_1-band. This is confirmed by the fact that a narrow absorption band with a frequency of 31,465 cm^{-1} is observed in the luminescence spectrum of naphthalene along with the 31,463 cm^{-1} band,[9] and also by the fact that the naphthalene preparations used in references 9 and 10 contained a large amount of β-methylnaphthalene, judging from the shapes of the luminescence spectra shown in these papers (the beginnings of these spectra are similar to the spectrum depicted in Fig. 1a). In this case, as seen from the figure, no luminescence is observed in the region of the A_1-band of crystalline naphthalene.

On increasing the temperature of the crystal to 77°K still another band (the B-band) appears in the luminescence spectrum of naphthalene. This band has a frequency of 31,623 ± 3 cm^{-1} and is polarized in the b-direction (Fig. 2). Its position coincides, within the limits of accuracy of the measurements, with the second strongly polarized B_1-band in the absorption spectrum of crystalline naphthalene at 77°K.[9] The intensity of this band is greater than the intensity of the band polarized along the a-direction (Fig. 2a). We note that our data on the luminescence spectrum of naphthalene at 77°K agree with the data of Wolf.[9]

We also point out that Wolf's conclusions about the direction of the moment of transition in a naphthalene molecule, which he based on an analysis of the ratios of the intensities of vibrational bands in the luminescence spectrum (without a 0 – 0-transition), and also on interpretation of the 31,065 cm^{-1} band as a band due to a transition from a vibrational level of the ground state to the zero level of the excited state (1 – 0-transition) and depending substantially on temperature, appear to be incorrect, inasmuch as that region of the luminescence spectrum pertains to the β-methylnaphthalene impurity in the naphthalene.[4] If the molecules of β-methylnaphthalene in naphthalene are oriented in the same way as the naphthalene molecules, one can draw tentative conclusions from Wolf's data about the direction of the transitions in the impurity molecules. As to transitions from thermally excited vibrational levels of the crystal ground state, the following section is devoted to this topic.

It is known that the intensity of luminescence due to the presence of impurities (this type of luminescence has the properties of luminescence of discreet centers), should decrease with increasing temperature.[12] In order to clarify the nature of the luminescence of crystalline naphthalene in the regions of the A_1- and B_1-bands, the luminescence spectra of the crystals were obtained at

Fig. 1

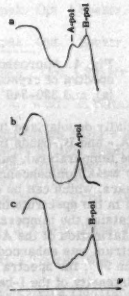

Fig. 2

Fig. 1. Microphotograms of the luminescence spectra of crystalline naphthalene (T = 20.4°K, unpolarized light). The arrow indicates the direction of decreasing concentration of β-methylnaphthalene in the specimens.

Fig. 2. Microphotograms of the luminescence spectra of crystalline naphthalene (T = 77°K). a, unpolarized light; b, a-component; c, b- component.

200-210, 293, and 330-340°K. The luminescence spectra of a naphthalene single crystal at 200-210°K are shown in Fig. 3.

A number of special features are observed in the spectrum: the A- and B-bands were smeared out and

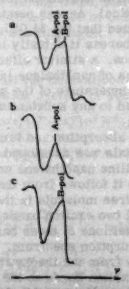

Fig. 3. Microphotograms of the luminescence spectra of crystalline naphthalene (T = 200-210°K). a, unpolarized light; b, a-component; c, b-component.

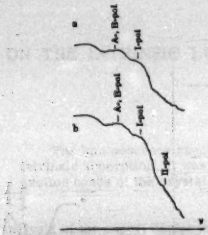

Fig. 4. Microphotograms of the luminescence spectra of crystalline naphthalene (T = 293°K (a), and 330–340°K (b), unpolarized light).

partially depolarized (they correspond in location with the A_1- and B_1-bands in the absorption spectrum at the same temperature), but in the short wavelength region a very weak luminescence band (I-band, ν = 31,900 cm^{-1}) appears, which can be compared with the 31,956 cm^{-1} band in the spectrum of crystalline naphthalene at 20.4°K.[11] On raising the temperature of the specimens to 293°K depolarization of the A- and B-bands in the luminescence spectrum was enhanced (on rotating the Glan-Thompson prism 90°, the spectra were practically unchanged) and the intensity of the I-band increased (Fig. 4a). The I-band was completely depolarized. Raising the temperature of the crystals to 330–340°K causes a visible intensification of the A-, B-, and I-bands and leads to the appearance of still another broad short wavelength band (II-band) in the luminescence spectrum located in the region of the A_2- and B_2- absorption bands.[11] Polarization is totally absent in the spectrum.

On raising the temperature, depolarization of the absorption bands of crystalline naphthalene (Fig. 5) (strongly polarized at 20.4°K) is also observed. In addition to this, thick single crystals of naphthalene (d ~ 7 mm) at 77°K showed a long wavelength absorption band (III-band, ν = 31,100 cm^{-1}) whose intensity was enhanced by increasing temperature. The III-band is located very near the 31,065 cm^{-1} band, but these bands are well separated in the spectra of the specimens containing large amounts of β-methylnaphthalene. The origin of the III-band is probably associated with transitions from a thermally excited electron-vibrational level of the ground state (1 – 0-transition). As was mentioned above, Wolf erroneously assumed that the 31,065 cm^{-1} was the 1 – 0-transition band, whereas it actually is due to the impurity β-methylnaphthalene. A similar effect is observed in the spectra of solutions of naphthalene in liquid solvents.[13]

Raising the temperature of the specimens to 330–340°K does not lead to any substantial changes in the absorption spectrum.

The theory of absorption and luminescence of light in molecular crystals was developed by Davydov.[7] The unit cell of crystalline naphthalene consists of two molecules; in this case it follows from the theory that to each excited state of a free molecule in the crystal there correspond in general two exciton bands. When the crystal absorbs light, transitions to these bands produce a doublet band in the absorption spectrum.

It also follows from the theory that in the case of transitions from exciton bands to the ground state, the luminescence of crystalline naphthalene must be strongly polarized, provided that the temperature is such that the translational symmetry of the crystal is not seriously disturbed.

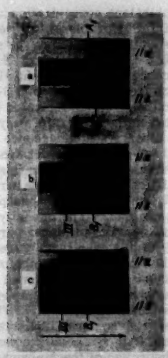

Fig. 5. Absorption spectra of crystalline naphthalene (d ~ 8 μ) in polarized light at different temperatures. Temperature (K°): a—77; b—200–210; c—293. The arrow points in the direction of increasing ν.

It was shown in Prikhot'ko's paper[11] that the strongly polarized A_1- and B_1-bands in the spectrum of crystalline naphthalene were associated with the crystalline state of the material. Data are presented in McClure's papers[10, 14] that indicate that these bands can be treated as components of the 0 – 0-transition doublet. If this is so, then the results obtained in the present paper can be explained in the following way. In naphthalene crystals with a high content of β-methylnaphthalene and other impurities, the absorbed light energy is transferred from the primary lattice to impurity molecules by migration of excitons through the crystal. The energy transferred to impurity molecules is then radiated in the form of luminescence. As the crystal is purified, the probability of collision of excitons with impurity molecules is reduced, and a luminescence appears which is associated with transitions from exciton states to the ground state, i.e., strongly polarized exciton luminescence. Since the spacing between the components of the doublet is greater than kT, then owing to the establishment of a quasi-equilibrium distribution in the excited states,[1] only one component (the A-band at 20.4°K), associated with the transition from the lowest excited level to the ground state is observed in the luminescence spectrum.

The analysis of the possible structure of the exciton bands given in reference 1 shows that, in general, at low temperatures exciton luminescence in molecular crystals must be extremely unlikely. When the temperature of the crystals is increased, however, i.e., when kT is increased and this energy approximates or exceeds the width of the band, the restriction on exciton luminescence must vanish, and one can expect an increase in the intensity of exciton luminescence in comparison with other forms of luminescence. In the case when kT becomes larger than the spacing between exciton bands, one can also expect the appearance of transitions from higher exciton bands. The increase of the probability of nonradiative transitions with increasing temperature can lead to the reverse process—a reduction in the overall intensity of the luminescence. These two processes are competitive. It is possible to determine from the experimental data which of these will prevail in any par-

ticular case. The data presented above show that in crystalline naphthalene the nonradiative transitions associated with increased temperature from the second, higher exciton band during the lifetime of the excited state are compensated by an increase in the population of this band due to an increase in kT. This also leads to the appearance of a strongly polarized B-band in the luminescence spectrum of crystalline naphthalene at 77°K, i.e., to a "flaring up" of the intrinsic luminescence of the crystal.

The fact that the B-band intensity in the luminescence spectrum at 77°K is higher than the A-band intensity may be associated with the fact that the oscillator strength of the B_1-band is significantly greater than that of the A_1-band. According to Wolf's data, the B_1-band intensity in the absorption spectrum is approximately 10 times greater than the A_1-band intensity.

As to the depolarization of the strongly polarized A- and B-bands at higher temperatures, this effect is probably associated with disturbance of the translational symmetry of the lattice by thermal fluctuations in the density, and by the formation of a large number of defects in the crystals at high temperatures.

Thus (1) the strong polarization of the A- and B-bands in the luminescence spectrum of crystalline naphthalene, which are in resonance with the A_1- and B_1-bands in the absorption spectrum at 77°K, (2) the increased intensity of these bands with increased temperature, and (3) the appearance under these conditions of new short wavelength bands in the luminescence spectrum, all make it possible to conclude that the luminescence of crystalline naphthalene in the region of intrinsic absorption (which occurs only in very pure specimens) is exciton luminescence.

In conclusion, we regard it our pleasant duty to express our appreciation to A. F. Prikhot'ko for his interest in the work and his valuable guidance.

REFERENCES

1. V. L. Broude, A. F. Prikhot'ko, and E. I. Rashba. Uspekhi Fiz. Nauk 67, 99 (1959).
2. A. F. Prikhot'ko. Izvest. Akad. Nauk SSSR, Ser. Fiz. 15, 608 (1951).
3. A. F. Prikhot'ko and M. T. Shpak. Opt. i Spektr. 4, 17, 30 (1958).
4. A. F. Prikhot'ko and M. T. Shpak. Opt. i Spektr. 6, 119 (1959).
5. A. F. Prikhot'ko and I. Ya. Fugol'. Opt. i Spektr. 4, 335 (1958).
6. D. Griessbach, G. Will, and H. C. Wolf. Z. Naturforsch. 11a, 791 (1956).
7. A. S. Davydov. Teoriya pogloshcheniya sveta v molekulyarnyi kristallakh. (The theory of light absorption in molecular crystals), Izd. Akad. Nauk Kiev, 1951.
8. G. Schiebe. Z. Elektrochem. 47, 73 (1941).
9. I. V. Obreimov and K. G. Shabaldas. J. Phys. (USSR) 7, 168 (1943).
10. D. S. McClure and O. Schnepp. J. Chem. Phys. 23, 1575 (1955).
11. A. F. Prikhot'ko. Zhur. Eksptl. i Teoret. Fiz. 19, 383 (1949).
12. V. L. Levshin. "Fotoluminestsentsiya zhidkikh i tverdykh veschectv." (Photoluminescence of Liquid and Solid Substances), 1951.
13. R. Passerini and I. Ross. J. Chem. Phys. 22, 1012 (1954).
14. D. S. McClure. J. Chem. Phys. 22, 1668 (1954).

STEADY-STATE LUMINESCENCE OF PHOSPHORS IN THE PRESENCE OF SEVERAL KINDS OF TRAPS

V. V. Antonov-Romanovskii

Received 18 June 1959

The kinetics of phosphorescence for steady state excitation are studied in the case when the traps differ very markedly only in depth and are occupied to only a slight extent. Under these conditions we can accurately calculate the distribution of charges among traps, and the nature of the dependence of (1) this distribution, (2) the brightness of luminescence of individual bands, and (3) photoconductivity on temperature and the intensity of the exciting light.

In references 1 and 2 we explained, in a very general way, certain regularities of the initial stages of luminescence decay and buildup for a phosphor containing several kinds of electron and hole traps. This was possible because in the initial stages of the process the redistribution of charges among traps predominates over recombination. This fact, combined with certain assumptions which are often realized experimentally, makes the equations of kinetics quasi-linear.

However, in the case of steady-state excitation, we obviously may no longer neglect the recombination process. The kinetic equations therefore turn out to be essentially nonlinear. However, the problem can be solved completely in this case also, and in very general terms as well, since the concentrations of charges on traps do not vary with time under steady-state conditions.

The kinetic equations for steady-state excitation can be obtained from the transient expressions given in reference 2 by setting all the derivatives equal to zero. We then obtain the following system of equations:

$$\omega_{0i}^{-} n_i^{+} \cdot n^{-} N^{-} + w_i^{+} n_i^{+} = \varepsilon_i^{+} (\gamma_i^{+} - n_i^{+}) n^{+} N^{+} + \varkappa_i^{+} (\gamma_i^{+} - n_i^{+}) E, \quad (1)$$

$$\omega_{0i}^{+} n_i^{-} \cdot n^{+} N^{+} + w_i^{-} n_i^{-} = \varepsilon_i^{-} (\gamma_i^{-} - n_i^{-}) n^{-} N^{-} + \varkappa_i^{-} (\gamma_i^{-} - n_i^{-}) E, \quad (2)$$

where

$$n^{\mp} N^{\mp} = \frac{\sum_k^{n^{\mp}} w_k^{\mp} n_k^{\mp} + \sum_k^{n^{\pm}} \varkappa_k^{\pm} (\gamma_k^{\pm} - n_k^{\pm}) E + \varkappa_0 \nu_0 E}{\sum_k^{n^{\pm}} \omega_{0k}^{\mp} n_k^{\mp} + \sum_k^{n^{\mp}} \varepsilon_k^{\mp} (\gamma_k^{\mp} - n_k^{\mp})}. \quad (3)$$

If we sum over Eqs. (1) and (2), then, taking Eq. (3) into account, we obtain the following equality, which is obvious for the steady state

$$\sum_1^{s^+}\sigma_{0i}^+ n_i^+\cdot u^- N^- + \sum_1^{s^-}\sigma_{0k}^+ n_k^-\cdot u^+ N^+ = \sum_1^{s^+} x_i^+(\nu_i^+ - n_i^+)E$$

$$+\sum_1^{s^-} x_k^-(\nu_k^- - n_k^-)E + \chi_0\nu_0 E, \qquad (4)$$

It indicates that the number of ionization acts is balanced by the number of recombination acts.

In exactly the same way, by again summing over Eqs. (1) and (2), but now taking account of Eq. (4), we obtain another equality, which is less evident:

$$\sum_1^{s^+} w_i^+ n_i^+ + \sum_1^{s^-} w_k^- n_k^- + \chi_0\nu_0 E = \sum_1^{s^+}\sigma_i^+(\nu_i^+ - n_i^+)\,u^+ N^+$$

$$+\sum_1^{s^-}\sigma_k^-(\nu_k^- - n_k^-)\,u^- N^-, \qquad (5)$$

It indicates that the number of trapping events, i.e., the number of nonrecombinatory departures of free charges from both bands, is compensated by the number of liberated trapped charges, and—no matter how strange this appears at first glance—by the number of ionizations in the host substance. The point is that $2\chi_0\nu_0 E$ free charges are formed during $\chi_0\nu_0 E$ ionization acts. Under steady state conditions, $\chi_0\nu_0 E$ ionization acts are compensated by $\chi_0\nu_0 E$ recombination acts. However, each recombination act results in the disappearance of not two free charges, but of one free and one trapped charge. Therefore $\chi_0\nu_0 E$ free charges uncompensated by recombinations remain in both bands. Numerically, this is exactly equal to the $\chi_0\nu_0 E$ ionization acts of the host substance. The left-hand side of Eq. (5) takes this circumstance into account.

If we sum over Eqs. (1) and (2) separately, however, and then subtract one of these sums from the other, we obtain an identity, which indicates that Eqs. (1) and (2) are dependent. This shows that Eqs. (1) and (2) are insufficient for the determination of all the $n_i^\mp$, so that one more condition is necessary. This condition follows from the principle of electrical neutrality, according to which it is necessary that

$$\sum_1^{s^-} n_k^- - \sum_1^{s^+} n_i^+ = 0, \qquad (6)$$

i.e., that the total of separated charges of both signs be equal.

Consider, however, the case in which part of the charges of either sign are localized at particularly deep traps so that the probability of the thermal ejection of the charges is practically zero. Consider also that the effective recombination cross sections at these traps are quite small, i.e., that for certain traps

$$w_i \approx 0 \text{ and } \sigma_i \approx 0, \qquad (7)$$

which seems to give a recombination case with unequal concentrations of the recombining partners. Similarly, the presence of donor levels of either sign, when an appreciable portion of them is dissociated thermally, seems to lead to a case where the concentrations of electrons and holes are unequal.

We should note that for strongly differing concentrations of the recombining partners, the expontiality is the special feature of the recombination, i.e., linearity or quasi-linearity of the process.

In general, we analyzed the case of unequal concentrations of recombining partners in references 1 and 2 when we studied the dominant recombination of charges liberated from certain traps of a special kind. Of course, the process was transitory in this case since it did not concern the entire luminescence decay or build-up period, but only its initial and intermediate stages. The parameters of this process did not remain constant even in the initial stages, but changed all the time due to the succession of trapping actions.

If the number of recombinations is appreciably smaller than the number of recaptures, i.e., if

$$\sum_1^{s^+}\sigma_{0i}^+ n_i^+\cdot u^- N^- + \sum_1^{s^-}\sigma_{0k}^+ n_k^-\cdot u^+ N^+ \ll \sum_1^{s^-}\sigma_k^-(\nu_k^- - n_k^-)\,u^- N^-$$

$$+\sum_1^{s^+}\sigma_i^+(\nu_i^+ - n_i^+)\,u^+ N^+, \qquad (8)$$

then, according to Eqs. (4) and (5)

$$\sum_1^{s^-} x_k^-(\nu_k^- - n_k^-)E + \sum_1^{s^+} x_i^+(\nu_i^+ - n_i^+)E \ll \sum_1^{s^-} w_k^- n_k^- + \sum_1^{s^+} w_i^+ n_i^+, \qquad (9)$$

i.e., the number of ionizations is appreciably smaller than the number of liberations of trapped charges.

In the subsequent discussion we shall assume that the influence of saturation is absent, i.e., that the inequality

$$n_i^\mp \ll \nu_i^\mp, \qquad (10)$$

is valid.

If the quantities $w_i^\mp$ form a rapidly decreasing series with increasing i,

$$w_i^\mp \gg w_{i+1}^\mp, \qquad (11)$$

while the quantities $\sigma_{0i}^\mp$ are on the contrary comparable (the "correct" case)

$$\sigma_{0i}^\mp \sim \sigma_{0i}^\mp,$$

then there exists a certain $j^\mp$ which divides the series of $w_i^\mp$ values into two parts, which satisfy the following conditions:

$$w_i^\mp \gg \sigma_{0i}^\pm \cdot u^\pm N^\pm \quad \text{for} \quad i \leqslant j^\mp, \qquad (13)$$

$$w_i^\mp \ll \sigma_{0i}^\pm \cdot u^\pm N^\pm \quad \text{for} \quad i > j^\mp. \qquad (14)$$

We then obtain from Eqs. (1) and (2)

$$n_i^\mp \approx \frac{\sigma_i^\mp \nu_i^\mp \cdot u^\mp N^\mp + x_i^\mp \nu_i^\mp E}{w_i^\mp}, \quad (i \leqslant j^\mp), \qquad (15)$$

$$n_i^\mp \approx \frac{\sigma_i^\mp \nu_i^\mp \cdot u^\mp N^\mp + x_i^\mp \nu_i^\mp E}{\beta_{0i}^\pm \cdot u^\pm N}, \quad (i > j^\mp). \qquad (16)$$

In accordance with this, we shall call "shallow" the traps for which $i \leqslant j^\mp$ and "deep" those for which $i > j^\mp$. Such a division is in the nature of a convention, since it obviously depends both on the temperature and on the intensity of the exciting light.

Insofar as the numerator on the right-hand side of (15) depends only weakly on i, we deduce from (15), taking (11) and (12) into account, that

$$n_1 \ll n_2 \ll \ldots \ll n_j, \qquad (17)$$

omitting the superscripts ± throughout.

On the other hand,

$$w_1 n_1 \sim w_2 n_2 \sim \ldots \sim w_j n_j. \qquad (18)$$

However, we obtain from (16), for the population of the deeper traps,

$$n_{j+1} \sim n_{j+2} \sim \ldots \sim n_m, \qquad (19)$$

but, on the other hand,

$$w_{j+1} n_{j+1} \gg w_{j+2} n_{j+2} \gg \ldots \gg w_m n_m.$$

It follows then from (17)–(20) that

$$n = \sum_{1}^{m^-} n_k^- \approx \sum_{j^++1}^{m^+} n_k^+, \tag{21}$$

$$\sum_{1}^{m^-} \sigma_{0k}^- n_k^- \approx \sum_{j^++1}^{m^+} \sigma_{0k}^+ n_k^+, \tag{22}$$

$$\sum_{1}^{m^-} w^- n_k^- \approx \sum_{1}^{j^+} w_k^+ n_k^+. \tag{23}$$

i.e., the storage of charges and recombination are governed primarily by the deeper traps, and the liberation of charges by the shallower ones.

With the help of (15) and (16), Eqs. (22) and (23) give us

$$\sum_{1}^{m^-} \sigma_{0k}^- n_k^- \cdot u^+ N^+ \approx \sum_{j^++1}^{m^+} \sigma_k^+ \nu_k^+ \cdot u^+ N^+ + \sum_{j^++1}^{m^+} \varkappa_k^+ \nu_k^+ \cdot E, \tag{24}$$

$$\sum_{1}^{m^-} w_k^- n_k^- \approx \sum_{1}^{j^+} \sigma_k^+ \nu_k^+ \cdot u^+ N^+ + \sum_{1}^{j^+} \varkappa_k^+ \nu_k^+ \cdot E. \tag{25}$$

It follows from (15) and (16) that in order to express the quantities $n_i^\mp$ in terms of the constants σ_{0i}, σ_i, ν_i, and w_i it is sufficient to express the quantities u^-N^- and u^+N^+ in terms of them.

With the help of (22)–(25), we obtain from Eq. (3) an equation connecting u^-N^- with u^+N^+:

$$\sum_{j^-+1}^{m^-} \sigma_k^- \nu_k^- \cdot u^- N^- + \sum_{j^++1}^{m^+} \sigma_k^+ \nu_k^+ \cdot u^+ N^+ = \sum_{1}^{j^-} \varkappa_k^- \nu_k^- \cdot E + \sum_{1}^{j^+} \varkappa_k^+ \nu_k^+ \cdot E + \varkappa_0 \nu_0 E. \tag{26}$$

This equation is symmetrical in the superscripts + and −. Hence we obtain the same equation by interchanging them. In order to determine u^-N^- and u^+N^+ it is therefore necessary to find another equation connecting them. This can be accomplished as follows:

From (6), taking account of (21) and (16), we obtain

$$n \approx \sum_{j^++1}^{m^-} \frac{\sigma_k^- \nu_k^- \cdot u^- N^- + \varkappa_k^- \nu_k^- E}{\sigma_{0k}^- \cdot u^+ N^+} \approx \sum_{j^++1}^{m^+} \frac{\sigma_k^+ \nu_k^+ \cdot u^+ N^+ + \varkappa_k^+ \nu_k^+ E}{\sigma_{0k}^+ \cdot u^- N^-}. \tag{27}$$

It follows from the form of Eqs. (26) and (27) that u^-N^- and u^+N^+ are proportional to E, hence n is independent of E. The quantity n is thus also not a function of $w_i^\mp$ and hence not of T. However, this independence of E and T is limited in character. It is valid only as long as the subscripts j^- and j^+ in the inequalities (13) and (14) do not vary with the variation of E or T.

Therefore, if we do not limit the range of variation of T or E, the quantity n will not remain constant at the instant the inequalities (13) and (14)(and hence also the equalities (15) and (16)) are violated. It will increase or decrease to a definite value until the inequalities (13) and (14) become valid again for some other value of j^- or j^+ (j^- or j^+ will change by +1 or −1). Afterwards, for a further change in T or E, the abovementioned inequalities can again be violated and the process will again be repeated, etc. This means that n (and also, according to (16), all the $n_i^\mp$ for which $i > j^\mp$) will vary in steps.

In order to determine the nature of these changes, i.e., to find whether there is an increase or decrease in the magnitude of n and $n_i^\mp$, and also of the conductivity, we carry out the following analysis:

Equations (26) and (27) can be represented in the form

$$S^- x^- + S^+ x^+ = K^- + K^+ + K^0, \tag{28}$$

$$n = \frac{Q^- x^- + L^-}{x^+} = \frac{Q^+ x^+ + L^+}{x^-}, \tag{29}$$

where

$$S^\mp = \sum_{j^\mp+1}^{m^\mp} \sigma_k^\mp \nu_k^\mp, \quad Q^\mp = \sum_{j^\mp+1}^{m^\mp} \frac{\sigma_k^\mp \nu_k^\mp}{\sigma_{0k}^\mp}, \quad K^\mp = \sum_{1}^{j^\mp} \varkappa_k^\mp \nu_k^\mp,$$

$$L^\mp = \sum_{j^\mp+1}^{m^\mp} \varkappa_k^\mp \nu_k^\mp, \quad K^0 = \varkappa_0 \nu_0, \tag{30}$$

$$x^\mp = \frac{u^\mp N^\mp}{E}. \tag{31}$$

According to Eqs. (28) and (29), the quantities x^- and x^+ (which we shall call the coefficients of electron and hole photoconductivity respectively) and hence the quantity n do not depend on either E or T until some subscript j^- or j^+ changes by +1 or −1, i.e., until there is a change in the division of the system of electron or hole traps into deep and shallow ones.

Let us consider what will happen to the quantities x^-, x^+ and n, and also to n_i^- and n_i^+ when, for example, j^- changes by $\Delta j^- = \pm 1$. We shall assume here that the quantities depending on j^- suffer only insignificant changes. We obtain then from Eqs. (28) and (29)

$$S^- \Delta x^- + S^+ \Delta x^+ = \Delta K^- - x^- \Delta S^-, \tag{32}$$

$$\left(\frac{Q^-}{x^+} + \frac{n}{x^-}\right) \Delta x^- - \left(\frac{Q^+}{x^-} + \frac{n}{x^+}\right) \Delta x^+ = -\frac{x^-}{x^+} \Delta Q^-. \tag{33}$$

where for $\Delta j^- = +1$ (an increase in T or a decrease in E)

$$\Delta S^- = -\sigma_{j^-+1}^- \nu_{j^-+1}^-, \quad \Delta Q^- = -\frac{\sigma_{j^-+1}^- \nu_{j^-+1}^-}{\sigma_{0\,j^-+1}^-},$$

$$\Delta K^- = +\varkappa_{j^-+1}^- \nu_{j^-+1}^-, \quad \Delta L^- = -\varkappa_{j^-+1}^- \nu_{j^-+1}^-, \tag{34}$$

while for $\Delta j^- = -1$ (a decrease in T or an increase in E)

$$\Delta S^- = +\sigma_{j^-}^- \nu_{j^-}^-, \quad \Delta Q^- = +\frac{\sigma_{j^-}^- \nu_{j^-}^-}{\sigma_{0\,j^-}^+},$$

$$\Delta K^- = -\varkappa_{j^-}^- \nu_{j^-}^-, \quad \Delta L^- = +\varkappa_{j^-}^- \nu_{j^-}^- \tag{35}$$

(The increments of all other constants are equal to zero.)

It follows from Eqs. (32)–(35) that the increments Δx^- and Δj^- are always of the same sign, i.e., $\Delta x^-/\Delta j^- > 0$.

Let us consider for simplicity the special case in which

$$K^\mp = 0 \quad \text{and} \quad L^\mp = 0, \tag{36}$$

i.e., when the exciting light directly ionizes only the host substance. In this case it is not difficult to obtain the relationships

$$\frac{K^0}{S^+} \frac{\Delta x^-}{x^+ x^-} = -\frac{1}{2} \frac{\Delta Q^-}{Q^-} - \sqrt{\frac{Q^+}{Q^-} \frac{\Delta S^-}{S^+}}, \tag{37}$$

$$\frac{K^0}{S^-} \frac{\Delta x^+}{x^- x^+} = \frac{1}{2} \frac{\Delta Q^-}{Q^-} - \frac{\Delta S^-}{S^-}. \tag{38}$$

$$\frac{\Delta n}{n} = \frac{1}{2} \frac{\Delta Q^-}{Q^-}. \tag{39}$$

Taking account of (35), we deduce from these formulas that on cooling, when $\Delta j^- = -1$, we always have $\Delta n > 0$ and $\Delta x^- < 0$, i.e., the concentration of trapped charges of both signs increases while the coefficient of electronic

photoconductivity x^- decreases. The converse holds during heating, when $\Delta j^- = +1$. The case of hole photoconductivity is more complicated. It behaves in the same way as electronic conductivity only if

$$\frac{1}{2}\frac{\Delta Q^-}{\Delta S^-} < \frac{Q^-}{S^-}. \tag{40}$$

We have an anomalous case, however, if

$$\frac{1}{2}\frac{\Delta Q^-}{\Delta S^-} > \frac{Q^-}{S^-}, \tag{41}$$

since here the coefficient x^+ of hole photoconductivity increases on cooling and decreases on heating!

Let us consider in more detail the meaning of inequality (41). Using (35) we obtain from (41)

$$\frac{1}{2\sigma_{0,j^-}^+} > \frac{\sum_{j^-+1}^{m^-} \sigma_k^- \nu_k^-}{\sum_{j^-+1}^{m^-} \sigma_k^+ \nu_k^-}. \tag{42}$$

Since the right-hand side of the inequality is nothing but the average effective value $(1/\sigma_{0,k}^+)_{av.}$ of the quantities $1/\sigma_{0,k}^+$, it follows from (42) that

$$\frac{1}{\sigma_{0,j^-}^+} > 2\left(\frac{1}{\sigma_{0,k}^+}\right)_{av.}. \tag{43}$$

This condition is not very rigid. It means that the inverse of the effective recombination cross section of holes with electrons on traps of the j^- kind should only exceed the average of the inverse of the recombination cross section of holes with electrons on deep traps by a factor greater than 2.

The light sums n_1^- and n_1^+, as distinguished from the total light sum n, will behave somewhat peculiarly, regardless of which of the inequalities (40) and (41) is obtained.

If the parameters of different kinds of traps, other than depth, differ but little from each other, then in deep traps ($j^\mp + 1 \leqslant 1 \leqslant m^\mp$) the concentrations of charges of each sign are comparable. It follows then from (21) that

$$n_1^\mp \approx \frac{n}{m^\mp - j^\mp - 1}. \tag{44}$$

Taking account of (44), using (30), (34), and (35), and assuming, for example, that $\Delta j^- = \pm 1$ while $\Delta j^+ = 0$ (i.e., assuming a change only in the system of electron traps) we derive from (39)—considering all increments insignificant—that

$$\left(\frac{\Delta Q^-}{Q^-} \approx \frac{1}{m^- - j^- - 1}\right) \quad \frac{\Delta n_1^-}{n_1^-} \approx \frac{1}{2}\frac{\Delta j^-}{m^- - j^- - 1}$$
$$\text{and } \frac{\Delta n_1^+}{n_1^+} \approx \frac{\Delta n}{n} \approx -\frac{1}{2}\frac{\Delta j^-}{m^- - j^- - 1}. \tag{45}$$

This result is very interesting. In the case of cooling, for example, or an increase in the intensity of the exciting light, while the concentrations of holes in deep traps (n_1^+) as well as the total quantity of stored separated charges (n) increases somewhat, the concentrations of electrons in deep traps (n_1^-) decrease to the same degree! The electrons and holes will obviously exchange roles if we now assume the converse, namely $\Delta j^- = 0$ while $\Delta j^+ = \pm 1$.

Thus, while n varies monotonically stepwise over a wide range of T or E values, the quantities n_1^- and n_1^+ also vary stepwise, but not monotonically. Furthermore, they vary in opposite directions as shown schematically in the drawing. The quantities n_1^- and n_1^+ seem to fluctuate around some average value. Therefore, the monotonic increase (or decrease) of n is caused only by the successive inclusion (or exclusion) of levels of either kind in (or from) the system of deep traps. The distribution of charges among the traps is obviously not in thermal equilibrium.

Let us consider the two limiting cases in which the traps are either all deep ($j^\mp = 0$) or all shallow ($j^\mp = m^\mp$). In the first case there is no further redistribution of charges among traps when T decreases or E increases.

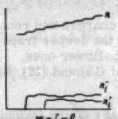

In the second case (in agreement with (15) and the fact that $\chi_1^\mp = 0$), the distribution of charges among all the traps will be in thermal equilibrium the whole time. Therefore, in the main, only the deepest traps determine the complete concentration of the separated charges

$$n \approx n_{m^-}^- \approx n_{m^+}^+, \tag{46}$$

i.e., it appears as if only the deepest traps (of both signs) existed in the phosphor. It is sometimes convenient to use this circumstance in studying the kinetics of phosphorescence. It is not difficult to show that in this limiting case

$$n \sim \sqrt{E}. \tag{47}$$

However, the situation will be entirely different if, on the contrary, $\chi_1^\mp > 0$ while $\chi_0 = 0$. In this case, for example, if $T \to 0$ or $E \to \infty$, the quantity $n \to \infty$; hence condition (10) is violated.

We carried out our study for the case when the stimulating action of the exciting light is negligibly small. Its presence can greatly complicate the study: The division of traps according to the probability $w_i^\mp$ of the ejection of charges from them can no longer be carried out taking only the trap depth into account, since the ejection will also depend on the stimulating action, which is proportional to the intensity E of the exciting light. If the various $w_i^\mp$ vary as much in magnitude here as in the case of purely thermal electron ejection, then the above treatment of the problem remains valid. However, there is a different sequence of traps according to the magnitude of $w_i^\mp$. It is perfectly obvious that the distribution of charges among traps will now, as before, be mainly in a state of thermal nonequilibrium.

Thus, the filling of the traps under prolonged excitation is not, as a rule, in a state of thermal equilibrium, the deviation being in the direction of a more uniform distribution of charges among the traps. The case is analogous to that of excitation of short duration when the charges distribute themselves among the traps according to their effective capture cross sections.

This result is very important since it implies that the initial distribution of charges among the levels is always in a state of thermal nonequilibrium. This is the case because every distribution occurs as a result of either a short or a prolonged excitation.

This validates the results obtained in reference 1, in which it is assumed that the initial distribution of charges among traps is far from thermal equilibrium.

Let us now consider the intensities of individual phosphorescence bands. Let us assume that the radiation arises as a result of the recombination of free electrons

with ionized luminescence centers. Then the brightness of the luminescence caused by the ionized luminescence centers of the i-th kind is

$$I_i = q_i \sigma_{0i} n_i^+ \cdot u^- N^-, \qquad (48)$$

where q_i denotes the radiation yield on recombination, i.e., it takes into account the losses which may arise within an excited center after recombination.

Let us consider, however, not the quantity I_i itself but another one which may be obtained by means of (31)

$$\frac{I_i}{q_i E} = \sigma_{0i}^- n_i^+ x^-, \qquad (49)$$

and which is proportional to the yield of the recombination of free electrons with ionized luminescence centers of the i-th kind.

Since the quantities n_i^+ and x^- suffer only "stepwise" variations when T or E vary, the same variation in magnitude will occur for the recombinatory yield of radiation, which according to Eq. (49) is proportional to the product of n_i^+ by x^-. Since the "steps" are not large here, it means that the fluctuation in the quantity $I_i/q_i E$ is also not sharp, particularly since the quantities n_i^+ and x^- vary in opposite directions (see above). It will be sharp only if the traps of the i-th kind will themselves move from the category of "deep" into the category of "shallow" traps when there is a catastropic decrease in the magnitude of n_i (external quenching caused by a sharply increased probability of the transfer of holes into the filled band).

In conclusion, let us note the following: The observed regularities will be strongly disrupted if the initial assumption is violated. This states that the traps of different kinds differ markedly only in the values of the probability of charges being ejected from them, i.e., in the values of w_i, but not in the values of σ_{0i}, σ_i, ν, and χ_i.

REFERENCES

1. V. V. Antonov-Romanovskii. Opt. i Spektr. 7, 376 (1959).
2. V. V. Antonov-Romanovskii. Opt. i Spektr. 7, 524 (1959).

STUDY OF THE ELECTROLUMINESCENCE OF A SUBLIMED ZnS-Mn PHOSPHOR

N. A. Vlasenko and Iu. A. Popkov

Received 15 June 1959

Pure zinc sulfide and metallic manganese were vacuum evaporated and heat treated to produce a sublimed ZnS-Mn phosphor; the latter's electroluminescence spectrum, brightness waves, and variation of integral brightness with applied field strength and frequency were studied, as well as certain electrical properties. It was shown that the electroluminescence of films—intrinsic electroluminescence—also is produced throughout the entire volume of the specimen. As the applied voltage is increased, the increase in brightness is much sharper than for powdered phorphors, and does not conform to any of the formulas suggested for them. Shallow donor levels (~ 0.1 ev) were detected in ZnS-Mn films; the ionization energy of the levels varies with the voltage applied to the specimen, which agrees with Frenkel's mechanism for thermal ionization aided by fields.

INTRODUCTION

Sublimed phosphors in the form of compact, homogeneous, transparent films are convenient for the study of luminescence and its associated phenomena. The study of the electroluminescence of sublimed specimens is particularly interesting, since due to their high transparency, homogeneity, and the absence of a binding dielectric, it ie possible to observe many quantitative characteristics which could not be measured accurately with powder specimens. Transparent electroluminescent films are also of great practical value, for example, for special purpose light sources, television screens, and image intensifiers, image converters, etc.

However, up to the present only two short papers on the electroluminescence of films have been published: Halsted and Koller[1] studied the electroluminescence of ZnS-Mn films obtained by Cusano's method[2] (reaction in the gas phase); Thornton[3] obtained electroluminescent zinc sulfide films activated with copper and manganese, by evaporation in a vacuum from the corresponding electroluminescent powder, followed by annealing.

One of us[4] has developed a new method of obtaining sublimed zinc sulfide phosphors; it has the advantages that it is possible to develop a film with specified characteristics (activator concentration, film thickness) and that fluxes and co-activators are absent. Specimens with reproducible properties can be obtained by this method and luminescence can be studied in substances of very simple chemical composition. The present work is devoted to the study of electroluminescence in a sublimed ZnS-Mn phosphor produced by this method.

PREPARATION OF SPECIMENS

The following procedure was used to prepare the ZnS-Mn specimens for electroluminescence studies. Pure zinc sulfide (phosphor quality) and metallic manganese were evaporated out of two tantalum crucibles onto a glass plate coated with a tin dioxide film (the transparent electrode) in a 10^{-3} mm Hg vacuum. After this, still under vacuum, the films were heat treated at 500-550°C, this was necessary both to diffuse the activator through the ZnS lattice and to give the films a good crystal structure. An aluminum film was vacuum-evaporated onto the prepared phosphor, and served as the second electrode.

In order to investigate the role of the phosphor/metal contact, in some specimens the phosphor was covered with a thin film of some good dielectric (polystyrene, for example) before the second (metallic) electrode was deposited.

EXPERIMENTAL RESULTS

The sublimed ZnS-Mn phosphor obtained by this method gives an orange luminescence under the action of a beam of electrons, X-rays, or ultraviolet rays, and also under an applied ac electric field.

In this work we studied the electroluminescence excited by a sinusoidal ac field. A ZG-10 audio oscillator was used as the source of sinusoidal voltage

Electroluminescence was observed both in specimens in which the metallic electrode was deposited directly on the phosphor, and in specimens in which a layer of a good dielectric was deposited between them.

With the excitation that we used, the electroluminescent brightness of the ZnS-Mn films depends on the concentration of the activator; the optimum concentration of manganese, as in the case of photoluminescence,[4] is 6×10^{-3} gm/gm. At this manganese concentration, specimens about 5μ thick had a luminescent brightness of 0.02 stilbs under an applied electric field of 4×10^5 volts/cm at a frequency of 3000 cps, the light yield then being about 3 lumens per watt.

The electroluminescence spectrum of these films is a simple band with a half-width of 0.20 ev and maximum located at 2.13 ev (582 mμ). The spectral composition of the radiation is almost independent of the size and frequency of the applied voltage. Altering the activator concentration does not change the electroluminescence spectrum either, whereas the photoluminescence spectrum shifts towards long wavelengths as the activator concentration is increased.[5]

We studied the light pulses given by the sublimed ZnS-Mn phosphor under different excitation conditions, using a double beam oscillograph. A signal proportional to the integral electroluminescence brightness was applied to the oscillograph directly from the photomultiplier in front of which the specimen was placed. Figures 1 and 2 give the results. In these Figures the upper oscillogram represents the light pulse, and the lower represents the voltage applied to the specimen. The negative half-cycle of the voltage oscillogram corresponds to the field polarity for which the negative potential is applied to the metallic electrode.

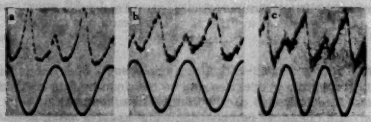

Fig. 1. Frequency (cps): a—100; b—400; c—1000.

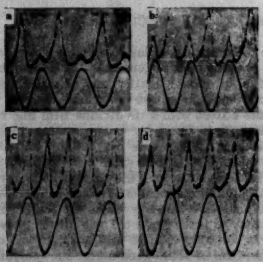

Fig. 2. Field strength (volts/cm): a—2×10^5; b—4.8×10^5; c—5.4×10^5; d—5.6×10^5.

At low frequencies, every half-cycle has a light pulse which is in phase with the applied voltage and symmetrical in shape. As the frequency of the field increases (Fig. 1) the amplitude of the peaks changes very little, but some asymmetry appears in them: after the negative half-cycle, the brightness does not fall to zero as the applied voltage goes through zero.

The amplitude ratio of two adjacent light pulses corresponding to different field polarities, depends on the specimen thickness and the excitation conditions; the thinner the phosphor film, the greater this dependence. Figure 2 shows the light pulses for a specimen 3μ thick. The Figure shows that the relative magnitudes of adjacent peaks depends greatly on the field strength: at E = 2×10^5 volts/cm the amplitude ratio of the peaks corresponding to the negative and positive half-cycles is 4.5; as the field is increased this ratio at first decreases to unity, then falls below unity. Figure 3 shows the variation of peak brightness with field strength. For curve 1, the aluminum is the negative electrode; for curve 2, it is the positive electrode. As the specimen thickness is increases, the difference between the rates of increase of the peaks vanishes, so that with a phosphor ~ 7.5 μ thick the peaks are almost equal in size, irrespective of the applied field. If the metallic electrode is not in direct contact with the phosphor there is no difference in the sizes of the peaks or their rates of increase.

The integral electroluminescent brightness of the sublimed ZnS-Mn phosphor grows very rapidly as the field increases.

To study this relationship the specimen was placed directly in front of a photomultiplier, since the radiation spectrum, as we mentioned above, is independent of the field strength. By changing the width of the slit between the specimen and the photomultiplier and by changing the amplification, we were able to measure brightness over a range of eight decades. The linearity of the photomultiplier and amplifier were checked in advance.

The variation of the brightness with the applied field strength was studied with specimens of different thicknesses, using the optimum concentration of manganese. Figure 4 gives the results for four specimens of different thicknesses at frequency 500 cps. The logarithm of the brightness is plotted on the y-axis, and the average field strength on the x-axis. The specimen thickness was measured interferometrically.

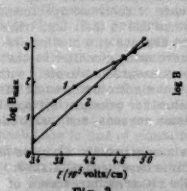

Fig. 3

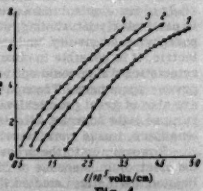

Fig. 4

Fig. 4. Thickness (μ): curve 1—1.5; curve 2—3.5; curve 3—5.5; curve 4—7.9.

The electroluminescent brightness increases by 6 to 8 orders of magnitude as the field is increased by a factor 5 to 6. At a given field strength the brightness increases with specimen thickness. The field strength at which it is still possible to observe electroluminescence

decreases as the phosphor thickness increases. Thin specimens, however, are more stable with regard to the electrical breakdown and hold up well under high fields.

Changes in the frequency of the applied field and in the temperature do not affect this relationship.

The frequency dependence of the brightness of an electroluminescent sublimed phosphor is the same as for powdered phosphors: at low frequencies the brightness is proportional to the frequency, and then saturation is observed. For ZnS-Mn films at frequencies greater than 5000 cps, the brightness scarcely changes at all if the resistance of the transparent electrode is low compared to the impedance of the specimen; below this frequency there is a considerable reduction in brightness as the frequency increases in this range.

Fig. 5. a—$E_{eff} = 3 \times 10^4$ volts/cm; b—$E_{eff} = 4 \times 10^5$ volts/cm.

We also studied certain electrical properties of electroluminescent specimens. Figure 5 shows typical oscillograms of the current flowing through the specimen (upper curves), and of the voltage applied to it (lower curves). At low fields (Fig. 5a), when there is still no electroluminescence, the current oscillogram is a sine wave shifted approximately 90 deg relative to the voltage sine wave. As the field is increased (Fig. 5b) the current waveform is strongly distorted and the current phase shift relative to the voltage becomes considerably less than 90 deg. This indicates nonlinearity of the current/voltage characteristic at high fields and a considerable increase in the real component of the admittance. Deviation from Ohm's law is observed at fields exceeding 3×10^4 volts/cm (see, for example, Fig. 6, in which curve 1 represents the relationship between the current and the magnitude of a dc field for one of the ZnS-Mn specimens).

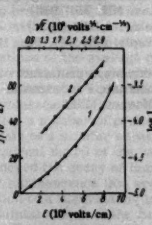

Fig. 6

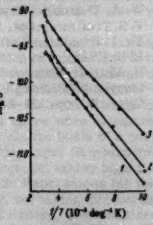

Fig. 7

Fig. 6. Curve 1—I against E; curve 2—log I against $\sqrt{E}$.

Fig. 7. Field strength (volts/cm): curve 1—2×10^3; curve 2—8×10^3; curve 3—3×10^4.

Specimens in which the metallic electrode is in direct contact with the phosphor have a slight rectifying action: their resistance is 20-50% greater when the metallic electrode is negative.

We studied the temperature dependence of the conductivity of ZnS-Mn in dc fields over the range of 115-340°K. Figure 7 gives the results. At low temperatures the variation of log σ with 1/T is a straight line, with a slope which varies somewhat with the magnitude of the applied field. At temperatures above 250°K ($1/T = 4 \times 10^{-3}$) the slope increases. The following values of the activation energy were obtained from the slope of the low-temperature portion: curve 1: 0.11 ev; curve 2: 0.098 ev; curve 3: 0.082 ev.

Electroluminescence in a sublimed ZnS-Mn phosphor is observed in fields an order of magnitude greater than for powdered ZnS phosphors (for the former, the range is 5×10^4 to 6×10^5 volts/cm; for the latter, 2×10^5 to 5×10^4 volts/cm). This is apparently due to the fact that in powder phosphors, the luminescence arises only at the grain surface,[8] where the local field considerably exceeds the average field. The presence of small regions of high field in powdered phosphors is usually associated[7,8] with the presence on the phosphor grain surfaces of a phase with high conductivity (Cu_xS or ZnO). The relatively low breakdown resistance of powdered phosphors is evidently related to their nonuniformity. ZnS-Mn films obtained as described above are uniform in their properties and chemical constitution, and it is not surprising, therefore, that they sustain considerably higher fields and give volume luminescence. The growth of brightness with thickness at a given field strength (Fig. 4) indicates that the electroluminescence is occurring throughout the volume of the film. The brightness of the films compared with powder specimens of the same thickness is related, apparently, to the volume luminescence of the former.

Noticeable luminescence appears at lower and lower field strengths as the specimen thickness is increased; this indicates the absence of an electroluminescence threshold, the apparent threshold being due to the limited sensitivity of the radiation detector.

The electroluminescence observed in the films must be attributed to intrinsic electroluminescence, and not to electroluminescence of injected carriers, because its characteristics do not change even when the metallic electrode is not in direct contact with the phosphor. The electrical measurements showed that considerable electroluminescence occurs, even with fields at which Ohm's law is no longer obeyed.

The brightness of the films increases with field strength considerably faster than in powdered phosphors: for the latter, the brightness changes by seven orders of magnitude with a 20- to 30-fold increase in field strength,[7-9] while in films this change in brightness occurs with a 5- to 6-fold increase in field strength. The slower increase in integral brightness for powder specimens is perhaps due to the field strength being very different at the different grains, due to their different dimensions and their nonuniform size distribution; in consequence of this each grain size will have its own rate of growth of brightness with field strength, while the measurements are made on the brightness averaged over the specimen. Another possible reason for the slower increase in brightness for powder specimens is that the applied field is distributed between phosphor grains and their surrounding dielectric in inverse proportion to the conductivity, and the conductivity of the phosphor rises sharply with the field, as was mentioned above, so that as the applied field strength is increased, the true field in the grains rises considerably more slowly than the average field. Due to the fine dispersion in films these phenomena should be less pronounced.

The variation of the brightness of ZnS-Mn films with the applied field does not conform to any of the numerous relationships of this type obtained for powdered phosphors.[4] Figure 8 shows (a) log B plotted against 1/V and (b) log B plotted against $1/\sqrt{V}$; these indicate that the following most frequently quoted formulas are not valid:

$$B = ae^{-\frac{a}{\sqrt{V}}} \tag{1}$$

and

$$B = ae^{-\frac{b}{V}}, \tag{2}$$

where B is the brightness, V is the applied field, and a and b are constants.

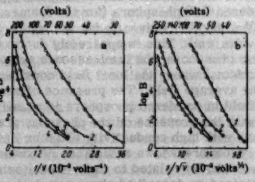

Fig. 8. Thickness (μ): curve 1—1.5; curve 2—3.5; curve 3—5.5; curve 4—7.9.

A V^n power law with n = 6-7 is approximately obeyed over a wide range. Our data are best described by the formula

$$B = ae^{b\sqrt{E}}, \tag{3}$$

as Fig. 9 shows clearly; here log B is plotted against $\sqrt{E}$. Significant deviation from this formula is observed only in thin specimens ($\lesssim 2\mu$).

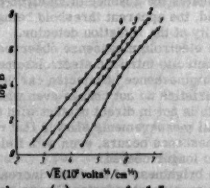

Fig. 9. Thickness (μ): curve 1—1.5; curve 2—3.5; curve 3—5.5; curve 4—7.9.

The current in ZnS-Mn films increases with the field in a similar manner (See Fig. 6, the straight line 2). Frenkel[10] obtained this relationship for the current theoretically in the region where Ohm's law is not obeyed. Assuming thermal ionization of atoms, aided by the field, Frenkel obtained the following expression for the probability of ionization

$$p = C \cdot e^{-\frac{\left(W - b\sqrt{\frac{eE}{\varepsilon_\infty}}\right)}{kT}} \tag{4}$$

where W is the activation energy with no field, e is the electronic charge, ε_∞ is the dielectric constant of the substance, C is a constant, k is Boltzmann's constant, and T is the absolute temperature. From this equation it follows that for impurity centers with low activation energy, a field of the order of 10^5 volts/cm can considerably affect the probability of ionization. As measurements of the temperature variation of conductivity have shown, there are shallow (~0.1 ev) donor levels in ZnS-Mn. The experimental variation of the activation energy with the applied field agrees with Eq. (4).

The rectifying action of specimens with a metallic electrode deposited directly on the phosphor is in all probability due to the formation at the metal-semiconductor interface of a layer impoverished in electrons.[11] The presence of a potential barrier in this region is also shown by certain properties of electroluminescence; for example, the different rates of increase of adjacent light pulses in thin specimens as the field is increased. As the thickness of the phosphor layer is increased the contribution of the region near the electrodes to the total brightness of the specimen becomes smaller, and the integral electroluminescent brightness ceases to vary with the direction of the field.

In conclusion the authors take this opportunity to express their deep gratitude to K. D. Sinel'nikov for suggesting the topic and to I. N. Shklyarevskii and V. K. Miloslavskii for their interest in this work, and for discussions.

REFERENCES

1. R. E. Halsted and L. R. Koller, Phys. Rev. **93**, 349 (1954).
2. D. A. Cusano. J. Opt. Soc. Am. **43**, 878 (1952).
3. W. A. Thornton. J. Appl. Phys. **30**, 123 (1959).
4. N. A. Vlasenko. Doklad na VII Vses. soveshch. po liuminestsentsii. (Report presented at the seventh All-Union conference on luminescence), Moscow, 1958.
5. P. Zalm, G. Diemer, and H. A. Klasens. Phil. Res. Rep., **9**, 81 (1954).
6. G. Destriau and H. F. Ivey. Proc. IRE **43**, 1911 (1955).
7. W. Lehmann. J. Electrochem. Soc. **103**, 24 (1956).
8. W. A. Thornton. Phys. Rev. **102**, 38 (1956).
9. V. S. Trofimov. Opt. i Spektr. **4**, 113 (1958).
10. Ya. I. Frenkel'. Zhur. Eksptl. i Teoret. Fiz. **12**, 1292 (1938).
11. N. Mott, R. Gurney. "Elektronnye protsessi v ionnykh kristallakh" (Electronic Processes in Ionic Crystals), pp. 199-211. Moscow, 1950.

THE INFLUENCE OF SECONDARY ABSORPTION AND EMISSION PROCESSES ON THE DURATION OF LUMINESCENCE OF A PLANE-PARALLEL LAYER

A. M. Samson

Received 14 May 1959

The influence of secondary absorption and emission processes on the duration of luminescence of a plane-parallel layer was studied. The formulas obtained make it possible to calculate the duration of luminescence under different conditions of irradiation and observation. There may be a considerable increase in the duration associated with high values of the quantum yield. The duration of the luminescence as observed through the layer is always greater than the corresponding duration observed by "reflection."

1. In general, the luminescence of a material in a volume of finite size originates not only under the direct action of external causes, but also by secondary absorption and emission processes. These processes affect the intensity, yield, laws of growth and decay, and other spectroscopic characteristics of the radiation emitted by the volume of material under consideration. This influence also depends on the degree of overlapping of the absorption and emission bands, the quantum yield per unit volume, the dimensions of the luminescing volume, and the conditions of irradiation and observation. Therefore, the character of the radiation emanating from the luminescent medium is determined not only by the particular properties of the atoms and molecules, but is also dependent to a considerable degree on the experimental conditions.

The effect of secondary absorption and emission processes on radiation characteristics is found to be especially strong in experiments with resonance radiation.[1-3] The growth and decay of luminescence require a longer time than in an elementary volume. Sometimes the duration of the luminescence is increased by 1 or 2 orders of magnitude. This phenomenon is called imprisonment of radiation.[1, 2] The marked increase in the duration of luminescence is also found in the study of the kinetics of luminescence, particularly in scintillation counter experiments.[4]

The increase in duration of luminescence due to secondary processes has not been adequately investigated theoretically. Early papers[1, 2] on this problem are based on the solution of diffusion equations. Later, it was shown[5-8] that the diffusion equation is not applicable to the propagation of photons, and that the solution of this problem must be based on an integro-differential equation that takes account of the special characteristics of photon propagation. However, it is difficult to solve such equations in general form.

In papers by Holstein,[7, 8] Biberman,[9] and Veklenko,[10, 11] evaluations of the average duration of luminescence from infinite slabs and a cylinder were obtained from the integro-differential equations. In Agranovich's work[13-14] on the luminescence of molecular crystals the average durations for a number of particular cases were calculated on the basis of a similar equation. On the basis of a one-dimensional model of the radiating layer Gamburzeff[15] considered the decay of luminescence, taking higher order luminescence into account. Expressions for the diffusion of a luminescing layer, but taking into account only luminescence of the first 2 orders, were obtained by Ivanov,[16] who made use of a similar model. Sobolev[17] proposes a solution for the nonsteady-state problem in a form that is more convenient for analysis; however, his solution also applies to the one-dimensional case. The laws of growth and decay of luminescence are also discussed in reference 18. However the analyses performed in this paper and also in reference 19 are not carried out rigorously, and certain important relationships are not examined.

References 20-22 are also devoted to an explanation of the influence of secondary absorption and emission on the nature of radiation emanating from a volume of finite dimensions under nonsteady-state conditions. More specifically, general expressions for the intensity of the radiation coming out of a plane-parallel layer are derived in reference 22 with an arbitrary dependence of the external source output on time. It was also shown that, in the general case, the decay of the luminescence is not exponential and that the laws of growth and decay are strongly dependent not only on the intrinsic properties of the medium but also on the angles of incidence and observation. The nonsteady-state luminescence of an infinitely thick slab, as it depends on the quantum yield of an elementary volume and the conditions of exposure and observation, was examined in detail.

This paper considers the average duration of the luminescence of a plane-parallel layer due to secondary absorption and emission processes under different experimental conditions.

2. We will understand the term "average duration" to mean the ratio of the average duration of luminescence of a layer to the average duration of the luminescence of an elementary volume τ_0. If the dependence of the intensity of the emerging radiation J(t) on time is known, this value is determined in the following way:

$$\bar{\tau} = \frac{\frac{1}{2}\int_0^\infty J(t)\, t\, dt}{\tau_0 \int_0^\infty J(t)\, dt}. \tag{1}$$

The expressions derived in reference 22 for the average durations are:

$$\bar{\tau}_R^{pul}(\gamma, \xi) = \frac{\gamma}{J_R^{st}(\gamma, \xi)} \frac{dJ_R^{st}(\gamma, \xi)}{d\gamma}, \quad \bar{\tau}_T^{pul}(\gamma, \xi) = \frac{\gamma}{J_T^{st}(\gamma, \xi)} \frac{dJ_T^{st}(\gamma, \xi)}{d\gamma}, \tag{2}$$

$$\bar{\tau}_R^{cont}(\gamma, \xi) = \frac{1}{2} \frac{\frac{d^2[\gamma J_R^{st}(\gamma, \xi)]}{d\gamma^2}}{\frac{dJ_R^{st}(\gamma, \xi)}{d\gamma}}, \quad \bar{\tau}_T^{cont}(\gamma, \xi) = \frac{1}{2} \frac{\frac{d^2[\gamma J_T^{st}(\gamma, \xi)]}{d\gamma^2}}{\frac{dJ_T^{st}(\gamma, \xi)}{d\gamma}}, \tag{3}$$

where $\bar{\tau}_R^{pul}$ and $\bar{\tau}_T^{pul}$ are the radiation durations of a layer with short excitation (by a pulse) with observation by "reflected" and "transmitted" light, respectively; $\bar{\tau}_R^{cont}$

and $\overline{\tau}_T^{\xi\,cont}$ are the same values with continuous preliminary irradiation; γ is the quantum yield of an elementary volume; $J_R^{st.}$ and $J_T^{st.}$ are the intensities of the radiation under steady-state conditions; η is the cosine of the angle of observation; ξ is the product of the cosine of the angle of incidence and the ratio of the absorption coefficient within an emission band to the absorption coefficient for the exciting radiation. The study of duration of luminescence $\overline{\tau}^{pul.}$ with a pulsed excitation system is important in connection with research on the resolving power of scintillation counters, for example. Average luminescence durations after instantaneously shutting off the steady-state conditions $\overline{\tau}^{cont.}$ are often determined in fluorometric studies.

The analysis carried out in this paper is applicable to the situation in which the light emitted by the system is confined to a narrow frequency interval, but the absorbed light can be of any frequency. If the frequency of the exciting radiation coincides with the emission frequency, we have a case of propagation of resonance radiation. The results of this paper are also applicable to the problem of sensitized fluorescence of monatomic vapors. The applicability of the results of this work to materials with arbitrary absorption and emission bands will be considered separately.

From formulas (2) and (3) it is seen that if the dependence of the radiation intensity on quantum yield is known for the steady-state conditions of exposure $J_R^{st.}$ and $J_T^{st.}$, then it is easy to determine the luminescence duration for any layer parameters and any experimental conditions.

3. As is known,[13, 14, 17] the intensities $J_R^{st.}$ and $J_T^{st.}$ can be found by the following formulas

$$\left.\begin{aligned} J_R^{st.}(\eta,\xi) &= \frac{\gamma}{4\pi}\frac{k(\nu_1)}{k(\nu_0)}J_{ext.}(\xi)\,\xi\,\frac{\varphi(\xi)\varphi(\eta)-\psi(\xi)\psi(\eta)}{\eta+\xi}\,,\\ -J_T^{st.}(\eta,\xi) &= \frac{\gamma}{4\pi}\frac{k(\nu_1)}{k(\nu_0)}J_{ext.}(\xi)\,\xi\,\frac{\varphi(\xi)\psi(\eta)-\varphi(\eta)\psi(\xi)}{\eta-\xi}\,. \end{aligned}\right\} \quad (4)$$

Here $J_{\quad}(\xi)$ is the intensity of the external radiation incident on the layer, ϕ and ψ are auxiliary functions introduced for the first time by Ambartsumyan; $k(\nu_1)$ is the absorption coefficient for the external radiation; $k(\nu_0)$ is the absorption coefficient within the emission bands. In the general case, the functions ϕ and ψ are determined from nonlinear integral equations for which there are no rigorous solutions.

Expressions for ϕ and ψ are proposed in reference 24:

$$\varphi(\xi)=\frac{(2\xi+1)(1-2\xi+\gamma\xi)}{1-k^2\xi^2}+\frac{4\gamma\xi(2\xi+1)}{1-k^2\xi^2}\,\frac{1-e^{-2ka}}{(2+k)^2-(2-k)^2e^{-2ka}}+\frac{8\gamma\xi(2\xi-1)}{1-k^2\xi^2}\,\frac{e^{-ka}-\frac{a}{\xi}}{(2+k)^2-(2-k)^2e^{-2ka}}\,,$$

$$\psi(\xi)=\varphi(-\xi)\,e^{-\frac{a}{\xi}}\,,\quad k=2\sqrt{1-\gamma}. \quad (5)$$

Here a is the optical thickness of the layer for the emission band frequency. The results obtained by using these formulas are in good agreement with the results of rigorous calculations.

In a number of cases the expressions for ϕ and ψ are greatly simplified:

(a) for an infinitely thick layer ($a = \infty$)

$$\varphi(\xi)=\frac{1+2\xi}{1+2\xi\sqrt{1-\gamma}}\,,\quad \psi(\xi)\equiv 0; \quad (6)$$

(b) for excitation of the system by weakly absorbed radiation ($\xi = \infty$)

$$\varphi(\infty)=\psi(\infty)=\frac{2}{k}\,\frac{(2+k)-(2-k)e^{-2ka}}{(2+k)+(2-k)e^{-2ka}}\,; \quad (7)$$

(c) for quantum yield equal to 1 ($\gamma = 1$)

$$\varphi(\xi)=\frac{(2\xi+1)(1+a-\xi)}{1+a}+\frac{(2\xi-1)\xi}{1+a}\,e^{-\frac{a}{\xi}}\,,$$

$$\psi(\xi)=\frac{(2\xi+1)\xi}{1+a}-\frac{(2\xi-1)(1+a+\xi)}{1+a}\,e^{-\frac{a}{\xi}}\,. \quad (8)$$

Substituting the values of $J_R^{st.}$ and $J_T^{st.}$ expressed in terms of ϕ and ψ (determined by formulas (5) and (8)) into (2) and (3), we obtain the average durations of the luminescence depending in explicit form on the parameters of the layer and the experimental conditions.

4. Let us consider the duration of luminescence of an infinitely thick layer. Substituting (4) into (2) and taking (6) into consideration, we obtain

$$\tau^{pul.}(\gamma,\xi)=1+\frac{\gamma\xi}{1+2\xi\sqrt{1-\gamma}}\,\frac{1}{\sqrt{1-\gamma}}+\frac{\gamma\eta}{1+2\eta\sqrt{1-\gamma}}\,\frac{1}{\sqrt{1-\gamma}}\,. \quad (9)$$

The expression for the duration of luminescence associated with instantaneously switching off the steady-state exciting source $\overline{\tau}^{cont}(\eta,\xi)$ is more complicated:

$$\tau^{cont.}(\gamma,\xi)=1+\quad (10)$$

$$\frac{\gamma}{2}\,\frac{\gamma\varphi(\xi)\varphi''(\gamma_1)+\gamma\psi''(\xi)\varphi(\eta)+2\gamma\psi'(\xi)\psi'(\eta)+2\psi'(\xi)\varphi(\eta)+2\varphi(\xi)\psi'(\eta)}{\varphi(\xi)\varphi(\eta)+\psi'(\xi)\psi(\eta)+\psi(\xi)\psi'(\eta)}$$

where ϕ is determined by formula (6) and ϕ' and ϕ'' are the first and second derivatives with respect to γ. It is seen from (9) and (10) that the average duration is strongly dependent not only on γ but also on η and ξ, especially when the values of γ are large. So $\overline{\tau}^{pul.}$ and $\overline{\tau}^{cont.}$ vary within the following limits:

$$1\le\tau^{pul.}(\eta,\xi)\le\tau^{pul.}(1,\infty),\quad 1\le\tau^{cont.}(\gamma,\xi)\le\tau^{cont.}(1,\infty). \quad (11)$$

where

$$\tau^{pul.}(1,\infty)=1+\frac{\gamma}{2(1-\gamma)}+\frac{\gamma}{1+2\sqrt{1-\gamma}}\cdot\frac{1}{\sqrt{1-\gamma}}\,. \quad (12)$$

$$\tau^{cont.}(1,\infty)=1+\frac{\gamma}{4(1-\gamma)}\cdot\frac{36-33\gamma+24\sqrt{1-\gamma}-6\gamma\sqrt{1-\gamma}}{(2-\gamma+4\sqrt{1-\gamma})(1+2\sqrt{1-\gamma})}\,. \quad (13)$$

An examination of (12) and (13) indicates that the values of $\overline{\tau}^{pul}(1,\infty)$ and $\overline{\tau}^{cont}(1,\infty)$ can be rather appreciable. For example with $\gamma = .51$, $\overline{\tau}^{pul}(1,\infty) = 1.82$ and $\overline{\tau}^{cont.}(1,\infty) = 1.86$; with $\gamma = .96$, $\overline{\tau}^{pul}(1,\infty) = 16.43$ and $\overline{\tau}^{cont.}(1,\infty) = 19.56$. As $\gamma \to 1$, the durations $\overline{\tau}^{pul.}$ and $\overline{\tau}^{cont.}$ become infinitely long.

5. Formulas obtained in a similar way for the average durations in the case of luminescence of a layer of finite thickness are considerably more complicated. Comparatively simple expressions for the average durations can be written only in certain cases. For example, with $\gamma = 1$

$$\tau_R^{pul.}(\eta,\xi)=1+\frac{\varphi'(\xi)\varphi(\eta)+\varphi(\xi)\varphi'(\eta)-\psi'(\xi)\psi(\eta)-\psi(\xi)\psi'(\eta)}{\varphi(\eta)\varphi(\xi)-\psi(\eta)\psi(\xi)}\,, \quad (14)$$

$$\tau_T^{pul.}(\gamma,\xi)=1+\frac{\varphi'(\xi)\psi(\gamma_1)+\varphi(\xi)\psi'(\gamma_1)-\varphi(\gamma_1)\psi'(\xi)-\psi'(\gamma_1)\psi(\xi)}{\varphi(\xi)\psi(\gamma_1)-\varphi(\gamma_1)\psi(\xi)}\,, \quad (15)$$

where ϕ and ψ are defined by formula (8), and the derivatives with respect to γ, ϕ', and ψ', are equal respectively to:

$$\psi'(\xi) = (2\xi+1)(2\xi-1)^2\xi + (2\xi+1)(1-4\xi^2)\xi\,\frac{a}{1+a} + \xi(2\xi+1)\left[a + \frac{a^3}{3(1+a)^2}\right] + (2\xi-1)\xi(1-4\xi^2)\,\frac{e^{-\frac{a}{\xi}}}{1+a} + \xi(2\xi-1)\left[a - \frac{a^3}{3(1+a)^2}\right]e^{-\frac{a}{\xi}}, \quad (16)$$

$$\psi'(\xi) = \psi'(-\xi)\,e^{-\frac{a}{\xi}}. \quad (17)$$

Let us consider in more detail the expressions for the duration of the luminescence corresponding to the intensity of the radiation coming out of the layer averaged over the directions under consideration. For the steady state these values are determined from ϕ and ψ in the following way:

$$J_R^{ext.}(\xi) = \frac{k(\gamma_1)}{k(\gamma_0)}\,J_{ext.}(\xi)\,\frac{1}{2\pi}\left[\varphi(\xi) - 1\right],$$

$$J_T^{ext.}(\xi) = \frac{1}{2\pi}\,\frac{k(\gamma_1)}{k(\gamma_0)}\,J_{ext.}(\xi)\left[\psi(\xi) - e^{-\frac{a}{\xi}}\right]. \quad (18)$$

Expression (18) can be easily derived from the integral equations defining ϕ and ψ and formula (4). Substituting (18) into (2) and (3), we obtain

$$\tau_R^{pul.}(\xi) = \frac{T\varphi'(\xi)}{\varphi(\xi) - 1}, \quad \tau_T^{pul.}(\xi) = \frac{T\psi'(\xi)}{\psi(\xi) - e^{-\frac{a}{\xi}}}, \quad (19)$$

$$\tau_R^{cont.}(\xi) = 1 + \frac{T}{2}\,\frac{\varphi''(\xi)}{\varphi'(\xi)}, \quad \tau_T^{cont.}(\xi) = 1 + \frac{T}{2}\,\frac{\psi''(\xi)}{\psi'(\xi)}. \quad (20)$$

The substitution of the appropriate expressions for ϕ and ψ into (19) and (20) leads to complicated relationships showing the dependence of the durations on γ, a, and ξ. Only in certain cases are relatively simple expressions obtained:

(a) The external radiation is almost totally absorbed at the front boundary of the layer ($\xi = 0$). This corresponds to either a strong absorption of the exciting radiation, or a very high (near 90 deg) angle of incidence. Expanding ϕ and ψ into a series in powers of ξ and confining ourselves to 2 terms of the expansion, we obtain

$$\tau_R^{pul.}(0) = 1 + \frac{\gamma}{2\sqrt{1-\gamma}}\,\frac{(1+\sqrt{1-\gamma})^2 - 4\sqrt{1-\gamma}\,(1+2a\gamma)\,e^{4a\sqrt{1-\gamma}} - (1-\sqrt{1-\gamma})^2\,e^{-8a\sqrt{1-\gamma}}}{\left[(1+\sqrt{1-\gamma})^2 - (1-\sqrt{1-\gamma})^2\,e^{-4a\sqrt{1-\gamma}}\right]\left[(1+\sqrt{1-\gamma}) - (1-\sqrt{1-\gamma})\,e^{-4a\sqrt{1-\gamma}}\right]}, \quad (21)$$

$$\tau_T^{pul.}(0) = 1 + \frac{\gamma}{2(1-\gamma)}\,\frac{2a\sqrt{1-\gamma}\,(1+\sqrt{1-\gamma})^2 - \gamma + e^{-4a\sqrt{1-\gamma}}\left[2a\sqrt{1-\gamma}\,(1-\sqrt{1-\gamma})^2 + \gamma\right]}{(1+\sqrt{1-\gamma})^2 - (1-\sqrt{1-\gamma})^2\,e^{-4a\sqrt{1-\gamma}}}. \quad (22)$$

With a yield equal to one ($\gamma = 1$) the durations of luminescence are

$$\tau_R^{pul.}(0) = \frac{3 + 12a + 12a^2 + 4a^3}{3(1+a)(1+2a)}, \quad \tau_T^{pul.}(0) = \frac{3 + 6a + 6a^2 + 2a^3}{3(1+a)}, \quad (23)$$

$$\tau_R^{cont.}(0) = \frac{45 + 270a + 540a^2 + 540a^3 + 300a^4 + 96a^5 + 16a^6}{15(1+a)(3+12a+12a^2+4a^3)}, \quad \tau_T^{cont.}(0) = \frac{45 + 135a + 225a^2 + 210a^3 + 180a^4 + 84a^5 + 14a^6}{15(3+6a+6a^2+2a^3)}. \quad (24)$$

(b) The external radiation is attenuated exponentially inside the layer as e^{-2x}, where x is the optical thickness of the layer for the frequency of the emission band ($\xi = \frac{1}{2}$). In addition to the directed light beam, a diffusion flux with a frequency equal to the frequency of the emission band (resonance luminescence the intensity of which does not depend on direction) is also attenuated according to approximately the same law.

For this case

$$\tau_R^{pul.}\left(\frac{1}{2}\right) = \frac{1}{\sqrt{1-\gamma}}\,\frac{(1+\sqrt{1-\gamma})^2 - 4\sqrt{1-\gamma}\,(1+2a\gamma)\,e^{-4a\sqrt{1-\gamma}} - (1-\sqrt{1-\gamma})^2\,e^{-8a\sqrt{1-\gamma}}}{\left[(1+\sqrt{1-\gamma})^2 - (1-\sqrt{1-\gamma})^2\,e^{-4a\sqrt{1-\gamma}}\right]\left(1 - e^{-4a\sqrt{1-\gamma}}\right)}, \quad (25)$$

$$\tau_T^{pul.}\left(\frac{1}{2}\right) = \frac{2\gamma e^{-2a\sqrt{1-\gamma}}\left[2a\sqrt{1-\gamma}\,(1+\sqrt{1-\gamma})^2 - \gamma + e^{-4a\sqrt{1-\gamma}}\left[2a\sqrt{1-\gamma}\,(1-\sqrt{1-\gamma})^2 + \gamma\right]\right]}{\sqrt{1-\gamma}\left[(1+\sqrt{1-\gamma})^2 - (1-\sqrt{1-\gamma})^2\,e^{-4a\sqrt{1-\gamma}}\right]\left[4\sqrt{1-\gamma}\,e^{-2a\sqrt{1-\gamma}} - (1+\sqrt{1-\gamma})^2\,e^{-2a} + (1-\sqrt{1-\gamma})^2\,e^{-2a-4a\sqrt{1-\gamma}}\right]} \quad (26)$$

The durations for $\gamma = 1$ are determined by the formulas

$$\tau_R^{pul.}\left(\frac{1}{2}\right) = \frac{3 + 6a + 4a^2}{3(1+a)}, \quad \tau_T^{pul.}\left(\frac{1}{2}\right) = \frac{3a + 6a^2 + 2a^3}{3(1+a)(1 - e^{-2a} - ae^{-2a})}, \quad (27)$$

$$\tau_R^{cont.}\left(\frac{1}{2}\right) = \frac{18a^3 + 96a^4 + 240a^5 + 300a^6 + 180a + 45}{15(1+a)(4a^2+6a+3)}, \quad (28)$$

$$\tau_T^{cont.}\left(\frac{1}{2}\right) = \frac{45 + 180a + 270a^2 + 210a^3 + 84a^4 + 14a^5}{15(1+a)(2a^2+6a+3)}. \quad (28)$$

(c) The layer is excited by weakly absorbed radiation ($\xi = \infty$). This case is realized in scintillation counters,[4] for example. Here the durations for "reflected" and "transmitted" radiation are equal to

$$\tau_R^{pul.}(\infty) = \tau_T^{pul.}(\infty) = \frac{(1+\sqrt{1-\gamma})^2 - 4\sqrt{1-\gamma}\,(1+\gamma a)\,e^{-2a\sqrt{1-\gamma}} - (1-\sqrt{1-\gamma})^2\,e^{-4a\sqrt{1-\gamma}}}{2(1-\gamma)\left(1 - e^{-2a\sqrt{1-\gamma}}\right)\left[1 + \sqrt{1-\gamma} + (1-\sqrt{1-\gamma})\,e^{-2a\sqrt{1-\gamma}}\right]}. \quad (29)$$

With $\gamma = 1$

$$\tau_R^{pul.}(\infty) = \tau_T^{pul.}(\infty) = 1 + a + \frac{a^2}{3}, \quad (30)$$

$$\tau_R^{cont.}(\infty) = \tau_T^{cont.}(\infty) = \frac{15 + 15a + 10a^2 + 20a^3 + 17a^4 + 5a^5}{5(3 + 3a + a^2)}. \quad (31)$$

It is seen from the formulas presented that variation of the experimental conditions leads to a change in the dependence of the average duration on the parameters of the layer. This is especially marked at high values of γ.

6. Tables 1 and 2 present the values of the average durations of $\overline{\tau}_R^{pul.}$ and $\overline{\tau}_T^{pul.}$ corresponding to the intensities of the luminescence with $\gamma = 1$, averaged over the directions considered. The tables were computed from formulas (19) in which ϕ, ψ, ϕ'_1 and ψ' were calculated in accordance with expressions (8) and (16).

Table 1. Values of $\overline{\tau}_R^{pul.}(\xi)$ with $\gamma = 1$

ξ	a = 0.5	1.0	1.5	2.0	3.0	4.0	5.0	7.0	10.0
0.0	1.39	1.72	2.05	2.38	3.04	3.70	4.36	5.69	7.68
0.2	1.52	2.01	2.47	2.94	3.86	4.79	5.72	7.58	10.4
0.4	1.55	2.13	2.72	3.31	4.50	5.69	6.88	9.27	12.9
0.5	1.56	2.17	2.80	3.44	4.75	6.07	7.39	10.0	14.0
0.6	1.56	2.19	2.86	3.55	4.97	6.40	7.85	10.8	15.1
0.8	1.57	2.22	2.94	3.71	5.31	6.97	8.66	12.1	17.2
1.0	1.57	2.25	3.00	3.81	5.56	7.41	9.32	13.2	19.2
1.2	1.57	2.26	3.02	3.89	5.75	7.77	9.87	14.2	20.9
1.4	1.57	2.27	3.07	3.95	5.90	8.05	10.3	15.1	22.5
1.6	1.57	2.28	3.09	3.99	6.08	8.28	10.7	15.8	23.9
1.8	1.58	2.28	3.10	4.03	6.12	8.47	11.0	16.5	25.2
2.0	1.58	2.29	3.12	4.05	6.20	8.63	11.3	17.1	26.3
3.0	1.58	2.30	3.16	4.14	6.45	9.14	12.3	19.0	30.6
5.0	1.58	2.32	3.19	4.21	6.66	9.59	13.0	20.9	35.3
10.0	1.58	2.32	3.22	4.26	6.82	9.96	13.7	22.5	39.5
∞	1.58	2.33	3.25	4.33	7.00	10.3	14.3	24.3	44.3

Tables 1 and 2 graphically demonstrate the dependence of the duration of luminescence on the layer thicknesses a and ξ. Inasmuch as ξ is proportional to the cosine of the angle of incidence and inversely proportional to the absorption coefficient of the exciting radiation, these tables also indicate the dependence of the duration of luminescence on the spectral composition of the exciting light. It is clear from the tables that the durations are extended by an increase in the thickness of the layer. The durations for "transmitted" radiation are always greater than the corresponding durations for "reflected" radiation. The latter figure increases with increasing ξ, reaching its maximum value at $\xi = \infty$. On the other hand, values of the durations for "transmitted" radiation decrease with increasing ξ, reaching a minimum at $\xi = \infty$. This minimum value of the duration for "transmitted" radiation is equal to the maximum value of the duration for "reflected" radiation.

Table 2. Values of $\overline{\tau}_T^{pul.}(\xi)$ with $\gamma = 1$

ξ	a = 0.5	1.0	1.5	2.0	3.0	4.0	5.0	7.0	10.0
0.0	1.72	2.83	4.30	6.11	10.8	16.7	24.1	42.7	80.7
0.2	1.85	2.70	4.14	5.95	10.6	16.6	23.9	42.5	80.4
0.4	1.82	2.55	3.87	5.56	10.1	16.1	23.4	42.1	80.0
0.5	1.81	2.51	3.77	5.41	9.85	15.8	23.1	41.7	79.7
0.6	1.81	2.49	3.69	5.27	9.57	15.4	22.6	41.3	79.3
0.8	1.80	2.45	3.59	5.03	9.10	14.7	21.7	40.2	78.1
1.0	1.80	2.43	3.52	4.92	8.74	14.0	20.8	38.9	76.7
1.2	1.80	2.41	3.48	4.83	8.48	13.5	20.0	37.7	75.1
1.4	1.59	2.40	3.45	4.76	8.28	13.1	19.4	36.5	73.3
1.6	1.59	2.39	3.43	4.71	8.12	12.8	18.8	35.4	71.5
1.8	1.59	2.39	3.40	4.66	8.00	12.5	18.4	34.4	70.2
2.0	1.59	2.38	3.39	4.63	7.90	12.3	18.00	33.6	68.1
3.0	1.59	2.36	3.34	4.53	7.60	11.7	16.8	30.7	61.6
4.0	1.59	2.36	3.32	4.48	7.45	11.3	16.2	29.1	57.5
5.0	1.59	2.35	3.31	4.45	7.36	11.1	15.8	28.2	54.9
10.0	1.59	2.34	3.28	4.39	7.18	10.7	15.1	26.2	49.8
∞	1.58	2.33	3.25	4.33	7.00	10.3	14.3	24.3	44.3

The dependence of the duration of luminescence observed by "transmission" and "reflection" on the thickness of the layer for different γ's is illustrated in Figs. 1 and 2. The curves for $\overline{\tau}^{pul.}$ are plotted in Fig. 1, and those for $\overline{\tau}^{cont.}$ in Fig. 2. The durations are calculated for the case in which $\xi = \frac{1}{2}$ and the intensity of the radiation is observed averaging over the directions considered. Specifically, the curves of Fig. 1 were computed from formulas (25)-(27).

It is clear from the figures that the increase of the average luminescence durations can be rather large, even with moderate values for the quantum yield of an

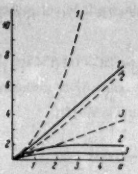

Fig. 1

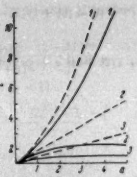

Fig. 2

Fig. 1. The dependence of the average luminescence duration on the optical thickness of the layer with preliminary pulsed excitation. The unbroken curves are the duration for "reflected" radiation. The broken curves are the duration for "transmitted" radiation. Curves 1—γ = 1.00; curves 2—γ = 0.75; curves 3—γ = 0.51.

Fig. 2. The dependence of the average luminescence duration on the optical thickness of the layer with preliminary continuous excitation. The unbroken curves are the duration for "reflected" radiation. The broken curves are the duration for "transmitted" radiation. Curves 1—γ = 1.00; curves 2—γ = 0.75; curves 3— γ = 0.51.

elementary volume. With γ's near 1, the increase in the luminescence duration relative to the duration for an elementary volume is appreciable, even with layers of comparatively small optical thickness. The luminescence durations associated with observation by "reflection" (solid curves) increase with increasing optical thickness and reach limiting values corresponding to the luminescence of an infinite layer. The durations by "transmission" (broken curves) increase indefinitely with increasing optical thickness a, their dependence on a being approximately linear for $\gamma < 0.75$. Therefore the increase in duration due to secondary processes is most strongly demonstrated in the observation of radiation that has "passed through." For example, for a = 5 and γ = 1 $\overline{\tau}_T^{pul.} = 23.1$, $\overline{\tau}_T^{cont.} = 17.4$; with a = 5 and γ = .75 $\overline{\tau}_T^{pul.} = 7.1$, $\overline{\tau}_T^{cont.} = 5.1$; the corresponding values $\overline{\tau}_R^{pul.}$ and $\overline{\tau}_R^{cont.}$ are 7.4 and 12.4, 2.0, and 2.25.

The values of $\overline{\tau}^{pul.}(\infty)$ for different layer thicknesses and different values of the quantum yield of an elementary volume γ are shown in Table 3. There is a very strong dependence on γ, especially for thick layers.

Table 3. Values of $\overline{\tau}^{pul.}(\infty)$

a	γ = 0.10	0.30	0.51	0.64	0.75	0.81	0.91	0.95	0.99	1.00
0.5	1.08	1.15	1.23	1.31	1.38	1.45	1.50	1.55	1.57	1.58
1.0	1.12	1.26	1.41	1.57	1.74	1.92	2.08	2.21	2.30	2.33
1.5	1.14	1.32	1.53	1.78	2.06	2.37	2.69	2.97	3.18	3.25
2.0	1.16	1.36	1.61	1.93	2.31	2.78	3.30	3.80	4.19	4.33
3.0	1.17	1.39	1.69	2.10	2.66	3.42	4.40	5.55	6.57	7.00
4.0	1.17	1.40	1.72	2.17	2.84	3.84	5.30	7.27	9.35	10.3
5.0	1.17	1.41	1.73	2.20	2.93	4.08	5.94	8.84	12.4	14.2
7.0	1.17	1.41	1.73	2.22	2.99	4.29	6.70	11.3	18.0	24.3
10.0	1.17	1.41	1.73	2.22	3.00	4.36	7.10	13.5	28.6	44.3
∞	1.17	1.41	1.73	2.22	3.00	4.37	7.22	15.0	55.0	∞

7. Observation of the luminescence duration by "transmission" is meaningful if the radiation that has "passed through" is sufficiently intense and experimentally measurable. Figure 3 is a graph of the dependence of the "reflection" coefficient $R = \phi\left(\frac{1}{2}\right) - 1$ (solid curves) and the "transmission" coefficient $T = \psi\left(\frac{1}{2}\right) - e^{-2a}$ (broken curves) on layer thickness for the steady state;

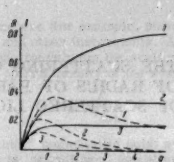

Fig. 3. The dependence of the "reflection" coefficient R and the "transmission" coefficient T on layer thickness. The unbroken curves are the "reflection" coefficient. The broken curves are the "transmission" coefficient. Curves 1—$\gamma = 1.00$; curves 2—$\gamma = 0.75$; curves 3—$\gamma = 0.51$.

i.e., immediately after turning off the continuous external source. The figure shows that the values of T are still rather appreciable for layer thicknesses $a \leq 5$, $\gamma \geqslant 0.75$ (for $\gamma = 1$ and $a = 5$, $T = 17\%$; for $\gamma = .75$ and $a = 5$, $T = 0.5\%$). Consequently, the increase in average luminescence duration under "transmission" measurement conditions, with high values of γ, is fully accessible to experimental observation.

8. A study of the nonsteady-state luminescence is conducted in references 20-23, and also in this paper. Our work is done under conditions such that there is a certain time interval between the disappearance and reappearance of a photon. We have called this interval "the average duration of luminescence" or "the average time that particles exist in the excited state for an elementary volume." Inasmuch as any interaction of light with matter, generally speaking, takes place after some time interval, the delay of luminescence due to the presence of radiation of higher order must occur in any medium and be independent of the nature of the interaction. For this reason, the considerable increase of average duration associated with observation by "transmission" can be used for determination of very short time periods associated with the interaction of light with matter. In addition to this work, there is a need for further studies that take account of the nonspherical distribution of radiation.

In conclusion, I express my appreciation to B. I. Stepanov for suggesting this theme and taking an interest in the work.

REFERENCES

1. A. Mitchell and M. Zemansky. "Rezonansnoe izluchenie i vozbuzhdennye atomy." (Resonance Radiation and Excited Atoms), GNTI, Moscow, 1937.
2. P. Pringsheim. "Fluorestsentsiya i Fosfore s tsentsiya." (Fluorescence and Phosphorescence), IL, Moscow, 1951.
3. A. V. Phelps. Phys. Rev. **110**, 1362 (1958).
4. J. Birks. "Stsintillyatsionnye schetchiki." (Scintillation Counters), IL, Moscow, 1955.
5. L. M. Biberman. Zhur. Eksptl. i Teoret. Fiz. **17**, 416 (1947).
6. R. Seiwert. Exper. Techn. d. Phys. **3**, Sonderheft "Spektroskopie," 6 (1955).
7. T. Holstein. Phys. Rev. **72**, 1212 (1947).
8. T. Holstein. Phys. Rev. **83**, 1159 (1951).
9. L. M. Biberman, Dokt. diss., Mosk. energ. inst. 1958 (Doctorate dissertation, Moscow Power Engineering Institute 1958).
10. B. A. Veklenko. Zhur. Eksptl. i Teoret. Fiz. **33**, 817 (1957).
11. B. A. Veklenko. Zhur. Eksptl. i Teoret. Fiz. **36**, 204 (1959).
12. V. M. Agranovich. Opt. i Spektr. **3**, 84 (1957).
13. V. M. Agranovich. Izvest. Akad. Nauk SSSR, Ser. Fiz. **23**, 40 (1959).
14. V. M. Agranovich and Iu. Iu. Konobeev. Opt. i Spektr. **6**, 648 (1959).
15. G. A. Gamburzeff. Z. Physik **55**, 553 (1929).
16. A. P. Ivanov. Opt. i Spektr. **2**, 800 (1957).
17. V. V. Sobolev. "Perenos luchistoi energii v atmosferakh zvezd i planet." (The Transport of Radiant Energy in the Atmospheres of Stars and Planets). GITTL, Leningrad, 1956.
18. S. F. Kilin and I. M. Rozman. Opt. i Spektr. **6**, 70 (1959).
19. M. D. Galanin. Trudy Fiz. Inst. Akad. Nauk SSSR **5**, 340 (1950).
20. A. M. Samson. Opt. i Spektr. **5**, 500 (1958).
21. A. M. Samson. Izvest. Akad. Nauk SSSR, Ser. Fiz. **22**, 1399 (1958).
22. A. M. Samson. Inzh. Fiz. Zhurn. **2**, 6 (1959).
23. A. M. Samson. Inzh. Fiz. Zhurn. **2**, 8 (1959).
24. A. M. Samson. Inzh. Fiz. Zhurn. **1**, 1 (1958).

DETERMINATION OF THE SIZE OF PARTICLES BY THE SCATTERING OF LIGHT
I. FORMULAS AND NOMOGRAMS FOR COMPUTATION OF RADIUS OF PARTICLES BY THE OPTICAL DENSITY AND BY INTENSITY OF SCATTERED LIGHT

I. Ya. Slonim

Received 28 April 1959

On the basis of the equations of Shifrin's theory of light-scattering, formulas are derived and nomograms are constructed for the determination of the sizes of particles of the dispersion systems, in which electrical properties of the particles deviate little from the properties of the surrounding medium.

I. INTRODUCTION

The basic advantage of the optical method of determination of the size of particles of dispersion systems is the possibility of following the processes in the system, without interfering with the course of these processes. This makes the method particularly valuable for the colloidal chemistry.

The literature dedicated to theory of light scattering and to practical applications of this method is very extensive (see, for example, the monograph of reference 1 and reviews of references 2 and 3.) The method proposed by Debye is widely used for determination of molecular weight of polymers from light scattering; optical methods are also used for studying latices and dispersions of polymers.[4-7] However, it should be noted that for a very important case, when the size of the particles approaches the wavelength of the light, computation with the formulas of the theory of Mie[8] is very complicated.

Considerably simpler expressions for the coefficient of scattering and the indicatrix of scattering are obtained[1] for dispersion systems in which electrical properties of the particles deviate but little from the properties of the surrounding medium. To these systems belong many important colloidal systems, and particularly latexes and water dispersions of high polymers. The equations of Shifrin's theory, and his tabulated values of the functions entering into them,[1,9] allow one to calculate the optical properties of these systems from the known sizes and the properties of the particles.

In colloidial chemistry the reverse problem is encountered more often; that is one of determining the size of particles by light scattering. The purpose of this article is the derivation, on the basis of equations of Shifrin's theory, of formulas for computation of the size of particles from the light scattered by a dispersion system.

II. INITIAL EQUATIONS OF LIGHT SCATTERING THEORY FOR GLOBULAR PARTICLES WHOSE PROPERTIES DO NOT DEVIATE MUCH [FROM THOSE OF THE MEDIUM]

The coefficient of scattering k_p, equal to the total light energy scattered by one particle in all directions, with the intensity of the incident flux equal to unity, is determined in first approximation by the equation:

$$k_p = \pi a^2 \alpha^2 F(z), \tag{1}$$

where a is the radius of the particle, α is the parameter characterizing the deviation of the properties of the particle from the properties of the surrounding medium.

$$\alpha = \frac{3}{4\pi}\left(\frac{m^2-1}{m^2+2}\right),$$

where m is the ratio of the indices of the particle and the medium

$$F(z) = \frac{2z^2}{z^2}\left\{\frac{z^2}{4} + 5z^2 + (4z^2 - 16)(\mathrm{Ci}\, z - \ln z - C_e) - 2z\sin z + 14(\cos z - 1)\right\}. \tag{3}$$

Ci z is the integral cosinus of z, C_e is Euler's constant equal to 0.577,215..., z is a parameter characterizing the ratio of the size of the particle to the wavelength.

$$z = \frac{8\pi a}{\lambda}, \tag{4}$$

where λ is the light wavelength in the medium, equal to the wavelength in vacuum, divided by the index of refraction of the medium.

The indicatrix of scattering is expressed by equation:

$$I_\beta = I_0 v^2 \frac{16\pi^4}{\lambda^4} \alpha^2 \left(\frac{1+\cos^2\beta}{2}\right) f^2(q), \tag{5}$$

where I is the intensity of light scattered by the particle at angle β to the direction of the incident pencil (See Fig. 1), I_0 is the intensity of the incident light, v is the volume of the particle,

$$f(q) = \frac{3}{q^3}(\sin q - q\cos q), \tag{6}$$

$$q = \frac{z}{2}\sin\frac{\beta}{2}. \tag{7}$$

III. DIRECTLY MEASURED QUANTITIES WHEN STUDYING LIGHT-SCATTERING OF DISPERSION SYSTEMS

If we exclude measurements of the degree of polarization, not investigated in this work, the study of light-scattering of a dispersion system includes: (a) measuring the intensity I′ of the transmitted light, and (b) measuring the intensity I_β of the light scattered under different angles (see Fig. 1). The measurement of I′ can be performed with the aid of spectrophotometers, photometers of different designs (for example, photometers FM and

Fig. 1

FM-56), colorimeters (for example, photoelectrocolorimeter FEK-N) and other instruments. As a result of the measurement, one reads from the scale of the instrument the value of the optical density of the system:

$$D = \lg \frac{I_0}{I_{instr.}}. \quad (8)$$

For the "white" nonmetallic sols, absorption of light by the particles is insignificant, and attenuation of the primary light pencil is conditioned only by scattering of light in accordance with the law:

$$I = I_0 e^{-\tau x}, \quad (9)$$

where τ is the turbidity, x the thickness of the system along the path of rays. In this case:

$$\tau = \frac{2.303D}{x}. \quad (10)$$

Applying a series of light filters, it is possible to determine the value of D for different λ. With an increasing wavelength, the optical density is decreasing. The dependence of D on λ may be represented[10] by the empirical equation:

$$D = \text{const}\, \lambda^{-n}, \quad (11)$$

where the index n depends on the size of the particles, but does not depend on λ.

Since in the final account the nature of light scattering is determined by the ratio of the size of the particle to the wavelength, it is obvious that Eq. (11) can be valid only within a sufficiently narrow interval of values λ.

For the determination of n, experimental data are put on a graph with the coordinates $\log D - \log \lambda$; a straight line is obtained, the slope of which is equal to n.

Sufficiently reliable measurements of light scattering by transmission methods may be obtained only for the systems with relatively larger values of τ, of the order of magnitude of 10^{-2} cm^{-1}. With small values of τ, of the order of magnitude of 10^{-3} to 10^{-4} cm^{-1}, more accurate results are obtained by means of direct measurement of I_β/I_0, conducted with the aid of nephelometers. Usually, measurements are made with values of $\beta = 45°$, 90°, 135°, and others (see reference 3, page 708). The value of τ rises monotonously with the increase in the size of particles in a constant total concentration; therefore, it can be used directly for the determination of a. But, simultaneously with the increase of the total amount of the scattered light energy with the increasing a, there occurs a forward expansion of the indicatrix. Therefore, the values of I_β for $\beta \neq 0$ first increase, and then decrease,[11] passing through numerous maxima and minima. The first maximum for I_{45} is observed at $z \approx 13.5$; for I_{90} at $z \approx 7$; for I_{90} at $z \approx 5.5$.

Within the interval, of interest to us, of values of z from 2 to 8, the values I_{90} and I_{135} will not anymore uniquely determine the value a; therefore, we shall present a table for determining a for I_{45} only, particularly because the nephelometer NFM manufactured here with a standard turbid prism permits the determination of the absolute value for I_{45}/I_0 only. The indicatrix of dispersion of particles which are small with respect to the wavelength is symmetrical, and in this case $I_{45}/I_{135} = 1$. For larger particles, the indicatrix is expanded, and $I_{45}/I_{135} > 1$.

The value of the ratio I_{45}/I_{135}, uniquely characterizing the asymetry of dispersion, is determined by the size of the particle, and it may be used for computing a.

Equations (1) and (5) were derived for one particle. Actually, we are investigating a system in which there are a great number of particles. If the distances between the particles are sufficiently large, it may be assumed that the intensity of light, scattered by 1 cm^3 of the system, is equal to the product of the intensity with one particle and the partial concentration (the number of particles in 1 cm^3) N_1. Under other equal conditions, values of τ and I_β/I_0 will be proportional to the volume concentration (the part of the system volume occupied by the dispersion phase) c_v, because:

$$N_1 = \frac{c_v}{v} = \frac{3c_v}{4\pi a^3}. \quad (12)$$

For a characterization of a system, one should not use the absolute values of τ and I_β/I_0, but their ratios to the concentration. To exclude the result of the mutual influence of the particles and their electric fields, it is necessary to conduct the measurements of τ and I_β/I_0 at several concentrations, and to extrapolate the values τ/c_v and I_β/c_vI_0 for an infinite concentration.

Let us denote the limiting values:

$$\lim \left(\frac{\tau}{c_v}\right)_{c_v \to 0} \equiv [\tau] \quad (13)$$

and

$$\lim \left(\frac{I_\beta}{I_0 c_v}\right)_{c_v \to 0} \equiv [I_\beta] \quad (14)$$

and call them, respectively, "the characteristic turbidity" and "the characteristic intensity of light scattering at angle β." Thus, as a result of the measurements, we shall obtain the values of the characteristic turbidity τ (cm^{-1}), of the exponent n in empirical equation (11), the characteristic intensity I_β (cm^{-1}) of light scattering at angle β, and the asymetry of the indicatrix, I_{45}/I_{135}, of light scattering. The formulas for determining the sizes of particles from these values will be given in the following section.

IV. FORMULAS FOR DETERMINING THE SIZE OF PARTICLES

(a) Determination of a from τ

The turbidity τ is equal to the total energy scattered by 1 cm^3 of the system:

$$\tau = k_p N_1. \quad (15)$$

Substituting from (1) the value of k_p into (15), the value of N_1 from (12), and taking into consideration that

$$a = \frac{z\lambda}{8\pi}, \quad (16)$$

we obtain

$$\tau = \frac{6\pi c_v}{z^3} a^2 F(z). \quad (17)$$

from where

$$[\tau] = \frac{a^2}{\lambda} 6\pi \frac{F(z)}{z}.$$

Let us denote

$$6\pi \frac{F(z)}{z} \equiv \varphi(z), \quad (18)$$

then

$$\varphi(z) = \frac{[\tau]\lambda}{a^2}. \quad (19)$$

The values $\varphi(z)$ for z from 2 to 8 for increments of 0.5 were computed and are given in the table; the intermediate values may be determined with a sufficient accuracy by a linear interpolation. The character of the

variation of $\varphi(z)$ with z can be seen on the graph (Fig. 2). For the determination of the size of particles from the known values of the indices of refraction of the particles and of the medium, and from the measured value of τ, we can compute α (Eq. (2)) and λ, and from formula (19) we shall find $\varphi(z)$. We can find from the table the corresponding value z and determine a from formula (16). The whole computation can be performed in a few minutes using a slide rule.

(b) Computation of a from n

From (1), (10), and (15) we obtain

$$D = \frac{\pi}{2.303} N_1 \pi a^2 a^2 F(z). \tag{20}$$

Obviously, only z is changing when λ is changing (under the condition that the value of the relative index of refraction of the particle remains constant, i.e., that the optical dispersion of the particle and of the medium are the same).

Therefore, Eq. (20) may be rewritten

$$D = \text{const} \cdot F(z). \tag{21}$$

Substituting into (11) the value of λ from (4), and taking into consideration that a is constant, we obtain

$$D = \text{const} \cdot z^n. \tag{22}$$

By comparing (21) and (22) we observe that in a restricted interval of wavelengths

$$F(z) = \text{const} \cdot z^n,$$

where from

$$\lg F(z) = n \lg z + \text{const}$$

and

$$n = \frac{\Delta [\lg F(z)]}{\Delta \lg z}. \tag{23}$$

The values of n were computed and they are given in the Table and on the graph (Fig. 2) for z from 2 to 8.

z	$\varphi(z)$	Increments	$i(45, z)$	Increments	I_{45}/I_{135}	Increments	n	Increments	z
2.0	25.12	21.18	2.365	2.207	1.155	0.099	3.812	—0.126	2.0
2.5	46.30	28.36	4.602	3.191	1.254	0.147	3.686	—0.113	2.5
3.0	74.66	35.1	7.793	4.29	1.401	0.174	3.573	—0.137	3.0
3.5	109.8	40.7	12.08	5.46	1.575	0.251	3.436	—0.152	3.5
4.0	150.5	44.5	17.54	7.55	1.826	0.304	3.284	—0.163	4.0
4.5	195.0	44.6	24.09	2.130	2.130	0.546	3.121	—0.161	4.5
5.0	241.6	46.6	32.18	8.09	2.676	0.546	2.960	—0.153	5.0
5.5	288.0	47.4	40.98	8.80	3.222	0.695	2.807	—0.148	5.5
6.0	335.4	46.9	50.92	9.94	3.971	1.083	2.659	—0.126	6.0
6.5	381.2	45.3	61.86	10.74	5.054	1.737	2.533	—0.076	6.5
7.0	425.5	44.3	73.18	11.32	6.791	2.766	2.457	—0.078	7.0
7.5	469.7	44.2	85.01	11.83	9.057	2.29	2.379	—0.050	7.5
8.0	511.6	41.9	97.26	12.25	25.47	11.22	2.329		8.0

Note: The increments of the values of functions are given for facilitation of interpolation.

As it could be expected, the value of n is near 4 when the values of z are small; because for small particles n = 4 in accordance with the Rayleigh equation.

As z increases, the value of n decreases, approaching the limit of 2 for the particles the sizes of which are larger than the wavelength. For the determination of the size of particles from the experimentally determined value of n, we find the value of z in the Table, and then the value of a in accordance with formula (16); for λ we shall take its average value in the region for which n is being determined.

(c) Computation of a from I_β

For the intensity of the light scattered at angle β by the system containing N_1 particles in 1 cm³, we obtain from Eq. (5)

$$I_\beta = I_0 v^2 \frac{16\pi^4}{\lambda^4} v^2 N_1 \left(\frac{1+\cos^2\beta}{2}\right) f^2(q).$$

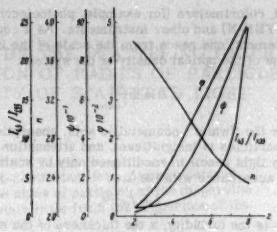

Fig. 2

Substituting for vN_1 the value c_v, and using the expression for z as may be derived from Eq. (16),

$$\frac{I_\beta}{I_0 c_v} = \frac{\pi^2 a^2 z^2}{24\lambda}\left(\frac{1+\cos^2\beta}{2}\right) f^2(q).$$

Let us denote:

$$\frac{\pi^2}{24} z^2 \left(\frac{1+\cos^2\beta}{2}\right) f^2(q) \equiv \psi(\beta, z). \tag{24}$$

Then,

$$[I_\beta] = \frac{a^2 \psi(\beta, z)}{\lambda}$$

and

$$\psi(\beta, z) = \frac{[I_\beta]\lambda}{a^2}. \tag{25}$$

The values $\psi(\beta, z)$ for $\beta = 45°$ and z from 2 to 8 are given in the Table. The computation of a from I_{45} is made exactly as it was done from τ (see Section (a)).

(d) Computation of a from I_{45}/I_{135}

It is seen from Eq. (5) that for the two values β_1 and β_2 symmetrical about the normal to the direction of the incident pencil, when $\cos^2\beta_1 = \cos^2\beta_2$, we have:

$$\frac{I_{\beta_1}}{I_{\beta_2}} = \frac{f^2(q_1)}{f^2(q_2)}.$$

We have computed the values of I_{45}/I_{135} for z from 2 to 8. With the aid of these values, given in the Table, and using the value of the asymetry of light scattering for I_{45}/I_{135}, one can easily find z, and then determine a from formula (16).

The determination of size of particles from n and from I_{45}/I_{135}, has the advantage of not requiring the measurement of the absolute values of light scattering. It is only necessary to find the dependence of the light scattering from the wavelength or from the direction of the scattered pencil; this can frequently be done more simply and with greater accuracy than the absolute measurements.

V. THE CONDITIONS OF APPLICABILITY AND THE ACCURACY OF THE FORMULAS DERIVED IN SECTION IV

(a) The Limits of z

The values of functions, given in the Table, permit computation of a for z from 2 to 8. For smaller particles, one may use also the Rayleigh equation. In accordance with our system of notation, the Rayleigh equation leads to the following computational formulas:

$$a = \frac{\lambda}{8\pi^2}\left(\frac{9[\tau]\lambda}{\alpha^2}\right)^{1/6}. \tag{26}$$

$$a = \frac{\lambda}{2\pi^2}\left(\frac{\pi\,[I_{45}]\,\lambda}{2n^2}\right)^{1/6}. \qquad (27)$$

When z = 1.5, the error arising from the use of Eq. (26) does not exceed 2%, and it is not greater than 1% when Eq. (27) is applied; the error rapidly decreases as z decreases.

For the particles with z greater than 8, the theoretical equations are not always applicable. The condition for the applicability of the equations is determined by the inequality

$$\frac{z}{4}(m-1) \leqslant 1, \qquad (28)$$

which is not satisfied for z greater than 8 if m = 1.5. One should note, however, that, with z greater than 8, the diameter of the particles exceeds 0.64λ; consequently, one can see these particles under a microscope.

(b) The Limits of m

The limiting values of m, for which the formulas of Section IV may be used, are determined from the inequality (28). The value of m does not exceed 1.5 in the majority of practically important cases; among them are particularly the water dispersions of polymers.

(c) Sphericity of Particles

The equations were derived for practically spherical particles; but they may be applied also in the case when the particles are oblong ellipsoids ("sticks") or flattened ellipsoids ("tablets"), provided, of course, that the ratio of the semiaxis is not great. Application of the formulas of Section IV to particles of a nonspherical form yields the radius of a sphere the volume of which is, in first approximation, equal to the volume of the particle. The error in determination of a is only 2% for oblong particles having the value of 2 for the ratio between their length and their diameter; the error reaches the value of nearly 5% when the ratio is 3; the values obtained for the radius are smaller than the true ones. The errors in a are also 2% and 5% for disk-shaped particles having the ratio of 2 and 3 between the diameter and thickness; but the values of a are higher than the correct ones.

(d) The Precision of the Formulas

The accuracy of the results obtained in determination of a from the formulas of Section IV depends on the size and the optical properties of particles; but even in the worse case the error, as it seems, does not exceed 5%. This accuracy is usually sufficient for studies in colloidal chemistry, as in dealing with colloidal systems the unavoidable errors arising from the polydispersion, from the formation of aggregates, and from the incomplete reproducibility of samples, etc., do not permit in any case the obtaining of more accurate results. In the cases where a greater accuracy is required, one may use the equations of the theory of second approximation; however, the computation will be more complicated, and it will have to be made for each case separately (see reference 1, p. 243).

VI. EXAMPLES OF APPLICATION OF THE FORMULAS FOR COMPUTATION OF PARTICLES SIZE

The value of τ was measured to be 0.4005 cm^{-1} for a sol of colophony,[12] produced by adding to water an alcohol solution of colophony, with a concentration of 155 mg/liter and at the wavelength of 710 mμ (in vacuum). The index of refraction of colophony is 1.548,[13] and its density, 1.08.

$$c_v = \frac{155 \cdot 10^{-3}}{10^3 \cdot 1.08} = 1.435 \cdot 10^{-4}, \quad \lambda = \frac{710 \cdot 10^{-7}}{1.33} = 5.34 \cdot 10^{-5}\ \text{cm},$$

$$m = \frac{1.548}{1.33} = 1.163, \quad \alpha = \frac{3(1.163^2-1)}{4(1.163^2+1)} = 0.025,$$

$$[\tau] = \frac{\tau}{c_v} = \frac{0.4005}{1.435 \cdot 10^{-4}} = 2.79 \cdot 10^3\ \text{cm}^{-1},$$

$$\psi(z) = \frac{[\tau]\lambda}{\alpha^3} = \frac{2.79 \cdot 10^3 \cdot 5.34 \cdot 10^{-5}}{0.025^3} = 238.$$

From the interpolation table, we find z = 4.96

$$a = \frac{z\lambda}{8\pi} = \frac{4.96 \cdot 5.34 \cdot 10^{-5}}{8\pi} = 1.06 \cdot 10^{-5}\ \text{cm}.$$

For the same sol, τ = 1.05 cm^{-1} at the wavelength of 488 mμ in vacuum.

$$\lambda_1 = \frac{488 \cdot 10^{-7}}{1.33} = 3.67 \cdot 10^{-5}\ \text{cm}, \quad \lambda_2 = 5.34 \cdot 10^{-5}\ \text{cm},$$

$$n = -\frac{\Delta \lg \tau}{\Delta \lg \lambda} = \frac{\lg 1.05 - \lg 0.4015}{\lg 5.34 - \lg 3.67} = 2.569.$$

For this value of n, the corresponding value of z is 6.36 in accordance with the Table. The average value of λ is

$$\lambda = \frac{(5.34 + 3.67) \cdot 10^{-5}}{2} = 4.505 \cdot 10^{-5}\ \text{cm},$$

$$a = \frac{6.36 \cdot 4.505 \cdot 10^{-5}}{8\pi} = 1.14 \cdot 10^{-5}\ \text{cm}.$$

The disagreement of 7% in comparison with the value of a obtained from τ, may possibly be explained by the fact that the value of the index of refraction used for colophony was one for red light and not for the average value of λ.

Using nephelometer NFM with light filter K-4, and at the wavelength of 541 mμ, the following values were determined for a latex of $c_v = 2 \times 10^{-3}$.

$$\frac{I_{45}}{I_0} = 6.4 \cdot 10^{-3}, \quad m = 1.20, \quad \alpha = 0.0305.$$

$$[I_{45}] = \frac{6.4 \cdot 10^{-3}}{2 \cdot 10^{-3}} = 320,$$

$$\lambda = \frac{541 \cdot 10^{-7}}{1.33} = 4.07 \cdot 10^{-5}\ \text{cm},$$

$$\psi(45, z) = \frac{[I_{45}]\lambda}{\alpha^3} = \frac{320 \cdot 4.07 \cdot 10^{-5}}{0.0305^3} = 14.0.$$

In accordance with the Table, z = 3.78,

$$a = \frac{3.78 \cdot 4.07 \cdot 10^{-5}}{8\pi} = 6.1 \cdot 10^{-6}\ \text{cm}.$$

VII. NOMOGRAMS FOR DETERMINING THE RADIUS OF PARTICLES

When studying the process taking place in colloidal systems, the necessity may be encountered for a great number of measurements of the sizes of particles. Nomograms have been constructed for facilitating these measurements.

The nomograms permit determining the radii of particles by four independent methods as was also the case with formulas of Section IV. To avoid a complication of nomograms, the determination of a from τ and from I_{45} is divided into two parts. First, using the known τ (or I_{45}), m, λ, and Nomogram 1 (Fig. 3) one determines the value of parameter z. Then a is found from z and λ from Nomogram 2 (Fig. 4). The determination of a from n and from I_{45}/I_{135} can be made readily from Nomo-

gram 2. The use of nomograms will be clear from the examples given in the illustrations.

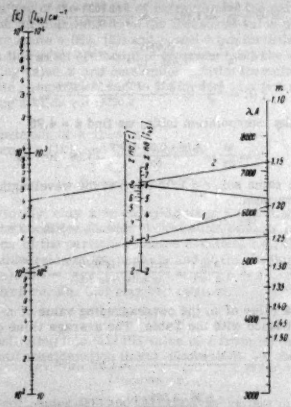

Fig. 3. Nomogram 1. Examples: 1, τ = 1100 cm^{-1}; m = 1.20; λ = 5470 A; z = 2.8. 2, I_{45} = 400 cm^{-1}; m = 1.15; λ = 6300 A; z = 5.9.

The nomograms can be used for determining the size of particles when the diameter of the particle is equal to from 0.16 to 0.64 of the wavelength. The limits of values of m are from 1.1 to 1.5; of λ, from 3000 to 8000 A; of I_{45}, from 10 to 10^4 cm^{-1}; of τ, from 10^3 to 10^5 cm^{-1}; of n, from 2.4 to 3.8; of I_{45}/I_{135}, from 1.2 to 20. These limits embrace the values which are usually encountered when studying latices, dispersion polymers, and similar systems.

When the ratio of the diameter of particles and the

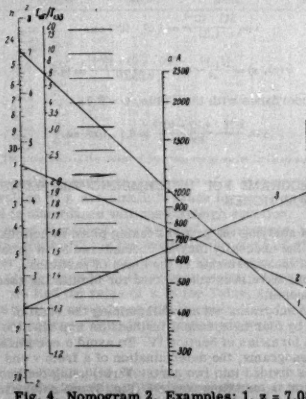

Fig. 4. Nomogram 2. Examples: 1, z = 7.08; λ = 3680 A; a = 1040 A. 2, n = 3.10; λ = 4200 A; a = 770 A. 3, I_{45}/I_{135} = 1.30; λ = 6100 A; a = 650 A.

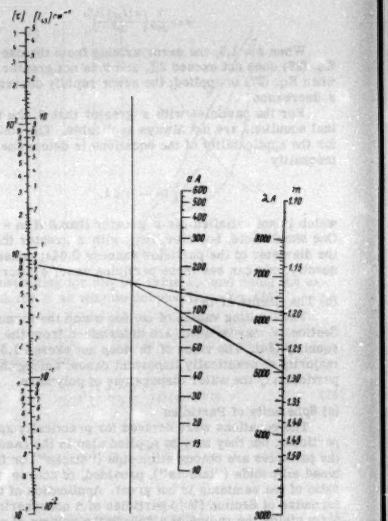

Fig. 5. Nomogram 3. Example: z = 8.12 cm^{-1}; λ = 5000 A; m = 1.20; a = 100 A.

wavelength is less than 0.15, the Rayleigh equation may be used, as the error will be less than 2%. Nomogram 3 (Fig. 5) was constructed for calculation of the radii of particles from τ and I_{45} on the basis of the Rayleigh equation.

REFERENCES

1. K. S. Shifrin. "Rasseyanie sveta v mutnoi srede." (Light Scattering in a Turbid Medium), GITTL, Moscow, Leningrad, 1951.
2. G. Junker. In "Nauka o kollоidakh" (Croyt, ed.) (The Science of Colloids), Vol. 1, p. 135, IL, Moscow, 1955.
3. W. West. In "Fizicheskie mеdody organicheskoi chimii" (Weissberger, ed.) (Physical Methods of Organic Chemistry), Vol. 4, p. 625, IL, Moscow, 1955.
4. P. Debye. J. Appl. Phys. Moscow, 17, 392 (1946).
5. P. V. Mochalov. Aggregativnaya and sorbtsionnaya ustoichivost' gidrosolei polistirola (Aggregative and Sorption Stability of Gidrosols of Polystirols), Dissertation, Moscow Mendeleyev Chemico-Technical Institute, Moscow, 1952.
6. A. I. Iurzhenko and B. P. Gusyakov. Kolloidnii Zhur. 14, 140, 414 (1952).
7. M. Herker. J. Polymer Sci. 28, 429 (1958).
8. G. Mie. Ann. Phys. 25, 377 (1908).
9. K. S. Shifrin. Trudy Glavn. Geofiz. Observ. 19, 255 (1950).
10. W. Heller, H. B. Klevens, and H. O. Oppenheimer. J. Chem. Phys. 14, 566 (1946).
11. K. S. Shifrin. Trudy Vsesoyuz. Zaoch. Lesotechn. Inst. No. 1, 33 (1955).
12. G. P. Luchinskii and E. S. Al'tman. Zhur. Fiz. Khim. 6, 57 (1935).
13. "Handbook of Chemistry and Physics" (Hodgman, ed.) 3rd edn. p. 2434, Cleveland, 1951.

SELECTIVE OPTICO-ACOUSTIC DETECTOR WITH ELECTRODYNAMIC MICROPHONE

N. A. Pankratov

Received 5 May 1959

An investigation was made of a selective optico-acoustic detector with an electrodynamic microphone. The sensitivity and noise were measured as functions of frequency, and the relations between noise and frequency were investigated with the microphone at different pressures. The threshold sensitivity of the detector was determined.

As was shown in references 1 and 2, in order to realize the threshold sensitivity of the chamber of an optico-acoustical detector the intrinsic noise of the microphone should comprise only a small proportion of the total noise of the detector. Under certain conditions —in particular, at low modulation frequencies—such a ratio of noises is actually observed in the case of an optical microphone.

In relation to the electrodynamic microphone it was pointed out that since the microphone coil and the detector chamber exist at the same temperature, the detector noise due to pressure fluctuations, calculated for the entire frequency range, cannot exceed the noise of the microphone coil. If this were not so, the equipartition law for distribution of energy fluctuations between the different degrees of freedom would be violated, since the microphone may be considered to be a system with two degrees of freedom—one electrical and one mechanical.

It follows that the inequality

$$\sum_{i}^{n} \sqrt{\overline{\Delta p_{n,i}^2}} \times u_i \leqslant \sum_{i}^{n} \sqrt{\overline{\Delta v_i^2}}, \qquad (1)$$

should hold, where

$$\sqrt{\overline{\Delta p_{n,i}^2}}$$

is the root mean square value of the pressure fluctuation of the gas in the chamber within the i-th interval of frequency; $\overline{u}_i$ is the mean sensitivity of the microphone in the ith interval of frequency; $\sqrt{\overline{\Delta v_i^2}}$ is the Johnson noise of the resistance of the microphone coil, the magnitude of which does not depend on the frequency range in which it is observed. This inequality is valid if n is sufficiently large.

There is considerable interest, however, in the ratio of noise levels in different regions of the frequency spectrum. As has been shown, the fluctuation of gas pressure in the chamber of a selective detector depends on the frequency range in which observations are made. Thus, if $(\omega\tau)^2 \gg 1$, where ω is the angular frequency and τ is the thermal time constant of the chamber, then as a result of thermal inertia the magnitude of the pressure fluctuation is inversely proportional to the frequency; that is, the pressure fluctuations are considerably larger at low frequencies than at high frequencies. This conclusion may be considered to have been demonstrated experimentally for small closed volumes such as a chamber. Van der Ziel's assertion[3] that fluctuations are independent of frequency apparently relates only to closed regions, where it is unnecessary to take account of fluctuations in the temperature and pressure of the small confined volume (although that author did not draw any detailed conclusions). It has also been stated that the noise of an electrodynamic microphone is determined by the electrical losses in the coil, and is independent of frequency; experimental support for this assertion has been put forward. A similar statement had been made previously by Iofe.[4] The authors cited have in mind broad-band radio broadcasting microphones, operating in the open. But this conclusion, as will be shown below, is not correct for a resonance microphone, or for microphones located in small closed spaces.

This paper reports work carried out in the investigation of different characteristics of selective optico-acoustic detectors in which electrodynamic resonance microphones are used.

METHOD OF INVESTIGATION

Measurement of the Dynamic Resistance of the Microphone

1. The dynamic resistance of the microphone was measured by the usual compensation method, the principles of which are illustrated in Fig. 1. An alternating current, produced by an audiofrequency generator ZG-10 was passed through microphone R_m and comparison resistance R. A vacuum tube voltmeter MVL-2M was used to alternately measure the voltage drop across the microphone and that across the comparison resistance R. The measurement amounts to finding a resistance R equal to R_m, as indicated by equality of the potential drops across these resistances. Measurements were carried out over the frequency range 50 to 1000 cps. Close to the resonance point of the microphone, where its resistance changes rapidly with frequency, measurements were made every 10-20 cps. In other regions, measurements were made every 50-100 cps.

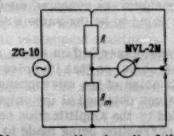

Fig. 1. Diagrammatic circuit of the compensation method.

In the frequency band under investigation, the inductance of the microphone coil and that of the comparison resistance were small enough to be neglected; that is, the measured quantities were pure resistances. The frequency dependence of the microphone resistance is explained by the fact that an additional electrical resistance, dependent on the mechanical resistance, is added to the resistance of the coil.

The added resistance is described by the relation

$$R_{add} = \frac{B^2 l^2 \cdot 10^{-9}}{z_{mech.}}, \qquad (2)$$

where $R_{add.}$ is the additional resistance in ohms; B is the induction in the gap; l is the length of the conductor; $z_{mech.}$ is the mechanical resistance in mechanical ohms.

At resonance, $z_{mech.}$ has a minimum; therefore the additional resistance, which is inversely proportional to it, has a maximum. In the equivalent circuit, the additional resistance and the intrinsic resistances of the microphone coil are in series.

The resistance values obtained were used in Nyquist's[8] formula to calculate the noise for a 4.5 cycle band, which was the bandwidth of the noise analyzer used used.[1,9] The results as computed were compared with experimental observations.

2. Some remarks should be made concerning the measurement of the amplification coefficient of an amplifier with a transformer input. The fact is that in the process of measurement, it became evident that if the input transformer is loaded by different resistances, the characteristics of the transformer change; that is, there is a displacement of the maximum in the transformation coefficient versus frequency curve. The resistance of resonance electrodynamic microphones is ohmic and depends on the frequency; hence in all measurements of the transformation coefficient, the input loading resistance connected to the primary coil of the transformer consisted of the microphone on which the subsequent measurements of dynamic resistance, noise, and sometimes the signal were to be made. (The packing of the microphone in the chamber of the detector was kept the same during the entire series of measurements.) The effect of the audiogenerator on the input resistance of the transformer was eliminated by the use of a decoupling resistance between the generator and the amplifier, a resistance being used that was considerably larger than that of the microphone.

Measurement of the Noise Spectrum of the Optico-Acoustic Detector with Resonance Electrodynamic Microphone

The measurement of the noise spectrum was carried out on the equipment described in reference 1. A few remarks should also be made in this connection.

In the measurement of the noise spectrum, the detector was carefully shielded from all kinds of interference: electrical, magnetic, acoustical, and mechanical. The precautions taken were apparently adequate, for the measurements were repeated many times, and the results were found to be the same within experimental error.

The input transformer had an ohmic resistance of the order of a few ohms, so that its noise was considerably less than the noise of the microphone and chamber.

The noise values obtained at the output of the analyzer were divided by the amplification coefficient of the whole circuit, a correction being made to take account of the role of the voltage divider comprised by the microphone resistance and the transformer resistance. In this manner the noise at the output terminals of the microphone was determined. The results were then compared with noise values calculated from the Nyquist formula for the dynamic resistance of a microphone.

RESULTS OF THE MEASUREMENTS

In Fig. 2. the logarithm of the frequency is plotted in cps as abcissae; the ordinates represent the root mean square noise expressed in volts. Curve 1 shows the values of noise observed experimentally; curve 2 is the predicted value of the measured resistance as computed by the Nyquist formula, and the straight line 3 is the noise of the microphone coil computed in a similar manner. It is clear that the maxima of the curves lie in the 540-550 cps region, and are nearly the same in magnitude. Below resonance, curve 2 is almost parallel to the axis of abscissae, since the resistance depends very little on the frequency, being determined mainly by the resistance of the coil (the additional electrical resistance is small, inasmuch as the elastic resistance of the movable system is very large).

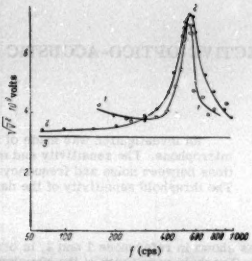

Fig. 2. Variation of the root mean square noise with frequency. Curve 1—experiment; curve 2—theory; curve 3—noise of the coil (calculated).

At the lower frequencies, curve 1 lies somewhat higher than curve 2, apparently due to the increase in noise of the input tube. At frequencies below 150 cps, measurements were difficult to carry out because the inductive impedance of the transformer decreased and became less than the resistance of the microphone. The separation of curves 1 and 2 in the region of resonance does not exceed 5-10% and is explained, apparently, by uncertainties in the determination of the parameters of the circuit—the band-width of the noise spectrum analyzer, the amplification factor of the amplifier, the resistance of the microphone, and the resistance of the transformer.

The results obtained agree quite satisfactorily, within the limits of accuracy of the experiments, with the generalized theorem of Nyquist.[8] In confirmity with that theorem, the thermal noise in an electrical system consisting not only of electrical circuit elements such as resistances, inductance coils, and condensers, but also including such passive electrical, electroacoustical, and electromechanical elements as antennae, microphones, galvanometers, etc., having the same temperature T, may be completely described by replacing these passive systems by equivalent electrical circuits having the same temperature.

At the resonance frequency, the noise voltage due to the added electrical resistance is approximately twice as great as the noise of the coil (R of the coil amounts to 150 ohms). In this frequency range, the additional resistance is fixed by the damping of the mechanical system and consists mainly of friction of the microphone coil and diaphragm in the air or gas which fills the chamber and the volume of the receiver beneath the diaphragm. This is easily proven by observing the change in dynamic resistance of the microphone with changes in the pressure of gas or air in the receiver chamber. Such measurements were carried out for several detectors with resonance electrodynamic microphones. The microphone under observation was placed in a glass flask in which the

pressure could be changed.

Figure 3 shows the dependence of the microphone resistance on the frequency for different gas pressures. Abscissae represent the frequency in cps; ordinates represent resistance in ohms. From comparison of the curves it is evident that with decrease of pressure, the resistance maximum of the microphone increases and is displaced toward lower frequencies. Curve 5 in this figure was obtained with the microphone in the chamber of the detector.

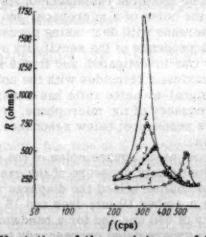

Fig. 3. Variation of the resistance of the microphone with frequency at different pressures of gas in the chamber. Pressure of gas (mm Hg): Curve 1—10; curve 2—100; curve 3—300; curve 4—760; curve 5—760.

The noise varies in approximately the same way as the resistance; noise measurements for this microphone are presented in Fig. 4. Qualitative comparison of Figs. 3 and 4 indicates that the noise and resistance change in roughly the same manner.

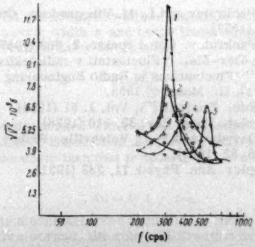

Fig. 4. Variation of noise of the microphone with frequency for different pressures of gas in the chamber. For numerical designation of the curves, see Fig. 3.

A shift in the maximum of resistance and noise is not observed for all microphones, however. Thus in Fig. 5, which shows the noise variation in a small microphone (diameter of the working part of the microphone membrane, 5 mm) there is no shift in the noise maximum. The shift in the maximum in Fig. 4 is apparently due to changes in the elastic resistance of the volumes on either side of the diaphragm. The increase in the resistance maximum comes from the decrease in the mechanical friction between the membrane and coil and the air in the gap. The noise observed increases with decreasing pressure; however, this does not indicate that the pressure fluctuations increase, since in this case there is a considerable increase in the sensitivity of the mechanical system toward the impact of individual air molecules. A certain analogy to this effect might be mentioned in the experiments of Kappler, in which he investigated the vibrations of mirrors suspended on fine wires, under the impact of air molecules at different pressures.[7]

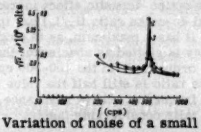

Fig. 5. Variation of noise of a small microphone with frequency at different pressures of gas in the chamber. Gas pressure (mm Hg): curve 1—760; curve 2—1; curve 3—100.

Inasmuch as the additional resistance is traceable to air friction, the observed level of noise voltage in the region of resonance over and above the noise of the coil is explained by the increased sensitivity of the microphone to fluctuations of pressure of the air or filling gas.

It is of some interest to determine the proportion of the noise contributed by the chamber of the detector acting as the volume on one side of the diaphragm. Since the volumes inside and outside the membrane are at the same temperature, and the membrane oscillates about the equilibrium position, the added resistance and noise are ascribable in equal degree to the volumes inside and outside the membrane. The magnitude of radiation flux corresponding to the root mean square noise is evaluated below.

Variation of the Sensitivity of the Detector with Frequency

The frequency dependence of the sensitivity of a selective detector with an electrodynamic microphone was investigated in the same region of the modulation frequency spectrum in which the noise was investigated. Results of the measurement are presented in Fig. 6, in which the logarithm of the frequency is plotted as abscissae, and the meter readings of the apparatus in relative units ($I_{rel.}$) as ordinates. As is evident from the figure, the sensitivity maximum of the receiver lies in the same region as the noise maximum, and coincides with the dynamic resistance maximum. Above resonance, the curve of sensitivity falls off sharply. This is explained by the fact that in that region, both the sensitivity of the microphone and the magnitude of the optico-acoustic effect decrease. Below resonance, the sensitivity also

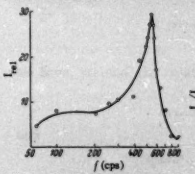

Fig. 6

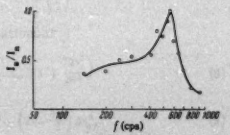

Fig. 7

Fig. 6. Variation of the sensitivity of the receiver with frequency.
Fig. 7. Variation of the signal-to-noise ratio with frequency.

decreases, but there is a frequency region where it is independent of frequency. In this region the decrease in sensitivity of the microphone is compensated by an increase in the optico-acoustic effect in the chamber of the detector with decreasing frequency. Further decrease in the sensitivity in the 50-100 cps region is explained by the fact that the sensitivity of the microphone decreases faster than the optico-acoustic effect increases.

The signal-to-noise ratio (I_s/I_n) has the same character; that is, it has a maximum, as is evident from Fig. 7 (the frequency is plotted as abscissae, the signal-to-noise ratio as ordinates). In the 100-300 cps region, the signal-to-noise ratio is still half the value observed at the resonance frequency. Above resonance, the signal-to-noise ratio falls considerably faster.

Root Mean Square Noise of the Selective Receiver

The radiation flux corresponding to the root mean square noise of the receiver which characterizes the threshold of sensitivity, is determined in the following manner. First, just as in the case of a detector with an optical microphone, a nonselective detector is used to determine the proportion of energy absorption in a chamber filled with the same gas as the detector, and having the same thickness as the chamber. The integral coefficient of absorption of the radiation of a Hefner candle for a chamber 10 mm thick amounts to about 10%. The signal produced by the radiation flux of the candle was amplified and measured by use of an oscillograph. Under the same conditions as were used to measure the signal, the peak noise was measured and divided by five to give the root mean square noise. For a detector with a chamber 10 mm deep and 1.6 cm in diameter, for modulation frequency of 640 cps and a bandwidth of 0.15 cps, the root mean square noise corresponded to a flux of 6×10^{-9} watts. The results obtained (taking account of the absorption coefficient) agree within the limits of experimental error with the magnitude of the noise of a selective detector with an optical microphone for a modulation frequency of 10 cps; this instrument's noise at 10 cps has been shown previously to be determined by the fluctuations of gas pressure in the chamber. From this it may be concluded that in an electrodynamic microphone detector, the noise is also due mainly to fluctuations of gas pressure in the spaces above and below the diaphragm of the microphone. The root mean square noise of the receiver does not depend on the frequency, in the region in which it was observed, as long as the noise is determined by pressure fluctuations.

CONCLUSIONS

On the basis of these experiments it is concluded that:

1. The noise spectrum of an optico-acoustical detector with an electrodynamic microphone has a maximum at the resonance frequency. Above resonance, the noise decreases and is determined by the resistance of the microphone coil. Below resonance, the noise is determined by the dynamic resistance of the microphone as distinguished from the resistance of its coil.
2. Both the noise of a microphone and its dynamic resistance increase with decreasing pressure.
3. The dependence of the sensitivity of the receiver on frequency was investigated, and it was shown that the sensitivity maximum coincides with the noise maximum.
4. The signal-to-noise ratio has a maximum at the resonance frequency of the microphone. It falls off sharply above resonance; below resonance, the decrease is insignificant.
5. The root mean square noise of the detector is fixed by fluctuations of pressure of the gas in the chamber and in the volume behind the diaphragm. In a receiver with a chamber 10 mm deep and 16 mm in diameter, at a frequency of 640 cps and for a bandwidth of 0.15 cps, the root mean square noise corresponds to a radiation flux of 6×10^{-9} watts.

The author expresses his thanks to Prof. M. L. Veingerov for his continuing interest and supervision of the work, and to A. S. Trufanov for his assistance in carrying out the measurements.

REFERENCES

1. N. A. Pankratov and L. M. Vinogradova. Opt. i Spektr. 7, 789 (1959).
2. N. A. Pankratov. Opt. i Spektr. 2, 662 (1957).
3. A. Van-Der-Ziel. "Fluctuatsii v radiotekhnike i fizike." (Fluctuations in Radio Engineering and Physics), IL, Moscow, 1958.
4. V. K. Iofe. Trudy IRPA, Vol. 1, 51 (1954).
5. R. Nyquist. Phys. Rev. 32, 110 (1928).
6. V. V. Davydov and V. G. Voishvillo. Prib. i Tekh. Eksp. 6, 82 (1958).
7. E. Kappler. Ann. Physik 11, 233 (1931).

THE CONFERENCE ON THE THEORY OF SPECTRAL INSTRUMENTS, MARCH 1959

A conference on the theory of spectral instruments and the technique of measurement of molecular spectra was organized by the Commission on Spectroscopy of the Academy of Sciences USSR, and the Section of Optics and Spectroscopy of the Leningrad House of Scientists from March 5-7, 1959. Taking part in the Conference were representatives of the Physical Institute of the Academy of Sciences, USSR, Moscow State University, the Physical Institute of the Leningrad State University, the State Optical Institute, the Institute of Petroleum, and, of other institutes. Below are published part of the lectures presented at the Conference, and presentations in the discussions.

DETERMINATION OF THE PARAMETERS, CHARACTERIZING THE TRUE CONTOURS OF ABSORPTION BANDS

I. V. Peisakhson

The apparatus function of a monochromator is determined by the width of its slits, by the diffraction effects, and aberrations of the optical system. It is possible to consider the apparatus to be free of aberrations if the width of the scattered figure, calculated using geometrical optics for an infinitely narrow slit, is not greater than the normal slit width. This condition is fulfilled, in particular, for the apparatus IKS-11, in those spectral regions in which NaCl and KBr prisms are used, and for slit heights limited to 10-12 mm also for LiF. For this situation, the apparatus function can be presented in the triangular form

$$A(x) = \frac{1}{\Delta\nu_e}\left(1 - \frac{|x|}{\Delta\nu_e}\right); \quad |x| < \Delta\nu_e, \tag{1}$$

the half-width of which is equal to

$$\Delta\nu_e = \sqrt{\Delta\nu^2 + \Delta\nu_0^2}, \tag{2}$$

where $\Delta\nu$ is the spectral width of the slits, related to their geometric width s and to the linear dispersion of the apparatus dl/dλ by the relation

$$\Delta\nu = \frac{s\nu^2}{\frac{dl}{d\lambda}},$$

and $\Delta\nu_0$ is the normal width of the slits, expressed in wave numbers. Expression (2), for not very wide slits, is more accurate than that proposed by a series of authors

$$\Delta\nu_e = \Delta\nu + \varphi \cdot \Delta\nu_0, \tag{3}$$

where φ is a constant. For slits five or more times greater than normal, the role of diffraction broadening of the slits is insignificant and can be neglected.

For significant aberrations there is also assumed an approximation of the apparatus function in a triangular form (1), and the influence of the monochromator optics on the results of the measurements can be characterized by one quantity—the effective spectral slit width $\Delta\nu_e$, i.e., by the half-width of the curve of its apparatus function.

If k(x) and K(x) are the true and observed optical densities (x is the distance on the wave number axis from some fixed point on the contour of the absorption band), then for an apparatus function of form (1) and for small $\Delta\nu_e$ we have

$$k(x) = K(x) + (|K'(x)|^2 - K''(x))\frac{\Delta\nu_e^2}{12}. \tag{4}$$

Let k_m and K_m be the true and observed maximum optical densities, b and b_0 be the corresponding values of the half-width of the band. Then for $\Delta\nu_e < b/2$

$$K_m = k_m - c_1\Delta\nu_e^2, \tag{5}$$

$$b^2 = b_0^2 + c_2\Delta\nu_e^2. \tag{6}$$

The coefficients c_1 and c_2 depend on the form of the form of the band, but for measurements for a given sample they are constant. Therefore, by measuring K_m and b for several values of the width of the slits, it is possible to determine k_m and b_0 by a linear extrapolation to an infinitely narrow slit of the dependences of K_m and b^2 on $\Delta\nu_e^2$, making no assumptions on the form of the band, except that it should be approximately symmetric.

It is also possible to calculate k_m approximately from the value of K(x) for three equidistant values of x:

$$k_m = K_m + \left[K_m - \frac{K(x_m + h) + K(x_m - h)}{2}\right]\frac{\Delta\nu_e^2}{6h^2}. \tag{7}$$

The expression in the square brackets is readily determined graphically (cf. the Figure).

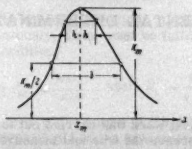

For contours of absorption bands, expressed by the Lorentz dispersion curve

$$K(x) = \frac{A}{x^2 + \left(\frac{b}{2}\right)^2},$$

we have, instead, the relationships

$$k_m = K_m\left(1 + \frac{2\Delta\nu_e^2}{3b^2}\right) \tag{8}$$

and

$$b_0^2 = b^2 - \left(2 - \frac{K_m}{3}\right)\Delta\nu_e^2, \tag{9}$$

giving values of k_m and b_0 with an accuracy not less than 2-3% for $\Delta\nu_e < 0.4b$ and $K_m \geq 2$.

MEASUREMENTS OF THE APPARATUS FUNCTION OF AN IKS-11 SPECTROMETER

O. D. Dmitrievskii and V. A. Nikitin

Using as a monochromatic source the emission line of a mercury lamp at 1.014μ (9859 cm^{-1}), we made measurements on the contour of the apparatus function of the IKS-11 spectrometer, serial no. 530032. For this the factory calibration of the monochromator was not changed, and only a verification of the correspondence of the width of the slits to that given by the scale, and a verification of the parallelism of the exit slit to the image of the entrance slit, were carried out. It was then established that to obtain true values of the width of the slits from the value indicated on the scale a correction of 0.02 mm must be made. The reproducibility of setting the slits was equal to $|\Delta s| = 0.01$ mm. The differences in the widths of the entrance and exit slits also did not exceed the limits 0.01 mm. The recording of the contours of the apparatus function was performed with the F-1 prism for the full height of the slits 20 mm, and for a scanning speed of 4.6 cm^{-1}/sec. A PbS photoconductor with an ac amplifier and recorder was used as a radiation detector. (The effective time constant of the system $\tau \approx 0.5$ sec.) The results of the measurements are presented graphically in Fig. 1. It is possible to see that for $s \leq 0.035$ mm the width of the apparatus function attains its very lowest value of 34 cm^{-1}, which significantly exceeds the diffraction limit of 4 cm^{-1}. This result shows that for measurements on the given apparatus (and, evidently, on many other serial numbers of the IKS-11) it is pointless to use slits less than 0.04 mm. The forms of the contours of the apparatus function are given in Fig. 2. As is expected, for slits $s > 0.05$ mm, the apparatus function has a form close to triangular, and for narrower slits approximates a Gaussian curve.

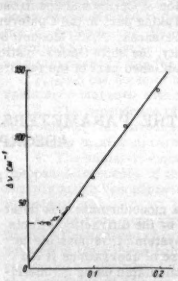

Fig. 1

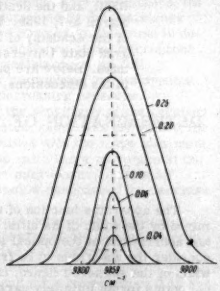

Fig. 2

Fig. 1. The dependence of the half-width of the apparatus function of the IKS-11 on the width of the slit for the F-1 prism. Solid line—the result of the usual calculation of the spectral width of the slits for a dispersion D = 677 cm^{-1}/mm. Circles and dashed line—the results of the experimental determination of the half-width of the apparatus function.

Fig. 2. Measurement of the contour of the apparatus function of the IKS-11 spectrometer (F-1 prism, 1.014μ). Numbers on the curves are the values of the corresponding widths of the slits (in mm).

EXPERIMENTAL DETERMINATION OF THE PARAMETERS OF INFRARED ABSORPTION BANDS IN LIQUIDS

D. N. Shchepkin

The present work was carried out to verify the relationships between the true and measured parameters of isolated absorption bands, presented in the paper of I. V. Peisakhson (cf. page 57).

The measurements were made using a Perkin-Elmer 12B apparatus with an LiF prism, a FEOU-18 amplifier, and a EPP-09 recorder. Before taking the measurements, the calibration of the apparatus was verified, and the geometric widths of the entrance and exit slits were checked. To exclude distortion, introduced by scanning, the measurements were made point by point. The results of the measurements are given in Tables 1-4 and in Figs. 1 and 2.

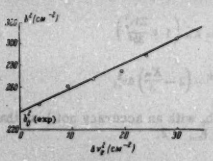

Fig. 1

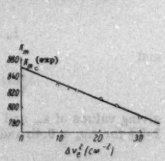

Fig. 2

The symbols in the figures and tables are:

s—the geometric slit width; $\Delta\nu_e$—the effective spectral slit width, determined by formula (2);* $\Delta\nu_0$—the normal slit width; b—the measured half-width of the band; b_0—the width of the band, determined by formula (9);* K_m—the optical density, measured at the absorption maximum; k_m—the optical density at the maximum, calculated for formula (7);* $b_{0(exp)}$—the width of the band, obtained by an extrapolation to zero slit width by formula (6)* $b^2 = b_0^2 + C_2 L \Delta\nu_e^2$; $k_{m(exp)}$—the optical density, obtained by an extrapolation to zero slit width by formula (5)* $K_m = k_m - C_1 \Delta\nu_e^2$.

*See paper by I. V. Peisakhson, this issue, p. 57.

Table 1 gives the values of b, K_m, k_m, k'_m, b_0, in their dependence on the spectral slit width for chloroform,

Table 1. Chloroform, νCH, 3020 cm^{-1}, Cell Thickness 0.026 mm, $\Delta\nu_0$ = 1.25 cm^{-1}

s (μ)	$\Delta\nu_s$ (cm^{-1})	b (cm^{-1})	$K_m = \ln I_0/I$	b_s (cm^{-1})	k_m	k'_m
30	2.02	15.6	0.851	15.4	0.861	0.864
50	2.92	16.1	0.828	15.8	0.848	0.850
70	3.70	16.4	0.819	15.7	0.847	0.846
80	4.42	16.6	0.814	15.6	0.853	0.856
90	4.94	17.0	0.805	15.7	0.850	0.846
100	5.46	17.5	0.791	15.9	0.843	0.835

Table 2. Methylethyl Ketone, 2νC = 0, 3417 cm^{-1}, Cell Thickness 0.096, $\Delta\nu_0$ = 1.6 cm^{-1}

s (μ)	$\Delta\nu_s$ (cm^{-1})	b (cm^{-1})	$K_m = \ln I_0/I$	b_s (cm^{-1})	k_m	k'_m
40	3.28	33.2	0.985	33.0	0.993	0.993
70	5.54	33.8	0.956	33.1	0.974	0.986
80	6.26	33.8	0.956	32.8	0.978	0.975
90	6.95	34.4	0.955	33.2	0.983	0.975
100	7.70	34.8	0.963	33.3	0.995	1.015
120	9.22	35.1	0.938	33.0	0.984	1.000

Table 3. Solution of Diphenylamine in CC14, 0.00745 mole/liter, νNH, 3437 cm^{-1}, Cell Thickness 2 cm, $\Delta\nu_0$ = 1.60 cm^{-1}

s (μ)	$\Delta\nu_s$ (cm^{-1})	b (cm^{-1})	$K_m = \ln I_0/I$	b_s (cm^{-1})	k_m	k'_m
60	4.8	26.0	1.815	25.1	1.84	1.83
80	6.25	26.4	1.780	25.4	1.84	1.83
110	8.3	27.0	1.745	25.2	1.85	1.84

Table 4

	Chloroform	Methylethyl ketone	Diphenylamine in CCl_4
b_0 (exp)	15.4	32.9	25.3
b_0	15.6	33.0	25.3
$k_{m(exp)}$	0.848	0.982	1.846
k_m	0.850	0.985	1.845
k'_m	0.850	0.958	1.835

in Table 2 the same for methylethyl ketone, in Table 3 the same for a solution of diphenylamine in CCl_4. Table 4 gives the means of the values of b, k_m, k'_m, $b_{0(exp)}$, $K_{m(exp)}$ for all three substances. Figures 1 and 2 show the dependence of b^2 and K_m on $\Delta\nu_s^2$ for chloroform.

The relative error of the different methods of calculating b_0 and k_m, determined by the scatter of the points, is 0.4-0.7%; the maximum deviations of the individual measurements from the mean do not exceed 1% for slit widths up to 0.4 times the band width.

DISTORTIONS IN SCANNING OF SINGLE-BEAM SPECTROMETERS

O. D. Dmitrievskii and V. A. Nikitin

In I. V. Peisakhson's paper* it was shown that the distortions on scanning lines and bands of Gaussian form in the case of detector-registering systems, close to exponential, are defined simply by a parameter K, showing how many times greater is the recording time of the band Δt than the time constant of the detecting system τ:

$$K = \frac{\Delta t}{\tau} = 0.85\frac{b}{v\tau}$$

(b is the half-width of the band, isolated by the monochromator; v is the scanning speed.) If the decrease of the observed band intensity at the maximum I_N by comparison with the original I is characterized by the ratio I_N/I, the broadening of the bands by the ratio b_N/b, and the displacement of the maxima by the quantity $\Delta(cm^{-1})$, then for $K > 1$ we have the simple relations

$$\frac{I_N}{I} \approx \frac{b}{b_N} \approx 1 \quad \text{and} \quad \Delta \approx v\tau.$$

The first of these shows the independence of the integrated intensity on the scanning speed, the second the independence of the shifts of the maxima on the width of the bands (for the condition $K > 1$, i.e., $\Delta t > \tau$).

The dependence of the ratios I_N/I and b_N/b on the parameter K can be described by the approximate formulas

$$\frac{b}{b_N} = \frac{I_N}{I} = 1 - \frac{2}{K^2} \quad \text{for} \quad 10 < K < \infty,$$

$$\frac{b}{b_N} = \frac{I_N}{I} = 1.03 - \frac{1}{2K} \quad \text{for} \quad 1 < K < 10.$$

An experimental verification of these formulas, carried out on an IKS-11 spectrometer, showed that they are in good agreement with experiment. Accordingly, setting the values of I_N/I and b_N/b guaranteeing the required accuracy of the measurements, the experimenter can determine the corresponding value of the parameter K and the permissible scanning speed by the condition

$$v = 0.85\frac{b}{\tau K} \approx 0.85\frac{\sqrt{s^2 + b_0^2}}{\tau K} \qquad (1)$$

(s is the effective spectral slit width, b_0 the true band width.) Simultaneously, there must be fulfilled the well-known energy condition:

$$s^2 \geq s^2_{min} = \frac{MU_n}{\sigma CB}, \text{ where } \overline{U}_n \sim \frac{1}{\sqrt{\tau}}. \qquad (2)$$

$\overline{U}_n$ is the noise level of the output of the detecting system, directly proportional to the square root of the time constant of the detector with "white noise"; σ is the sensitivity of the detector; B is the brightness of the source; C is a constant, characterizing the transmission of the monochromator and its dispersion in the spectral interval s; M is the ratio of signal to noise.

The relations (1) and (2) completely describe the interrelations of the three fundamental quantities s, τ, and v, characterizing the method of the measurement specified by the parameters K and M, quantitatively defining the magnitude of the systematic and random errors of the measurements. Since the three quantities s, τ, and v are connected by only two conditions (1) and (2), one of them can always be arbitrarily chosen by the experimenter; after this choice, the other two quantities are determined simply from conditions (1) and (2). In contrast to τ and v the shoice of s is limited still by an independent condition. Specifically, the spectral slit width s, as a rule, must be less than the width of the measured lines or bands b_0. As a sufficient requirement, even in the case of quantitative measurements, it is possible to specify

*This issue, p. 57.

the condition $s \leq b_0/2$, with which one can make a sufficiently complete calculation of the optical distortions of the contour of the bands; for example, with the help of the methods stated in the communications of I. V. Peisakhson and D. N. Shchepkin.

REFERENCE

1. O. D. Dmitrievskii, B. S. Neporent, and V. A. Nikitin. Uspekhi Fiz. Nauk **64**, 447 (1958).

INFLUENCE OF SCANNING AND THE CHOICE OF THE OPTIMUM CONDITIONS OF MEASUREMENT

G. G. Petrash

The systematic distortions, introduced by the spectral apparatus as a whole* into the distribution $\varphi(\lambda)$ being measured, are investigated, using the Fourier analysis method. With the assumption of small systematic errors for the distribution $h(\lambda)$ at the output of the spectral apparatus the following formula is obtained

$$h(\lambda) = \varphi(\lambda + \Delta) + \varphi''(\lambda + \Delta)\,(aS^2 + b\tau^2 v^2).$$

Here, S is the width of the apparatus function of the monochromator, a is a coefficient depending on the form of the apparatus function, τ is the characteristic of the inertia of the recording system* (the time constant), v is the scanning speed, b is a coefficient related to the form of the transformation function of the recording system, Δ describes the displacement of all of the curve as a whole.

*That is, distortions introduced both by the monochromator and by the recording system.

*The term "recording system" combines the detector, amplifier, and recorder.

The formula is valid for any form of $\varphi(\lambda)$ and for a broad class of apparatus functions and transformation functions of the recording systems.

The constant shift as a whole, Δ, can be accounted for readily in the calibration and does not introduce additional distortions, since in the first approximation the systematic errors are proportional to $\varphi''(\lambda)$ and the $(aS^2 + b\tau^2 v^2)$.

A rational choice of the conditions of measurement, however, cannot be made from an examination only of the systematic errors, since a decrease of the systematic errors resulting from a decrease of S and τ always leads to an increase in the random errors. Practically, this is the only factor limiting the decrease of S as well as τ. This circumstance leads to the impossibility of a separate assignment of the errors of the different origins and to the necessity of calculating them together.

Such a combined calculation shows that, for a typical infrared spectrometer, the relative mean square error of the measurement of the optical density D reaches a minimum if the following optimum conditions are fulfilled:

1. The magnitude of the absorption must be $\approx \frac{1}{3}$.[1]

2. The systematic errors associated with the scanning are four times less than the systematic errors resulting from the slits.

3. The general systematic error approximately equals the random error.

4. The optimum time constant is connected to the optimum slit width and the scanning speed by the relation which does not depend on the form of $\varphi(\lambda)$.

$$\tau_m v = \frac{S_m}{2}\sqrt{\frac{a}{b}}.$$

5. The optimum width of the slits, S_m, depends not only on the property of the instrument, but also on the width γ and form of $\varphi(\lambda)$. If $\varphi(\lambda)$ and the properties of the instrument are fixed, then

$$S_m = \gamma c\left(\frac{Ev}{\gamma^3}\right)^{1/5}, \quad c = \text{const}.$$

The parameter E is the mean square random error for unit slit width and time constant. If the measurement conditions are chosen as indicated, then the general error of the measurement of the optical density D is defined by the expression

$$P_m^2 = \frac{\overline{\Delta D^2}}{D^2} = A\left(\frac{Ev}{\gamma^3}\right)^{4/5}$$

(the parameter A depends on the properties of the instrument and on $\varphi(\lambda)$, and, furthermore, its decrease is possible only as a result of a decrease of v, i.e., as a result of an increase of the time of measurement).

In correspondence with this analysis for errors, not exceeding 10-20%, for practical work it is possible to give the following recommendations:

1. For work with different v and τ it is essential to take account of a change of the displacement Δ (for the case where the recording system is equivalent to an RC circuit: $\Delta = \tau v$).

2. Since for $\tau > \tau_m$ the systematic errors grow sharply, and for $\tau < \tau_m$ the errors increase as a result of the random ones, but relatively slowly, then it is possible, while not losing much by comparison with the optimum, to choose τ roughly in order that the errors resulting from the scanning be small. For this it is required that τv be five to ten times less than S.

3. The choice of the width of the slits must be derived from the dependence on the width γ of the structure being measured and, to a lesser degree, from the dependence on the form (for more details cf. reference 2).

In conclusion, it is noted that no methods of exclusion of the systematic errors resulting from the scanning should be recommended (in distinction from the methods of excluding slit distortions), since this gives no gain by comparison with a simple decrease of the inertia of the recording system to the record.

REFERENCES

1. G. G. Petrash and C. G. Rautian. Inzh. Fiz. Zhurn. 1, 61 (1958).
2. G. G. Petrash and C. G. Rautian. Inzh. Fiz. Zhurn. 1, 80 (1958).

ON MEASUREMENTS ON DOUBLE BEAM SPECTROMETERS

L. A. Gribov

All of the distortions of the record of the spectra, introduced by the registering part of a double-beam infrared spectrometer (of the type IKS-14) can be divided into three categories: (1) errors resulting from the inertia of the instrument, connected with the speed of scanning the spectrum (dynamic errors); (2) errors related to the finite voltage sensitivity of the servo motor; and (3) random errors, produced by the noise of the instrument. Such a division is not completely valid, but for the majority of practical cases is fully satisfactory. An analysis of the operation of double-beam instruments allows us to show a series of simple methods providing a choice of those conditions of the recording, for which the distortions are sufficiently small and can be evaluated.

The dynamic errors can be decreased most if the parameters of the amplifier-registering part are chosen by the appearance of the reaction of the system to an entering step-function signal, and the scanning speed from a graph of the dependence of the recorded intensity of the narrowest line in the spectrum being studied on the scanning speed.[1] The error from the voltage sensitivity of the servo motor can be determined by the following simple technique. The instrument is set by hand on some absorption band, and then, with the servo motor turned off, the photometric wedge is shifted from the equilibrium position. When the servo motor is turned on, the apparatus will return towards the old position as long as the error-signal is not equal to the voltage sensitivity of the servo motor. Shifting the pen of the instrument to the right and to the left of the chosen position, we determine the doubled magnitude of the error in the sections of the spectrophotometer scale.

A voltage sensitivity of the servo motor not equal to zero leads to a situation where, even for infinitely small scanning speeds, the apparatus will still lag behind the true appearance of the spectral curve. Accordingly, there will always be retained errors in the intensity, half-width, and wavelength of the recorded absorption bands. The last, as is readily shown, will depend on the half-width of the absorption band. It is advisable to take account of this circumstance in construction and use by means of graduated graphs. If an estimation of the errors from the voltage sensitivity of the servo motor is made, then in the recorded spectral curve the corresponding corrections can be readily introduced.

The presence of instrument noise is a necessary condition to obtain a spectral recording of the greatest possible accuracy. Indeed, the appearance of not too noisy peaks means first, that the instrument is working in the most sensitive region, and, secondly, a graphical averaging through the noise provides the possibility of finding the least distorted spectral curve from the output of the instrument.

The enumerated simple techniques, accessible to each experimenter, allow the distortion introduced in the spectral record by the registering part of the double-beam spectrophotometer to be significantly decreased. A further increase of the accuracy of double-beam spectrophotometers, in my opinion, can be achieved only by transition to automatic control of the scanning speed.

REFERENCE

1. L. A. Gribov. Prib. i Tekh. Eksp. No. 2, 65 (1958).

ON THE METHOD OF INTERFERENCE MODULATION

V. M. Arkhipov

In connection with the development of the method of interference modulation[1-11] it proves interesting to examine some of its possibilities and, in particular, the connection between the theoretical resolution fixed by the dispersing element (in the case examined by us, a diffraction grating), and the theoretical resolution of the apparatus in which the interference modulation is applied.[12-15] Let us assume that for a sufficiently small entrance aperture (without considering interference) the resolution of the instrument is defined for two lines of particularly small width with the wavelengths λ and $\lambda + \delta\lambda$ only by the theoretical resolving power of the diffraction grating used (Fig. 1). The quantity $\delta\lambda$ is chosen in correspondence with the Rayleigh criterion. A similar distribution of the intensities would occur, for example, in the focal plane of the usual autocollimated spectrometer with that grating for which, as is well known,

$$R\alpha_0 = \tan i, \qquad (1a)$$

where R is the theoretical resolving power of the grating, α_0 is the angular distance between the center of the dif-

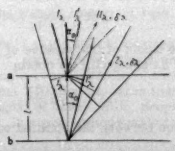

Fig. 1. The calculation of the interference difference of the path of the diffracted beams. I_λ and 1_λ—the beams diffracted from the plates a and b of the interferometer and corresponding to the diffraction maximum of the wavelength λ; I'_λ and $1'_\lambda$—the same for the wavelength λ, corresponding to the half-width of the scattering diffraction circle; $II_{\lambda+\delta\lambda}$ and $2_{\lambda+\delta\lambda}$—the same for the wavelength $\lambda + \delta\lambda$, corresponding to the maximum of the scattering diffraction circle.

raction pattern and the point of intersection of the resolved contours, and i is the diffraction angle. Generally, $\tan i = 0.5/1$; therefore, for simplicity, we put

$$R\gamma_0 = 1. \tag{1b}$$

We bring into the study the interference modulation of the rays diffracted from two gratings. For this it is essential to change by some means the path difference between the interfering beams at a constant speed. Let us determine to which band of frequency of modulation correspond the diffraction circles for the wavelengths λ and $\lambda + \delta\lambda$, and the difference between these bands of frequency of modulation. (It is assumed that the presence in the electric spectrum of a signal of harmonics of higher order, stipulated by the finiteness of the interference train, does not influence the band of the frequencies of modulation, corresponding to the diffraction circle of scattering.)

We assume that the beams corresponding to the center of the diffraction circle of wavelength λ go along the optic axis of the interferometer and interfere in the center of the field of the interferometer (Fig. 2). If the optical path difference between the plates of the interferometer is changed by the quantity l in time t, then the frequency of modulation of the beams (I_λ, 1_λ), corresponding to the center of the diffracted circle for the wavelength λ, is written as

$$f_\lambda = \frac{2l}{\lambda t}. \tag{2}$$

For the beams (I_λ', $1_\lambda'$), corresponding to the half-width of the diffraction circle, the frequency of modulation for the wavelength is expressed as

$$f'_\lambda = \frac{l(1+\cos\alpha_0)}{\lambda t}. \tag{3a}$$

For small α_0

$$f'_\lambda = \frac{2l}{\lambda t} - \frac{l\alpha_0^2}{2\lambda t}. \tag{3b}$$

From this the half-width of the band of frequencies of modulation for the wavelength λ using (1b) equals

$$\Delta f_\lambda = f_\lambda - f'_\lambda \approx \frac{f_\lambda}{4R^2}. \tag{4}$$

The frequency of modulation of the beams ($II_{\lambda+\delta\lambda}$, $2_{\lambda+\delta\lambda}$), corresponding to the center of the diffraction circle for the wavelength $\lambda + \delta\lambda$, analogously with (2), equals

$$f_{\lambda+\Delta} \approx \frac{2l}{(\lambda+\delta\lambda)t}. \tag{5}$$

And for the bands of frequencies of modulation of wavelength $\lambda + \delta\lambda$ using (1b) we obtain

$$\Delta f_{\lambda+\Delta} \approx 2f_{\lambda+\Delta}\frac{1}{R^2}. \tag{6}$$

The distance between the maxima of the bands of

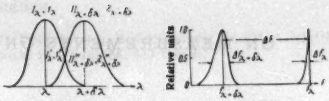

Fig. 2 Fig. 3

Fig. 2. Distribution of the intensities in the diffraction picture for two monochromatic lines according to Rayleigh. (Regarding notation see the legend to Fig. 1.)
Fig. 3. An amplitude representation of the modulated circles of scattering corresponding to two monochromatic lines on a scale of frequencies of modulation.

frequencies of modulation from (2) and (5), using (1b), equals

$$\Delta F = f_\lambda - f_{\lambda+\Delta} \approx \frac{f_{\lambda+\Delta}}{R}. \tag{7}$$

In Fig. 3 the results obtained on a scale of frequencies of modulation are presented. From the data presented it is possible to draw two fundamental conclusions:

1. By the use of interference modulation it is possible, with the help of sufficiently narrow-band detector-amplifier arrangement, to obtain a gain in light intensity as a result of an increase of the entrance aperture of the interferometer for a resolution defined, for example, by a diffraction grating.

2. By the use of interference modulation it is possible, with the aid of a sufficiently narrow-band detector-amplifier arrangement to obtain a gain in resolution in the neighborhood of R times by comparison with the resolution of a grating.

REFERENCES

1. J. Strong. J. Opt. Soc. Am. 47, 354 (1957).
2. L. Genzel and R. Weber. Z. angew. Phys. 10, 195 (1958).
3. L. Genzel and R. Weber. Z. angew. Phys. 10, 1 (1958).
4. P. Fellgett. J. phys. radium 19, 187, 237(1958).
5. J. Strong and G. Vanesse. J. phys. radium 19, 192 (1958).
6. N. G. Bakhshiev. Abt. Svid. No. 108418, Sept. 15, 1956.
7. N. G. Bakhshiev. Opt. i Spektr. 2, 816 (1957).
8. J. Connes. J. phys. radium 19, 197 (1958).
9. P. Tacquinot. J. phys. radium 19, 223 (1958).
10. H. Gebbie. J. phys. radium 19, 230 (1958).
11. L. Mertz. J. phys. radium 19, 233 (1958).
12. P. Ramsay, J. Opt. Soc. Am. 24, 253 (1934).
13. T. H. Schroeder and P. Ramsay. J. Opt. Soc. Am. 30, 355 (1940).
14. P. Connes. Opt. Acta 4, 136 (1957).
15. P. Connes. J. phys. radium 19, 215 (1958).

DISCUSSION

V. M. Chulanovskii. In the papers of I. V. Peisakhson and D. N. Shchepkin the possibility was shown of determining the true values of the absorption coefficient at the maximum and of the half-width of not too narrow infrared absorption bands on a common apparatus. Experience shows that these measurements must be carried out under the conditions of absence of distortions introduced by scanning, namely, by the measurement of the spectra "by points with a record." For each of the chosen wavelengths a record of the light currents I and I_0 is produced by alternately placing the cell with solution and solvent in front of the slit (cf. Figure).

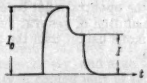

The features of such a recording are:

(a) Errors connected with the inertia of the system are completely removed, and the noise is readily averaged on the horizontal axes.

(b) A frequent check of the zero removes the necessity of control measurements, unavoidable for the records of band contours on single-beam instruments.

(c) It is not necessary to record all of the points of the curve—a proper choice of the points shortens the time of obtaining the spectral characteristics.

(d) The errors of the measurement, as experience has shown, is almost an order less than for the record of continuous contour.

A. V. Iogansen. Already in 1953 we had made measurements of the apparatus function of the IKS-11 spectrometer in the region of 1.014μ, using a photoelement as the detector and diaphragming the slit to 0.2-0.1 of its full height. For a LiF prism we obtained the following magnitudes of the half-width of the apparatus function (in microns):

Width of the Slit (μ)	Half-width of the apparatus function $\Delta\nu_{eff}$ for the slit height	
	4 mm	30 mm
20	32	47
30	39	53

Since for the region beyond 3μ there is still no reliable method of measurement of the half-width of the apparatus function, $\Delta\nu_{eff}$, then it becomes expedient to carry out measurements of $\Delta\nu_{eff}$ in the near infrared region and to extend the results of the measurements to longer wavelengths and to other prisms with the corresponding corrections for diffraction and the curvature of the slits. It would be desirable to have band standards for the determination of $\Delta\nu_{eff}$ in different regions of the spectrum. For this purpose there should be set up, in one of the laboratories, a special project on the measurements of the parameters of absorption bands using instruments of high resolution.

S. G. Rautian. It is possible to trust the calculated methods of the determination of the apparatus function of a monochromator only in the absence of aberrations, but even in this case the analysis of the question is not sufficiently complete. In particular, a calculation of the partial coherence of the illumination of the exit slit of the monochromator is desired. In the absence of aberrations it is essential to measure the apparatus function, and the working out of reliable methods of such measurements presents most important problems. I completely agree with A. V. Iogansen that it is essential to make measurements of the absorption coefficient of a series of narrow and broad lines on instruments of high resolving power.

Practically, I consider the following to be by far the most important recommendations issuing from the paper of G. G. Petrash: the systematic distortions arising from the registering system must be several times less than the distortions due to the apparatus function of the monochromator. This is true for single and double-beam instruments, for any apparatus functions, and types of spectra. This recommendation remains in force even for reduction to the ideal monochromator. The second interesting result is the separation of the effects of the shift of the spectrum and of the distortion of its form. Since, for small distortions, the shift does not depend on the form of the spectrum, it is possible to neglect it. From this viewpoint the undesirability of those setups is shown, in which the scanning speed is changed in correspondence with the slope of the signal.

In connection with the communication of V. M. Arkhipov, it is essential to emphasize that all of the advantages of interference spectroscopy are located in the optical part of the mounting, i.e., in the interferometer itself, and are by no means connected with those new ways of registration of the beam, which arise with the use of the interferometer in the capacity of a dispersing system (the new method of current modulation, etc.).

G. G. Petrash. The method contained in the paper of V. A. Nikitin and O. D. Dmitriev regarding a choice of the conditions of measurement does not lead to a minimum of the errors and, accordingly, does not guarantee the optimum conditions of measurement. This is connected with the following reasons:

(a) The random and systematic errors depending on the very same parameters (s, τ) are defined by conditions not connected with one another.

(b) They do not take account of the systematic errors arising from the influence of the slits of the monochromator and playing a most important role.

L. A. Gribov. I would like to emphasize once more the principal difference between single and double-beam instruments. Single-beam instruments measure directly the energy current E(t); double-beam instruments measure the error signal of observation, proportional to the derivative E′(t). In a particularly wide interval of slow

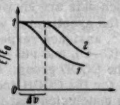

Dependence of the ratio E/E_0 on the scanning speed v for single-beam (curve 1) and double-beam (curve 2) instruments. Δv is the working interval of the scanning speeds for double-beam spectrophotometers.

scanning speeds the ratio E/E_0 (E—measured, E_0—true value) is practically constant and equal to one, in contrast with single-beam instruments (cf. Figure). The introduction of automatic regulation of the scanning speed guarantees a constant error signal of observation, i.e., it practically completely eliminates the necessity of the consideration of errors connected with scanning in double-beam spectrometers.

B. S. Neporent. The question of the simultaneous calculation of systematic and random errors must be decided in a sufficiently general form. The determination of the minimum total error (for conditions of a low value of these errors) has significance only for the limited, although frequently applied, conditions of the experiment. Besides, the presentation of the square of the total error as a sum of the squares of the systematic and random errors and, accordingly, the fixing of conditions rigidly determining the optimum parameters (the speed of recording v, the time constant τ, and the width of the slits s), are not the only ones possible. Taking account of the fact that in practice the relations between the slit width and the width of the band being measured, on one hand, and between the speed v and time constant τ on the other, can be changed within broad limits, we did not consider it necessary in reference 1 to postulate optimum relations between the systematic and random errors. A particular spectroscopic problem may require the reduction to a minimum mainly of errors of one origin only. As was shown in the communications of I. V. Peisakhson and D. I. Shchepkin, even significant errors connected with the apparatus function can be readily excluded with a particularly high degree of reliability by the corresponding treatment of the records. Having in mind the application of such a procedure, it would not be advisable, for example, to introduce into the determination of the total error errors connected with the apparatus function (the term as^2 in formula (81) in reference 2).

It should also be noted that in some cases it was necessary to determine the contour of the band, in others its area, and in others the intensity at the maximum and the half-width. Also, the rapid methods of measurement of the spectra produce particular demands on the errors. In their dependence on all of these factors the conditions of recording of the spectra must be chosen. In this scheme the formulation of general relations between s, v, and τ can be more useful than the proposal of "universal" regimes.

REFERENCES

1. O. D. Dmitrievskii, B. S. Neporent, and V. A. Nikitin. Uspekhi Fiz. Nauk **64**, 447 (1958).
2. S. G. Rautian. Uspekhi Fiz. Nauk **66**, 475 (1958).

SHORT COMMUNICATIONS

THE CHARACTERISTIC FREQUENCIES OF THE HYDROPEROXIDE GROUP, C—O—O—H

M. A. Kovner, A. V. Karyakin, and A. P. Efimov

Received 8 May 1959

The various applications of hydroperoxide compounds make the determination of their spectral features a problem of current interest; i.e., the establishment of some set of frequencies which characterize the COOH group and make its identification possible. In the present work, the vibrational frequencies of the hydroperoxide group are considered. The infrared spectra of hydroperoxides have been repeatedly studied, and this has made it possible to pick out the frequencies 840, 880, 1155, 1325, and 3450 cm^{-1} as typical of the C—O—O—H group.[1,2] These frequencies have been conjecturally assigned to δ(COOH), ν(O—O), ν(C—O), δ(O—H), and ν(O—H). A theoretical investigation of the problem of the characteristic frequencies of the hydroperoxide group is evidently of interest; it has proved expedient to limit ourselves, in the first stage, to the calculation of the vibrational frequencies of the four-atom model molecule C—O—O—H.

For the calculation, it is necessary to have on hand experimental data on the vibrational spectra of deuterated hydroperoxides. Such data are known only for cumene hydroperoxide,[3] in the spectrum of which 800, 855, 995, 1155, and 2550 cm^{-1}, assigned respectively to δ(COOD), ν(O—O), δ(O—D), ν(C—O), and ν(O—D), were picked out as frequencies of the COOD group. Analysis of the quoted sets of frequencies for the COOH and COOD groups permits us to draw the conclusion that these sets are incomplete; first, a nonlinear chain of four atoms must possess six frequencies; and secondly, numerous experimental data indicate that the vibrational frequencies of an XYZ angle (where the atoms X, Y, Z are heavy) are of the order $\delta(XYZ) < 600$ cm^{-1}. Consequently, the δ(COO) frequency is missing from the set. This deduction is confirmed as a result of a new study of the infrared spectrum of cumene hydroperoxide in the region down to 400 cm^{-1}, in which a very intense line with the frequency 585 cm^{-1} was observed (see Figure); this is assigned by us to δ(COO). The corresponding frequency in the COOD group is unfortunately not known. Since the assignment of the frequencies 880, 1155, 1325, and 3450 for COOH

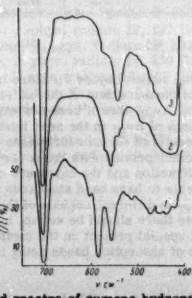

Infrared spectra of cumene hydroperoxide (1), dimethylphenylcarbinol (saturated solution in cumene) (2), and cumene (3). UR-10 spectrometer, cell thickness 0.01 mm.

and 855, 995, 1155, and 2250 cm^{-1} for COOD is undoubted, the frequency 840 cm^{-1}, previously conditionally designated as δ(COOH), must be assigned to the vibration of the dihedral angle γ between the COO and OOH planes.

In order to complete the calculation, it is necessary, furthermore, to have on hand exact data on the geometry of the hydroperoxide group in cumene. These, unfortunately, are lacking, and we have made use of the only data known to us, namely, data on the geometry of the hydroperoxide group in performic acid.[3] The equilibrium values of the bond lengths and angles of this group are: (C—O) 1.35 A; (O—O) 1.49 A; (O—H) 1.02 A; ($\angle$COO) 105°; ($\angle$OOH) 100°. For the dihedral angle mentioned above, the value 95° ± 25°, found from dipole moment values, has been given in reference 4 (the H_2O_2 and t-butyl hydroperoxide molecules). We have taken the equilibrium dihedral angle equal to 90°, which simplifies the calculation considerably. In Table 1 are presented the elements of the 6th-order kinematic-coefficient matrices, evaluated with the given values of the bond lengths and angles, with the "spectroscopic" masses of H and D equal to 1.088 and 2.126 respectively, and also with the introduction of the generally accepted unit of length 1.09 A. The ratio Π of the determinants of these matrices for COOD and COOH, which equals the ratio of the squares of all six frequencies of the two molecules, equals 0.176, while on replacement of the "spectroscopic" masses of H and D by the actual ones it takes on the value 0.164.

Table 1. Kinematic Coefficients and Force Constants of the Hydroperoxide Group

Bonds and angles	Kinematic coefficients	Force constants (10^5 cm^{-2})	Bonds and angles	Kinematic coefficients	Force constants (10^5 cm^{-2})
C—O, C—O	0.159	8.233	O—O, OOH	—0.0171	0.500
C—O, COO	—0.048	0.400	O—O, O—H	—0.012	0
C—O, O—O	—0.018	0	O—O, χ	0	0
C—O, OOH	0	0	OOH, OOH	1.309	1.300
C—O, O—H	0	0	OOH, O—H	—0.049	0.500
C—O, χ	0.008	0	OOH, χ	0.039	0
COO, COO	0.197	2.589	O—H, O—H	1.068	11.160
COO, O—O	—0.053	0.400	O—H, χ	0.013	0
COO, OOH	0	0.120	χ, χ	1.415	0.490
COO, O—H	0	0	OOD, OOD	0.751	1.300
COO, χ	0.069	0	O—D, O—D	0.580	11.160
O—O, O—O	0.136	5.566	χ, χ (COOD)	0.841	0.490

Let us return to the question of the set of 21 force constants which correspond to the C—O—O—H chain. The vibrational frequencies of COOH and COOD, even though there are only 12, could serve to determine them. However, as already noted, the frequency δ(COO) in COOD is unknown, and one can only assume that it is very close to 585 cm^{-1}, since it should not change markedly on deuteration. On the other hand, from the large difference in the χ, χ kinematic coefficients for COOH and COOD it follows that the χ frequency in COOD must be considerably lower than 800 cm^{-1}, and therefore the assignment of the observed 800 cm^{-1} frequency to this vibration is doubtful.

Thus there remain 10 experimental frequency values to be used for determining the force constants. Obviously one cannot get along without some preliminary assumptions. It is natural to suppose that the force constants for the interaction of angles and bonds which have no atoms in common are equal to zero. Furthermore, the force constant for the interaction of two adjacent bonds is usually taken equal to zero. Finally, it is permissible to assume the vanishing of the force constants for the interaction of the coordinate χ with all the remaining coordinates, since for a planar configuration of the chain this coordinate would be completely uncoupled by symmetry. With the assumptions just enumerated, 11 force constants remain unknown.

The force constant for the interaction of the COO and OOH angles may be taken equal to the force constant for the interaction of the transversely oriented angles in the CH_3OH molecule,[5] i.e., 0.12. In just the same way, we have taken the values of the CO, COO and OO, COO force constants equal to 0.40 and the OO, OOH and OH, OOH constants equal to 0.50, in analogy with the values for the CO, COH and OH, COH force constants in methyl alcohol.[5]

The remaining six most important (diagonal) force constants were determined by the variational method, and the values shown in Table 1 were obtained for them. These force constants are close to the analogous values in the molecules of related compounds. It must be noted that the possible errors in the geometric parameters entail errors in the determination of the force constants, but they do not influence the interpretation of the frequencies. The frequencies calculated according to the data of Table 1 and the observed frequencies are compared in Table 2.

Table 2. Calculated and Observed Vibrational Frequencies of the COOH and COOD Groups (cm^{-1})

COOH			COOD		
Bonds and angles	Calculated	Observed	Bonds and angles	Calculated	Observed
COO	586	585	COO	549	—
χ	834	840	χ	680	—
O—O	886	880	O—O	873	855
C—O	1156	1155	OOD	997	995
OOH	1321	1325	C—O	1156	1155
O—H	3450	3450	O—D	2539	2550

It would have been of considerable interest to study the infrared spectrum of cumene deuterohydroperoxide in the lower frequency region, but the correctness of the values of the two estimated COOD frequencies can be seen from the product rule: for Π = 0.164 and 0.176, the product of the squares of these two frequencies would have to equal 0.136 and 0.146 respectively, while the product of the squares of the calculated (and unobserved, Table 2) frequencies equals 0.139. This value is entirely reasonable, since it is known that the "spectroscopic" masses somewhat overestimate the effect of anharmonicity.

The sufficiently good agreement attained between the calculated and observed frequencies permits us to conclude that the frequencies of Table 2 form a set which is characteristic for the hydroperoxide group. As shown by study of the kinetics[6] of reactions which involve the hydroperoxides of benzene derivatives, the activation energy of these reactions does not depend on the length of the radicals. The constancy of the activation energy is consistent with the idea that the structure of the electron cloud of the hydroperoxide group is constant, which finds expression in the constancy of its vibrational frequencies. The kinetic peculiarities of different hydroperoxides indicate, evidently, not a difference in the activation energies, but a difference in steric factors, which depend on the structure of the radicals. A. D. Stepukhovich drew our attention to these circumstances.

The authors offer their thanks to academician A. N. Terenin for his interest in the work.

REFERENCES

1. A. V. Karyakin and V. A. Nikitin. Izvest. Akad. Nauk SSSR, Ser. Fiz. 17, 635 (1953).
2. A. V. Karyakin. Dokt. diss., Moscow State University, 1958;
V. A. Nikitin. Kand. diss., State Optical Institute, 1959.

3. P. A. Giguere and A. Weingartshoffer. Can. J. Chem. 30, 821 (1952).
4. M. T. Rogers and T. W. Campbell. J. Am. Chem. Soc. 74, 4742 (1952).
5. B. I. Stepanov. Zhur. Fiz. Khim. 19, 497 (1945).
6. M. Szwarc. Chem. Revs. 47, 75 (1950).

VARIATION IN THE DURATION OF LUMINESCENCE OF TRIVALENT GADOLINIUM AND TERBIUM IONS IN THE SYSTEM SULFURIC ACID-WATER, AS A FUNCTION OF COMPONENT CONCENTRATION

E. V. Kondrat'eva

Received 27 May 1959

We noted previously that the afterglow time τ for $Gd_2(SO_4)_3$ and $Tb_2(SO_4)_3$ solutions in a sulfuric acid-water system is approximately three times as long as τ for aqueous solutions of the same salts.[1,2] Measurements of τ for Gd^{+++} and Tb^{+++} in the sulfuric acid-water system enable us to draw certain conclusions concerning the change of structure of sulfuric acid solutions when diluted by water.

X-ray studies of the structure of sulfuric acid solutions[3,4] have not revealed how the structure of the acid varies when water is added.

We added water drop by drop to a solution of $Gd_2(SO_4)_3$ in concentrated H_2SO_4. After each addition of the water, the solution was carefully mixed. When the solution had cooled to room temperature, we measured τ. The experimental technique is described in reference 2. We found that when water is added up to a concentration corresponding to the composition H_2SO_4-H_2O (~16% H_2O by weight), the duration of luminescence remains the same as for concentrated sulfuric acid. When the content of water changes from 16 to 26%, which corresponds to a transition from the composition H_2SO_4-H_2O to H_2SO_4-$2H_2O$, τ decreases from 2×10^{-2} to 6×10^{-4} sec. The latter value corresponds to the duration of luminescence of aqueous solutions of $Gd_2(SO_4)_3$. Further addition of water does not bring about any further change in τ (Fig. 1). We found that the results are independent of the concentration of gadolinium in the solution within the limits 0.5-0.05%.

We found quite similar results for solutions of $Tb_2(SO_4)_3$ in water. (See Fig. 2.) These investigations were carried out in the 0.1-0.01% concentration range.

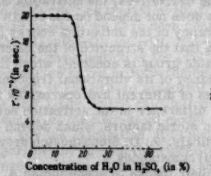

Fig. 1

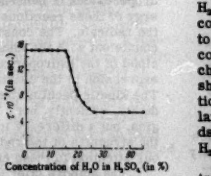

Fig. 2

Fig. 1. Variation of the duration of luminescence of $Gd_2(SO_4)_3$ in the sulfuric acid-water system as a function of water concentration.
Fig. 2. Variation of the duration of luminescence of $Tb_2(SO_4)_3$ in the sulfuric acid-water system as a function of water concentration.

It is known that the structure and intensity of the luminescence spectra of rare earth elements in solution are determined primarily by the immediate ionic environment.[5,7] We may assume that the quantity τ, which is almost entirely determined by the probabilities of nonradiative transitions,* is also primarily dependent on this environment.

*This has been shown in reference 8 for solutions of terbium salts. We may assume, on the basis of a comparison of the duration of luminescence of Gd^{+++} in solutions[1] and crystals,[9] that the same thing holds for solutions of gadolinium salts.

Apparently, the presence of small concentrations of water in sulfuric acid solutions of $Gd_2(SO_4)_3$ and $Tb_2(SO_4)_3$ (up to the composition H_2SO_4-H_2O) corresponds to a solution structure in which the H_2O molecules cannot be in the first coordination zone around the lanthanide ions.

Further addition of water changes the structure of the solution in such a way that the H_2SO_4 molecules in the first coordination zone around the rare earth ions are gradually replaced by water molecules. The structural changes cease when the composition H_2SO_4-$2H_2O$ is attained.

The sulfuric acid-water system is one of the few examples of liquid binary systems in which certain properties change discontinuously.

This system was studied in detail by D. I. Mendeleev.[10] In studying the dependence of ds/dp on p in the sulfuric acid-water system (where s is the specific gravity at 0°C and p the percent concentration of H_2SO_4), Mendeleev found that the corresponding curve has discontinuities at certain points. The most pronounced discontinuities in the derivative corresponded to the compositions H_2SO_4-H_2O and H_2SO_4-$2H_2O$. Mendeleev called the points of discontinuity or jumps "characteristic" points. According to Mendeleev, the existence of "characteristic points" is connected with the formation in the solutions of definite chemical compounds: the more stable the compound, the sharper the discontinuities in the property vs. composition curves. Mendeleev established the fact that the largest jump and the largest change in the slope of the ds/dp derivative correspond to the characteristic point H_2SO-$2H_2O$.

It is at this same composition that the largest contraction (decrease in the volume of the solution formed as compared to the sum of the component volumes) is observed and the largest amount of heat liberated when H_2SO_4 and H_2O are mixed. All this indicates the stability of the chemical compound formed.

It is obvious from the above that a change in the structure of the solution occurs at the "characteristic" points.

The duration of luminescence varies quite differently when a small amount of H_2SO_4 is added to an aqueous solution of $GdCl_3$. (Here water remains the main com-

ponent of the solution.) In this case there is a gradual decrease in the value of τ from 2.0×10^{-3} (for $GdCl_3$ in water at 15°C) to 6.0×10^{-4} sec (for $Gd_2(SO_4)_3$ in water at 15°C). (See Fig. 3.) No "jump" in τ is observed. This can apparently be explained as follows: In this case there is no rearrangement of the solvate sheaths; water molecules remain in the first coordination zone around the Gd^{+++} ions.

This conclusion agrees with recently published data,[11] according to which the coordination number of all ions in dilute aqueous solutions is four, which is the coordination number of water molecules in purely aqueous solutions.

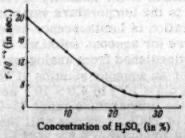

Fig. 3. Variation of the duration of luminescence of $GdCl_3$ in aqueous solution as a function of the amount of sulfuric acid added.

REFERENCES

1. E. V. Kondrat'ev. Opt. i Spektr. 5, 214 (1958).
2. E. V. Kondrat'ev and V. B. Ustinov. Vestnik Leningrad Gosudarst. Univ. No. 4 (1959).
3. A. F. Skryshevskii. Sbornik "Stroenie i fizicheskie svoistva veshchestva v zhidkom sostoyanii." (Collection, The Structure and Physical Properties of a Substance in the Liquid State) pp. 27, 28, Kiev. Izd. Univ. (Kiev. Univ. Pub.), 1954.
4. A. V. Romanov. Avtoreferat dissertatsii. (Author's abstract of thesis.)
5. A. N. Zaidel and V. Rotshtein. Doklady Akad. Nauk SSSR 57, 587 (1947).
6. E. Sayre, D. Miller, and S. Freed. J. Chem. Phys. 26, 109 (1957).
7. D. Miller, E. Sayre, and S. Freed. J. Chem. Phys. 29, 454 (1958).
8. E. V. Kondrat'ev. Opt. i Spektr. 6, 427 (1959).
9. G. H. Dieke and L. A. Hall. J. Chem. Phys. 27, 465 (1957).
10. D. I. Mendeleev. Izbrannye sochineniya. (Selected Works), 3, (1934).
11. A. F. Kapustinskii. Zhur. Fiz. Khim. 32, 1648 (1958).

A STUDY OF THE DURATION AND INTENSITY OF LUMINESCENCE OF TRIVALENT GADOLINIUM AND TERBIUM IONS IN SOLUTIONS

E. V. Kondrat'eva and G. S. Lazeeva

Received 27 May 1959

In previous communications we reported[1,2] certain results of a study of the duration of luminescence of Gd^{+++} and Tb^{+++} in solutions. Here we study the duration and intensity of the luminescence of Gd^{+++} and Tb^{+++} in solution in more detail. The experimental arrangement and measurement procedure were described in references 1 and 2. We studied the luminescence of solutions of $Gd_2(SO_4)_3$ and $Tb_2(SO_4)_3$ in water and sulfuric acid and of $GdCl_3$ and $TbCl_3$ in water. The salts were prepared by conventional methods from Gd_2O_3 and Tb_2O_3. The major part of the measurements for solutions of gadolinium salts were carried out at concentrations of 0.5-0.1%. We also verified that the duration of luminescence and the temperature dependence of the luminescence intensity do not vary over the concentration range 1-0.1%. For solutions of terbium salts, the measurements were performed in the concentration range 0.1-0.01%.

1. Gd^{+++}. The luminescence spectrum of Gd^{+++} in solution consists of two narrow bands with maxima at 3110 and 3060 A.[1,3] The ratio of the intensities of the two bands was determined by photographic photometry and was found to be

$$\frac{I_{3110}}{I_{3060}} = 25.$$

(The average arithmetical error of 20 measurements ~4%.)

This result was obtained for measurements of the luminescence spectrum of $GdCl_3$ in water. For solutions of $Gd_2(SO_4)_3$ in water and sulfuric acid, the ratio of intensities is approximately the same and does not vary appreciably over the concentration range 1.0-0.01%.

For Gd^{+++} it is of particular interest to determine separately the lifetime of each of the levels $^6P_{7/2}$ and $^6P_{5/2}$. Unfortunately, the intensity of the band $\lambda_{max} = 3060$ A is so low that only coarse measurements could be performed. These were furthermore restricted to an aqueous solution of $GdCl_3$ at gadolinium concentrations of around 1% and at t = 15°C. (The luminescence of this solution is brighter than that of all the other gadolinium solutions which we studied.) The value of τ_{3060} was found to be 10^{-3}-10^{-4} sec. The value of τ_{3110} for the same solution is 2×10^{-3} sec.

We should note that there are references in the literature to the fact that the lifetime of closely neighboring levels of trivalent rare earth ions can be different.[4,5]

The problem of the temperature quenching of the luminescence of lanthanide ions has been studied very little. In a series of papers published prior to 1957, the duration of luminescence of trivalent lanthanide ions in crystals and solutions of ionorganic salts was studied at room temperature only. No data were given indicating the presence of quenching.[6-9] Vavilov and Sevchenko tried to find the influence of temperature and solvent on the luminescence yield of solutions of terbium, europium, and samarium salts, but none was found.[10] In 1957, Dieke and Hall published data on the duration of luminescence of certain lanthanide crystals at different temperatures.[4] These data indicate that τ is almost independent of temperature.

As stated previously,[1,2] our investigations have shown that the luminescence of Gd^{+++} and Tb^{+++} in sul-

furic acid and aqueous solutions is subject to temperature quenching. For Gd* salts, this influence is very pronounced in all solutions studied. Over the temperature range of 2-95°C, τ of an aqueous solution of $GdCl_3$ decreases approximately by a factor of 12, τ of an aqueous solution of $Gd_2(SO_4)_3$ by a factor of 20, τ of a solution of $Gd_2(SO_4)_3$ in 96% sulfuric acid by a factor of 50. The results of the measurements are shown in Fig. 1. The intensity of Gd^{+++} luminescence also decreases with increasing temperature.

*All of the measurements of I and τ for Gd are made for the band λ_{max} = 3110 A. Due to the low intensity of the band λ_{max} = 3060 A, we were only able to note, when looking at the signal on an oscilloscope screen, that its afterglow duration also decreases strongly with a rise in temperature

The temperature variations of the duration and intensity of afterglow are similar. Figure 2 shows the temperature dependence of the duration and intensity of luminescence of an aqueous solution of $GdCl_3$. A similar dependence was alwo observed for solutions of $Gd_2(SO_4)_3$ in H_2O and in H_2SO_4.

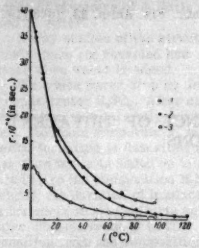

Fig. 1

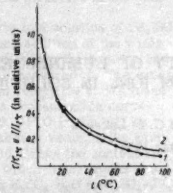

Fig. 2

Fig. 1. Temperature dependence of τ. 1—$GdCl_3$ in water; 2—$Gd_2(SO_4)_3$ in H_2SO_4; 3—$Gd_2(SO_4)_3$ in water.

Fig. 2. Relative variation with temperature of the intensity and duration of luminescence of an aqueous solution of $GdCl_3$. Curve 1—$\tau/\tau_{20°C}$; curve 2—$I/I_{20°C}$.

The decrease of I and τ with increasing temperature is apparently due to an increase in the probability of radiationless transitions, i.e., to an increase in the interaction of the radiating ion with solvent molecules.

The quantum yield of luminescence is

$$\gamma_l = \Sigma A \cdot \tau.$$

(ΣA is the sum of the probabilities of radiating transitions.)

If ΣA does not vary with temperature, then the dependence on temperature of the quantum yield should be similar to the temperature dependence of afterglow duration. A change in luminescence intensity can be identified with a change in quantum yield only in the case where the energy absorbed does not vary over the temperature interval being studied. On the basis of the fact that the variations of I and τ with temperature are almost parallel for all solutions studied, we may conclude that the decrease with temperature of the intensity of luminescence is caused primarily by a change in the quantum yield.

2. Tb^{+++}. It is known that the spectrum of the luminescence of the trivalent terbium ion in solutions consists of seven bands, 100-200 A wide, with maxima corresponding to wavelengths λ_{max} = 4890, 5450, 5890, 6200, 6480, 6700, and 6810 A.[11] All seven bands correspond to transitions from the $^5D_4$ level to components of the ^7F level.[9]

For solutions of terbium salts, we measured τ seperately for each of the bands λ_{max} = 4890, 5450, and 5890 A. We found that at room temperature τ is the same for these three bands and has the same temperature dependence. For the solution of $Tb_2(SO_4)_3$ in 96% H_2SO_4, the value of τ increased by, say, a factor of 8 as the temperature varied from 2 to 100°C, but did not change any further up to 250°C. (See Fig. 3.) The temperature variation of the intensity of luminescence is very similar to the temperature variation of the duration. The duration of luminescence depends very little on temperature for aqueous solutions of $Tb_2(SO_4)_3$ and $TbCl_3$, as distinguished from analogous solutions of gadolium salts. For an aqueous solution of $Tb_2(SO_4)_3$, τ decreases from 5.5×10^{-4} to 4.0×10^{-4} sec, i.e., by less than 30% for the temperature range 15-98°C. For aqueous solutions of $TbCl_3$, τ varies still less in the same interval (by only 10%)—from 5.5×10^{-4} to 4.9×10^{-4} sec. We should note that at t = 15°C the values of τ for aqueous solutions of $TbCl_3$ and $Tb_2(SO_4)_3$ coincide but differ by a factor greater than three for the analogous gadolinium salts.

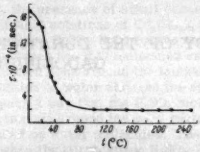

Fig. 3. Temperature dependence of τ for the $Tb_2(SO_4)_3$ solution in concentrated H_2SO_4.

CONCLUSIONS

1. The luminescence of $Gd_2(SO_4)_3$ and $Tb_2(SO_4)_3$ in aqueous and sulfuric acid solutions and of $GdCl_3$ and $TbCl_3$ in aqueous solutions is subject to temperature quenching.

2. The temperature dependence of τ is much more pronounced for solutions of gadolinium than terbium salts.

3. The luminescence of sulfuric acid solutions of $Gd_2(SO_4)_3$ and $Tb_2(SO_4)_3$ is subject to much greater temperature quenching than the luminescence of aqueous solutions of the same salts.

4. The dependence of τ on anions is more pronounced for gadolinium than for terbium salts.

REFERENCES

1. E. V. Kondrat'ev. Opt. i Spektr. 5, 214 (1958).
2. E. V. Kondrat'ev and V. B. Ustinov. Vestn. Leningrad Gosudarst. Univ. No. 4 (1959).
3. R. Tomaschek and E. Mehnert. Ann. Physik. 29, 306 (1937).
4. G. H. Dieke and L. A. Hall. J. Chem. Phys. 27, 465 (1957).
5. M. V. Fok. Opt. i Spektr. 2, 127 (1957).
6. A. N. Seidel. Nature 139, 248 (1937).
7. A. N. Zaidel' (Seidel) and Ya. I. Larionov. Uspekhi Fiz. Nauk 21, 211 (1939).

8. B. Rinck. Z. Naturforsch. 3a, 406 (1948).
9. H. F. Geissler and K. H. Hellwege. Z. Physik. 136, 293 (1953).
10. S. I. Vavilov and A. N. Sevchenko. Doklady Akad. Nauk SSSR 27, 541 (1940).
11. A. N. Zaidel' (Seidel), Ya. Larionov, and A. N. Filippov. Zhur. Eksp. i Teoret. Fiz. 9, 17 (1939).

ON THE RATIO BETWEEN THE SIGNAL FROM A COMPONENT BEING DETERMINED AND THE SIGNAL FROM THE TOTAL RADIATION FLUX FOR INFRARED GAS ANALYZER

A. O. Sall'

Received 28 May 1959

Inaccuracies of an absorptive analyzer[1-6] depend on the ratio F of the signal originating from a change of the composition of the component, being determined in the mixture under analysis, from zero to the maximum concentration (corresponding to the end of the scale of analyzer) to the signal from the total flux.[7-10] Usually

$$F = \frac{\int_0^\infty I\,(1 - e^{-ku})\,\varphi d\nu}{\int_0^\infty I\varphi d\nu},$$

where ν is the wave number, $I(\nu)$ is the spectral intensity of the fluxes under comparison, $k(\nu)$ is the coefficient of absorption of the component being determined, u is the product of the concentration of the component being determined in the mixture under analysis and the length of the working camera, and $\varphi(\nu)$ is the spectral sensitivity of the receiver.

When comparing the sensitivity of various absorption meters, it is also important to know the relationship $F = F(u)$. In many cases, for the first approximation, one could consider that the highest sensitivity has such an analyzer which permits attainment of the required numerical value of F with the smallest value of u. For instance, in order to get $F = 0.1$, with an unselective source and unselective receiver of radiation in the infrared analyzer, it is necessary to have the value of u of the average order of magnitude of 10^3–10^5 mm%. In an optico-acoustical gas analyzer the same values of F are readily obtained with u = 10–100 mm%.

The sensitivity of the gas analyzer can be increased also by separating from the total flux the required spectral region by means of a periodical change of the quantity of the component under determination in the path of both fluxes of the radiation being compared.[3] Such a change can be realized by using modulating cameras with a moving reflecting mirror.[9, 10] The vibrations of an elastic reflecting plate are effected by means of an electromagnet, the winding of which is fed by alternating current. Furthermore, as was shown by investigations, for actuating the winding it is better to use only one half of the cycle of the alternating current (with previous rectification of the semicycles), or an alternating current consisting of periodically repeated impulses (preferably rectangular). In that case:

$$F = \int_0^\infty I\,(1 - e^{-ku})\,(e^{-kw} - e^{-2kw} + \varphi_H)\,\varphi d\nu \times \left[\int_0^\infty I\,(e^{-kw} - e^{-2kw} + \varphi_H)\,\varphi d\nu\right]^{-1},$$

where w is the product of the concentration of the component being determined in the modulation camera and the amplitude of the change of the path of a ray in it, η is the ratio of the minimum thickness of the layer, occuring at the moment of the approach of the reflecting surface to the window, to the maximal thickness of the layer, which is obtained at the maximum distance of the reflecting surface from the window of the modulation camera, and φ is the relative change of the flux, falling on the receiver, resulting from the movement of the reflecting surface (in the absence of the gas which absorbs the radiation in the modulation camera.)

With the amplitude of the movement of the reflecting surface of about one milimeter, $\varphi_H \leq 10^{-2}$. By passing the fluxes through the modulation cameras filled with the component being determined and having two windows, and changing the distance between the windows, it is possible to get $\varphi_H \leq 10^{-3}$.

The sensitivity of such a gas analyzer is less than the sensitivity of an optico-acoustical gas analyzer. Indeed, if the absorption spectrum of the component being determined consists of well separated lines of the same intensity, and the spectrum of the source is such that $\varphi_a = 10^{-3}$, then for an optico-acoustical gas analyzer we have A = 0.1.[10] When calculating the value of A for the gas analyzer with nonselective sources and receivers, and fluxes which are modulated selectively, it is necessary to change φ_a to φ_H. If we take $\varphi_H \approx 10^{-3}$, we get

$$A \simeq 0.1 \times \frac{10^{-2}}{10^{-3}} = 100.$$

Using the data from reference 10, with F = 0.3 and A = 100, we have $(k_0 u)_{min} \approx 4 \times 10^4$ instead of $(k_0 u)_{min} \approx 1$, which was valid for the optico-acoustical gas analyzer.

If we denote by w the product of the effective thickness of the radiating layer in a selective gas source[11] and the concentration of radiating component, then for a gas analyzer with nonselective receiver the curves of $u = u(w)$ with F = const. will have the same shapes as the curves given in reference 10. Parameter A in that case is determined by the emitting efficiency of the windows and walls of the source and their temperature. The value of A is independent of the spectral sensitivity of the receiver, if the latter is constant within the spectral regions of the radiation of the heated gas, and of the windows and the walls of the receiver. By periodically changing the temperature of emitting gas in the source,[12] one could reduce the value of A almost to those obtained with the optico-acoustical gas analyzer. In that case η is equal to the ratio of the thickness of the passive layer at the window of the source to the effective thickness of the emitting layer.

The Figure shows the curves with $F(u, w) = \text{const.}$, which were obtained with $\eta = 0$ for the ideal case of a

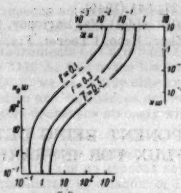

The dependence, from values u and w, of the ratio of the signal from the gas to the signal from the total radiation flux.

band which consisted of lines of an equal intensity. In the lower left-hand part of the illustration, F depends on the maximum value of the coefficient of absorption k_0, and on the top right-hand part it depends on the value of the generalized coefficient of absorption χ.[15] In the region of validity of the square root law,[15] u and w are connected by a proportional relationship.

In the region of validity of the law of square root, with $u \ll w$ and $\eta = 1$ we have

$$F \simeq \int_0^\infty (1 - e^{-kw})\,(e^{-kw\eta} - e^{-kw})\,dv \left[\int_0^\infty (e^{-kw\eta} - e^{-kw})\,dv\right] \simeq$$

$$(\sqrt{w} - \sqrt{u+w} - \sqrt{w\eta} + \sqrt{u+w\eta})\,(\sqrt{w} - \sqrt{w\eta})^{-1} \simeq \sqrt{\frac{u}{w}} + \eta - \sqrt{\eta},$$

from which

$$u \simeq (F^2 + 2\sqrt{\eta}F)\,w.$$

Generalizing for the case of small w, we have

$$u \simeq \frac{bF}{k_0} + (F^2 + 2\sqrt{\eta}F)\,w$$

or

$$F \simeq \sqrt{\left(\frac{0.5b}{k_0 w} + \sqrt{\eta}\right)^2 + \frac{u}{w}} - \left(\frac{0.5b}{k_0 w} + \sqrt{\eta}\right),$$

where b is a numerical coefficient, usually not exceeding 3 or 4.[15] From the result of experiments conducted with the optico-acoustical gas analyzer, we obtained

$k_0 b^{-1} \simeq 0.01$ (mm% CH_4)$^{-1}$ and $k_0 b^{-1} \simeq 0.04$ (mm% CO_2)$^{-1}$.

Example: Let us investigate, as an example, the calculation of the optimum value of u for the optico-acoustical gas analyzer.

We put $w < w_M = 10^3$ mm%; F = 0.1–0.2; $k_0 = 0.02$ (mm%)$^{-1}$; $\eta = 0.06$ (in the case of an optico-acoustical gas analyzer, the coefficient η can be determined as the ratio of the thickness of the passive layer at the window of the radiation receiving camera[7, 10] to the length of the ray path in it). Then we shall obtain

$$\frac{bF}{k_0} \simeq 5\text{–}10 \text{ mm\%} < u < \frac{bF}{k_0} + (F^2 + 2\sqrt{\eta}F)\,w_M = 65\text{–}150 \text{ mm\%}.$$

If we reduce u, while not changing F (what is obtained by a suitable change of w), then the error representing the deviation of the scale of the gas analyzer from a uniform one is usually decreased. Therefore, it is desirable to choose the smallest one from the possible values of u, which secure the necessary values of F.

One of the reasons which prevents the reduction of u is the increase of inaccuracy caused by the change of the concentration of the component, being determined, in the surrounding air.[8, 10] Let the possible differences of the air intervals be L' = 2 mm, and the possible change of the concentration in the air of the component being determined be c' = 0.01%. If we accept that the permissible value of this error should not exceed the order of magnitude of 10^{-3}, that is, 0.1% (relative), then we have

$$u > \Delta L' c' \left(\frac{\Delta c}{c}\right)^{-1} = 2 \times 0.01 \times 10^3 = 20 \text{ mm\%}.$$

For the optico-acoustical gas analyzers with a gas compensation,[8, 10, 14] developed by the SKB of analytical instrument manufacture, it is accepted that 20 mm% $\leqslant$ u $\leqslant$ 100 mm%.

REFERENCES

1. V. M. Chulanovskii. "Vvedenie v molekulyarnyi spektral'nyi analiz." (Introduction to the Molecular Spectral Analysis), GTTI, Moscow, Leningrad, 1951.
2. M. L. Veingerov. Doklady Akad. Nauk SSSR 19, 687 (1938); Dokt. Diss., State Optical Institute, 1940; Zav. Lab. No. 4, 426 (1947).
3. K. F. Luft. Rev. optique 33, 501 (1954).
4. N. N. Shumilovski and A. A. Sokolov. Avtomatik. i Telemekh. 14, 328 (1953).
5. N. A. Slovokhotova. Zav. Lab. No. 7, 835 (1954).
6. V. A. Pavlenko. Sovremennye gazoanalizatory (The Modern Gas Analyzers) Sb. "Lonitopribor." Novye teploenergeticheskie proizvodstviennye pribory regulatory. (The New Thermo-Power Industrial Instruments and Regulators), Mashgiz, 1953; Zav. Lab. No. 7, 868 (1954).
7. A. O. Sall'. Zhur. Tekh. Fiz. 26, 157 (1956).
8. A. O. Sall'. Priborostroienie No. 6, 14 (1956).
9. A. O. Sall'. Opt. i Spektr. 5, 316 (1958); Avtorsk. svid. (Author's Certificante) No. 109939.
10. A. O. Sall'. Zhur. Tekh. Fiz. 29, 330 (1959).
11. A. O. Sall' and S. B. Stanevich. Opt. i Spektr. 7, 256 (1959).
12. A. O. Sall'. Opt. i Spektr. 7, 576 (1959).
13. W. M. Elsasser. "Heat Transfer by Infrared Radiation in the Atmosphere." New York, 1942; K. Ya. Kondrat'ev. "Perenos dlinnovolnovogo izlucheniya v atmosfere." (The Transfer of Longwave Radiation in the Atmosphere), GTTI, Moscow-Leningrad, 1950.
14. A. O. Sall'. Opt. i Spektr. 7, 432 (1959).
15. A. O. Sall'. Priborostroienie No. 9, 12, (1956).

DISTRIBUTION OF THE SPIN DENSITY IN THE DIBENZENECHROMIUM CATION

S. I. Vetchinkin, S. P. Solodovnikov, and V. M. Chibrikin

Received 1 June 1959

Dibenzenechromium (DBCr) is one of a recently discovered class of compounds which have been called "Sandwich-type compounds." The outstanding characteristic of compounds of this typs is that the metal atom is bonded not with a separate carbon atom but simultaneously with the entire π-system of the aromatic hydrocarbon.[1,2]

For the investigation of the DBCr cation we used the method of electron paramagnetic resonance by means of which it was possible to obtain information on the distribution of the spin density in the molecule. Papers 3-6 report the discovery of the electron paramagnetic resonance spectrum of the DBCr cation and its substitutions both in polycrystalline form and in solution. In these same works it was found that the spectrum of dilute solutions of the DBCr cation and its substitutions has hyperfine structure.

This paper is concerned with the investigation of the spin density distribution in the dibenzenechromium cation. Conclusions about the spin density distribution were drawn on the basis of analysis of the hyperfine structure of electron paramagnetic resonance spectra taken in highly dilute solutions.

EXPERIMENTAL RESULTS

To determine the spin density distribution, solutions of the DBCr cation were investigated and also solutions of DBCr cations with isopropyl and cyclohexyl substitutions in both benzene rings. Figure 1 shows the DBCr cation spectrum taken in an acetone solution at a temperature of −70°C. The hyperfine structure observed depends on the interaction of the unpaired electron with the proton magnetic moment. From the relationship of the intensity of the hyperfine structure components and from the constancy of the hyperfine splitting (3.6 ± 0.5 oersteds) it follows that the unpaired electron interacts with protons of both benzene rings, indicating that all twelve protons are equivalent.

The effect of introducing substitutions into a DBCr benzene ring has also been investigated.[7] It was found that the introduction of hydrocarbon substitutions does not change the magnitude of the hyperfine splitting. At the same time it was established that the number of components of hyperfine structure in the spectra of DBCr substitutions corresponds to the number of remaining protons in both benzene rings. Upon more detailed investigation we found that in the spectrum of the dicumenechromium cation each component of the principal proton hyperfine structure additionally splits into a triplet with a distance between the triplet components approximately 1.0 oersted in magnitude. The additional triplet splitting leads us to ascribe the splitting to both α-protons of the isopropyl substitutions. Figure 2 shows the spectrum of the dicumenechromium cation taken in an acetone solution at a temperature of −90°C. A similar spectrum taken under the same conditions was obtained for the DBCr cation having a cyclohexyl substitution in both rings.

It has been reported in another work[8] that upon investigation of a DBCr cation solution additional hyperfine

Fig. 1 Fig. 2

Fig. 1. Spectrum of an acetone solution of the dibenzenechromium cation at −70°C.
Fig. 2. Spectrum of an acetone solution of the dicumenechromium cation at −90°C.

splitting was discovered and was ascribed to the interaction of the unpaired electron with the magnetic moment of the Cr^{53} isotope, a naturally occurring isotope. Figure 3 shows a spectrum of the DBCr cation in which, at the edge of the base line, is seen the extremes of the hyperfine structure components which depend on the presence of the Cr^{53} isotope (I = 3/2). The middle components are not seen against the background of the base signal. The magnitude of the hyperfine splitting between components of the chromium hyperfine structure in the DBCr cation is 19.0 oersteds.

Fig. 3. Spectrum of the dibenzenechromium cation with hyperfine structure resulting from the interaction of an unpaired electron with the magnetic moment of the Cr^{53} isotope.

All the spectra displayed were taken on the electron paramagnetic resonance spectrometer described in reference 9.

SPIN DENSITY DISTRIBUTION IN THE DIBENZENECHROMIUM CATION

Investigation of semiquinone substitutions[10] has shown that if in the π-system of an aromatic compound the spin density is not zero then the spectrum of such a compound shows additional hyperfine structure components resulting from the splitting due to the α-protons of the aliphatic substitution. Furthermore it is found that the additional hyperfine splitting should be of the same order of magnitude as that due to the protons of an aromatic ring.

Our discovery of additional proton hyperfine splitting in the spectrum of dicumenechromium (cf. Fig. 2) allows

us to draw a conclusion about the existence of spin density in the system of the benzene rings of the DBCr cation. McConnell and Chestnut[11] have proposed a mechanism of indirect interaction which explains the hyperfine splitting due to a proton of a CH fragment of an aromatic ring.

These authors have shown that the magnitude of the proton hyperfine splitting is proportional to the spin density on the p_z orbital of the adjacent carbon atom. It was also shown that the constant of proportionality Q is, to a first approximation, constant for all aromatic radicals and ion radicals.

If it is assumed that Q also remains constant for the case of metal-aromatic compounds then from the observed values of the proton hyperfine splitting (3.6 oersteds) it follows that the spin density on the p_z orbital of each carbon atom equals 0.16. Having concluded that the protons are equivalent it is possible to conclude further that the spin density at each carbon atom is the same. Thus the spin density in the π-system of both benzene rings equals 1.92. In order that the spin density of the DBCr cation, summed over the entire molecule, be normalized to unity it is necessary to assume that the spin density on the atomic orbitals of the chromium be opposite in sign to that on the benzene rings and equal to 0.92. The necessity of normalizing the spin density to unity stems from the fact that the DBCr cation has one unpaired electron.[3]

In support of the supposed spin density distribution we note the agreement of the magnitude of the proton hyperfine splitting in the DBCr cation and in the negative benzene ion.[12] In the DBCr cation the proton hyperfine splitting equals 3.6 oersteds which gives a spin density in the π-system of each benzene ring equal to 0.96; in the negative benzene ion the spin density in the π-system of the ring equals 1.00 while the proton hyperfine splitting is 3.75 oersteds. It has been found[13] in inorganic compounds of chromium (Cr_2O_3) that the splitting between hyperfine structure components of the chromium atom is 18.4 oersteds. Moreover the spin density on the atomic orbital of chromium is 1.00. If it is assumed that there are approximately the same small amounts of the S state of chromium in the DBCr cation and in the Cr_2O_3, then the agreement of the magnitudes of the hyperfine splitting due to the chromium atoms in these compounds may also be cited as experimental support for the supposed spin density distribution in the DBCr cation.

In papers 3 and 7 it was assumed that the proton hyperfine splitting can be explained by direct interaction of the unpaired electron located on the chromium atomic orbital, for example on the d_{z^2} orbital,[14] with the protons of the C—H bonds of benzene. To evaluate the possibility of such an interaction we calculated the upper limit of the magnitude of the hyperfine splitting in the dicumene-chromium cation. It was assumed that the interaction mechanism between the unpaired electron orbitals and the C—H bonds of the benzene ring was analogous to the mechanism of configurational interaction developed by McConnell[11] for C—H fragments. As distinct from McConnell's calculation we were concerned with the interaction of the unpaired electron located on the d_{z^2} chromium orbital and not on the p_z orbital of carbon. All remaining parameters were taken from McConnell.[11] On the basis of these assumptions the calculation of the upper limit of proton hyperfine splitting in dicumene-chromium gives the following values: (a) for protons of the benzene rings $\Delta H_{Cr-H} \leq 22$-10 oersteds where the experimentally determined value is 3.6 oersteds; (b) for an α proton of an isopropyl substitution $\Delta H_{Cr-H} \leq 0.04$-0.11 oersteds as compared with an experimental value of 1.0 oersted.

The lack of agreement between the calculated and experimental values of the hyperfine splitting due to an α-proton substitution confirms that the mechanism of direct interaction between an electron located on the d_{z^2} orbital of chromium and the protons of the C—H bonds of benzene cannot explain the observed proton splitting in the DBCr cation.

In conclusion the authors express their deep appreciation to Yu. A. Sorokin and G. A. Domrachev for the synthesis of the compounds used in these experiments.

REFERENCES

1. A. N. Nesmeyanov and E. G. Perevalova. Uspekhi Khim. **27**, 1 (1958).
2. M. E. Dyatkina. Uspekhi Khim. **27**, 57 (1958).
3. Iu. D. Tsvetkov, V. V. Voevodskii, et al. Doklady Akad. Nauk SSSR, **115**, 118 (1957).
4. G. K. Razuvaev, Iu. A. Sorokin, et al. Doklady Akad. Nauk SSSR, **113**, 1293 (1957).
5. R. D. Feltham, P. Sogo, and M. Calvin. J. Chem. Phys. **26**, 1354 (1957).
6. B. Elschner and S. Herrog. Z. Naturforsch. **12a**, 860 (1957).
7. V. V. Voevodskii, Iu. N. Molin, and V. M. Chibrikin. Opt. i Spektr. **5**, 90 (1958).
8. N. N. Bubnov and V. M. Chibrikin. Zhur. Fiz. Khim. **33**, 1891 (1959).
9. N. N. Bubnov and A. G. Semenov. Prib. i Tekh. Eksp. **1**, 92 (1959).
10. B. Venkataraman and G. Fraenkel. J. Chem. Phys. **23**, 588 (1953).
11. McConnell and D. B. Chestnut. J. Chem. Phys. **28**, 107 (1958).
12. S. I. Weismann, T. R. Tuttle, and E. de Boer. J. Phys. Chem. **61**, 28 (1957).
13. A. A. Manenkov and A. M. Prokhorov. Zhur. Eksptl. i Teoret. Fiz. **28**, 755 (1955).
14. M. E. Dyatkina and E. M. Shustrovich. Zhur. Neorganicheskoi Khim. **4**, 402, 553 (1959).
15. E. O. Fischer and W. Hafner. Z. Naturforsch. **10b**, 665 (1955).

TEMPERATURE QUENCHING IN CERTAIN ORGANIC SCINTILLATORS

A. F. Kulakova and S. M. Rozman

Received 3 June 1959

The luminescence yield of organic substances in the condensed phase depends on the specific energy losses of the exciting charged particles: the yield decreases with increasing specific loss.[1,2] For example, the average luminescence yield of crystalline anthracene for 5 Mev protons is about 42% of the yield for high velocity electrons (≳ 500 kev); for 5 Mev α-particles the yield is about 10%. This so-called α, β-ratio is approximately 0.1 for all other organic crystals, plastic and liquid scintillators.[3,4] While the differences in yield are large, as between excitation by α-particles and high speed electrons, there is little or no difference between the duration of luminescence in the two cases (τ_α and τ_β, respectively).[3]

According to Galanin's theory[5] all these facts are explained by the quenching of luminescence due to localized heating along the path of the ionizing particle. In this case it is assumed that the luminescence is completely quenched in the inner part of the track and that the luminescence yield is dependent on the number of activations in the outer part of the track. Since the duration of the "thermal peak" is relatively short (≈10^{-11} sec), complete quenching requires that the quantum yield of fluorescence η be of the substance in the heated condition be equal to 0.001 of the quantum yield at the "regular" temperature η_0. The actual effective quantum yield in the region of the "thermal peak" is

$$\eta_{eff} = \eta_i + (\eta_0 - \eta) \exp\left(-\frac{t_1}{\tau}\right),$$

where t_1 is the duration of the "peak," and τ is the average duration of the excited state of the molecules at the temperature of the "peak." From the condition for complete quenching ($\eta_{eff} < 0.01\eta_0$) and the well-known relationship between the duration τ and the quantum yield η we obtain

$$\frac{\eta}{\eta_0} < \frac{t_1}{4.6\tau_0},$$

where τ_0 is the average lifetime of the excited state at "regular" temperature. Since $\tau_0 \gtrsim 2 \times 10^{-9}$ sec and $\tau_1 \lesssim 2 \times 10^{-11}$ sec,[5] it follows that

$$\eta < 2 \times 10^{-3} \eta_0.$$

Furthermore, the theory in reference 5 suggests that in the inner part of the track temperature quenching is practically absent, i.e., the decrease in yield is abrupt (within a narrow range of temperature change), which satisfies the $\tau_\alpha \approx \tau$ condition.

We have undertaken an investigation of the relationship between the yield of some organic scintillators and temperature in order to check the basic premises of the Galanin's theory[5] regarding the nature of this relationship. According to the data of Herforth and Kallmann[6] an abrupt decrease of the yield ensues when the organic crystals are melted (excitation by γ-rays). Naphthalene, diphenyl, and phenanthrene were investigated. In the latter two, the intensity of luminescence decreased by a factor of only 10-20 when they were molten. We measured the temperature-yield relationship in dibenzyl and stilbene when they were excited by β-particles (Ce^{144}-Pr^{144}) and α-particles (Po^{210}) (Fig. 1). The results obtained (Fig. 2) show that an abrupt decrease in yield is observed when both crystals are melted. In the case of excitation of stilbene by α-particles, the yield decreases by a factor of approximately 10^2. A slight increase is observed under β-excitation; this is apparently associated with Cerenkov radiation. The increase observed under α excitation could be due to luminescence of the air above the melt (the vapor pressure above the melt is not high). In order to exclude this possibility, an opaque aluminum foil was placed directly on the melt. As a control, the apparent decrease of luminescence caused by a BS-8 filter was measured.

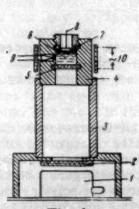

Fig. 1

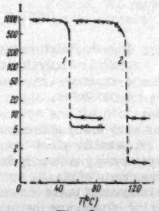

Fig. 2

Fig. 1. Cross section of the apparatus. 1, FEU-29 in a steel jacket. 2, Filter: BS-8 or quartz. 3, Textolyte tube. 4, Body of the container. 5, Fused quartz. 6, The substance under investigation. 7, Aluminum foil, about 4μ. 8, Source of α- or β-radiation. 9, Thermocouple. 10, Heating element.

Fig. 2. Relationship between the luminescence yield I of dibenzyl (1) and stilbene (2) crystals and temperature T. O-excitation by α-particles, x-excitation by β-particles.

The relationship between the luminescence yield of stilbene and the temperature satisfies the requirements of Galanin's theory[5]: an increase of temperature by $\Delta T \approx 100°$ above room temperature may lead to practically complete quenching of luminescence in $t \approx 2 \times 10^{-11}$ sec.*

*A thermal peak of duration $\approx 2 \times 10^{-11}$ sec corresponds to an instantaneous liberation of approximately 500 Mev per cm of track. In reference 5 a momentary source of heat is considered.

The second requirement of this theory is also satisfied. The agreement is not as good for dibenzyl. If the results reported in reference 6 are considered, one could conclude that the degree of quenching due to melting is dependent on individual properties of the substance. This is also verified by the fact that many organic substances which possess low melting points luminesce strongly in the liquid state (toluene, xylene, styrene, benzene, and others). According to the data of Belikova and Galanin[7] the quantum yield of toluene at room temperature is 0.01, and that of o-xylene is 0.03. In addition to this, the fact that liquid scintillators of high luminescence yield do exist does not agree with the assumption that the solvents pos-

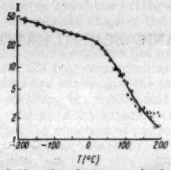

Fig. 3. Relationship between the luminescence yield I of polyvinyltoluene and temperature T. o-excitation by α-particles, x-excitation by β-particles.

sess very low quantum yields for fluorescence ($<10^{-3}$

A peculiar yield-temperature relationship exists in polystyrene and in polyvinyltoluene, which are basic components of plastic scintillators. Figure 3 contains the results of these measurements for polyvinyltoluene. Worthy of note are the relatively small decrease of yield on melting, and the absence of any abrupt change, which contradicts both requirements of Galanin's theory.[3]

We therefore conclude that temperature quenching due to localized heating in the track of an ionizing particle cannot be the principal cause of the dependence of the radioluminescence yield on the density of excitation or on the specific loss of energy of exciting particles.

REFERENCES

1. J. B. Birks. "Scintillation Counters." Pergamon Press, 1955.
2. F. D. Brooks. "Organic Scintillators," Progr. in Nuclear Phys. 5, (1956).
3. H. Kallmann and G. J. Bruckner. Phys. Rev. 108, 1122 (1957).
4. M. D. Galanin and Z. A. Chizhikova. Opt. i Spektr. 4, 196 (1958).
5. M. D. Galanin. Opt. i Spektr. 4, 758 (1958).
6. L. Herforth and H. Kallmann. Ann. Physik 4, 231 (1949).
7. T. P. Belikova and M. D. Galanin. Opt. i Spektr. 1, 168 (1956).

EXCITATION OF RECOMBINATION LUMINESCENCE IN THE FUNDAMENTAL ABSORPTION BANDS OF CERTAIN HALIDES

I. V. Yaek and G. G. Liid'ya

Received 10 June 1959

It is known[1-3] that the luminescence of activator ions is excited in the fundamental absorption bands of the alkali halide phosphors (exciton bands, "band-band" transitions). The transfer of energy from the host substance to the activator can occur here either by means of a moving excitation without current, i.e., by means of excitons, or as a result of electron-hole processes. In the latter case the following alternatives are possible: (1) electron recombination luminescence, in which free electrons recombine with holes trapped at (or near) luminescence centers; and (2) hole recombination luminescence, in which holes recombine with electrons trapped at (or near) luminescence centers. A special study is required to ascertain the relative contributions of the three above-mentioned processes to the excitation of luminescence in alkali halide phosphors.

Until now, the excitation spectra of steady state luminescence were usually measured when a study was made of the mechanism of transfer of energy from the host substance to the luminescence centers. As in references 6-8, we studied not only these spectral characteristics but the excitation spectra of recombination luminescence (phosphorescence) as well. The range of investigation was also extended to cover the fundamental absorption bands corresponding to exciton formation and to "band-band" transitions.

We chose the iodides (KI:Tl, KI:In, CsI:Tl, RbI:Tl, CdI_2:Pb) as the substances for our study, whose long wavelength fundamental absorption bands are in a region accessible to us, $\lambda > 185$ mμ.

The excitation spectra of phosphorescence described here are determined by the relation $I_{st}(\nu) = I^*_{st}/B(\nu)$ where I^*_{st} is the intensity of afterglow at the time t after the end of excitation, and $B(\nu)$ is the intensity of the exciting light. This formula gives the spectral distribution of the phosphorescence yield under conditions of total absorption (neglecting reflection losses).

The excitation of phosphors in the 186-225 mμ region was carried out by a condensed spark with Zn, Cu, Al electrodes through a focal monochromator. In the region $\lambda > 210$ mμ excitation was also performed with a hydrogen lamp through the monochromator of the SF-4 spectrophotometer. The quantity B was determined by means of an anthracene screen.

Phosphorescence was recorded by a photoelectric photometer consisting of an FEU-19 photomultiplier, a dc amplifier, and a recording potentiometer EPP-09.

A special check showed that under the conditions of the experiment, the intensity of luminescence in the spectral range investigated is proportional to the intensity of the exciting light.

Figure (a) gives the data for KI:Tl (6×10^{-2}mol % in the crystal), and Fig. (b) for RbI:Tl. Curve 1 represents the matrix absorption spectrum, curve 2 the phosphorescence excitation spectrum, and curve 3 steady state luminescence in each case. The structure of the excitation spectra of the other substances studied is essentially the same. Three regions may be distinguished in the absorption spectrum: the activator absorption ($^1S_0 - {}^3P_1$ and $^1S_0 - {}^1P_1$ transitions in Tl^+ ions), the exciton absorption (ex), and the absorption corresponding to the "band-band" transitions (e + p). (Cf., for example, reference 9.) The steady state luminescence and the phosphorescence of the phosphors which we investigated is excited in all these regions. In addition, in the phosphorescence excitation spectrum of KI:Tl a band appears at 225 mμ which corresponds either to the $6^1S_0 - 7^1S_0$ transition in Tl^+ ions or to the excitation of iodide ions near Tl^+. (In TbI:Tl this band was resolved only at a low temperature.)

The existence of the following regularities can be established in all the phosphorescence excitation spec-

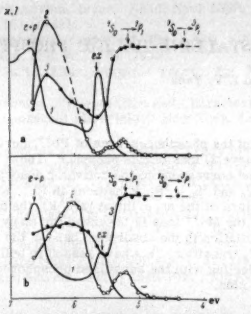

tra of the alkali halide phosphors which we studied:

1. The ratio $I_{ph}(e + p)/I_{ph}(^1S_0 \rightarrow {}^1P_1)$ depends strongly on activator concentration. It is greater than 1 for high concentrations and less than 1 for low concentrations. As shown by an estimate, the magnitude of the yield for "band-band" excitation cannot be explained by the superposition of an activator absorption band over the fundamental absorption region.

2. $I_{ph}(e + p) > I_{ph}(ex)$. It follows from this inequality that the electron-hole excitation mechanism is not the same as the exciton mechanism. (In principle, excitons can arise when free electrons and holes recombine.) The electron-hole mechanism of transfer of energy from the host to the activator is quite efficient for afterglow.

3. $I_{ph}(ex) < I_{ph}(^1S_0 \rightarrow {}^1P_1)$. Hence we cannot explain the excitation of afterglow in the activator by a "splitting off" of the exciton as was assumed in reference 10.

4. $I_{ph}(^1S_0 \rightarrow {}^1P_1) \gg I_{ph}(^1S_0 \rightarrow {}^3P_1)$. This rule agrees well with the assumption that the excitation of afterglow in the activator absorption bands is caused by a photothermal ionization of luminescence centers.

In all the phosphors studied, the recombination luminescence in the exciton bands is excited with a yield which differs from zero but is smaller than in the neighboring bands.

A sharp increase in the phosphorescence yield is observed to the left of the exciton band (about 5.9 ev for KI:Tl, KI:In, and RbI:Tl, and about 6.3 ev for CsI:Tl). In references 9 and 11 it is assumed that the "band-band" transitions are realized in this region. It is natural to consider our results as confirming this point of view. In experiments on the study of the external photoeffect,[8] of which our experiments are the counterpart for luminescence, the sharp increase in the yield of the external photoeffect begins at a shorter wavelength region (close to 7.3 ev for KI and RbI, and close to 6.4 ev for CsI). From the difference between these quantities we can estimate the magnitude of the electron affinity of the corresponding crystals, which is found to agree with earlier work.[9]

To show whether electron recombination luminescence occurs when excitation occurs in the matrix, we measured the stimulation spectra of the optical flash (SSOF) after KI:Tl was excited in the region corresponding to the "band-band" transitions and also in the exciton and activator absorption bands. For all these types of excitation, SSOF for KI:Tl with a not too high thallium concentration coincides with the F-absorption band. At higher thallium concentration shorter wavelength stimulation bands appear in addition to the F-band. We may assume that they correspond to the activator capture centers for electrons.

The spectrum of the formation of F-centers in KI:Tl (which was determined by comparing the intensities of the flash stimulated in the F-band with phosphorescence) coincides in the main with the phosphorescence excitation spectrum. The decay of the afterglow and the decrease in the flash when periodically stimulated in the F-band, run a parallel course. The electrons which are thermally liberated from the F-levels must therefore play an essential part in the afterglow. Since only electrons are liberated during stimulation in the F-band, the experiments described show that it is electron recombination luminescence which is excited in the region of the absorption bands of both the activator and the host substance. We certainly do not say that hole recombination luminescence is impossible. The experiments described in references 3 and 7 testify to the converse. The existence of activator capture centers for electrons, in principle, creates conditions for the realization of hole recombination luminescence.

This work was carried out under the direction of Ch. B. Lushchik, to whom the authors wish to express their gratitude.

REFERENCES

1. A. N. Terrenin and F. D. Klement. Uchenye Zapiski Leningrad Gosudarst. Univ. Ser. Fiz. Nauk 1, 73 (1935).
2. Z. L. Morgenshtern. Doklady Akad. Nauk SSSR 105, 2 (1955).
3. Ch. B. Lushchik and G. G. Liid'ya. Doklad na VII Soveshch. po liuminestsentsii v Moskve (Report at the 7th Conf. on Luminescence in Moscow, 1958).
4. G. G. Liid'ya. Trudy Inst. Fiz. i Astron. Akad. Nauk Eston. SSR, No. 10, 196 (1959).
5. K. Teegarden. Phys. Rev. 105, 1222 (1957).
6. W. Bunger. Z. Physik, 66, 311 (1930).
7. Ch. B. Lushchik, Kh. F. Kyaembre, and I. V. Yaek. Doklad na VII Soveshch. po liuminestsentsii v Moskve (Report at the 7th Conf. on Luminescence in Moscow, 1958).
8. I. V. Yaek. Trudy Inst. Fiz. i Astron. Akad. Nauk Eston. SSR No. 10, 166 (1959).
9. E. A. Taft and H. R. Philipp. J. Phys. Chem. Solids 3, 1 (1957).
10. Ch. B. Lushchik and V. I. Volin. Trudy Inst. Fiz. i Astron. Akad. Nauk Eston. SSR No. 7, 311 (1958).
11. N. F. Mott and R. W. Gurney. "Electronic Processes in Ionic Crystals." Oxford University Press, and IL, Moscow, 1950.

THE SENSITIZED PHOSPHORESCENCE OF CRYSTALLINE HALIDE PHOSPHORS

V. Ya. Kark, Ch. B. Lushchik, and I. V. Yaek

Received 10 June 1959

It has been proved that the phosphorescence of activated alkali halide crystals is not metastable, but recombinatory.[1-3] However, the detailed mechanism of the recombination luminescence has not been ascertained. The majority of papers assume that the phosphorescence of alkali halide crystals involves the ionization of luminescence centers at activation, and the subsequent recombination of electrons with the ionized centers.[1-4] In our laboratory we have observed recombination luminescence in alkali halide crystals activated by divalent Mn^{++} and Pb^{++} ions, whose further ionization is highly improbable. This led to the supposition that phosphorescence may arise without the luminescence centers being ionized.*

*Analogous considerations with reference to sulfide phosphors were stated earlier by Pringsheim.[5]

The following hypothesis was formulated: A peculiar sensitized phosphorescence may exist in which there is a radiationless transfer of the energy liberated at the recombination of electrons and holes to unionized luminescence centers.[6-8] Such a mechanism makes possible the hole recombination luminescence of centers where radiation arises as a result of the recombination of holes with trapped electrons. Hole recombination luminescence of alkali halide phosphors activated by Tl^+, In^+, and Ga^+ ions has actually been observed.[9-10] However, since it can arise at the recombination of holes with electrons trapped at luminescence centers, its existence cannot as yet be considered a proof of a sensitized mechanism of phosphorescence.

The search for a sensitized phosphorescence of crystals* was continued. We studied the phosphorescence excitation spectra of the multiactivated phosphor KBr:Tl:In. (The method of measurement was described in reference 13.) It was found that the recombination luminescence of Tl^+ ions is excited when absorption occurs in the thallium absorption bands, while indium phosphorescence is excited when absorption occurs in the indium absorption bands.[10,13] It is as if the phosphor remembered the nature of the excitation. Sensitized phosphorescence is not found in KBr:Tl:In. Following the suggestion of one of us, Shvarts and Sirnitis carried out a detailed investigation of the sensitized fluorescence of a series of multiactivated phosphors.[14] They succeeded in observing the transfer of energy from Pb^{++} to Mn^{++} ions in NaCl:Pb:Mn and KCl:Pb:Mn phosphors in agreement with the data of U.S. investigators. (Cf., for example, reference 15.) They also found a transfer of energy from the Tl^+ and In^+ to the Mn^{++} ions in the NaCl:Tl:Mn and NaCl:In:Mn phosphors. Malysheva observed a similar effect for the $CdBr_2$:Pb:Mn and CdI_2:Pb:Mn systems.[16]

*Let us note that the mechanism of this phenomenon differs essentially from the sensitized phosphorescence of organic molecules[11] and the sensitized luminescence of ZnS phosphors caused by hole migration (cf., for example, reference 12).

We made an attempt to find the phenomenon of sensitized phosphorescence in systems in which sensitized fluorescence is observed. We selected the $CdBr_2$:Pb:Mn phosphor, which has a fairly intense recombination luminescence.[9] The Figure shows the excitation spectra of the phosphorescence of Pb^{++} (curve 1) and Mn^{++} (curve 2) ions of this phosphor. These spectra coincide and correspond to the activator absorption of lead ($^1S_0 \rightarrow {}^1P_1$ and $^1S_0 \rightarrow {}^3P_1$ transitions in Pb^{++} ions). At the temperature of the experiment (293° K), the phosphorescence of the Mn^{++} ions is observed for many seconds after excitation in the absorption band of the Pb^{++} ions ($^1S_0 \rightarrow {}^3P_1$ transition). We have reason to believe that we are dealing with the sensitized phosphorescence of $CdBr_2$:Pb:Mn.

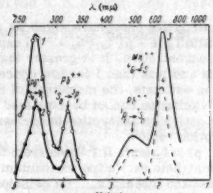

The phosphorescence excitation spectra (curves 1, 2) and the emission spectra (curves 3, 4) of the phosphor and $CdBr_2$:Pb:Mn.

The Figure shows also the emission spectrum of the $CdBr_2$:Pb:Mn phosphor (curve 3) for excitation in the 3.9 ev absorption band, which corresponds to the electron transition $^1S_0 \rightarrow {}^3P_1$ in the Pb^{++} ions. Two bands appear in emission. The short wavelength one is also observed in the $CdBr_2$:Pb phosphor and corresponds to the $^3P_1 \rightarrow {}^1S_0$ transition in the Pb^{++} ions. The long wavelength one arises after manganese is introduced into $CdBr_2$:Pb and corresponds to $^4G \rightarrow {}^6S$ transitions in the Mn^{++} ions. The Figure also shows (curve 4) qualitative data concerning the phosphorescence spectrum of $CdBr_2$:Pb:Mn. These data were obtained after excitation in the 3.9 ev band by measuring the intensity of phosphorescence through a large number of optical filters. The closeness of the emission spectrum obtained at the instant of excitation to that obtained during phosphorescence is natural whenever the resonance transfer of energy to the Mn^{++} ions is realized after the creation of excited Pb^{++} ions as a consequence of a series of intermediate recombinatory processes.

The presence of sensitized phosphorescence can appreciably influence the kinetics of relaxation processes in crystals. Luminescence of the same spectral composition can arise when electrons recombine with trapped holes or holes recombine with trapped electrons in several different recombination centers. This effect was taken into account quantitatively in references 8 and 17.

REFERENCES

1. V. V. Antonov Romanovskii. Trudy Fiz. Inst. Akad. Nauk 2, 130 (1942).

2. I. A. Parfianovich. Izvest. Akad. Nauk SSSR, Ser. Fiz. 13, 161 (1949).
3. Ch. B. Lushchik. Trudy Inst. Fiz. i Astron Akad. Nauk Eston. SSR No. 1, 57 (1955).
4. I. P. Shchukin. Zhur. Eksptl. i Teoret. Fiz. 29, 834 (1955).
5. P. Pringsheim. "Preparation and Characteristics of Solid Luminescent Materials." New York, London, 1948.
6. Ch. B. Lushchik and F. N. Zaitov. Trudy Inst. Fiz. i Astron. Akad. Nauk Eston. SSR No. 4, 53 (1956).
7. Ch. B. Lushchik, F. N. Zaitov, V. Ya. Kark, L. A. Teiss, and I. V. Yaek. Mater. V Soveshch. po liuminests. (Conference on Luminescence), Tartu, 1956; Isvest. Akad. Nauk SSSR, Ser, Fiz. 21, 693 (1957).
8. Ch. B. Lushchik and V. I. Volin. Trudy Inst. Fiz. i Astron. Akad Nauk Eston. SSR No. 7, 311 (1958).
9. P. A. Khellenurme. Trudy Inst. Fiz. i Astron. Akad. Nauk Eston. SSR No. 7, 340 (1958).
10. Ch. B. Lushchik, Kh. Kyaembre, and I. V. Yaek. Mater. VII Soveshch. po liuminests. (Conference on Luminescence), Moscow, 1958.
11. A. N. Terenin and V. L. Ermolaev. Doklady Akad. Nauk SSSR 85, 547 (1952).
12. M. V. Fok. Opt. i Spektr. 2, 475 (1957).
13. I. V. Yaek. Trudy Inst. Fiz. i Astron. Akad. Nauk Eston. SSR No. 10, 166 (1959).
14. K. K. Shvarts and U. A. Zirnitis. Trudy Inst. Fiz. i Astron. Akad. Nauk Eston. SSR No. 11, 3 (1959).
15. J. Schulman, R. Ginther, and C. Klick, J. Electrochem. Soc. 97, 123 (1950).
16. A. F. Malysheva. Mater. VI Sovesch. po liumnests. (Conference on Luminescence), Leningrad, 1958.
17. K. S. Rebane. Trudy Inst. Fiz. i Astron. Akad. Nauk Eston. SSR No. 8, 105 (1959).

THE RELATION BETWEEN PHOTOELECTRIC CHARACTERISTICS OF AN ELECTROPHOTOGRAPHIC LAYER AND THE CHARACTERISTICS OF LONGITUDINAL PHOTOCONDUCTIVITY

P. M. Podvigalkin

Received 8 April 1959

An electrophotographic layer is a photosensitive semiconductor layer of high resistivity on a conducting substrate, with an electric charge deposited on its surface. This charge forms an electric field inside and outside the layer. Such a system is electrically equivalent to an electric double layer: One electric layer is formed by the surface charge, the other by the screening charge induced in the volume of the semiconductor and in the substrate, the latter charge being equal in magnitude (but opposite in sign) to the surface charge. The potential of the electrophotographic layer is a parameter which can be measured directly, and is important from the practical point of view. The potential V of an electric double layer depends on the charge density q of the electric layer according to the well-known relation

$$V = \frac{4\pi q d_{eff.}}{\varepsilon}, \qquad (1)$$

where ε is the dielectric constant of the medium and $d_{eff.}$ the effective thickness of the layer, which depends on the charge distribution in each of the electric layers in a direction perpendicular to the layer.

When the electrophotographic layer is illuminated, its potential falls more rapidly than in the dark. This permits one to obtain a potential "map" which depicts the distribution of illumination on the surface, i.e., to obtain a latent electrophotographic image. As shown in Eq. (1), a variation in potential may be due to a variation in q, $d_{eff.}$, or ε.

Experimental data show that photoconductivity is the basic mechanism which causes a variation in potential under illumination in selenium and zinc oxide, which are at present the materials most commonly used for electrophotographic layers. Hence, to find the photoelectric characteristics of the electrophotographic layer, we must solve the problem of the conduction of the photocurrent in the semiconductor layer in a non-steady state, using the methods of electrodynamics. At the same time we must take into account the following: On the one hand, the external voltage is not steady (electrical variation), since the potential of the layer decreases during exposure; on the other hand, the luminous excitation is not steady (light flux variation). The latter is due to the fact that the exposure of the electrophotographic layer is performed by a single light pulse, which is more or less rectangular.

The general scheme for solving such problems has been well worked out (cf., for example, reference 1). It consists in the simultaneous solution of Poisson's equation and the kinetic equations, taking account of the variation in charge carrier concentration in levels and bands produced both by transition to other levels (thermal and light "ejection," recombination and trapping processes) and at the expense of diffusion processes and the drift of carriers in the external electric field. In addition, the following data must be known: the boundary and initial conditions, the energy diagram of the semiconductor, the equilibrium concentrations, the mobilities of the charge carriers, and the magnitude of the applied voltage. This problem cannot be solved for actual electrophotographic layers because of the complexity and lack of knowledge of conditions arising in these layers—the peculiar nature of the "upper" electrical contact, the necessity (resulting from the presence of strong electric fields in semiconductors) of taking into account thermoelectronic and collision ionization effects, etc.

In the first stage of a theoretical investigation of the process of formation of a latent electrophotographic image, it is expedient to establish the relation between the photoelectric characteristics of an electrophotographic layer in the non-steady state and its characteristics under "electrically" steady conditions. Under these conditions, i.e., for constant external voltage (static mode of operation) the electrophotographic layer is merely a "longitudinal" photoresistor.[2] If we find such a relation we shall be able to use the characteristics of the semiconductor material measured under simpler conditions than those of the electrophotographic process

to predict the properties of the electrophotographic layer prepared from this material. It will also indicate means for improving the photographic characteristics of the layers.

In the general case, the variation of the potential of an electrophotographic layer under illumination is determined by the equation

$$-\frac{dV}{dt}=J(V,\ E,\ t). \tag{2}$$

where E is the illumination and t the time.

It is not difficult to show that if the potential variation is mainly due to a decrease in the surface charge and the screening charge (their "recombination"), then J(V, E, t) has the meaning of a current density through the layer (per unit capacity) measured under electrically steady conditions. Let us assume that J(V, E, t) can be represented as the sum of the densities of the dark current $J_T(V)$ and the photocurrent $J_\phi(V, E, t)$. Equation (2) can then be written as

$$-\left[\left(\frac{dV}{dt}\right)_T+\left(\frac{dV}{dt}\right)_\phi\right]=J_T(V)+J_\phi(V,\ E,\ t). \tag{3}$$

Since we are interested in the variation of potential under the action of light, we must solve the equation

$$-\left(\frac{dV}{dt}\right)_\phi=J_\phi(V,\ E,\ t). \tag{4}$$

We shall solve Eq. (4) for a special form of the function $J_\phi(V, E, t)$, assuming that the layer is illuminated by a monochromatic light pulse of rectangular shape. Let the photocurrent be a function of a power of V: $J_\phi \sim V^m$ and let the relaxation of the photocurrent be symmetrical and exponential, i.e.,

$$J_\phi(V,\ E,\ t)=\sigma'_{\phi\phi}(E)\left(1-e^{-\frac{t_e}{\tau}}\right)e^{-\frac{t-t_e}{\tau}}V^m, \tag{5}$$

Here $\sigma'_{\phi\phi}=J_\phi^m/V^m$ is the steady state "longitudinal" photoconductivity $\sigma_{\phi\phi}(E)$ of the layer divided by $C_{eff.}=\varepsilon/4\pi d_{eff.}$ and by V^{m-1}; τ is the photocurrent relaxation time (τ may be a function of E but we shall assume it to be independent of V), t_e is the exposure time of the layer.*

*Since we are dealing with "longitudinal" photoresistivity, the assumption that the relaxation of the photocurrent is symmetrical and exponential does not imply that the function $\sigma_{\phi\phi}(E)$ is linear and that τ is independent of E.

In this case the solution of Eq. (4) has the form

$$\ln\frac{V}{V_0}=\frac{1}{1-m}\ln\left\{1-\frac{1-m}{V_0^{1-m}}\sigma'_{\phi\phi}(E)\left[t_e+\tau\left(e^{-\frac{t_e}{\tau}}-1\right)e^{-\frac{t_n-t_e}{\tau}}\right]\right\}, \tag{6}$$

where t_n is the instant the potential of the layer is being measured ($t_n \geq t_e$). Equation (6) may be called the equation of the characteristic curve of the latent image, since it gives a relation between the potential V of the layer, its illumination E, and the exposure t_e.

Equation (6) represents the final result of exposing the electrophotographic layer, taking into account the "after effects" of the light. If the quantities t_e and t_n are given the meaning of running coordinates, the same equation gives the curve for the decrease of the potential under illumination by a rectangular light pulse. Here Eq. (6) is resolved into two equations. The first

$$\ln\frac{V}{V_0}=\frac{1}{1-m}\ln\left\{1-\frac{1-m}{V_0^{1-m}}\sigma'_{\phi\phi}(E)\left[t+\tau\left(e^{-\frac{t}{\tau}}-1\right)\right]\right\} \tag{7}$$

represents the portion of the curve of the decrease in the potential of the layer under illumination for $t \leq t_e$. The second equation corresponds to $t \geq t_e$.

$$\ln\frac{V}{V_0}=\frac{1}{1-m}\ln\left\{1-\frac{1-m}{V_0^{1-m}}\sigma'_{\phi\phi}(E)\left[t_e+\tau\left(e^{-\frac{t_e}{\tau}}-1\right)e^{-\frac{t-t_e}{\tau}}\right]\right\}. \tag{7'}$$

Let us consider the limiting case of Eq. (6) assuming $(t_n - t_e)/\tau \gg 1$. In this case Eq. (6) assumes the simpler form

$$\ln\frac{V}{V_0}=\frac{1}{1-m}\ln\left\{1-\frac{1-m}{V_0^{1-m}}\sigma'_{\phi\phi}(E)\,t_e\right\}. \tag{8}$$

We shall call Eq. (8) the equation of the limiting characteristic curve. The limiting characteristic curve shows the dependence of the potential of the layer on E and the exposure t_e under conditions such that the "after effect" of the light is fully utilized. It is interesting to note that in the case which we are considering (the symmetrical relaxation of the photoconductivity), Eq. (8) does not contain τ, the relaxation time for the photoconductivity.

The Figure shows schematically the curve for the potential decay of the illuminated electrophotographic layer (solid curve) and the limiting characteristic curve (dotted curve) for the cases $t_e < \tau$ and $t_e > \tau$.

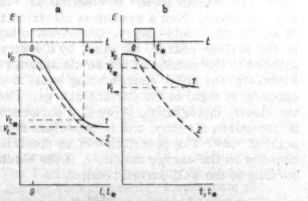

The decay curves of the potential V of the illuminated electrophotographic layer (curves 1) and the limiting characteristic (curves 2) for the case (a) of $t_e > \tau$ and (b) of $t_e < \tau$.

In conclusion, I should like to express my thanks to S. G. Grenishin for his interest and valuable advice.

REFERENCES

1. A. I. Gubanov. "Teoriya vypryamlyaiushchego deistviya poluprovodnikov." (Theory of the Rectifying Action of Semiconductors), Moscow, 1956.
2. V. E. Lashkarev. Zhur. Eksptl. i Teoret. Fiz. 18, 953 (1948).

THE OPTICAL SOCIETY OF AMERICA

Why should you join OSA?

There is no other association of opticists in existence to promote and disseminate knowledge in this field. The Optical Society of America was organized in 1916 "to increase and diffuse the knowledge of optics in all its branches pure and applied, to promote the mutual interests of investigators of optical problems, of designers, manufacturers and users of optical instruments and apparatus of all kinds, and to encourage co-operation among them".

What about the advantages of membership?

You receive three monthly publications:

THE JOURNAL OF THE OPTICAL SOCIETY OF AMERICA: *This is the official publication of OSA*

OPTICS AND SPECTROSCOPY: *an English translation of the leading scientific journal of the USSR Academy of Sciences in this field*

PHYSICS TODAY: *as OSA is a member society of the American Institute of Physics, OSA members receive this publication**

From JOSA and OPTICS AND SPECTROSCOPY you will not only learn what your American colleagues are doing, but also discover what the Russians are working on in your field. Together these two journals publish the work of American and Russian scientists in all branches of optics and spectroscopy, including X-ray, ultraviolet, visible, infrared and microwave, filters, lens design, thin layer optics, geometric optics, electron optics, diffraction gratings, electroluminescence, wave mechanics, thermal radiation backgrounds, detectors, infrared polarizers, and their many applications in science and industry.

You will also receive announcements and programmes of all meetings (OSA holds at least two a year) and, even if you cannot attend many of these, you will know what is going on in your area. And you can submit a paper and have it given by proxy.

Who can join?

OSA invites to membership all who are interested in any branch of optics, either in research, in teaching, in optical applications, in the manufacture and distribution of optical equipment of all kinds, or in physiological and medical optics.

What are the membership dues? $13.00 per annum.

How can you join?

Write Dr. Mary E. Warge, Executive Secretary, Optical Society of America, 1155 16th Street, N. W., Washington 6, D. C., for an application form.

*OSA members may also subscribe to other AIP publications at a reduced rate.

OPTICAL SOCIETY *of* AMERICA

1155 SIXTEENTH STREET, N. W. WASHINGTON 6, D. C.

ANNUAL REVIEWS
RUSSIAN TRANSLATION PROGRAM

Annual Reviews, Inc., is a non-profit corporation engaged in the publication of ten Reviews that cover a number of the sciences from Psychology to Nuclear Science. The reviews, 20 or 25 in number, published in each annual volume, are written by scientists from all over the world. When the scientific literature from the USSR began to enter this country in the postwar years, Annual Reviews attempted to make the contents available to its readers by publishing in several of the Reviews, a special chapter entitled, "The current status of _____ in the USSR." Such articles were written by scientists of native linguistic competence, resident in the western world, who, at the same time, were well recognized by their colleagues for their scientific competence.

Although this effort was pursued for three years, it was finally largely abandoned because of the difficulties that were experienced in attempting to evaluate the present status of, for examples, optics, in one 30-page chapter. Fortunately, by this time, translation programs had begun to develop. These have made it possible for Annual Reviews to subscribe to 31 of the translated periodicals and to make these available to its authors, some 200 in any given year, who are interested in the contents. Thus, papers on optics in Russian are distributed among at least 20 authors, each a specialist in his field, instead of leaving to a single author the very difficult task of reviewing the whole of the Russian literature in optics. The recipients are completely free to review or to discard the material received. In the case of one of its Reviews, Annual Reviews is still using the earlier approach, largely because a substantial portion of the original literature is not encompassed by present translation programs.

INSTRUMENT SOCIETY OF AMERICA
FOREIGN TRANSLATION PROGRAM

The Instrument Society of America was awarded a grant by the National Science Foundation to continue the translation and publication of the 1959 issues of English editions of four leading Russian technical journals:

The Russian original of Measurement Techniques (Izmeritelnaia Tekhnika) was published as a monthly in 1959 by the Committee of Standards, Measures and Measuring Instruments of the Council of Ministers, USSR. There are approximately 100 pages per issue with articles of particular interest to all who are engaged in the study and application of fundamental measurement.

Instruments and Experimental Techniques (Pribory i Tekhnika Eksperimenta) is published bi-monthly by the Academy of Sciences, USSR. Over 175 pages per issue deal with articles on function, construction, application and operation of instruments in various fields of experimentation.

The Russian monthly Automation and Remote Control (Avtomatika i Telemekhanika) is published by the Institute of Automation and Remote Control of the Academy of Science, USSR with approximately 150 pages per issue. It is considered to be the leading Soviet journal in the automatic control field and contains articles on all phases of automatic control theories and techniques.

Industrial Laboratory (Zavodskaya Laboratoriya) is published by the Ministry of Light Metals, USSR. This monthly contains articles on instrumentation for analytical chemistry and physical and mechanical methods of material research and testing. There are approximately 125 pages per issue.

For information write Instrument Society of America, 313 Sixth Avenue, Pittsburgh 22, Pennsylvania.

DISCUSSION 63

V. M. Chulanovskii
A. V. Iogansen
S. G. Rautian
G. G. Petrash
L. A. Gribov 63
B. S. Neporent 64

SHORT COMMUNICATIONS

The Characteristic Frequencies of the Hydroperoxide Group, C—O—O—H . . . . . M. A. Kovner, A. V. Karyakin, and A. P. Efimov 64

Variation in the Duration of Luminescence of Trivalent Gadolinium and Terbium Ions in the System Sulfuric Acid-Water, as a Function of Component Concentration . . . . . E. V. Kondrat'eva 66

A Study of the Duration and Intensity of Luminescence of Trivalent Gadolinium and Terbium Ions in Solutions . . . . . E. V. Kondrat'eva and G. S. Lazeeva 67

On the Ratio between the Signal from a Component being Determined and the Signal from the Total Radiation Flux for Infrared Gas Analyzer . . . . . A. O. Sall' 69

Distribution of the Spin Density in the Dibenzenechromium Cation . . . . . S. I. Vetchinkin, S. P. Solodovnikov, and V. M. Chibrikin 71

Temperature Quenching in Certain Organic Scintillators . . . . . A. F. Kulakova and S. M. Rozman 73

Excitation of Recombination Luminescence in the Fundamental Absorption Bands of Certain Halides . . . . . I. V. Yaek and G. G. Lilid'ya 74

The Sensitized Phosphorescence of Crystalline Halide Phosphors . . . . . V. Ya. Kark, Ch. B. Lushchik, and I. V. Yaek 76

The Relation between Photoelectric Characteristics of an Electrophotographic Layer and the Characteristics of Longitudinal Photoconductivity . . . . . P. M. Podvigalkin 77

EDITOR'S NOTE

Comments on the scientific content of the translated Russian articles published in OPTICS AND SPECTROSCOPY are invited. They should be addressed as a Letter to the Editor of the Journal of the Optical Society of America and forwarded to the Editor of that journal, Dr. W. R. Brode, National Bureau of Standards, Washington 25, D.C.

VOL. VIII, NO. 1 OPTICS AND SPECTROSCOPY JANUARY 1960

CONTENTS

An Investigation of the Intensity Ratio of the Polarized Components in the Radiation of the "Luminous" Electron . . . F. A. Korolev and O. F. Kulikov 1

Ground States of Bound Paramagnetic Rare Earth Ions in an External Magnetic Field . . . N. V. Afanas'eva 4

Spectroscopic Determination of the Nuclear Moments of the Odd Isotopes of Gadolinium . . . N. I. Kaliteevskii, M. P. Chaika, I. Kh. Pacheva, and E. E. Fradkin 6

Enhancement of Sensitivity in the Spectral Isotope Analysis of Lead . . . M. S. Kashtan, E. V. Sobotovich, and T. N. Khlopina 11

Electronic Absorption Spectra of Some Indan Homologs . . . M. M. Kusakov, E. A. Prokof'eva, and M. V. Shishkina 13

Relation between Vibration Frequencies of Isotopic Molecules (the Sums Rules and the Rules for the Product Sums of the Frequency Square Powers) . . . L. M. Sverdlov 17

Frequencies of the Fundamental Vibrations of the SO_3 Molecule . . . G. A. Khachkuruzov 19

On Polarization Relationships in Raman Spectra of Molecules with a High Degree of Conjugation . . . Ya. S. Bobovich and M. Ya. Tsenter 22

Study of the Interaction between Pyridine and Water by Infrared Absorption Spectra . . . A. N. Sidorov 24

Determination of the Absolute Value of Parameters Characterizing Intensity in the Infrared Absorption Spectrum in the Cases of the Absence of Time Distortions II. . . . V. M. Chulanovsky, I. V. Peisakhson, and D. N. Shchepkin 28

The Dispersion Curve of Gaseous n-Pentane . . . E. F. Yamshchikov 29

On the Intrinsic Luminescence of Crystalline Naphthalene . . . M. T. Shpak and E. F. Sheka 32

Steady-State Luminescence of Phosphors in the Presence of Several Kinds of Traps . . . V. V. Antonov-Romanovskii 35

Study of the Electroluminescence of a Sublimed ZnS-Mn Phosphor . . . N. A. Vlasenko and Iu. A. Popkov 39

The Influence of Secondary Absorption and Emission Processes on the Duration of Luminescence of a Plane-Parallel Layer . . . A. M. Samson 43

Determination of the Size of Particles by the Scattering of Light. I. Formulas and Nomograms for Computation of Radius of Particles by the Optical Density and by Intensity of Scattered Light . . . I. Ya. Slonim 48

Selective Optico-Acoustic Receiver with Electrodynamic Microphone . . . N. A. Pankratov 53

THE CONFERENCE ON THE THEORY OF SPECTRAL INSTRUMENTS, MARCH 1959 . . . 57

Determination of the Parameters, Characterizing the True Contours of Absorption Bands . . . I. V. Peisakhson 57

Measurements of the Apparatus Function of an IKS-11 Spectrometer . . . O. D. Dmitrievskii and V. A. Nikitin 58

Experimental Determination of the Parameters of Infrared Absorption Bands in Liquids . . . D. N. Shchepkin 58

Distortions in Scanning of Single-Beam Spectrometers . . . O. D. Dmitrievskii and V. A. Nikitin 59

Influence of Scanning and the Choice of the Optimum Conditions of Measurement . . . G. G. Petrash 60

On Measurements on Double-Beam Spectrometers . . . L. A. Gribov 61

On the Method of Interference Modulation . . . V. M. Arkhipov 61

(Contents continued on inside back cover)